Molecular Tweezers with Additional Binding Sites against Protein Aggregation

Dissertation

Department of Organic Chemistry
University of Duisburg-Essen

By

Som Dutt

From Muzaffar Nagar, India

Essen 2012

Referee: Prof. Dr. Thomas Schrader

Co-Referee: Prof. Dr. Carsten Schmuck

Chairperson: Prof. Dr. Hans-Curt Flemming

Date of disputation: 03.12.2012

This work was performed during the period from July 2009 to October 2012 at the department of Organic Chemistry, University of Duisburg-Essen, campus Essen, under the supervision of Prof. Dr. Thomas Schrader.

_____

Som Dutt

Acknowledgement

I would like to express my sincere gratitude to Prof. Dr. Thomas Schrader for offering me PhD position on such an important topic. His broad research experience and profound knowledge have been very valuable throughout this work.

I am also deeply thankful to Prof. Dr. Frank-Gerrit Klärner for providing his valuable advices and logical thoughts during my work.

I am very much thankful to Prof. Dr. Carsten Schmuck for becoming co-referee my thesis.

I am also very much thankful to Prof. Dr. Hans-Curt Flemming for chairing the disputation.

I would also like to thank to Prof. Gal Bitan and his coworkers at University of California (LA, USA) and, Dr. Elsa Sanchez Garcia and her coworkers at MPI Mulheim, Germany for working in their collaboration.

Mr. Heinz Bandmann and Dr. Torsten Schaller measured the NMR, Mr. Klaus Kowski performed the ITC measurements and helped me even beyond their actual duties. I would like to thank all of them. I would also like to thanks Mr. Werner Karow and Mr. Winfried van Hoof for MS measurements and Mrs. Heike Wolle for the HPLC and peptide synthesis, Mrs. Ingeborg Reiter and Jessica Kunter for their help.

I thanks to all the former and present colleagues; Constanze Wilch, Max Sena Peters, Thomas Gersthagen, Andrea Sovislok, Patrick Gilles, Peter Talbiersky, Juila März-Berberich, Marco Hellmert, Jolanta Polkowska, Marc Blecking, Caroline Blecking, Patricia Latza, Kai Bernitzki, Wenbin Hu, Kirsten Wenck, Eva Zeppenfeld and Miao Li for supporting and keeping a lovely atmosphere in the laboratory.

I would also like to thanks to Prof. Dr. Gebert Haberhauer and his co-workers for their friendly behavior and lovely atmosphere.

At last, but most important, I wish to thank my family, especially my parents and my wife Deepika for their endless love, understanding and emotional support. This work would have not been accomplished without their support and encouragements.

To My Parents

Thesis Abstract

My doctoral thesis aims at the development of molecular tweezers with increased affinity and specificity for amyloidogenic proteins. A particular focus lies on the amyloid-β protein, a major pathological hallmark of Alzheimer's disease. In Klärner group, a molecular tweezer called the phosphate tweezer was developed which selectively binds to the amino acid lysine and arginine both in peptides and proteins, and thereby inhibits the aggregation and toxicity of amyloid proteins. However, the symmetrical prototype which carries two phosphate anions at its periphery, does not distinguish between well-accessible lysines on a protein surface. In my thesis I try to develop symmetrical and unsymmetrical molecular tweezers with new recognition sites, which become selective for a given protein/epitope.

In the first part of the work, I explored the chemical and biological effects of replacing the phosphate anions by other anionic groups of biological relevance. For this purpose, I synthesized the sulfate tweezer and carried out comparative binding studies among the phosphate, phosphonate, sulfate and methyl carboxylate tweezers with basic amino acids and relevant peptide guests. Using NMR, fluorescence, ITC, and molecular simulation, I observed substantial differences in the binding characteristics of all the four tweezer types toward their peptide guests.

In collaboration, we studied the inhibition potential of the phosphate tweezer against the pathologic aggregation of the islet amyloid polypeptide (IAPP), a protein involved in the type II diabetes. For more structural insight, I carried out an investigation about complexes between the tweezer and IAPP fragments by NMR, fluorescence and ITC experiments. Biological experiments and QM/MM calculations were performed in collaborations.

In the second part of my work, I synthesized several unsymmetrical molecular tweezers that carry a phosphate group on one side and several different linkers on the other side of tweezer's central benzene ring. These tweezers with attached linker units display varying affinities for lysine and arginine derivatives from milimolar to micromolar. Biological experiments of these unsymmetrical tweezers are currently underway in Prof. Bitan's lab (neurology, UCLA). Lastly, I developed an even more general and potent synthetic route for the synthesis of unsymmetrical molecular tweezers which keep both the phosphate groups on the tweezer. One of the two phosphate groups is substituted with an alkyne or an ester linker unit. The alkyne linker tweezer can be coupled with an azide containing recognition site via alkyne-azide click reaction, whereas,

the ester linker tweezer can be coupled with an amine containing recognition site to synthesize more powerful unsymmetrical molecular tweezer.

Content

1	**Introduction**	1
1.1	Alzheimer's disease	1
1.2	Amyloid proteins involved in pathology of Alzheimer's disease	2
1.3	Protein recognition by artificial synthetic receptors	5
1.3.1	Inhibition of potassium channels	6
1.3.2	Control over the tetramerization domain of mutant P53-R337H protein	8
1.3.3	Protein camouflage in cytochrome c–calixarene complexes	10
1.4	Receptor molecules for amino acids	11
1.5	Molecular tweezers	14
2	**Goal of the work**	18
2.1	Role of different peripheral anions	18
2.2	Role of different linker groups on monophosphate tweezers	21
3	**Results and Discussion**	23
3.1	Synthesis	23
3.1.1	Synthesis of the tweezer precursors	23
3.1.2	Synthesis of the phosphate tweezer 133	25
3.1.3	Synthesis of the sulfate tweezer 161	26
3.1.4	Synthesis of 1st generation unsymmetrical linker tweezers	27
3.1.5	Synthesis of the 2nd generation unsymmetrical tweezers	33
3.2	Binding Studies	36
3.2.1	Binding studies of the anionic tweezers	36
3.2.2	Binding comparisons among the four anionic tweezers	55
3.2.3	Biological evaluation of the anionic tweezers against aggregation and toxicity of Aβ42 and IAPP	64
3.2.4	Studies of the 1st generation unsymmetrical linker tweezers	67
3.2.5	Solvent polarity effects on complexation	76
3.2.6	Study of the phosphate tweezer **133** binding to IAPP	80
4	**Summary and outlook**	87
4.1	Summary	87

4.1.1 Symmetrical anionic tweezers 87
4.1.2 Unsymmetrical phosphate tweezers 89
4.2 Outlook 92
4.2.1 2nd generation unsymmetrical tweezers 92
4.2.2 Structure based design of the molecular tweezers for Aβ peptide 93

5 Experimental part 97
5.1 Material and method 97
5.2 Synthesis 101
5.2.1 Synthesis of the sulfate tweezer 161 101
5.2.2 Synthesis of the unsymmetrical linker tweezers 104
5.2.3 Synthesis of 2nd generation unsymmetrical bis phosphate tweezers 136
5.3 NMR titration 145
5.4 Fluorescence titrations 149
5.4.1 Fluorescence titrations of the phosphate tweezer **133** 149
5.4.2 Fluorescence titrations of the sulfate tweezer 161 155
5.4.3 Fluorescence titration of the unsymmetrical tweezers 175
5.5 Isothermal titration calorimetry (ITC) studies of the tweezers 133 and 161 Complexes 188
5.5.1 ITC experiments of the phosphate tweezer 133 complexes 188
5.5.2 ITC experiments of the sulfate tweezer 161 complexes 194
5.6 Crystal structure 196
5.6.1 Crystalstructure of dimethoxyphosphate octyltweezer **182** 196

6 References 208

List of Abbreviations

Aβ	Amyloid-β
AcArgOMe	*N*-Acetyl arginine methylester hydrochloride
AcCysOMe	*N*-Acetyl cysteine methylester hydrochloride
$(AcCysOMe)_2$	*N*-Acetyl cystine methylester hydrochloride
AcLysOMe	*N*-Acetyl lysine methylester hydrochloride
Ac_2O	Acetic anhydride
AD	Alzheimer's disease
APP	Amyloid precursor protein
CD	Circular dichroism
CLR	Clear (molecular tweezer)
COSY	Correlation spectroscopy
DA	Diels-Alder
DCM	Dichlormethane
DDQ	2,3-Dicyano-5,6-dichloro-*p*-benzochinone
DIPEA	Diisopropylethylamine
DMAP	4-dimethylaminopyridine
DMF	Dimethylformamide
DMSO	Dimethylsulfoxide
DNA	Deoxyribonucleic acid
EM	Electron microscope
eq	equivalent
et al.	And other (Latin: et alii)
Et_3N	Triethylamine
F.L.	Fluorescence
HR-MS	High resolution mass spectroscopy
I	Intensity
IAPP	Islet amyloid polypeptide
ITC	Isothermal Titration Calorimetry
KOH	Calcium hydroxide
MD	Molecular Dynamics
MP	Melting point
MS	Mass spectroscopy
MT	Molecular tweezer
MTT	3-(4,5-Dimethylthiazol-2-yl)-2,5-diphenyltetrazolium bromide
MW	Molecular Weight
NAD^+	Nicotinamide adenine dinucleotide
$NADP^+$	Nicotinamide adenine dinucleotide phosphate

NaOH	Sodium hydroxide
NMA	N-Methylmorpholine
NMNA	*N*-Methyl nicotinamide iodide
NMR	Nuclear Magnetic Resonance
p53	Tumor Protein p53
PBS	Phosphate Buffered Saline
PyBOP	benzotriazol-1-yl-oxytripyrrolidinophosphonium hexafluorophosphate
RNA	Ribonucleic acid
RT	Room Temperature
SAM	*S*-Adenosylmethionine
THF	Tetrahydrofuran
ThT	Thioflavin T
TMSBr	Trimethylsilylbromide
UV	Ultraviolet

1 Introduction

Proteins constitute an essential part in organisms and nearly participate in all the cellular processes. Regulation of cellular growth, cell signaling, immune re1sponse, trafficking of molecules and cell differentiation are important protein functions.[1] Proteins are synthesized in the ribosome as linear heteropolymers or polypeptides of amino acids which share a common molecular backbone but differ in their variable side chains.[2] These linear molecules are folded into highly specific compact three dimensional structures. The position of all atoms and their collective motion determines the properties of the proteins. A number of factors are assisting protein folding, but particularly molecular chaperones which are present in all type of cellular compartments, provide a favorable environment which helps to correct conformational errors.[3,4] Only correctly folded proteins can selectively and specifically interact with other molecules. Therefore, for the proper functioning of a protein, it has to be ensured that it is correctly folded into its thermodynamically most stable native state. Failure of proteins to fold correctly or remain correctly folded often is the origin of pathological diseases.[5] Amyloids are proteins whose misfolding causes several so-called amyloidogenic diseases including Alzheimer's disease and type-II diabetes etc. To date there is no cure for these diseases, therefore, the development of small molecule therapeutics for the treatment of these amyloid related diseases is a prime objective. Similarly, this thesis aims at developing molecular tweezers against Alzheimer's disease, which are able to prevent amyloid-β (Aβ) peptide misfolding and aggregation, and secondly, molecular tweezers against type II diabetes, which are able to counteract islet amyloid polypeptide (IAPP) misfolding and aggregation.

1.1 Alzheimer's disease

Alzheimer's disease (AD) is a progressive neurodegenerative disease that initially appears as temporary memory loss and difficulty with daily tasks, and gradually causes decline of mental faculties, dementia, and finally to death.[6,7] This is a disease of old age, typically affecting people in the eighth or ninth decade of life with incidence numbers rising steeply after age 65. Currently, AD has no cure. Whereas, several major diseases are decreasing gradually, AD is sharply increasing. In 2009, the Alzheimer's Association has reported that current estimates of AD prevalence worldwide is 29.4 million,[8] with the US contributing the highest number of 5.3 million.[9] The life span of patients with AD is eight years on average and may extend up to 20 years from the onset of symptoms.[10] During the long years of illness, the patients, families,

caretakers, and society in general suffer emotionally and financially. Current cost estimates of care for patients with AD in the US are > $148 billion a year and worldwide estimates are > 315 billion a year.[11] If no cure is found in the near future, AD will become an epidemic.[12,13]

1.2 Amyloid proteins involved in pathology of Alzheimer's disease

The protein associated with Alzheimer disease is a 37-42 amino acid residue peptide called amyloid-β (Aβ). The original source of Aβ is the abnormal proteolysis of the amyloid precursor protein (APP), an integral membrane protein whose primary function is not well known.[14] In the AD patient, Aβ42 and Aβ40 accumulate into Aβ fibrils and deposit as senile plaques into the brain and have been considered the major cause of neurotoxicity and neuronal cell death.[15] Today, however, it is generally accepted that pre-fibrillar soluble oligomers are the primary neurotoxic agents.[16,17,18] A pictorial sketch of the amyloid cascade is depicted in Figure 1.1 and a stepwise cascade outline is found in Figure 1.2.

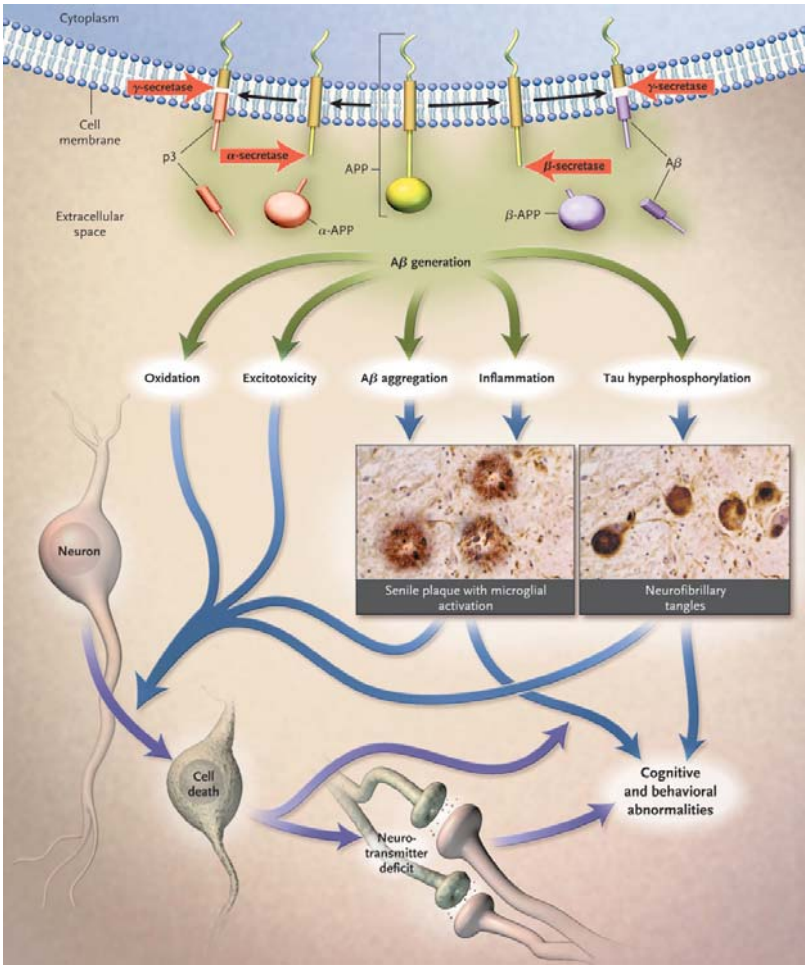

Figure 1.1 Putative amyloid cascade.[7]

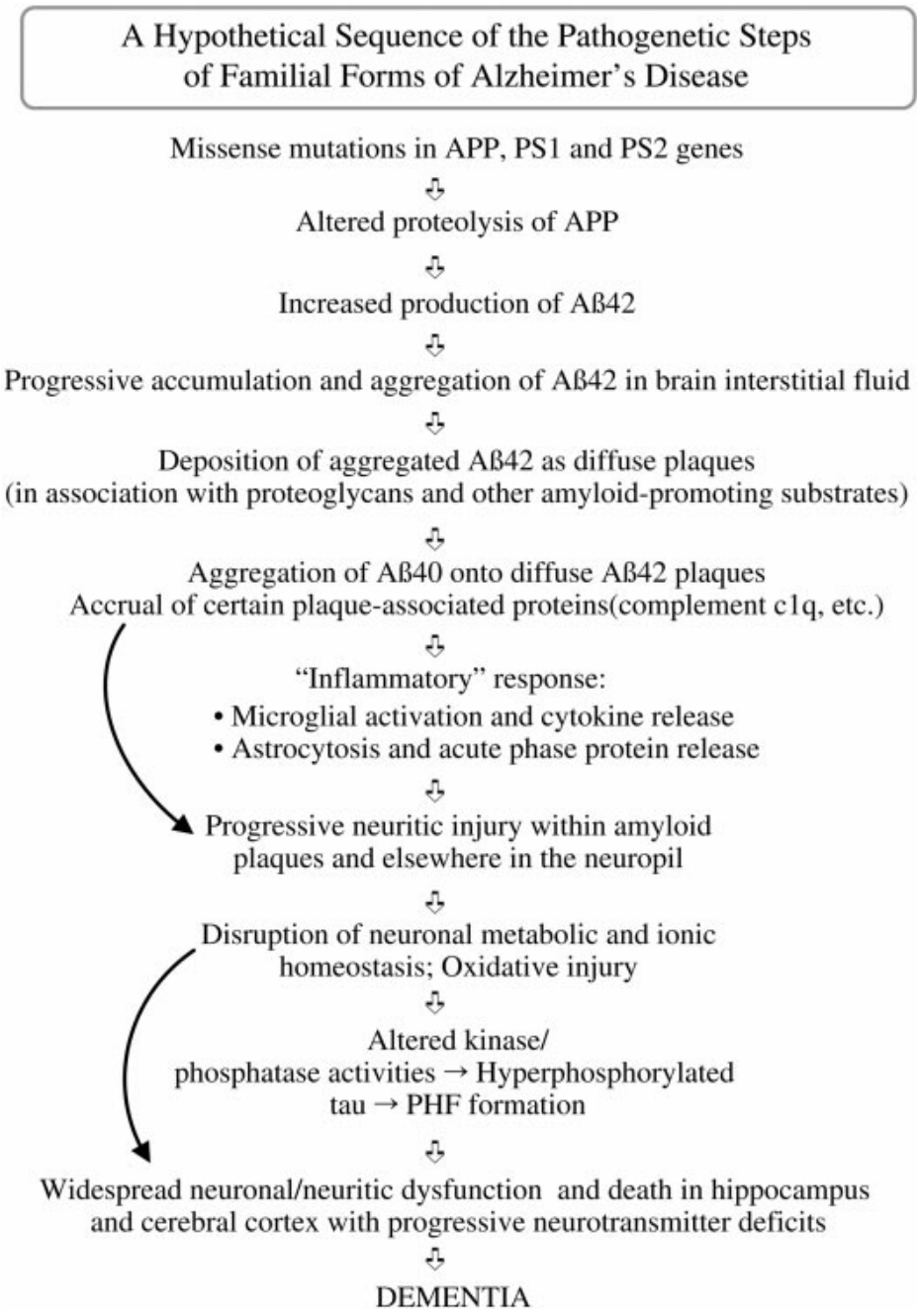

Figure 1.2 A hypothetical sequence of pathologenic step of familial form of Alzheimer's diseases.[6]

Due to the metastable and non-crystalline nature of Aβ aggregates, structural studies of Aβ have been difficult.[19,20] However, in recent years, significant progress has been made in obtaining high-resolution NMR structures of both Aβ fibrils[21,22], and pre-fibrillar assemblies of Aβ.[23] Using solid-state NMR techniques, Lührs *et al.* have reported that in amyloid fibrils, Aβ molecules are organized in parallel β-sheets.[24] In these β-sheets each monomer is folded into two β-strands connected by a turn (U-turn) in the region Aβ (22-30) as shown in Figure 1.3.

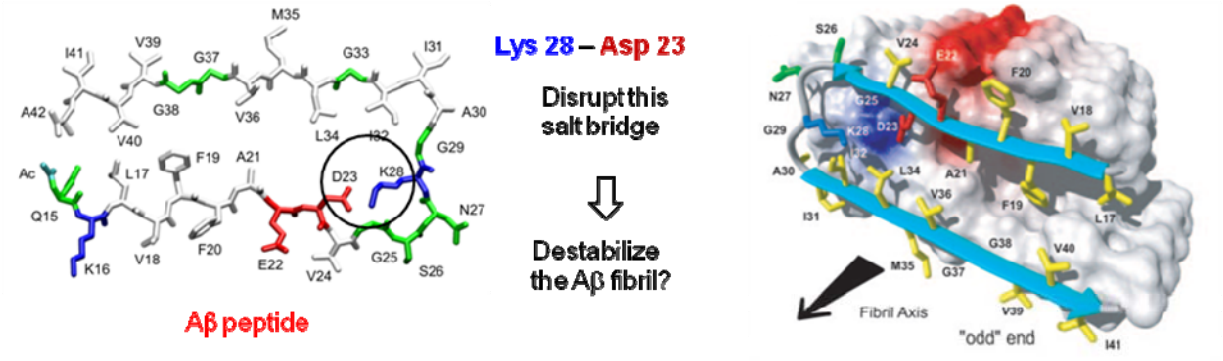

Figure 1.3 Left: Aβ (17–42) peptide in which a salt bridge between K28 and D23 is highlighted by the black circle. Right: Lühr's structure of amyloid-β fibril, indicating a β-sheet shown by cyan arrows.[24]

Within this turn, a salt-bridge between the side chains of Asp-23 and Lys-28 has been identified as a key stabilizing interaction.[25,26,27] Because this turn appears to be the first structural element observed along the pathway of Aβ folding, Lazo *et al.* suggested that it nucleates Aβ folding and assembly.[28]

In principle, a salt-bridge may also be formed between Lys-28 and Glu-22.[29] The NMR data of Lazo *et al.* could not distinguish between these two possibilities and suggested that both could co-exist. Follow up modeling studies suggested that a Glu22–Lys28 salt bridge actually predominated over Asp23–Lys28 in the initial turn (Figure 1.4).[30]

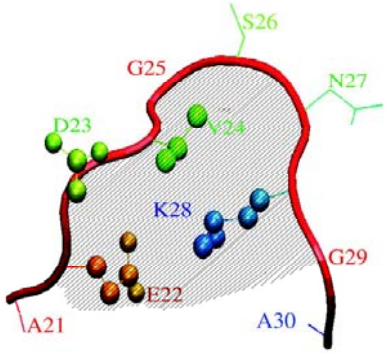

Figure 1.4 Model of central turn in Aβ. The model is based on NMR data and molecular dynamic simulations.[29]

Apart from participating in electrostatic interactions, the alkyl chain of the Lys-28 side-chain forms hydrophobic interactions with the side chain of Val-24, which were reported to be crucial for stabilization of the initial turn in Aβ.[28,31,32] Similarly, the alkyl chain of Lys-16 can contribute in hydrophobic interactions with residues in the central hydrophobic cluster of Aβ (CHC, residues 17–21) and thereby stabilize intra- and/or intermolecular contacts involved in β-sheet formation and aggregation. Therefore, the two Lys residues in Aβ, and in particular Lys-28, appear to be crucial in Aβ folding and self-assembly. With this information in mind, Bitan *et al.* hypothesized that a reagent capable of interacting specifically with Lys residues might inhibit the crucial electrostatic and hydrophobic interactions the Lys side chains participate

in and thereby inhibit Aβ folding, assembly, and toxicity.

1.3 Protein recognition by artificial synthetic receptors

Most of the biological processes rely on the association of two or more proteins which is a highly precise molecular recognition phenomenon. Therefore, synthetic receptor molecules that can bind or interact with proteins can be of great importance. In particular, those receptor molecules are valuable that operate in aqueous solution, bind selectively to a target protein through noncovalent interactions and can modulate or alter protein activities. However, a number of challenges are associated with the design of small molecular receptors that can efficiently control or regulate the activity of a protein.[33,34] Some of these comprise (1) the complex irregular topology of most protein surfaces rendering many surface-exposed residues sterically inaccessible, (2) the large contact area which is usually required for efficient competition with natural protein-protein interactions (> 1000 $Å^2$), (3) the high number of identical amino acid residues on a protein surface, among which only few are suited for protein inhibition by external complexation, and (4) the high degree of solvation of polar surface-bound amino acid residues in proteins. On the other hand, supramolecular chemistry has gone a long way since the Nobel Prize was awarded to Cram, Lehn and Pedersen in 1987. Today we can calculate with reasonable precision all kinds of noncovalent interactions and we know how to construct receptor molecules for almost any given target.

In recent years several pioneering supramolecular systems have been developed that were used to stimulate or retard protein activities. These have been summarized in several excellent reviews.[34,35,36,37,38,39] Some of the first approaches have been developed in the Hamilton group: initial efforts focused on hot spots of basic proteins around the active site. Porphyrins, calixarenes and cyclodextrins were chosen as molecular platforms with attached peripheral arms for lateral recognition of charged amino acid residues. Among the above supramolecular host molecules, cone shaped calix[n]arenes can accommodate functional groups in their hydrophobic cavities and have great potential in protein surface recognition.[40,41,42,43,44] In most of these early examples, multiple electrostatic interactions towards charged amino acids were combined with dispersive interactions towards the unpolar ligand platform, further enhanced by the hydrophobic effect (exclusion of solvent molecules). Impressive results have been obtained when the artificial inhibitors were complementary in shape and charge distribution to the respective protein epitope.
In my thesis I summarize recent work and progress in the direction of rational design of small

molecule receptors that efficiently interfere with the biological function of a protein–some of which are therapeutically relevant.

1.3.1 Inhibition of potassium channels

In a rational approach to design small molecule inhibitors of proteins, Trauner *et al* developed synthetic inhibitors of potassium channels.[45] The latter are gated membrane pores for the regulated flux of metal cations which are essential for organisms as diverse as archaebacteria and humans.[46] Potassium channels control transmembrane potential and thereby vital cellular functions such as excitability, proliferation secretion and volume regulation. Each channel is formed by four protein subunits which self-assemble into a central pore. Some simple organic molecules are known to block these pores, such as the tetraethylammonium cation. A number of natural inhibitors have also been identified from scorpions, snakes, spiders and other organisms, but none of them takes advantage of the four-fold symmetry of the homotetrameric ion channels.

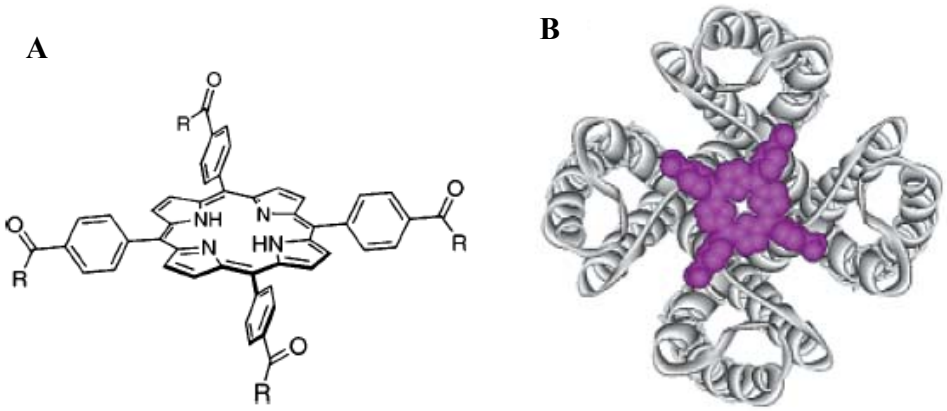

Figure 1.5 (A) Tetraphenylporphyrin derivatives, designed to block hot spots in potassium channels (R = -NH_2^+-$(CH_2)_n$-NH_3^+); (B) tetraphenylporphyrin (violet) docked onto its preferred binding site on the channel entrance.[45]

In their seminal work, Trauner *et al.* proposed that fourfold symmetrical porphyrin scaffolds may be able to bind all four channel subunits simultaneously, resulting in a strong polyvalency effect. As a consequence his group synthesized and tested several cationic tetraphenylporphyrin (TPP) derivatives which bind to the four subunits of voltage-gated potassium channels of the K_v1.x class such as "Shaker" and "K_v1.3". From a competitive binding assay with a hongotoxin (^{125}I-$HgTX_1$A19Y/Y37F), a number of TPP derivatives, all decorated with a positively charged periphery, were found to bind to these potassium channels with nanomolar affinities (e. g., for compound **3**, K_i = 20 nM). On the other hand, porphyrins with negatively charged groups did not

compete with hongotoxin binding, suggesting that the high affinity originates from specific interactions between cationic groups on the porphyrins and negatively charged (aspartate) residues located on the hot spots of each channel subunit. Electrophysiological experiments demonstrated, that cationic compounds indeed significantly inhibites the “Shaker” current in a reversible manner; however, complete inhibition was not attained even at high concentrations, raising the question whether the porphyrin really binds to all four channel subunits simultaneously, as proposed in the binding model (Figure 1.5).

The putative binding mode of TPP derivatives on potassium channels has been the subject of further mechanistic studies.[47] Solid state NMR spectroscopy was combined with electrophysiological and pharmacological experiments in order to investigate structural alterations of the K^+ channels. However, in contrast to the Trauner model, all structural data according to Ader pointed to deep penetration of the porphyrin into the channel pore with simultaneous insertion of one of its positively charged arms along the channel axis where the protonated amine group interacts with K^+ ion binding sites. It was argued that although the synthetic porphyrin fulfilled the 4-fold symmetry requirement it did not utilize it, because its flat structure did not fit the conical shape of the channel pore and thus only partially inhibited the channel current in a nonspecific way.

In another combined effort to design and synthesize more selective ligands for this job, Trauner and de Mendoza later reported about a family of multivalent calix[4]arene ligands which bind to the surface of K_v1.x channels in a reversible manner.[48] In contrast to flat porphyrins, these calix[4]arenes possess a conical C_4-symmetry which is perfectly complementary to the shape of the K_v channels’ outer vestibule, thus providing features for optimal binding. Trauner and de Mendoza synthesized and evaluated a large number of calix[4]arenes with neutral, positively or negatively charged upper rims and free-OH or crown ether loops at their lower rims.

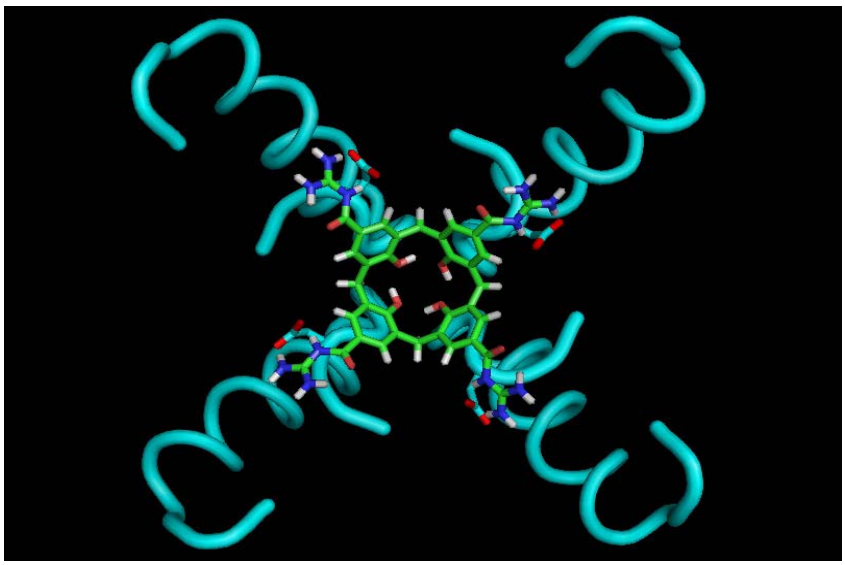

Figure 1.6 Calix[4]arene docked on the crystal structure of human valtage dependent $K_v1.2$ potassium channel. The Asp-379 side chains are represented, showing the 4-ion-pair, hydrogen-bonded contacts with the guanidinium residues of the calix[4]arene.[48]

Molecular dynamics and electrophysiological experiments were performed to investigate the structural and functional aspects of the interaction between these calix[4]arene derivatives and potassium channels. Ligands with cationic (guanidine and arginine) substituents at the upper rims bind the protein with high affinity by interacting with an anionic Asp-379 residue, which is conserved in all the potassium channels of the $K_v1.x$ subfamily. Simultaneously, the lower rim adorned with free hydoxyls is embedded inside the channel pore where it establishes a cyclic array of four hydrogen bonds in the turret loop (Figure 1.6).

By contrast, calixarene ligands substituted with carboxylate, neutral or ammonium groups at the upper rims do not show significant inhibition effects on the "Shaker" ion current. Thus, simple guanidinylated phenols shows no inhibition effect even at 50 μM, strongly indicating the importance of multivalency and preorganization present in the active calix[4]arenes.

1.3.2 Control over the tetramerization domain of mutant P53-R337H protein

Protein P53 is also called the tumor suppressor protein or the "genome guardian". It is a transcription factor, responsible for mediating cell cycle arrest or apoptosis when its DNA is damaged.[49] Mutations in P53 were found to initiate around 50% of all kinds of human cancer. Human P53 protein contains 393 amino acids and is structurally as well as functionally divided

into four domains. Two identical protein chains, each consisting of an α-helix and a β-strand, fold into an intertwined secondary structure called “dimer”, stabilized through a major ion-pair interaction between Arg-337 and Asp-352 (Figure 1.7A). The active form of the protein is a tetramerization domain in which two of these dimers are held together by strong hydrophobic and hydrogen bonding interactions. In the mutant P53-R337H, Arg-337 is replaced by histidine which is unable to form the ion pair bridge with Asp-352 because the histidine is not fully protonated at physiological conditions. This mutation destabilizes the whole tetramerization domain and renders the organism susceptible to tumor setup.

Further, the development of effective synthetic P53 ligands came from the Giralt and de Mendoza groups, who again used the shape complementary of a calixarene platform to the conical cavity of a self-assembled protein.[50] It was reasoned that combination of the calixarene’s cone conformation with appropriately positioned positively charged groups would efficiently complement the hydrophobic environment inside the protein tetramer and the negatively charged glutamate residues located on its outer surface. ^{1}H-STD NMR, ^{15}N-^{1}H-HSQC NMR, Differential Scanning Calorimetry (DSC), and MD simulations were all used to characterize this protein-ligand binding process.

Intriguingly, already the simple conical calix[4]arene ligand (Figure 1.7B) meets the above mentioned criteria. Two of these calix[4]arene molecules sit like corks in the hydrophobic clefts of the protein, which recovers its tetramer integrity and thus protein begins to work again (Figure 1.7C). The four guanidiniomethyl groups at the upper rim of this calix[4]arene undergo electrostatic and hydrogen bonding interactions with Glu-336 and Glu-339 and the calixarene’s hydrophobic surface together with both crown ether loops at lower rim fit nicely and cooperatively into the hydrophobic pocket of the P53 tetramer assembly, stabilizing the whole ensemble.

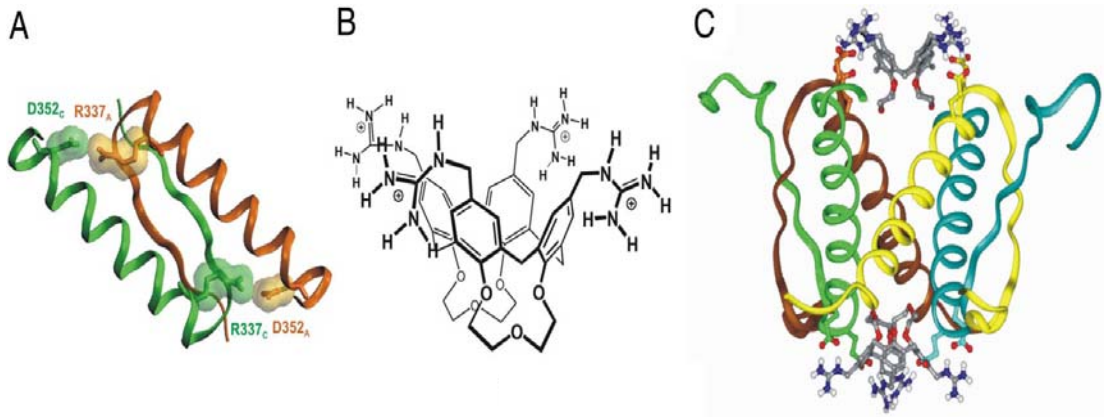

Figure 1.7 Protein p53TD and docking of ligand 1. (A) Primary p53 dimer showing the two major R337–D352 interactions. (B) Tetraguanidiniomethylcalix[4]arene ligand. (C) Two calix[4]arene molecules with guanidiniomethyl groups stabilizes the mutated tetramerization domain of the tumor suppressor P53 protein. [50]

1.3.3 Protein camouflage in cytochrome c–calixarene complexes

Recently, Crowley *et al.* were successful to generate a crystal structure of *p*-sulfonatocalix[4]arene complexing the surface of cytochrome c.[51] Cytochrome c is known as a pseudospecific binder to its protein partners involved in redox processes and apoptosis. NMR titration data revealed that the binding process involves two or more binding sites; however, binding affinities were estimated only in the range of 0.8-1.6 mM. In the crystal structure is shown that three sulfonatocalix[4]arene molecules bind to three different lysine residues (Lys89, Lys4 and Lys22) in two crystallographically separate molecules of Cyt c (Figure 1.8). Clearly, the ligand binds to lysine by encapsulating the amino acid side-chain and by forming at least one hydrogen bond between its peripheral sulfonate anions and the ammonium cation of lysine. Electrostatic contributions were investigated by varying the ion concentration. In the absence of 50 mM NaCl the binding affinities increased by a factor of 1.6, indicating the decrease in electrostatic screening effects of ions. Though, the effects of sulfonatocalix[4]arene on the reactivity of Cyt c have not yet been carried out, these crystal structures are first of its kind and very encouraging towards the supramolecular approaches of biological interference.

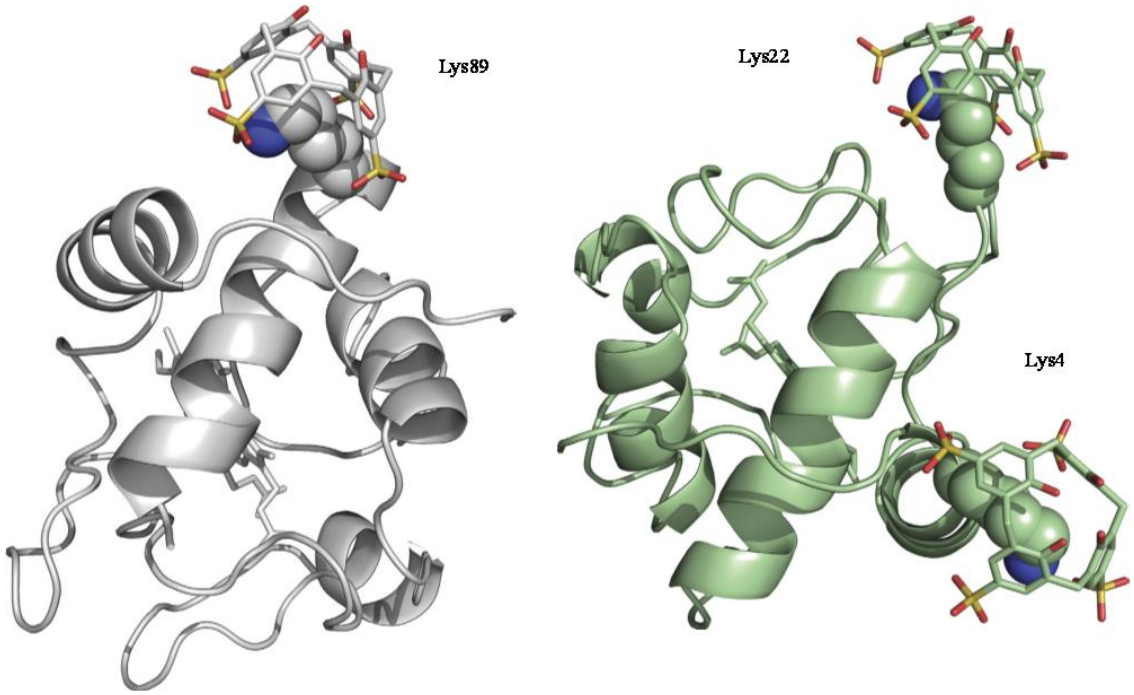

Figure 1.8 Crystal structure of sulfonatocalix[4]arene complexed at three different lysines on two different molecules of cytochrome c (Cyt c).[51]

All the above examples showed how rationally designed molecules can use non-covalent interactions to bind to selected residues on the surface of large proteins.

1.4 Receptor molecules for amino acids

Most of the artificial receptor molecules utilize the multivalency to bind proteins and to date no receptor molecule is reported which is amino acid specific and interferes with biological process of proteins. Amino acid specific receptors can be of great importance in modern medicinal chemistry. For example, there are only a few amino acids or sequences of amino acids that contribute most to the structural and functional aspects of a protein or enzyme. The group of these key amino acids is called hot spot.[52] Therefore, such key residues in a protein could be attractive targets for amino acid specific receptors. The artificial receptors can be modified and developed to interact with a specific region in a protein and therefore, become protein selective.

In the supramolecular chemistry community, a number of artificial receptor molecules have been developed for amino acids. Pioneering work came from *Cram* (binaphthyl crown ethers),[53] *Sessler* (sapphyrins),[54,55,56] *Chin* (coordination complexes),[57] *de Mendoza* (chiral bicyclic guanidines)[58,59] and *Sanders* (zinc porphyrins).[60] Later amino acid specificity was achieved by crown ethers adorned with a "recognition unit" (lysine, *H.-J. Schneider, B. König*),[61,62] glycoluril

clips (aromatic amino acids, *R. Nolte*),[63,64] polycyclic pyridines (arginine, *T. Bell*),[65] macrocyclic Tröger's base derivatives (lysine/arginine, *D. Dougherty*),[66] zinc and copper chelate complexes (histidine, *B. König, E. V. Anslyn*),[67,68] boronic acids (homocysteine, *R. Strongin*),[69] guanidiniopyrroles (aspartate, glutamate, *C. Schmuck*),[70,71] cucurbit [7]uril (phenylalanine, *A. R. Urbach*)[72] etc. All represent powerful mono- or ditopic host molecules with functionalities complementary to the side chains of proteinogenic amino acids. Some of these also operate in water, but very few cases have been reported where these receptor molecules are able to interfere with biological processes.

In particular, basic amino acids lysine and arginine play vital role in biological processes.[73] Histones are specifically acetylated and deacetylated at side chain ammonium group of lysine to activate or repress gene regulation (transcription).[74,75] RNA binding proteins are arginine rich and bind through specific electrostatic interactions with phosphate anions in the neucleotide backbone, for example; arginine rich transcriptional activator *Tat* and *Rev* are involved in the replication step of human immunodeficiency visus type 1 (HIV-1).[76,77] Further, KAA sequence is an important building block in the bacterial cell walls.[78] Lysine peptide KLVFF is associated with Aβ aggregation in Alzheimer's disease.[79] The RGD sequence is another important recognition element found in many proteins that interact with integrins on cell surface.[80]

Though basic amino acids are crucial in protein's structures and functions, there are only selected potential artificial receptors for these amino acids. For example, apart from our research group, two receptors are known for amino acid lysine and arginine. Polycyclic pyridines developed by Bell *et al.* is an interesting example that bind guanidinium group of arginine through multiple arrays of hydrogen bonds and known as Bell's arginine cork (Figure 1.9), however, in aqueous solution only 1100 μM affinity (K_d) is achieved.

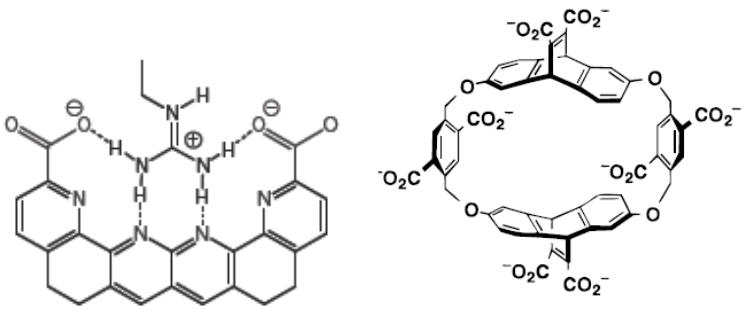

Figure 1.9 Structures of Bell's arginine cork[65] (left) and Dougherty's cylcophane receptor for arginine.[66]

Substituted cyclophanes, developed by Dougherty group, are another class of potential receptors (Figure 1.9) having the best affinity of 200 μM for arginine. These carboxylic cyclophane receptors are arginine selective over lysine and form complexes by utilizing the cation-л, electrostatic and hydrophobic interactions. Certain calix[4]- and -[5]arenes have also been identified that binds to lysine and arginine.[41,42,44] König *et al.* attached two crown ethers via a suitable linker to bind diammonium lysine, however, in aqueous buffer solutions the binding was almost immeasurable ($K_a < 10\ M^{-1}$).[62]

In the below example is shown how the strong binding of lysine is achieved in proteins. Methylated lysine histone (for example; H3K4me3) is associated with transcription start site of active genes. Crystal structures of histone H3K4me3 bound by plant homeodomain (PHD) finger of human BPTF are obtained (Figure 1.10).[81] Interestingly, in the crystal structure, a cage of aromatic amino acids of the protein BPTF is formed surrounding the trimethylated lysine side-chain of histone. An affinity of 3 μM was estimated for BPTF binding to H3(1-15)K4me3 using calorimetric measurements. This is an interesting example where only one lysine residue play critical role in biological recognition through hydrophobic and cation-л interactions.

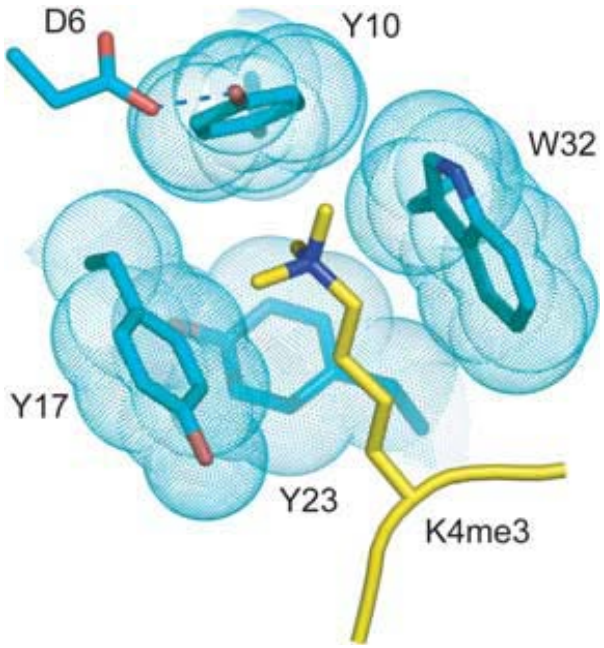

Figure 1.10 Crystal structure of protein BPTF bound to H3K4me3. In yellow is shown trimethylated lysine and in cyan aromatic residues of PHD domain of protein BPTF.[81]

1.5 Molecular tweezers

In recent years, our group has explored new mechanisms of supramolecular interference with protein and peptide activity by means of molecular clips and tweezers.[82,83,84,85] Molecular clips draw the biologically active part of the respective cofactor (NAD^+ or $NADP^+$) into their cavities and are able to reversibly inhibit enzymatic processes.[83,86] On the other hand, molecular tweezers encapsulate the side chain of Lys and Arg amino acids[87] and prevent the protein aggregation events.[88] The phosphonate tweezer was the first water soluble artificial receptor that bind to lysine with the dissociation constant, K_d = 200 μM in neutral phosphate buffer. Later on, even much higher affinity was achieved by the phosphate analog that binds to lysine in neutral phosphate buffer with 20 μM affinity[83]. Therefore, the phosphate tweezer was proved to be more water soluble and highly selective artificial receptor molecule for lysine. The structures of the two tweezers and electrostatic potential surface of the phosphate tweezer are shown in Figure 1.11.

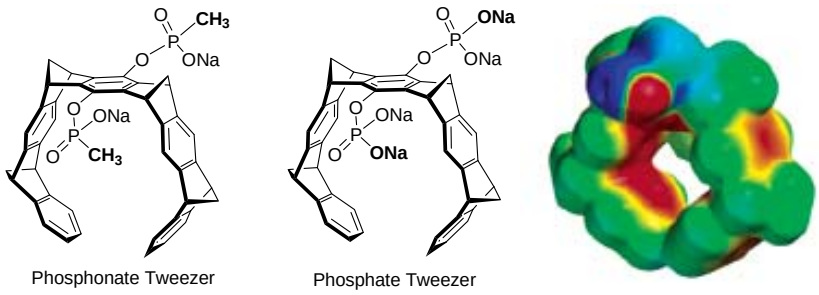

Figure 1.11 Structures of the phosphonate and the phosphate tweezers developed in the Schrader and the Klärner groups, and electrostatic potential surface of the phosphate tweezer showing high electron density cavity (right).[89]

These molecular tweezers adorned with anionic phosphate or phosphonate groups on the central benzene ring feature electron-rich and torus-shaped cavity. The exquisite selectivity for lysine or arginine is achieved through threading the amino acid side-chain into the cavity and locking the phosphate/phosphonate and ammonium/guanidinium ions by the salt-bridge formation. NMR and ITC titrations showed the enthalpy driven complex formation between the tweezers and lysine/arginine which results from van-der Waals and electrostatic interactions. Molecular modeling studies provided structural insights of a complex formed by these molecular tweezers with lysine or arginine guests (Figure 1.12).[87]

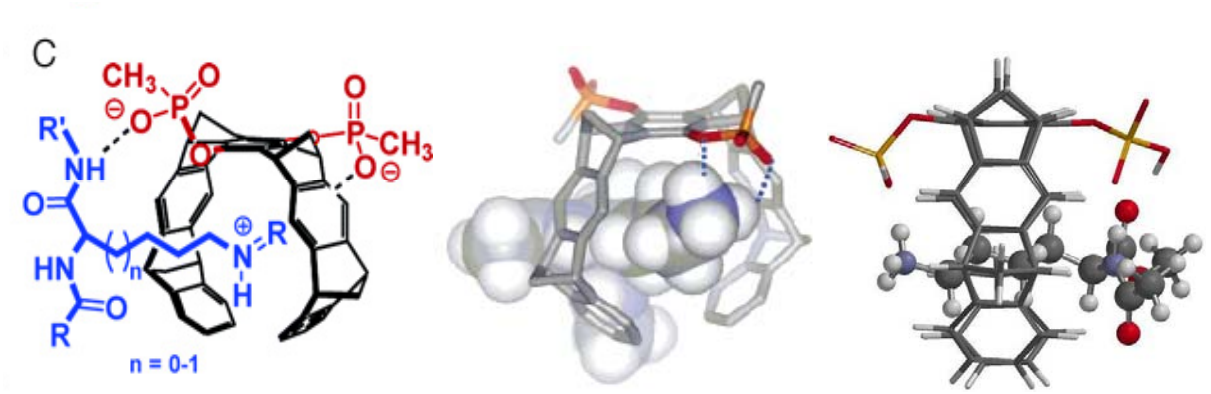

Figure 1.12 Left: schematic drawing of lysine/arginine binding to phosphonate tweezer; Middle: calculated structure of the phosphonate tweezer- AcLysOMe complex;[87] Right: calculated structure of the phosphate tweezer-AcLysOMe complex.[89] Both the structures were calculated using conformational search (Macro Model, Amber*/water, 5000 steps).

Given the low micromolar affinities in aqueous solution towards basic amino acids, the phosphate tweezer possesses high potential to interfere with the biologically relevant peptide or proteins in which lysine or arginine residues play crucial roles. This hypothesis was explored by Prof. Bitan at UCLA who work on the structure-based inhibitors of amyloid proteins involved in Alzheimer's disease and type II diabetes etc. Prof. Bitan in collaboration with our group investigated the inhibition potential of the molecular tweezers against aggregation and toxicity of the amyloid proteins.[88] Biophysical and cell assays studies suggested that the phosphate tweezer is capable of inhibiting the aggregation and toxicity of multiple amyloidogenic proteins. Using the mass spectrometry and solution-state NMR it was shown that the phosphate tweezer binds to the lysine residues in the amyloid-β protein and disrupts the hydrophobic and electrostatic interactions which are thought to be crucial for the nucleation of aggregation process. With its great potential, the phosphate tweezer was named CLR01.

Bitan *et al.* investigated the inhibition of aggregation processes of Aβ42 by the phosphate tweezer using Thioflavin T (ThT), circular dichroism (CD), electron microscope (EM) etc techniques. The decrease or no change in ThT fluorescence in the presence of the phosphate tweezer indicated the prevention of protein aggregation (Figure 1.13b). The same samples of ThT experiments were analyzed into electron microscope which showed long needle shaped fibrils of amyloid proteins in absence of CLR01, while only amorphous structures in the presence of CLR01 were observed (Figure 1.13e).

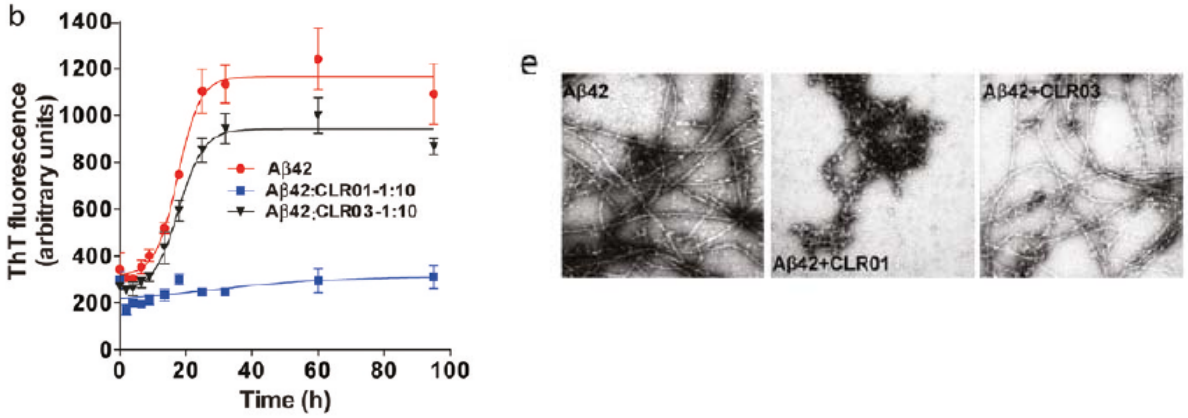

Figure 1.13 (b) CLR01 inhibition of Aβ42 aggregation measured by ThT fluorescence. (e) Morphological analysis of Aβ42 in the absence or presence of phosphate tweezer (CLR01) was examined at the end of each aggregation reaction. Phosphate spacer (CLR03) was used as a negative control.[88]

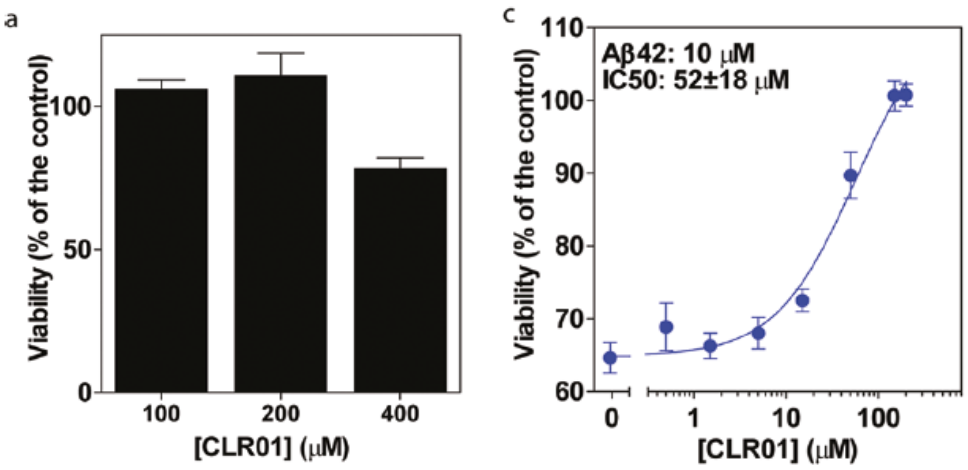

Figure 1.14 Dose-dependent inhibition of toxicity of amyloidogenic proteins by CLR01. (a) Increasing concentrations of CLR01 were incubated with differentiated PC-12 cells for 24 h. (c) Oligomers of protein Aβ42 were added to differentiated PC-12 or RIN5fm cells in the absence or presence of increasing CLR01 concentrations. Cell viability were measured using the MTT reduction assay.[88]

The toxicity and rescue effects of CLR01 on the cells in the presence of amyloid aggregates were tested in cell viability assays. The results indicated that CLR01 is not toxic upto a high concentration of 200 μM and only at about 400 μM little toxicity of CLR01 was observed (Figure 1.14a). On the other hand, CLR01 rescued the cell viability from the toxicity of various proteins aggregates. At about 100 μM concentration of CLR01 cells were rescued and restored into fully functioning state (Figure 1.14c).

These intriguing results lead to further develop the molecular tweezers into more powerful and selective receptors. To understand the importance of the phosphate groups, it is necessary to replace them with other different anions of similar nature and investigate the role of each anion in the binding process and inhibition potency of the respective tweezers. Since the diphosphate tweezer is symmetrical and cannot be selective to a particular protein target, it is also necessary to transform at least one of the phosphate groups into an additional protein specific or amino acid sequence specific binding unit.

2 Goal of the work

My doctoral thesis aims at the development of molecular tweezers with increased affinity and specificity for amyloidogenic proteins. A particular focus lies on the amyloid-β protein. The molecular tweezer **133** with two phosphate groups operates in aqueous medium and selectively binds to the amino acids lysine and arginine both in peptides and proteins.[89,90] Recently this tweezer was reported to inhibit the aggregation and toxicity of amyloid proteins.[88] It is evident that the strong binding of the phosphate tweezer **133** to lysine or arginine resulted from specific hydrophobic, electrostatic and cation-л interactions. The development of molecular tweezers will be approached in two parts.

2.1 Role of different peripheral anions

The phosphate groups on tweezer **133** not only render the tweezer water-soluble, but are also essential to lock the ammonium or guanidinium cations of basic amino acids into an internal ion pair. Therefore, replacing the phosphate anions with other anionic groups of biological relevance would be an interesting study which may result in improved tweezer design, if the differences in the binding characteristics of anionic groups can be explored. Phosphates, carboxylates and sulfates are ubiquitous in biological structure, function and regulation. The sulfate group has pulled more attention in developing new substances with pharmacological importance.[91,92,93,94,95,96,97] Despite the similar structure and pyramidal shape of phosphate and sulfate, they are highly specific in biological systems. For example; phosphate-binding protein (PBP) selectively transport the phosphate anions in biological process, while unable to recognize other polyanionic groups such as sulfate.[98] On the other hand, sulfate-binding protein, involved in the active transport of sulfate, is highly specific for sulfate and do not bind to phosphate.[99] Another interesting example is the heparin binding to antithrombin-III (AT-III). This binding is achieved through AT-III interactions with sulfate groups in sugar units of heparin. Boeckel et al showed that the replacement of a particular sulfate group by a phosphate group resulted in the inactive analog of pentasaccharide domain.[100]

Apart from the biological systems, many groups have explored the functional aspects of artificial receptors that are substituted with these anionic groups. Klärner *et al.* studied the supramolecular properties of several molecular clips substituted with phosphate, phosphonate and sulfate anions (Figure 2.1).[101] Interestingly, they found substantial difference in the binding characteristics of these clips as shown in Table 2.1. The phosphate clip **18h** binds substantially stronger to caffeine

and **SAM** compared to the sulfate clip **36** and the phosphonate clip **18g**. On the other hand, the sulfate clip **36** binds to **NMNA** and Kosower Salt more strongly compared to the clips **18h** and **18g**.

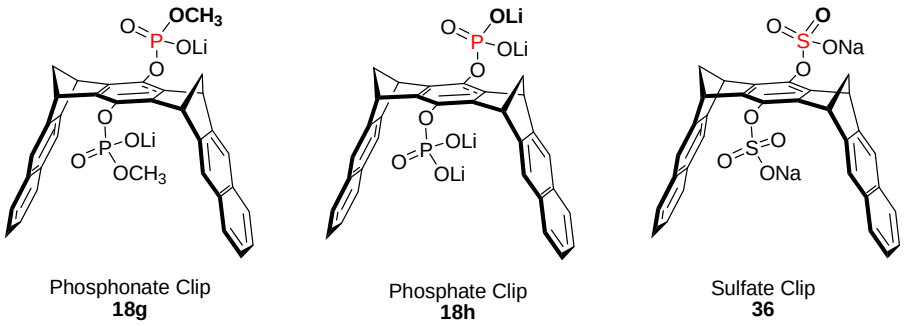

Figure 2.1 Structures of the three anionic clips studied in the Klärner group.[101]

In another example, Nilsson *et al.*[102] synthesized a series of O2-anion-substituted galactopyranosides and studied their binding to arginine-rich proteins galactins. In the comparison study of sulfate and phosphate substituted ligand, they found sulfated ligand were several fold superior over the phosphate substituted ligand. There could be several factors like; charge, resonance stabilization of charge and solvation of anions, etc that affect the selectivity and specificity of the ligands containing these anionic groups.

Though, phosphate and phosphonate tweezers have already been synthesized and studied in Klärner and Schrader groups, the binding comparisons among the phosphate, phosphonate, sulfate and carboxylate anionic tweezers have not yet been investigated. These studies should be of great importance, in particular, when we would like to develop molecular tweezers as therapeutic candidates. Therefore, specific and selective binding characteristics and toxicity effects of these anionic tweezers should also be screened in biological system.

Table 2.1 comparisons among the dissociation constants of the sodium sulphate naphthalene clip 36, the tetralithium phosphate clip 18h and the dilithium phosphonate clip 18g in buffered water solution (pH= 7.2) measured by means of ^{1}H NMR titration experiments at 25 ºC.

Guest	Host		
	36 K_d [µM]	**18h K_d [µM]**	**18g K_d [µM]**
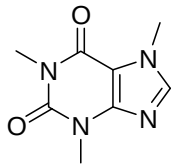 Caffeine	345	23	105
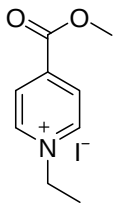 Kosower Salt	12[a]	53	1190
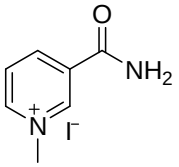 NMNA	6	30	88
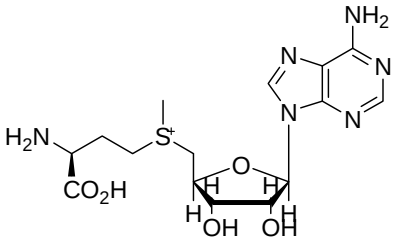 SAM	1064	185	833

[a] Measured in pure D_2O[101]

In the first part of this thesis, the effects of these anionic groups on the tweezer will be investigated (Figure 2.2). For this reason, the sulfate tweezer **161** will be synthesized for the first time to carry out comparative binding studies among phosphate, phosphonate, sulfate and carboxymethyl tweezers with derivatives of basic amino acids and relevant peptide guests such as KAA, KLVFF, RGDFV and IAPP fragments.

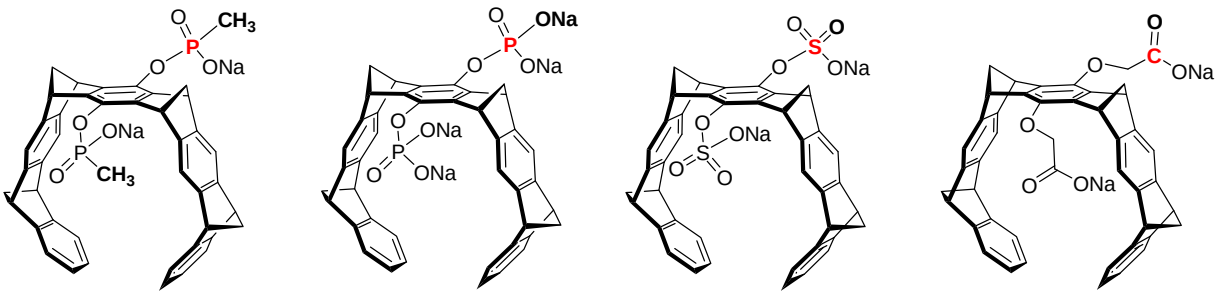

Figure 2.2 Structures of the four symmetrical anionic tweezers substituted with phosphonate, phosphate, sulphate and methylcarboxylate anions.

Due to the difference in basicity, shape, charge, solvation and stereoelectronic properties of the four anions, these tweezers are supposed to provide substantial differences in the binding characteristics toward their peptide guests. Guest binding studies will be performed by NMR, fluorescence, ITC experiments and molecular modeling simulation.

2.2 Role of different linker groups on monophosphate tweezers

The symmetrical prototype which carries two phosphate anions at its periphery, does not distinguish between well-accessible lysine residues on a protein surface. To develop further their diagnostic as well as therapeutic potential these new lead structures must become protein- or peptide-specific, and thus avoid unwanted side effects. Since only one phosphate is used for ammonium- or guanidinium recognition, the other one may be replaced by a second binding site, connected to the parent tweezer by a suitable linker, which corresponds to the distance between both functional groups on the protein surface. Therefore, in the second part of this work, I will develop unsymmetrical tweezers which carry additional recognition sites and hence become selective for a given protein epitope.

Earlier observations from substituted neutral tweezer derivatives in organic media quite often demonstrated self-inclusion of extended aliphatic side chains, with the result, that guest affinities remained very modest, if binding was not blocked at all. This unsatisfying behavior poses the open question, if also in buffered aqueous solution, certain linkers block the cavity entrance to our anionic phosphate tweezers, and prevent free access of amino acid and peptide guests?

Common linkers which are often used in synthetic drug candidates to combine an alcohol with another active part of the molecule are mainly based on ether and ester functionalities. Ethers are

usually preferred over esters because of their greater hydrolytic stabilities. On the other hand, polar chains are considered to avoid unwanted hydrophobic clustering as well as increase water solubility of the resulting drug candidates.

Several unsymmetrical molecular arginine and lysine tweezers which carry the above-mentioned linker units on one side and a phosphate anion on the other side of their central hydroquinone will be synthesized. These linkers which cover a broad range of polarities as well as anchor points for the covalent attachment of the secondary binding site will be attached to the parent hydroquinone by ester and/or ether junctions. The new unsymmetrical tweezers with attached linker units will be studied to evaluate the effects of their individual linker groups in complex formation. Only the best candidates will be equipped with recognition sites to achieve protein specificity.

Our group has already established a close collaboration with Prof. Bitan's laboratory (Department of Neurology, UCLA, U.S.A.) who will carry out biological studies of every new tweezer type about its influence on the aggregation of amyloidogenic proteins. The required chemical studies will be performed by myself.

3 Results and Discussion

3.1 Synthesis

3.1.1 Synthesis of the tweezer precursors

The starting molecular tweezers required in this work are the dihydroxy tweezer **121** and the monohydroxy acetoxy tweezer **120**, that were developed in the group of Prof. Klärner and were first synthesized by Kamieth.[103] The diacetoxy tweezer **119** served as the parent tweezer for both the starting precursors and was synthesized from the bisdienophile **107** (spacer) and the diene **115** (side wall) through the Diels-Alder (DA) reaction.

The Spacer **107** was synthesized in five steps as shown in Scheme 3.1 starting from p-benzoquinone and cyclopentadiene. The DA-adduct **103** obtained in the first reaction was converted into the 1,4-hydroquinone intermediate **104** by triethylamine and subsequently was oxidized into the corresponding quinone derivative **105** by using p-benzoquinone as oxidizing agent. The *syn* and *anti* products were produced through the DA reaction of **105** and cyclopentadienes. The *syn* product **106** was purified by crystallization and converted into diacetoxy spacer **107** using acetic anhydride and DMAP in pyridine.

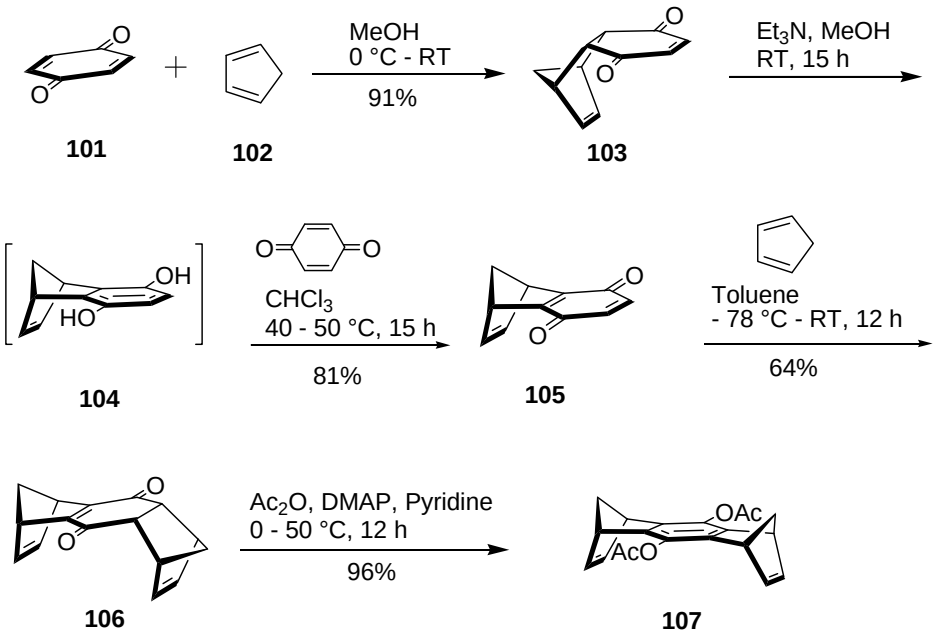

Scheme 3.1 Synthesis of the bisdienophile **107** (spacer).

The diene **115** was synthesized in 7 steps (Scheme 3.2). The first step of the synthesis was the Diels-Alder reaction of indene and maleic anhydride. The reaction proceeds by refluxing the

reaction mixture at > 200 ^{o}C where indene converted into *1H*-indene which undergoes a [4+2] cycloaddition with maleic anhydride and produced the adduct **110** in 20-40 % yield. In the next step, *cis* dimethylester **111** was produced by the estrification of anhydride **110** in the presence of acetyl chloride as acid catalyst. Then cis-dimethylester **111** was converted into thermodynamically more stable trans-dimethylester **112** using sodium methoxide. The *trans* diemethylster **112** was then reduced into *trans* diols **113** using $LiAlH_4$. Chlorination of the *trans* diols **113** was carried out using the triphenylphosphine dichloride as a chlorinating agent and finally, the elimination of chlorides was conducted in alkaline media (KOH in THF) at 40^{o}C to obtain the diene **115**.

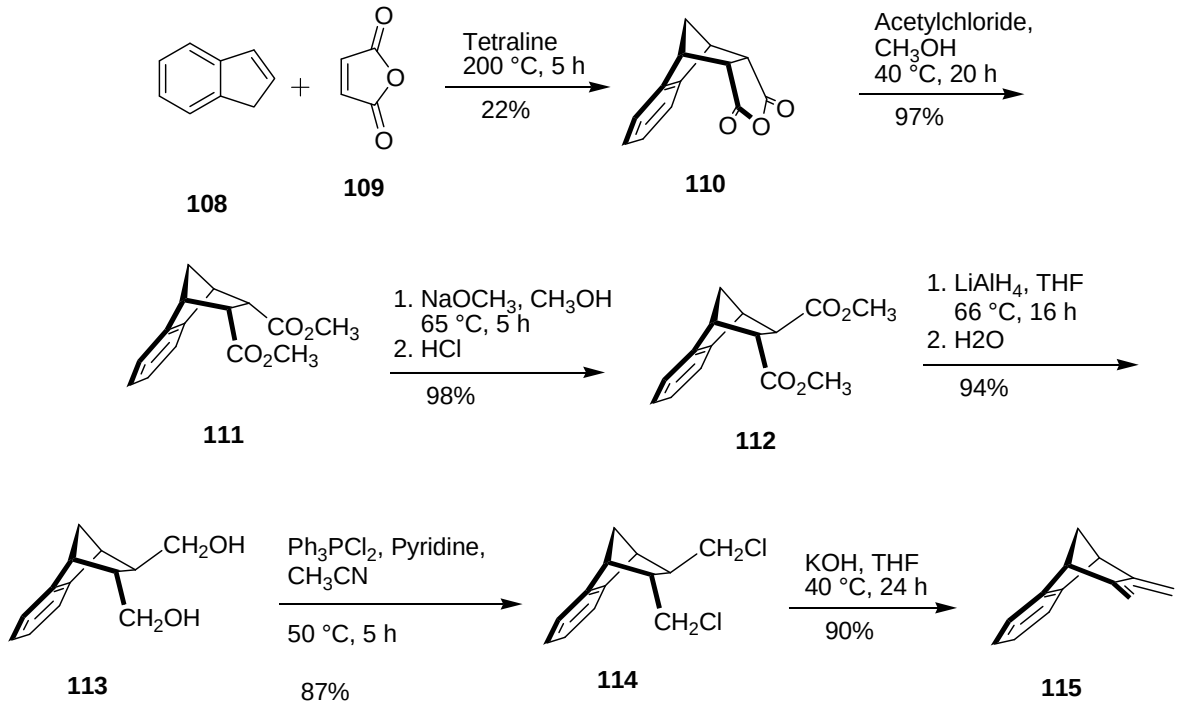

Scheme 3.2 Synthesis of the diene **115** (side wall).

The most critical reaction in the synthesis of the tweezers is the coupling reaction of the diene **115** and the bisdienophile **107** (Scheme 3.3). One molecule of the bisdienophile and two molecules of the diene were coupled by [4+2] cycloaddition. This reaction required high pressure and temperature and therefore was performed in the sealed ampoules at 170 ^{o}C under inert atmosphere for four days. The resulting adduct **118** was then oxidized into the corresponding diacetoxy tweezer **119** using DDQ as oxidizing agent in the refluxing toluene. The dihydroxy tweezer **121** was obtained by the reduction of acetoxy groups of the tweezer **119** using $LiAlH_4$, whereas the monohydroxy acetoxy tweezer **120** was synthesized by selective removal of one acetyl group of **119** in alkaline NaOH.

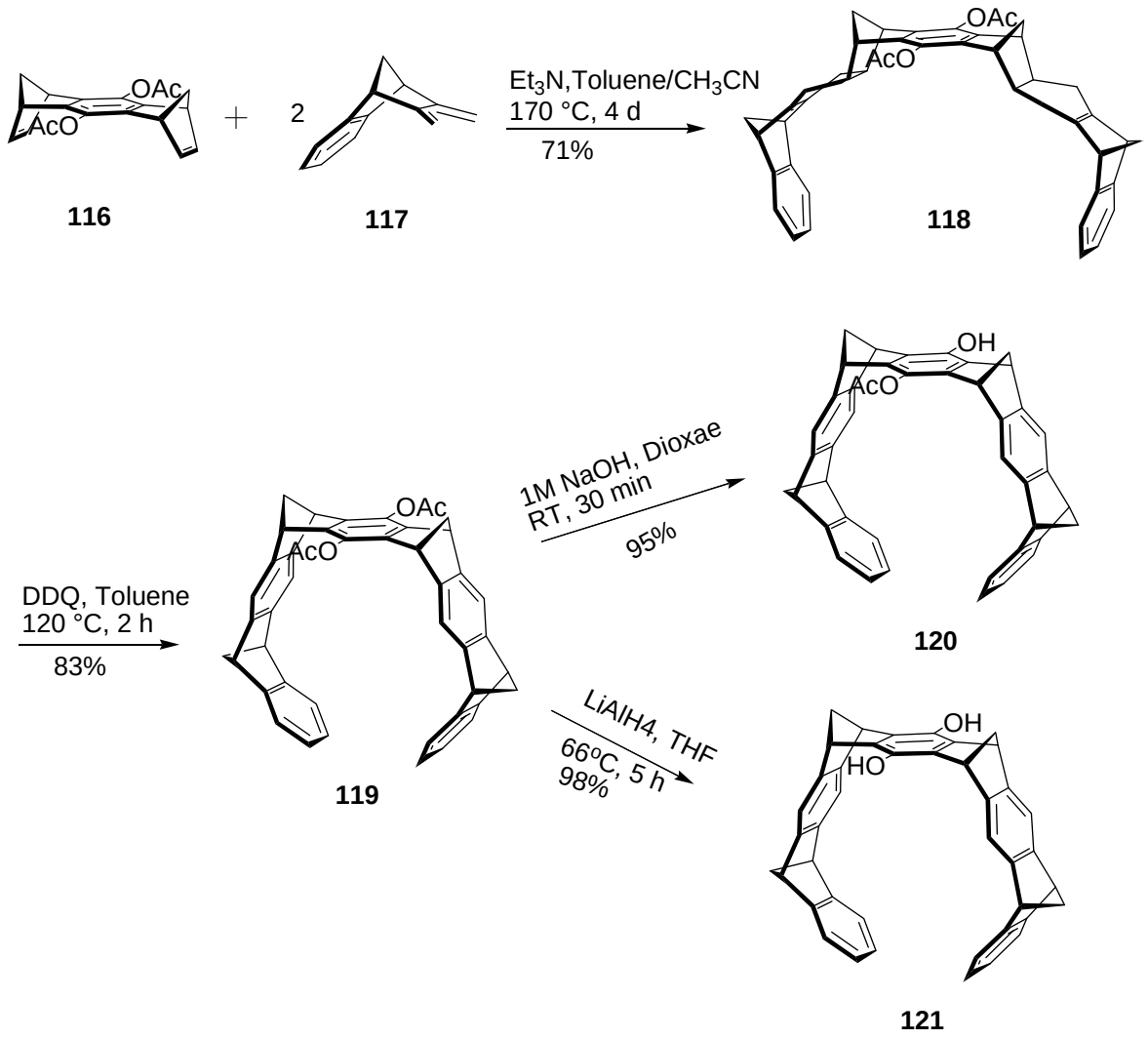

Scheme 3.3 Synthesis of the dihydroxy tweezer **121** and the monohydroxy-acetoxy tweezer **120**

3.1.2 Synthesis of the phosphate tweezer 133

The phosphate tweezer **133**, was synthesized for the first time by Bastkowski[89] in the Klärner group (Scheme 3.4). The phosphate tweezer **133** was synthesized on a large scale to conduct more new experiments and to perform biological studies in several collaborations worldwide. Several projects were undertaken in collaboration on the tweezer **133**, in particular with Prof. Bitan at UCLA. Prof. Bitan is responsible for biophysical and biological studies of the tweezers. The phosphate tweezer **133** was synthesized by the phosphorylation of the dihydroxy tweezer **121** with phosphoroxy chloride. The intermediate tetrachloride **122** was washed several times with diluted aqueous HCl followed by hydrolysis in THF/H_2O. The resulting crude product **123** was washed several times with aqueous HCl solution. Neutralization of the tweezer **123** was

performed with aqueous NaOH in methanol to produce sodium salt of the phosphate tweezer **133**. After washing the solid crude with minimum amount of dichloromethane or acetonitrile pure phosphate tweezer **133** was obtained.

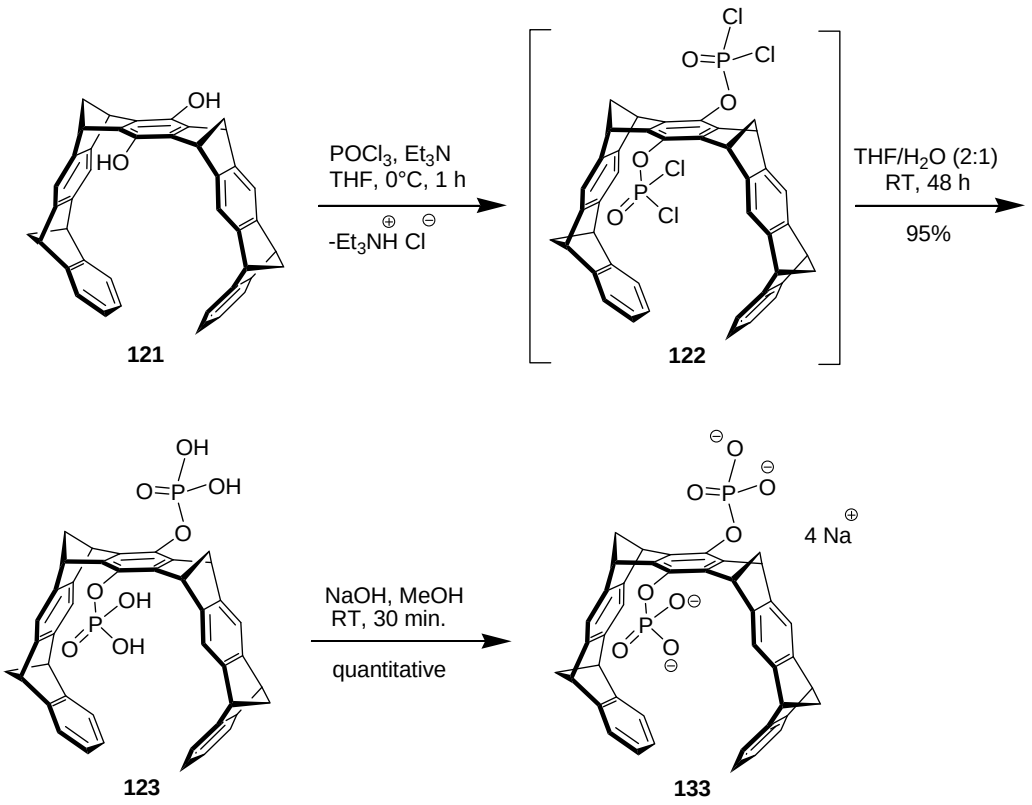

Scheme 3.4 Synthesis of the phosphate tweezer **133**.

3.1.3 Synthesis of the sulfate tweezer 161

The sulfate tweezer **161** was synthesized as shown in Scheme 3.5 using the optimized protocol by Cartagena.[101] To incorporate the sulfate groups into the tweezer, the dihydroxy tweezer **121** was treated with sulfur trioxide pyridinium complex in refluxing anhydrous pyridine. Initially, 4 eq. of SO_3·Py complex were added and after 24 hour 3 eq. of the complex were additionally added to the reaction mixture. Basic work up by $NaHCO_3$ furnished the sodium salt of sulfate tweezer **161**. The final product was then purified by redissolving the crude in ethanol and subsequent filtration.

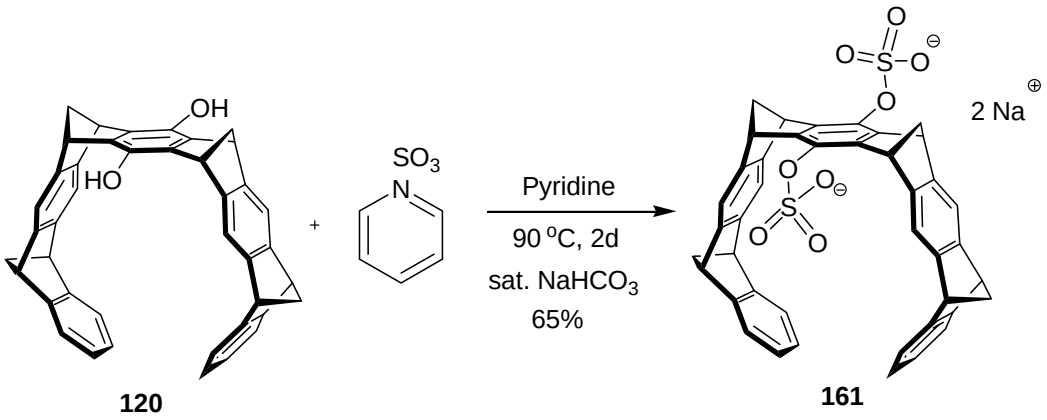

Scheme 3.5 Synthesis of the sulfate tweezer **161**.

3.1.4 Synthesis of 1st generation unsymmetrical linker tweezers

Possible pathways

In the past years, our group has been interested in designing and modifying the symmetrical tweezers to the unsymmetrical tweezers to make them more selective and specific. Usually, in the unsymmetrical tweezers one phosphate group is replaced by some other auxiliaries or recognition units. The recognition units are required to read a protein sequence or make additional interactions with a target protein. The other phosphate group on the tweezer is required for the tweezer's water solubility and ion pair interactions with the cationic ammonium or guanidinium groups of a guest.

There can be several pathways to make unsymmetrical tweezers. Three possible paths are shown in the schemes below. In the path 1 (Scheme 3.6), starting material is the dihydroxy tweezer 121. The first step of the path 1 can either be a nucleophilic substitution reaction of tweezer's phenoxide with acyl or alkyl halides in the presence of an alkali base such as K_2CO_3 or a coupling reaction with a carboxylic group using PyBOP and N-Methylmorpholine. The latter conditions have been employed by Talbiersky.[90] The first step of path 1 is uncontrolled with respect to the reaction of two hydroxyl groups of the tweezer 121 and therefore, the disubstituted tweezer 136 is also formed along with the required mono substituted tweezer 135. In the second step, phosphorylation of the second hydroxy group of the tweezer 135 was achieved using phosphoroxy chloride but the yield of the product in the first step is less than 50 % which makes this approach less suitable.

Path 1

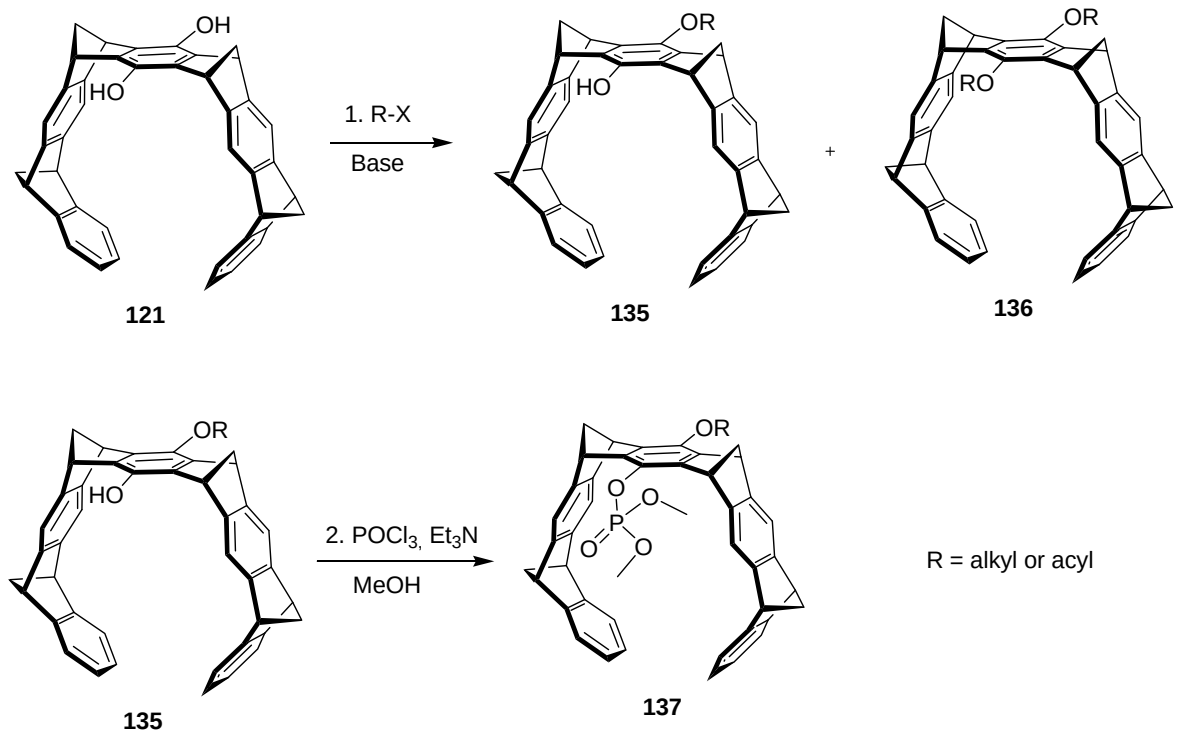

Scheme 3.6 Synthetic scheme for the preparation of unsymmetrical phosphate tweezers starting from the dihydroxy tweezer **121** through path 1.

The phosphodichloride intermediate can be directly hydrolyzed by water to produce the required phosphate tweezer. However, when the phosphorylation did not work completely, the separation of unreacted starting material and product was very difficult due to the highly polar free phosphate group on the tweezer. Even more, the phosphate group was cleaved during the normal silica gel column chromatography. Therefore, instead of direct hydrolysis, the phosphodichloride intermediate was reacted with methanol to get dimethylphosphate precursor **137**. After the column chromatography purification and removal of the protecting methyl groups by trimethylsilyl bromide pure product was obtained in good yield.

The monohydroxy acetoxy tweezer **120** was synthesized to minimize the loss of the starting material by the formation of the disubstituted acyl or alkyl precursors.[103] However, excess of NaOH used in his protocol produced mixture of the monoacetoxy tweezer, the dihydroxy tweezer and the starting diacetoxy tweezer. Further, the product formation could not be monitored by TLC because all these tweezers were having same R_f value. Therefore, only one acetyl group was hydrolyzed by using 1.1 eq. NaOH, but allowing the reaction for longer time (20 hours). Though,

compared to path 1 there is one extra step in path 2 but good yield obtained by path 2 make it more suitable over path 1.

Path 2 and 3

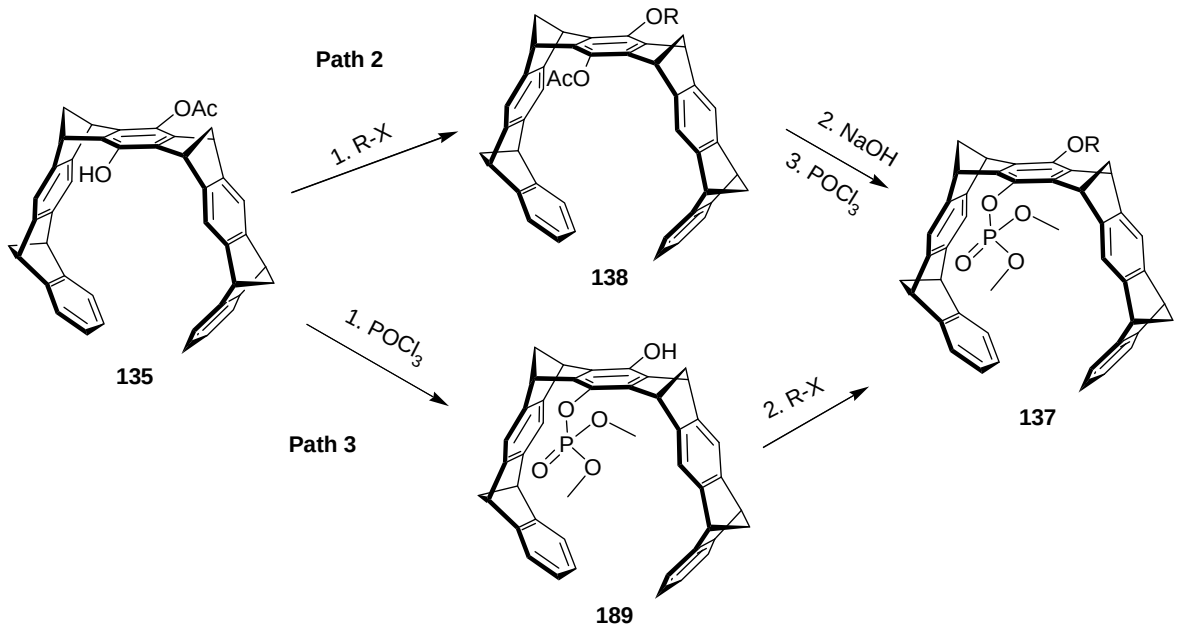

Scheme 3.7 Synthetic scheme for the preparation of unsymmetrical phosphate tweezer by path 2 and path 3.

Path 3 was recognized during the synthesis of the acetoxy phosphate tweezer **193.** As a convenience, esterification of the intermediate phosphoryl chloride with excess methanol also cleaved the acetyl group and directly furnished the tweezer **189**. After column purification, the tweezer **189** was obtained in 65% overall yield. Product can also be purified by crystallization in methanol. Initial attempts to alkylate or acylate the tweezer **189** were successful and the protected phosphate group appeared stable under the basic conditions. Following the path 3, there are two advantages: 1) phosphorylation of each new tweezer will not be required as in other two paths; 2) in the same pot acetyl group can be cleaved to furnish the required monohydroxy dimethylphosphate tweezer **189**. Therefore, path 3 proved to be the convenient path, and majority of the new unsymmetrical tweezers were prepared following the path 3.

3.1.4.1 Synthesis of the acetoxy phosphate tweezer 193

To understand the effects of ester junction, we synthesized the acetoxy phosphate tweezer **193**. Acetoxy group was attached to the hydroxyl group in the tweezer **189** using acetyl chloride and triethylamine (Scheme 3.8). In the next step, complete dealkylation on phosphorus using

trimethylsilylbromide TMSBr in CH_2Cl_2 leads to the acetoxy phosphate tweezer **193**. For complete removal of both methyl esters on phosphorus, TMSBr qualified as a powerful reagent, which acts under mild conditions and leaves ester as well as ether links untouched. Due to acetyl group sensitivity towards sodium hydroxide, we used the acetoxy tweezer **193** without neutralization of its phosphate group by NaOH.

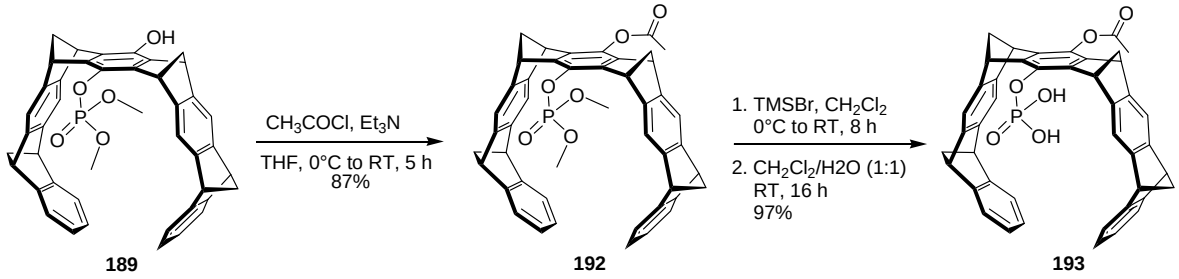

Scheme 3.8 Synthesis of the acetoxy phosphate tweezer **193**

3.1.4.2 Synthesis of the octyl phosphate tweezer 195

To investigate the hydrophobic interactions in the unpolar region of Aβ, we synthesized the tweezer **195** substituted with a long octyl chain. The monohydroxy dimethylphosphate tweezer **189** was deprotonated to generate the nucleophilic phenoxide anion, which reacted with 1-bromooctane and produced the tweezer **182**. Both the methyl esters on phosphorous were removed by TMSBr in the same way as for the tweezer **193**. Treating the resulting free phosphate tweezer with 2 eq. of aqueous NaOH in methanol furnished the sodium phosphate salt of the octyl tweezer **195**. Previously, initial attempts were made to prepare **195** according to path 2 but the phosphorylation followed by hydrolysis to generate directly free phosphate tweezer did not furnish pure product. Further, purification of the resulted crude was difficult as the free phosphate group ($-OPO_3H_2$) was cleaved during the silica gel column chromatography.

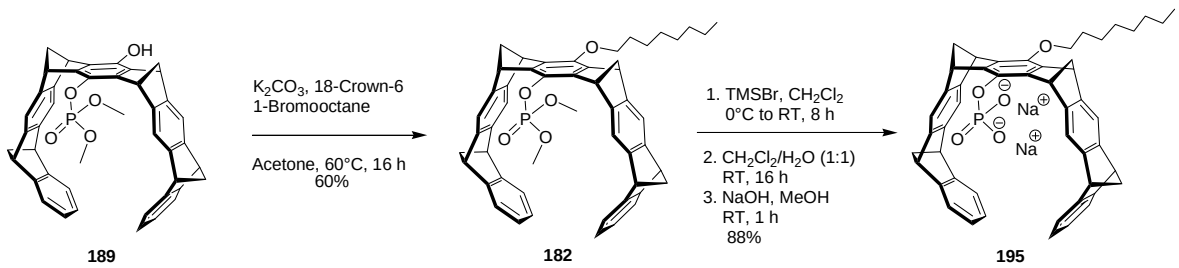

Scheme 3.9 Synthesis of the octyl phosphate tweezer **195**.

3.1.4.3 Synthesis of the ethoxycarboxymethyl phosphate tweezer 196

We designed the tweezer **196** to keep the ester group in the linker, but to avoid the more susceptible phenolic ester group we shifted the ester group one carbon farther and converted the phenolic ester into an alkyl ester. With this molecule, we expect that due to the carboxylic ester group, the linker will avoid to interact with the cavity. Further, the ester group will make the linker soluble in the aqueous solution. Also, a recognition site can be easily coupled with the carboxylic group. The tweezer **196** was prepared in the similar way as the tweezer **195**. Here, Finkelstein conditions were established by addition of KI in acetone, so that bromide was smoothly displaced from ethyl bromoacetate by the tweezer's phenoxide. The reaction completed in 16 hour in refluxing acetone while at room temperature 4 days were required. After column chromatography purification the tweezer **191** was obtained in 73% yield.

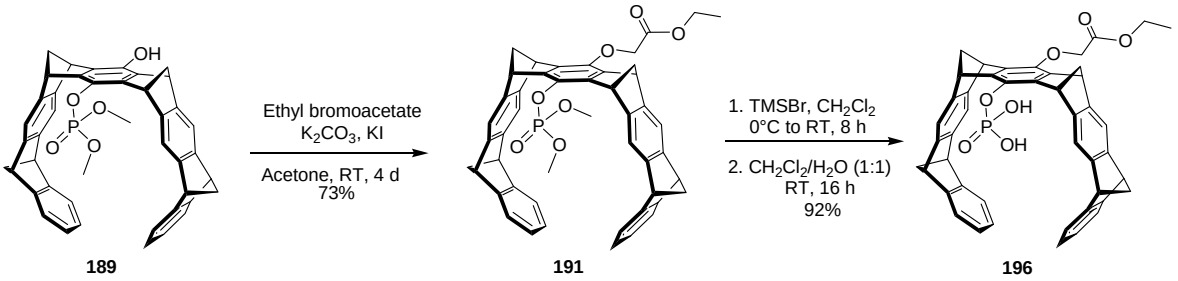

Scheme 3.10 Synthesis of the ethoxycarboxymethyl phosphate tweezer **196**.

In the Next step, methyl groups on phosphorous were cleaved selectively using TMSBr and without affecting other functionality like the ethyl ester. Neutralization of the phosphate group with NaOH also partially hydrolyzed the ethyl ester group. Therefore, the tweezer **196** was used as such without the neutralization of its phosphate group by NaOH.

3.1.4.4 Synthesis of the glycerol phosphate tweezer 198

Epoxides are reactive towards a large number of nucleophiles (O, N, C and S).[104,105,106,107] To explore different type of linkers at the tweezer we chose to utilize epoxide chemistry. Herein, we designed an epoxide containing tweezer **164.** Such epoxides can provide several advantages in the tweezer synthesis, such as: 1) epoxide group can be opened with a variety of nucleophiles; 2) depending on the acidic or basic conditions, epoxides can be opened to generate primary or secondary hydroxy group; 3) new hydroxy group generated will add to the tweezer's solubility in

water; 4) hydroxy group can also participate in guest interactions and; 5) hydroxy group provides anchor point for further functionalization of the tweezer.

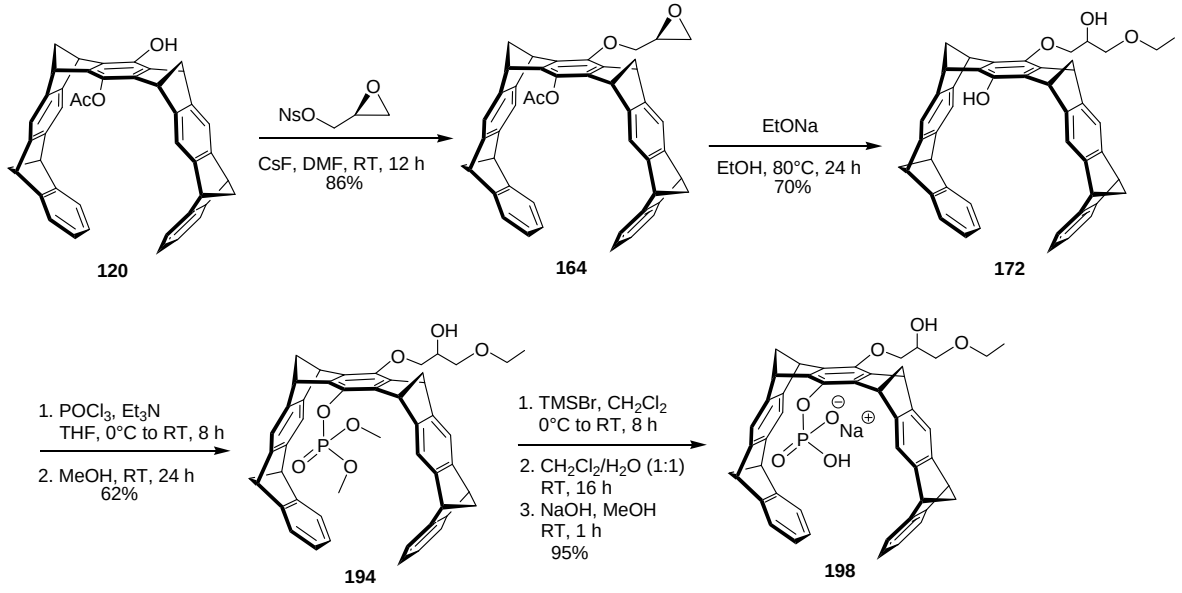

Scheme 3.11 Synthesis of the glycerol phosphate tweezer **198**.

Using this approach, the glycerol phosphate tweezer **198** was synthesized in which the linker is consists of a glycerol backbone (Scheme 3.11). Treatment of the monohydroxy precursor **120** with glycidyl nosylate in the presence of caesium floride furnished the respective epoxide ether **164**. Following a protocol from Furukawa and Otera[108], a 6-fold excess of CsF was employed which serves a dual purpose: one equivalent deprotonates the phenol as a non-nucleophilic base and generates the highly nucleophilic caesium phenoxide, another equivalent binds the resulting sulfonic acid. The nitrobenzenesulfonate (Ns) derivative directs the nucleophilic attack exclusively to the C-1 position, so that no racemization occurs at C-3. During subsequent ring opening with excess sodium ethoxide, the acetoxy group was once more simultaneously cleaved, leading to the intermediate **172** with a phenolic and a secondary aliphatic hydroxy moiety. This reaction can later be used to introduce the second binding site from alcohols or amines. Phosphorylation with $POCl_3/Et_3N$ takes place exclusively on the phenolic group of the tweezer **172**, and generates, after hydrolysis and neutralization, the mono sodium salt of the glycerol phosphate tweezer **198**.

All the new 1st generation linker tweezers as well as their intermediates have been fully characterized by spectroscopic methods. The existence of the phosphate moiety has been

unequivocally established by HRMS and ^{31}P NMR spectroscopy. The unsymmetrical tweezers are all soluble in water (1-50 μM). However, for NMR measurements at millimolar concentrations, methanol was added to the aqueous buffer (CD_3OD/D_2O phosphate buffer).

3.1.5 Synthesis of the 2nd generation unsymmetrical tweezers

Recently, we designed a new approach to make unsymmetrical tweezers that can overcome the problems such as poor water solubility, low affinity and self inclusion of linker. We adopted synthetic route similar to DNA synthesis.[109,110] Installing one phosphate in its protected form on one side of the central benzene ring (**189**), a trivalent phosphorous was attached on the other side in order to obtain phosphoramide intermediate **246**. This was achieved in 90% yield by reacting phenolic -OH group of the tweezer **189** with phosphorylating reagent, *N,N*-Diisopropylmethylphosphonamidic chloride in presence of DIPEA. To the intermediate **246**, two different linkers were attached that can later be coupled with a recognition unit.

2nd generation linker 1: the tweezer **247** was synthesized with a linker unit that has a terminal carboxylic ester group. Such an ester group can be selectively hydrolyzed and coupled with alcohol- or amine-containing recognition units. In the last step, the protecting groups can be cleaved to furnish the desired unsymmetrical tweezer molecule. The reaction of phosphoramide tweezer **246** with alcoholic linker methyl glycolate and subsequent oxidation of trivalent phosphorous to pentavalent phosphorous by t-butyl hydroperoxide produced the fully protected product **247** in 50% yields (Scheme 3.12). For the lower yield of **247**, it can be suspected that excess of alcoholic linker replaced with the tweezer on the trivalent phosphorous in **246**. To examine the effect of oxidizing reagent, iodine can be used for the oxidation of the trivalent phosphorous. Initial attempts to deprotect the methyl ester of phosphate were made using LiBr and TMSBr. LiBr is a mild method for the cleavage of methyl group on phosphorous, but even 30 eq. of LiBr partially cleaved the methyl ester groups and did not produced the final product **252**. TMSBr, though, cleaved all the methyl groups, but the final product **251** was not obtained pure. In future, more elaboration of the deprotection step will be required to obtain the clean product.

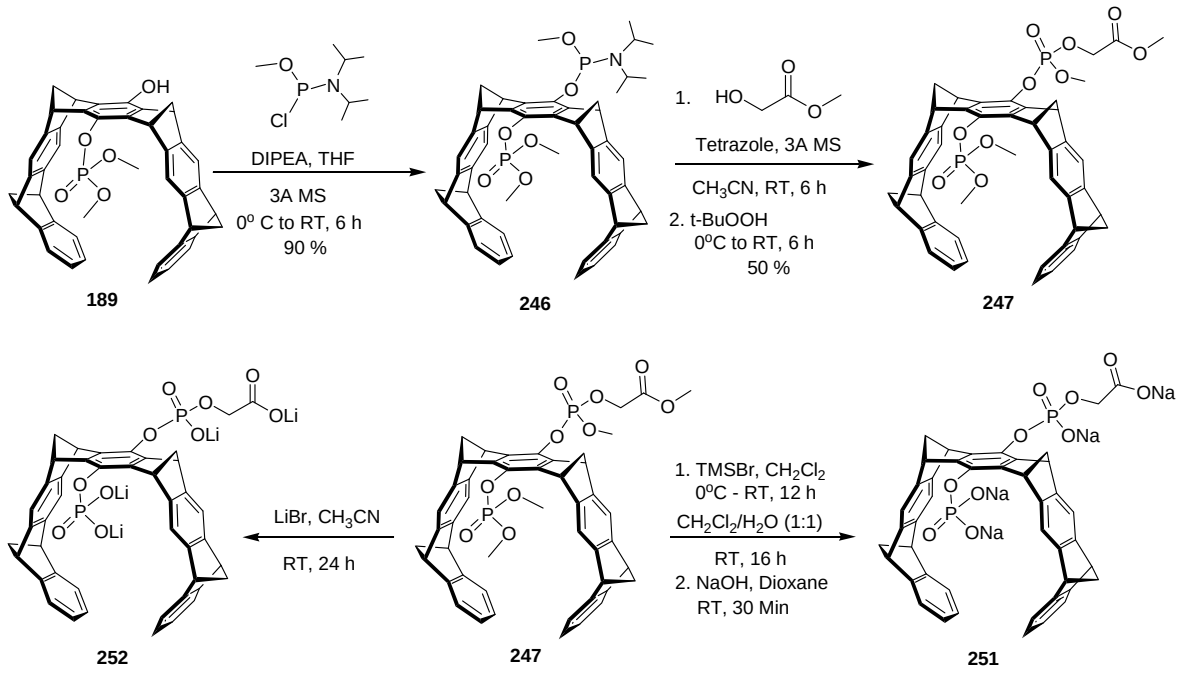

Scheme 3.12 Synthesis of the carboxylic ester linker tweezer **251**/**252**.

Hydrolysis of phosphate diesters by suitably placed nucleophile has been reported.[111] Further, the hydrolysis rate could be enhanced by divalent metal ions such as Mg^{2+} and Zn^{2+}. In the below depicted example, an intramolecular cyclic phosphate ester was formed by the exocyclic attack of a carboxylic oxygen on the phosphorous, liberating the phenoxide as a leaving group in a reversible manner. The similar hydrolysis mechanism can be expected in our case when we neutralized the deprotected tweezer with NaOH to obtain the tweezer **251**. Therefore, to avoid such a highly favorable five or six membered ring formation, one could use a longer linker separating the ester and hydroxyl groups by three or more atoms. Another possibility could be that a recognition unit should be synthesized with a hydroxyl group that can react with phosphoramide **246**.

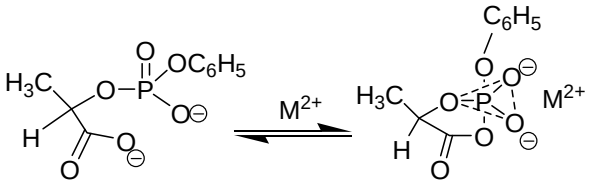

2nd generation linker 2: a linker that has a terminal alkyne group can be more potent. A terminal alkyne provides the great advantage that a tweezer and a recognition unit can be coupled in water. A molecular tweezer such as **257** and a recognition unit with azide functionality can easily be prepared and then could be coupled by the famous cupper catalyzed click reaction. To explore further the synthetic utility of the trivalent phosphorous, the tweezer **248** was prepared in 50 % yield by the reaction of **246** and 3-butyn-1-ol (Scheme 3.13). Here, the deprotection of the methyl groups shall be carried out, for which TMSBr can be used as a potential reagent.

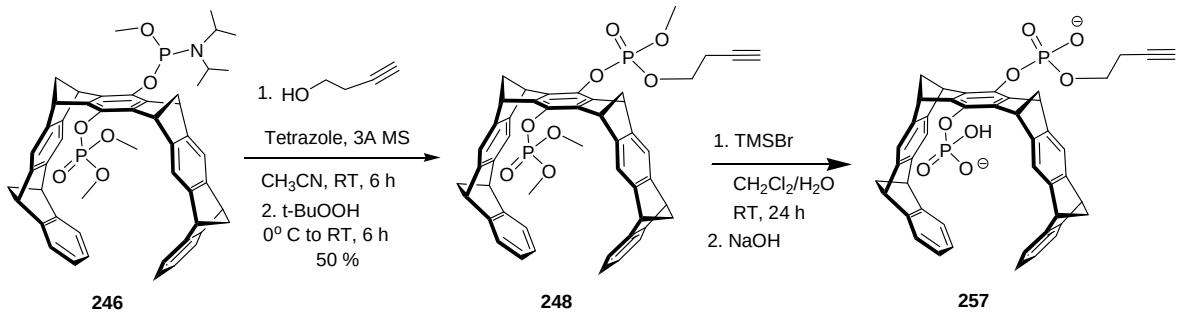

Scheme 3.13 Synthesis of the alkyne linker tweezer **248**/**257**.

3.2 Binding Studies

3.2.1 Binding studies of the anionic tweezers

Rational design of the artificial receptor molecules for a given target lies in the heart of non-covalent interactions between the two species. Therefore, in the proper designing of receptor molecules, it is essential to understand several aspects of the molecular interactions through the different techniques. In this chapter we investigated the self associations and the guest binding of the different anionic tweezers shown in Figure 3.1.

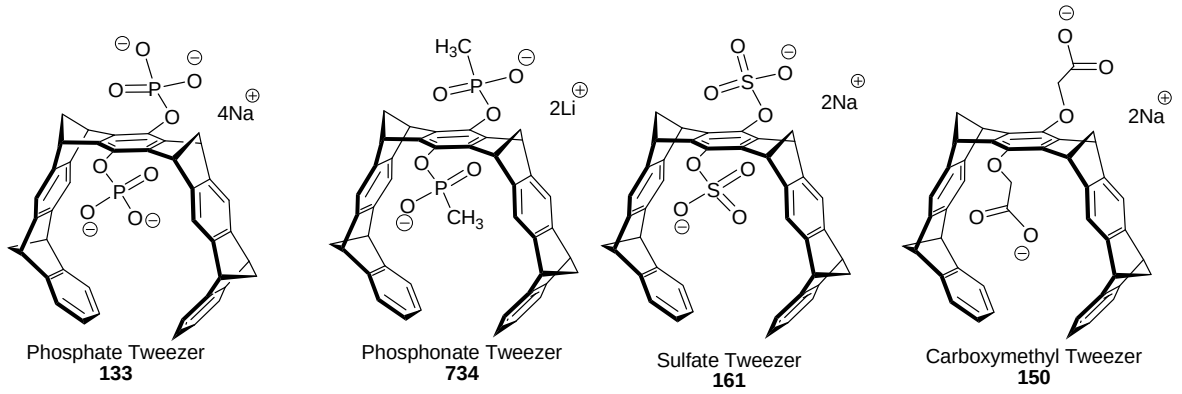

Figure 3.1 Structures of the four symmetrical anionic tweezers synthesized to date.

The work discussed in this section was performed by several colleagues of our group and Klärner group and, I am very much thankful to them. Synthesis and studies of the tweezer **133** were performed by Frank Bastkowski[89], Peter Talbiersky[90] and me. The tweezers **161**, **734** and **150** were synthesized and studied by me, Michael Fokkens[112] and Constanze Wilch[113] respectively.

3.2.1.1 Self association properties of the sulfate tweezer 161 - comparison with other anionic tweezers

The tendency of an artificial receptor molecule to self-assemble can lower the receptor's ability to complex a guest molecule. Therefore, a potential receptor should have low affinity to self-assemble for optimum function under the desired conditions. It is known that the phosphate tweezer **133** weakly self assemble into the dimer (K_{dm} = 60 μM) in aqueous solution. Expectedly, the tweezer **161** also shows the different chemical shift patterns of aromatic protons in D_2O and methanol-d_4. The aromatic signals in methanol are sharp and split while the signals in D_2O are broad and shifted. These changes indicate that distinct supramolecular assemblies are formed in

the two solvents. Concentration dependent ^{1}H-NMR dilution titration of the tweezer **161** in aqueous phosphate buffer produces the dimerisation constant K_{dm} = 370 M^{-1} (Table 3.1).

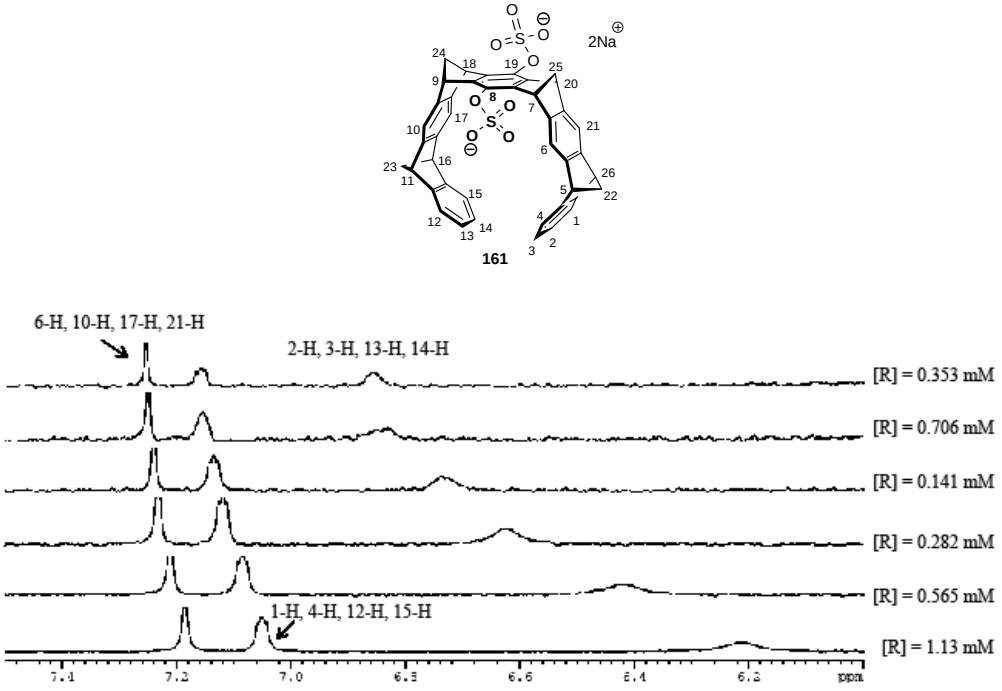

Figure 3.2 Concentration dependent ^{1}H-NMR signals of the sulfate tweezer **161** in phosphate buffer (10 mM, pH 7.2) at 25°C.

From the NMR titration it is obtained that the protons 2-H, 3-H, 13-H and 14-H are highly dependent on the tweezer concentration and influence most ($\Delta\delta_{max}$ ~ 2.0 ppm) due to the magnetic anisotropy from the aromatic rings of the second tweezer molecule (Figure 3.2). Other aromatic protons are only weakly shifted ($\Delta\delta_{max}$ ~ 0.3 ppm) and the chemical shifts of the non-aromatic protons of **161** are independent of the tweezer concentration.

Molecular modeling calculations were performed for the monomeric **161** and the dimeric $\mathbf{161}_2$ tweezers. The resulted minimum energy structures are listed in Figure 3.3. In the monomeric structure of the tweezer **161**, both the anionic sulfate groups are pointed upward away from the electron rich cavity. The calculated structures of the dimer $\mathbf{161}_2$ supports the chemical shift pattern observed by the ^{1}H-NMR titration. The calculated entangled dimer $\mathbf{161}_2$ is also quite similar to the calculated phosphate tweezer dimer $\mathbf{133}_2$.

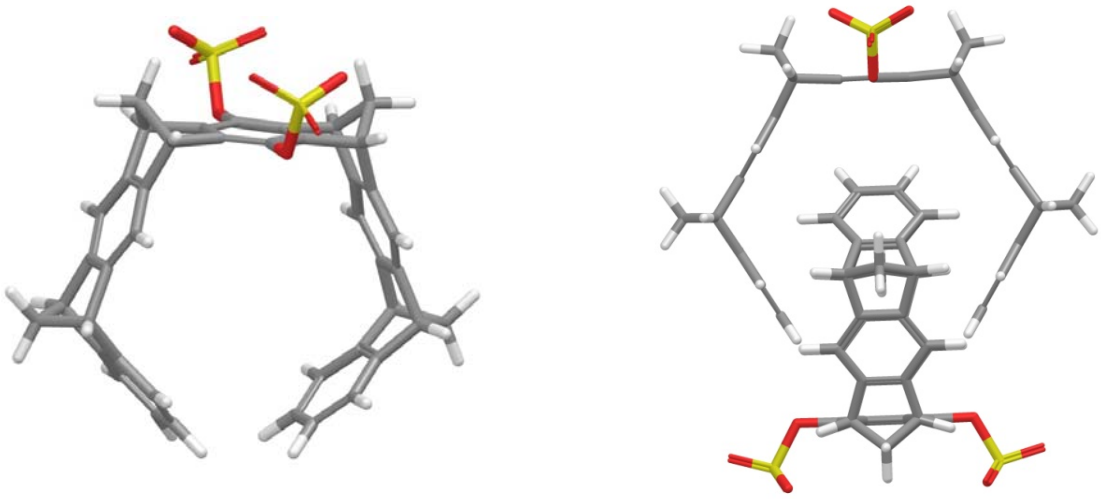

Figure 3.3 Molecular modeling structures of the sulfate tweezer **161** (left) and its dimer $\mathbf{161}_2$ (right) obtained by the Monte-Carlo Simulation (Maestro 9.2, OPLS_2005, water, 5000 steps).

Self association properties of the four anionic tweezers were compared to understand the effects of the different anions. Experimental data on the measured dimerisation constants (K_{dm}) and maximum chemical shift difference ($\Delta\delta_{max}$) are listed in the Table 3.1. Unexpectedly, dimerisation of the sulfate tweezer **161** is stronger than the dimerisation of the phosphate tweezer **133.** On the other hand, the phosphonate tweezer **734** and the carboxymethyl tweezer **150** do not self-assemble. Since the hydrophobic skeleton is common in all the tweezers, the difference in their dimerisation must arise due to the different anionic groups.

The calculated structure of the tweezer **161** (Figure 3.4) shows that negatively charged sulfate groups pointed are upward away from the electron rich tweezer's cavity, resulting into the completely opened cavity. On the other hand, the phosphate groups in the tweezer **133** can be expected partially protonated that can exist in $-PO_3^{2-}$ and $-OPO_3H^-$ forms at the neutral pH. In addition, the phosphate groups can move freely up and down with a small difference in their conformational energy. The calculated minimum energy structure of the monoprotonated phosphate tweezer shows that the phosphate groups are pointed down and insert the hydrogen atoms of the phosphate groups into the tweezer's cavity. This creates the partial steric hindrance at the cavity of the tweezers. Furthermore, the phosphate groups are strongly solvated compared to the sulfate groups due to the more negative charge on the phosphate groups. Therefore the bigger size of the solvation shells of the phosphate groups can again create the steric hindrance at the cavity of the tweezers. All these observations suggest that the sulfate tweezer **161** has more opened cavity compared to the phosphate tweezer **133** that allow the former to self-assemble strongly compared to the later. Moreover, it is found that the sulfate tweezer **161** is slightly less

soluble in compared to the tweezer **133** in aqueous solutions because the tweezer **161** has higher aggregation tendency.

Table 3.1 Self association constants K_{dm} [M^{-1}] and association induced maximum chemical shifts $\Delta\delta_{max}$ [ppm] of aromatic protons of the phosphate tweezer **133** and the sulfate tweezer **161** in phosphate buffer (10 mM, pH 7.2). Phosphonate and carboxymethyl tweezers do not show self association and therefore not listed here.

Receptor	K_{dm} [M^{-1}]	$\Delta\delta_{max}$ [ppm]
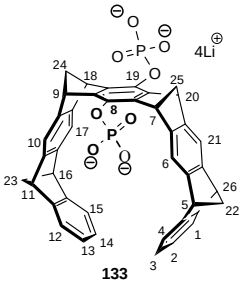 **133**	60 ± 17 % [89]	2.23 (2-H, 3-H, 13-H,14-H), 0.37 (1-H, 4-H, 12-H, 15-H), - 0.28 (6-H, 10-H, 17-H, 21-H),
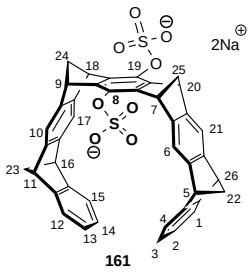 **161**	370 ± 21 %	2.02 (2-H, 3-H, 13-H,14-H), 0.31 (1-H, 4-H, 12-H, 15-H), 0.26 (6-H, 10-H, 17-H, 21-H),

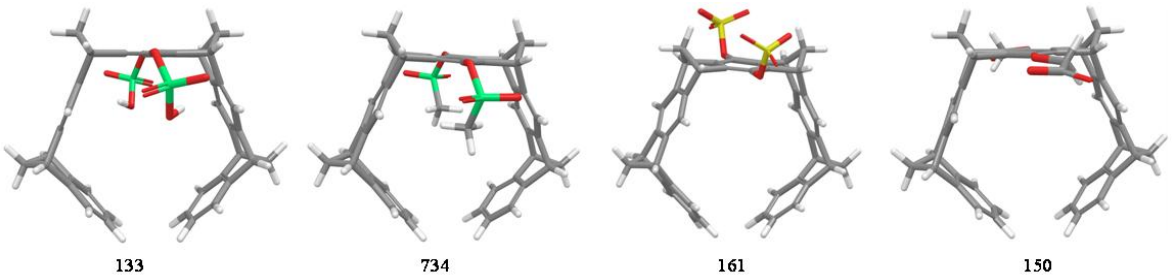

Figure 3.1 Molecular modeling structures of the four anionic tweezers obtained by conformational search (Maestro, OPLS_2005, water, 5000 steps). The structures of the tweezers **133**, **734** and **150** were re-produced again.

The molecular modeling structure of the phosphonate tweezer **734**[112], shows that the methyl groups on phosphorous are pointed down into the tweezer's cavity that can prevent the dimer formation by providing steric hindrance for the other molecule of the tweezer. Carboxymethyl tweezer **150** does not provide any significant concentration dependent chemical shift, and therefore, no dimerisation is expected for this tweezer. However, molecular modeling structures

do not show completely upward or downward orientation of carboxymethyl groups. But one thing might be expected that longer length and more flexibility of carboxymethyl groups create the steric impact at the cavity and on the dimmer formation of this tweezer.

Overall, we have shown the effects of different anionic groups on the self association behavior of the tweezers. The sulfate tweezer ($-OSO_3^-$, **161**) being the least bulky tends to aggregate strongly compared to the other tweezers. The dimerisation of the tweezers are substitution dependent (size of the anion) in the order; $-SO_3$ (**161**) > $-OPO_3H^-$(**133**) > $-OCH_2CO_2^-$(**150**) ≈ OPO_2CH_3 (**734**). It is important to note that the above mentioned factors about the different anionic tweezers can also affect their binding with the guests. Further, the dimerisation constants of all the tweezers are small and can be ruled out when strong complex can be formed with a guest molecule.

3.2.1.2 Studies of the sulfate tweezer 161 complexes

The most important parameter in the association of the two or more different molecular species is the association constant (K_a) or the dissociation constant (K_d). The dissociation constant is a measure of the binding affinity between a host and a guest that is influenced by the non-covalent intermolecular interactions. For all the guests, dissociation constants were obtained using fluorescence titration experiments. NMR titration and isothermal calorimetric titration experiments were performed for the selected guest molecules. Molecular modeling was performed to gain more structural insight into host-guest complexes. Since, until now no crystal structure of a tweezer and an amino acid or protein guest has been generated, all the above mentioned methodologies were performed to understand several chemical and structural aspects of the complexes formed by the tweezers. Although, the NMR titrations alone provides substantial structural information through chemical shift differences of host and guest protons, but the fluorescence spectrometry was used more routinely. Further, ITC measurements were performed to obtain thermodynamic data such as; enthalpy and entropy of a complex.

3.2.1.2.1 Studies of the sulfate tweezer 161 complexes by ^{1}H-NMR titration spectrometry

The complex formation between a receptor molecule and a guest molecule can be easily detected by the ^{1}H-NMR spectrum of the receptor-guest mixture. In a standard ^{1}H-NMR titration experiment, complexation-induced chemical shifts ($\Delta\delta_{obs}$) of the guest protons are measured with varied receptor concentrations and constant guest concentration. In an alternative method, called

the dilution titration method, complexation-induced chemical shifts ($\Delta\delta_{obs}$) of the guest protons are measured in a 1:1 mixture of the receptor/guest at overall different concentrations. Using both the methods, complexation-induced maximum chemical shifts ($\Delta\delta_{max}$) of guest protons and association constant K_a can be calculated by the use of equation 3.1 and performing the program TableCurve.[114,115,116,117,118]

$$\Delta\delta = \frac{\Delta\delta_{max}}{[G]_t} \cdot \left(\frac{1}{2}\left([H]_t + [G]_t + \frac{1}{K} \right) - \sqrt{\frac{1}{4} \cdot \left([H]_t + [G]_t + \frac{1}{K} \right)^2 - [H]_t \cdot [G]_t} \right) \qquad \text{Equation 3.1}$$

$\Delta\delta_{obs}$: Observed chemical shift difference

$\Delta\delta_{max}$: Maximum complexation-induced chemical shifts of the guest protons

$[G]_t$: Total concentration of the guest

$[H]_t$: Total concentration of the host

K_a : Association constant

The NMR titration spectroscopy was used to study the host-guest complex formation for selected guests. Experimentally measured dissociation constants and complexation-induced maximum chemical shifts for the selected protons of the lysine and arginine derivatives are given in the Table 3.2.

Table 3.2 Dissociation constants K_d [µM] of the sulfate tweezer **161** with lysine and arginine derivatives and complex induced chemical shift difference $\Delta\delta_{max}$ [ppm] of guest protons in the phosphate buffer (10 mM, pH 7.2).

Guest	$\Delta\delta_{max}$ [ppm]	K_d [µM]
Ac Lys OMe	3.75 (6-H), 4.41 (5-H), 2.64 (4-H), 1.29 (3-H), 0.37 (2-H)	12 ± 11 %
Ac Arg OMe	3.86 (5-H), 2.51 (4-H), 1.32 (3-H), 0.42 (2-H)	88 ± 5 %

The dissociation constants of the tweezer **161** for protected lysine and arginine are in low µM range. The tweezer **161** shows affinity of 12 µM to **AcLysOMe** while 7 times lower affinity to AcArgOMe. The complete titration spectra for complex **161@AcLysOMe** are shown in Figure 3.5. The spectra indicate almost complete saturation of the lysine signals at 3:1 stoichiometry of host/guest in which 6-H and 5-H protons of the lysine are shifted most (~ 3.7 ppm and ~ 4.3 ppm respectively). These strong upfield shifts of the lysine side-chain provide evidence for the inclusion of the alkyl side-chain into the tweezer's cavity.

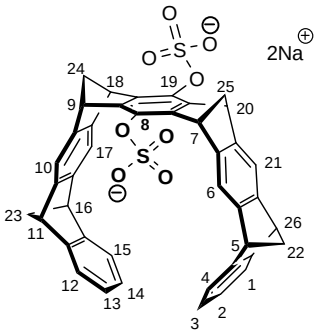

161

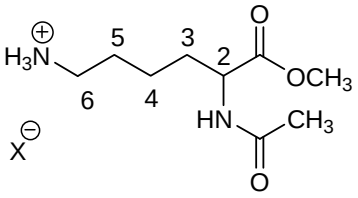

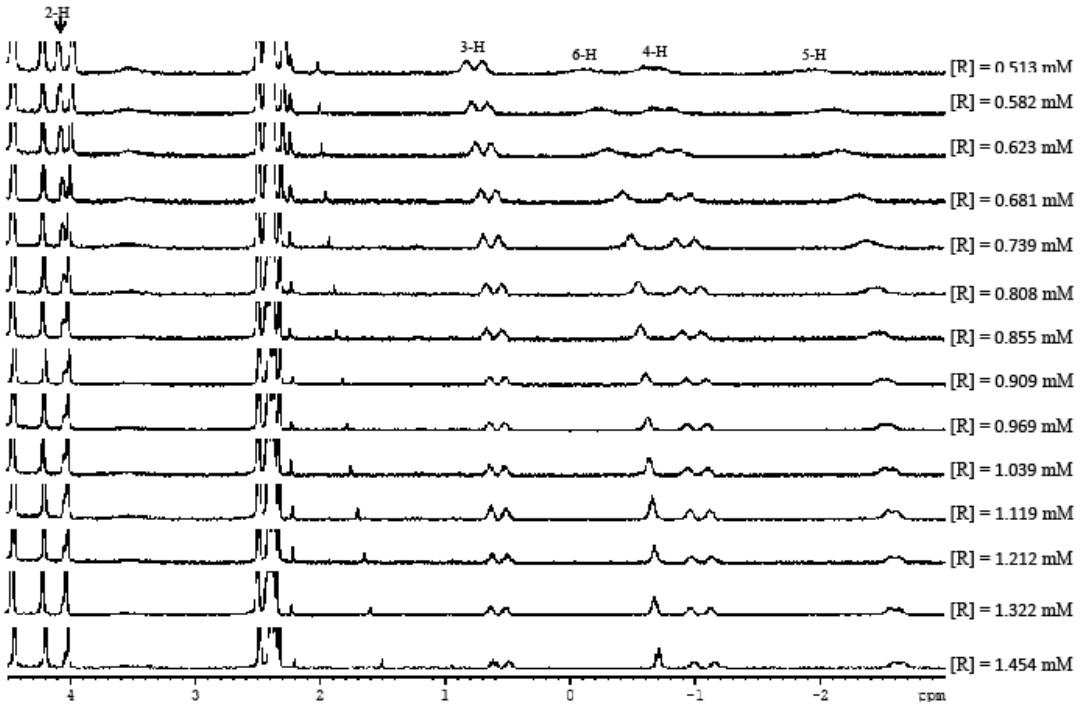

Figure 3.5 ^{1}H-NMR titration spectra of the sulfate tweezer **161** and AcLysOMe in phosphate buffer (10 mM, pH 7.2) at 25^{o}C. The concentration of AcLysOMe was kept constant at 0.572 mM. The protons of guest are mentioned on the top spectrum.

The complete titration spectra for complex **161**@AcArgMe are shown in Figure 3.6. All the guest protons were shifted upfield and among them proton 5-H and proton 4-H are the most shifted protons (3.6 ppm and 2.3 ppm respectively). These shifts indicate the complex formation by the inclusion of the guanidinium side-chain of the arginine into the tweezer's cavity. The lower affinity for arginine is attributed to the bigger size and desolvation penalty of guanidinium moiety inside the tweezer's cavity.

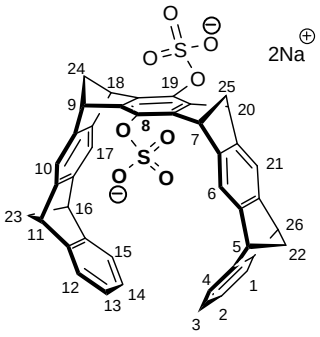

161

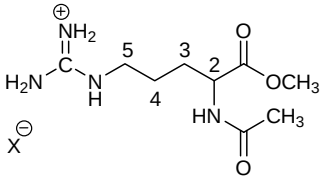

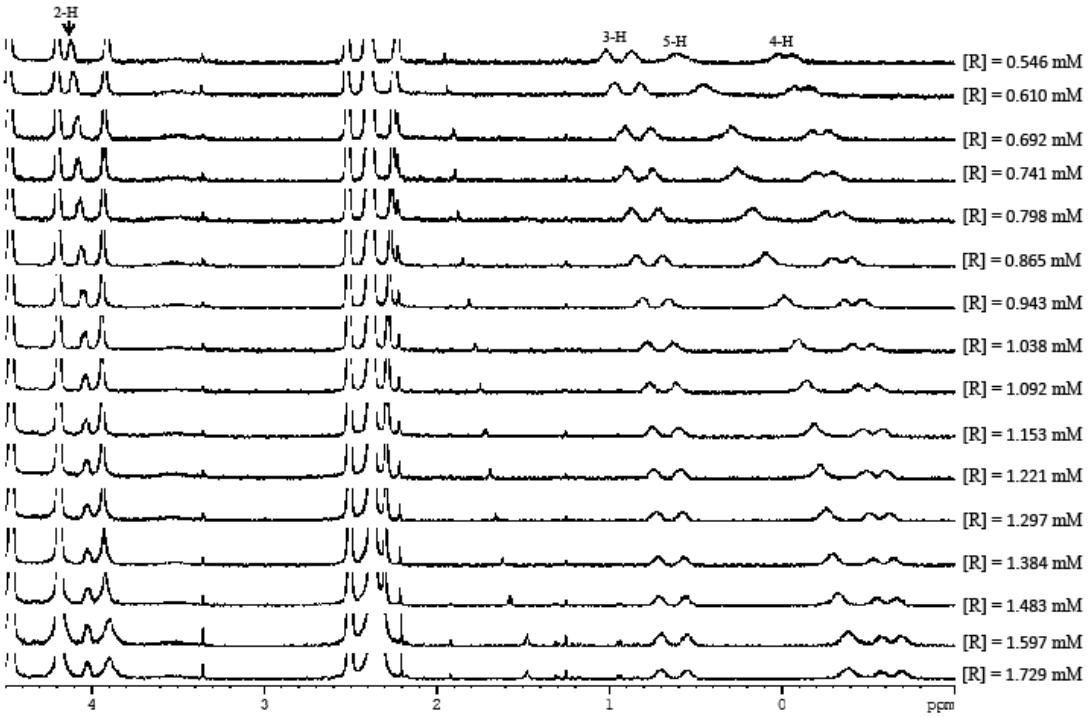

Figure 3.6 ^{1}H-NMR titration spectra of the sulfate tweezer **161** and AcArgOMe in phosphate buffer (10 mM, pH 7.2) at 25^{o}C. The concentration of AcArgOMe was kept constant at 0.560 mM. The protons of arginine are mentioned on the top spectrum.

3.2.1.2.2 Studies of the sulfate tweezer 161 complexes by fluorescence spectrometry

To measure the association/dissociation constants of a complex, fluorescence spectrometry is more efficient and convenient tool compared to ^{1}H-NMR or ITC spectrometry. Less amount (micromolar concentration) of a receptor and the least time required compared to the other methods makes this technique most suitable. Binding affinities of the sulfate tweezer **161** for a large number of amino acid derivatives and peptide guests were measured using this methodology. The obtained dissociation constants (K_d) are listed in the Table 3.3.

Table 3.3 Dissociation constants K_d [μM] of the sulfate tweezer **161** with lysine and arginine derivatives and, peptides in the phosphate buffer as measured by the fluorescence titration spectroscopy.

Guest	Solvent, pH	K_d [μM]
Ac Lys OMe	**PB, 200 mM, pH 7.6**	**28 ± 2 %**
Ac Arg OMe	**PB, 200 mM, pH 7.6**	**178 ± 4 %**
Ac Lys OMe	PB, 10 mM, pH 6.2	16 ± 3 %
Ac Arg OMe	PB, 10 mM, pH 6.2	69 ± 4 %
Ac Lys OMe	**PB, 10 mM, pH 7.2**	**19 ± 3 %**
Ac Arg OMe	**PB, 10 mM, pH 7.2**	**77 ± 5 %**
Ac Lys OMe	PB, 10 mM, pH 8.6	18 ± 5 %
Ac Arg OMe	PB, 10 mM, pH 8.6	88 ± 5 %
H Lys OH	**PB, 10 mM, pH 7.6**	**227 ± 6 %**
H Lys OH	**PB, 10 mM, pH 6.2**	**173 ± 15 %**
H Arg OH	PB, 10 mM, pH 7.6	699 ± 15 %
H Arg OMe	PB, 10 mM, pH 7.6	160 ± 6 %
KAA	**PB, 10 mM, pH 7.6**	**303 ± 5 %**
KAA	**PB, 10 mM, pH 6.2**	**184 ± 12 %**
KLVFF	PB, 10 mM, pH 7.6	38 ± 11% [a]
IAPP(1-7)	PB, 10 mM, pH 7.6	110 ± 6 %
cRGDFV	PB, 10 mM, pH 7.6	n.d.
Ac Lys OMe	**PBS, 10 mM, pH 7.2**	**31 ± 4 %**
KAA	PBS, 10 mM, pH 7.2	397 ± 3 %
AcLysOMe	**Methanol**	**20 ± 6 %**
Ac Arg OMe	**Methanol**	**276 ± 7 %**

PB: phosphate buffer

PBS: phosphate buffer saline with 150 mM NaCl

n.d.: Not Determined.

a: Strong shift of fluorescence maximum ($\Delta\lambda$ ~ 20 nm, blue shift) and intensity of new maximum increase after addition of ~ 5 equivalent guests.

The structures of all the amino acid derivatives and peptide guests discussed in this thesis are given in Figure 3.8 (lysine guests) and Figure 3.9 (arginine guests). The biological importance of all these peptides has been described in the section 1.3. The dissociation constants obtained by the ^{1}H-NMR titration experiments and the fluorescence titration experiments are in good agreement. The small differences in the dissociation constants are apparently due to the different concentrations used in the two methods. Surprisingly, the tweezer **161** shows a wide range of affinities ranging from 700 μM to 16 μM for different guests. Under the similar conditions, the most differed binding behavior is observed among the protected and unprotected amino acids.

For example, the binding affinity for the unprotected lysine (HLysOH) is 227 μM which is about 12-fold lower than the affinity for the protected lysine (AcLysOMe).

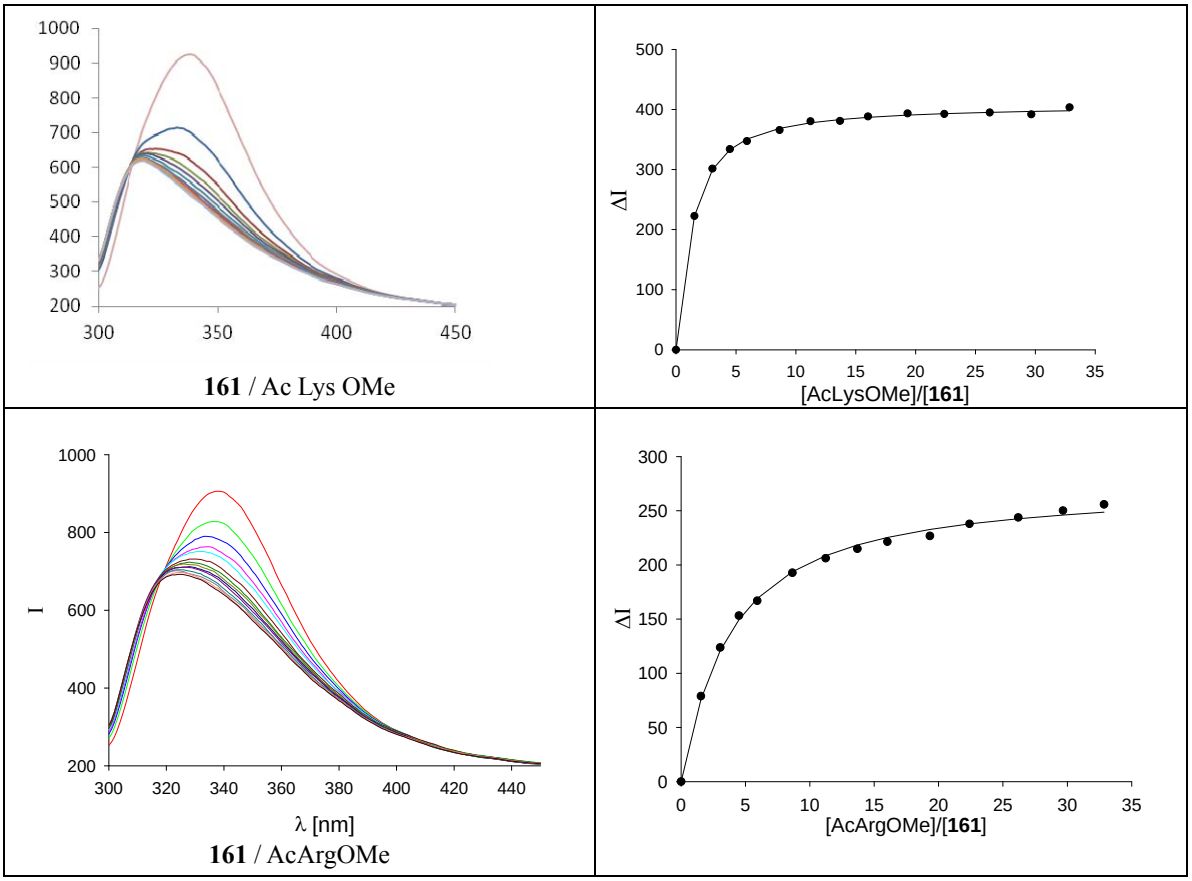

Figure 3.7 Selected guest concentration dependent emission spectra of the tweezer **161** (left) in aqueous phosphate buffer (10 mM, pH 7.6) and the non linear curves obtained by SigmaPlot[119] (right).

Similar trends of the sulfate tweezer **161** binding are also observed for the arginine guests, for example; the tweezer **161** binds to HArgOH with about 9-fold lower affinity compared to AcArgOMe. In addition, it is found that the sulfate tweezer **161** binds strongly to the N/C-protected amino acids and failed to bind comparably to the N/C-free amino acids or peptides (Table 3.3). For the longer peptide $IAPP_{1-7}$, the tweezer **161** shows moderate, but still 6-fold lower affinity (110 μM) compared to AcLysOMe. Interestingly, protecting the C-terminus of the arginine, as in HArgOMe, increase the affinity by 4-fold compared to the N/C-free arginine.

HLysOH

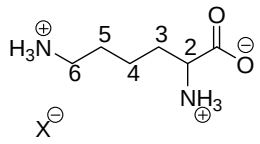

KLVFF

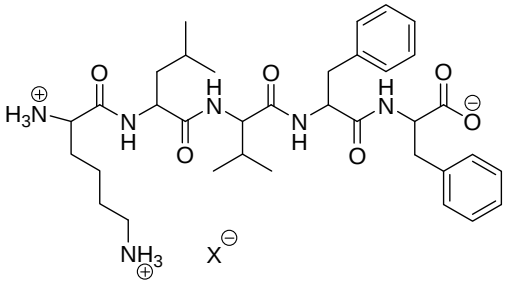

AcLysOMe

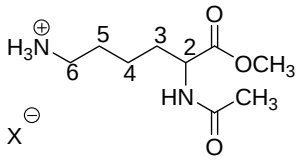

KKLVFF

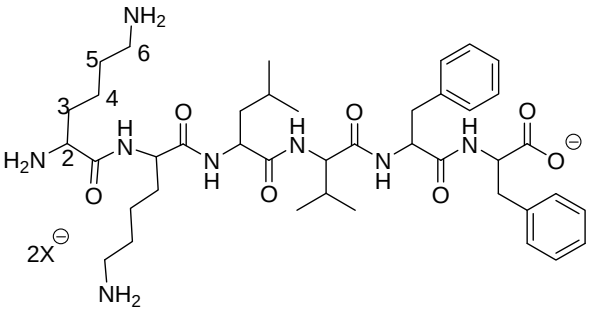

KAA

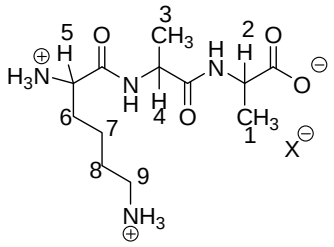

IAPP1-7 (KCNTATC)

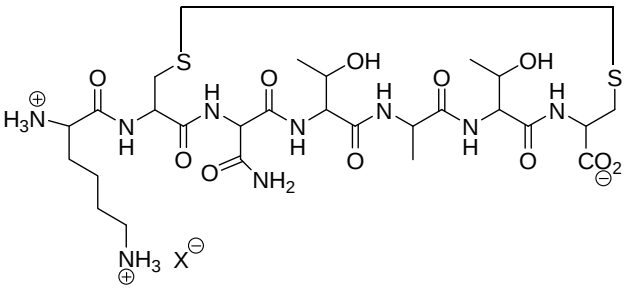

AcCysOMe

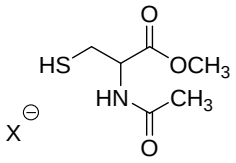

(AcCysOMe)$_2$

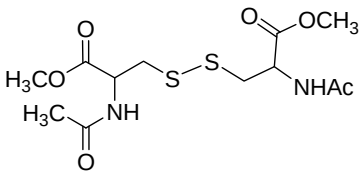

Figure 3.8 Structures of the lysine- and cysteine-containing peptide guests.

The structural differences between the protected and free amino acids are based only on their amine and carboxylate functional groups. Due to this reason, the differences in the tweezer binding affinity towards these guests is aroused through the electrostatic and hydrogen bonding interactions between the sulfate anion of the tweezer and the free or protected amine and carboxylic groups of the amino acid backbone. From the experimental and structural details, it is found that that the electrostatic repulsions between the anionic sulfate and the anionic carboxylate

reduce the strength of the complex. These data highlight the importance of the appropriate electrostatic and hydrogen bonding interactions between the tweezer's anion and the backbone of an amino acid or a peptide in the formation of a strong complex.

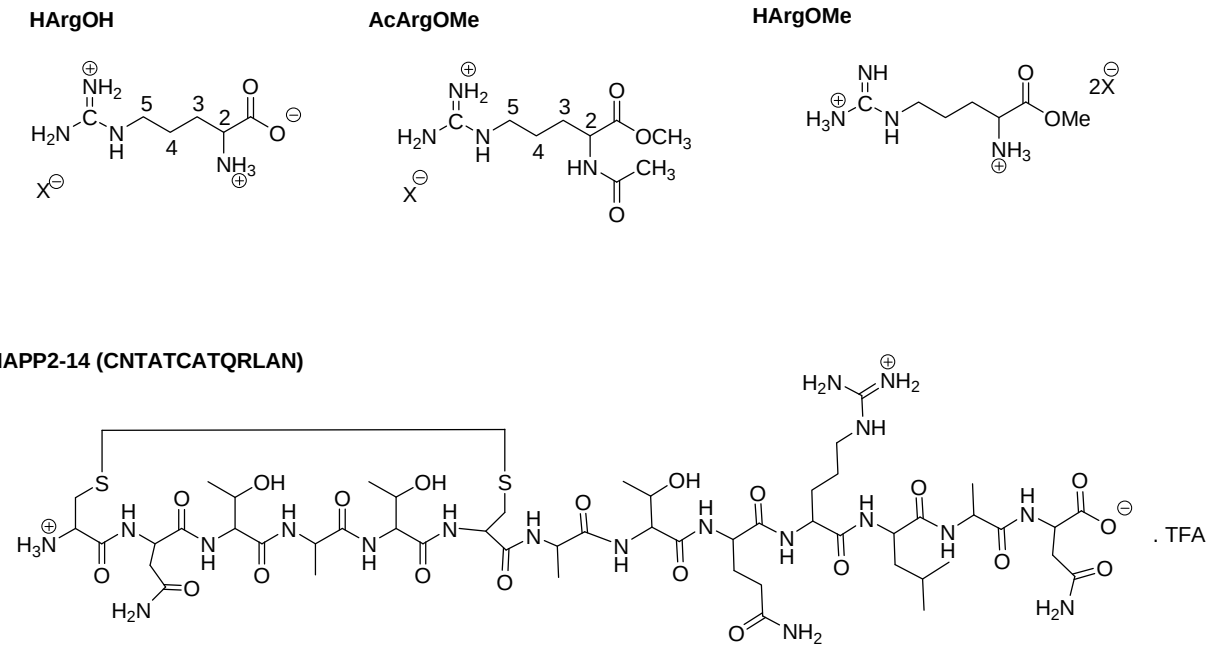

Figure 3.9 Structures of the arginine derivatives and arginine-containing peptide guests.

The effects of the pH, the buffer concentration, the ionic strength and the solvent on the complex stability were also investigated (Table 3.3). No substantial effects of the varied pH (6.2 to 8.5) are observed on the tweezer binding to the protected lysine and arginine; however, the effects are significant for the free amino acids and peptide KAA. When the pH is reduced from 7.6 to 6.2, the tweezer affinities for the N/C-free guests is increased almost by a factor of 2. The reduction in the pH increases the population of the protonated ammonium and carboxylate groups of the amino acid backbone and therefore, the electrostatic and hydrogen bonding interactions between the tweezer and the guest are enhanced.

The effects of the buffer concentration and saline are similar on the complex stability. When the buffer concentration is increased from 10 mM to 200 mM, the binding affinities of the tweezer **161** are reduced from 19 μM to 28 μM for the protected lysine and from 77 μM to 178 μM for the protected arginine. These results indicate the screening effects of the buffer ions. Obviously, the ionic interactions are not the major forces responsible for the stability of the complexes.

Complex formations by the sulfate tweezer **161** in the solvents other than water were also investigated. Due to close similarity of methanol to water, methanol served as another good

solvent. Surprisingly, complex formed between the tweezer **161** and AcLysOMe in methanol has same affinity to the complex formed in aqueous buffer. The ^{1}H-NMR spectra of a 1:1 mixture of the tweezer **161** and AcLysOMe in methanol-d_4 showed almost the similar chemical shift pattern of AcLysOMe protons as in the aqueous buffer. The 4-fold low affinity of the complex **161@**AcArgOMe indicates different impact of methanol on this complex. The NMR chemical shifts of the guest protons are also not influenced as large as in the buffer solution. Surprisingly, in methanol, fluorescence of the tweezer **161** is increased with the guest addition and is reverse to the fluorescence quenching occurred in the aqueous solutions. Proper reasons for the fluorescence inversion in the methanol are not yet understood.

3.2.1.2.3 Studies of the phosphate tweezer 133 complexes by fluorescence spectroscopy

The binding of the tweezer **133** for the lysine, arginine and cysteine derivatives were investigated using fluorometric titration experiments (Table 3.4). The tweezer **133** shows about 2-3 times lower affinities to arginine derivative AcArgOMe compared to lysine derivative AcLysOMe. The effects of buffer ions concentrations on the guest binding of the phosphate tweezer **133** are similar to those of the tweezer **161.** Binding of the tweezer **133** to cysteine (AcCysOMe), disulfide cystine $(AcCysOMe)_2$ and IAPP peptide fragments were also investigated as a part of the project, "inhibition of aggregation and toxicity of IAPP protein by the molecular tweezer **133**". Only 2-4 % change in the fluorescence of the tweezer **133** is observed with cysteine or cystine derivatives, indicating no binding of the tweezer **133** to these guests. The binding of the tweezer **133** with IAPP fragments will be discussed in the last section of this chapter.

Table 3.4 Dissociation constants K_d [μM] of the phosphate tweezer **133** with lysine, arginine and cysteine derivatives and, IAPP peptide fragments in phosphate buffer as measured by the fluorescence titration spectroscopy.

Guest	Solvent, pH	K_d [μM]
Ac Lys OMe	PB, 200 mM, pH 7.6	17 ± 6 % [90]
Ac Lys OMe	PB, 10 mM, pH 7.6	9 ± 6 %
Ac Arg OMe	PB, 200 mM, pH 7.6	61 ± 2 %
Ac Arg OMe	PB, 10 mM, pH 7.6	20 ± 5 %
AcCysOMe	PB, 10 mM, pH 7.6	-
$(AcCysOMe)_2$	PB, 10 mM, pH 7.6	-
IAPP(1-7)	PB, 10 mM, pH 7.6	9 ± 6 %
IAPP(2-14)	PB, 10 mM, pH 7.6	104 ± 4 %
AcLysOMe	Methanol	66 ± 11 %

-: no binding, only 2-4 % changes in the tweezer's fluorescence.

3.2.1.2.4 Isothermal calorimetric titration (ITC) studies of the sulfate tweezer 161 complexes and the phosphate tweezer 133 complexes

Isothermal titration calorimetry[120] is another important method from which we not only measure the association constants but also other important thermodynamic parameters such as enthalpy, entropy and stoichiometry of the complex formation are measured in just a single experiment. In an ITC experiment, the heat evolved or absorbed is measured during the addition of a guest solution into a host solution. The thermodynamic data for the complexes of the tweezers **161** and **133** with lysine- and arginine-containing guests determined by the VP-ITC[121] are listed in the Table 3.5. The binding affinities determined by the ITC measurements are in agreement with the data obtained by the fluorometric and the ^{1}H-NMR titration experiments. The enthalpy determined for the complex **161**@AcLysOMe formation is highly favorable (ΔH = -8.3 kcal/mole) but the entropy of the complex formation is unfavorable (-TΔS = 2.1 kcal/mole), resulting in an overall decreased affinity. On the other hand, the entropy determined (-TΔS = 0.387 kcal/mole) for the complex **161**@AcArgOMe is only slightly unfavorable but the observed enthalpy (ΔH = -5.9 kcal/mole) is substantially lower than the enthalpy for the complex **161**@AcLysOMe. The more negative ΔH determined for AcLysOMe indicates that the tweezer **161** binds enthalpically more tightly to AcLysOMe compared to AcArgOMe. These results suggest that the entropy loss by the association of the tweezer **161** and lysine or arginine guest is more than the entropy gain by the release of solvent molecules into the bulk solvent.[122] Obviously, the loss in the degree of freedom of the host and guest, in particular, by the restricted motion of the tightly complexed lysine, is responsible for the more entropy loss of the complex **161**@AcLysOMe.

Table 3.5 Dissociation constants (K_d), enthalpy (ΔH), entropy (ΔS), Gibbs free energy and stoichiometry (n) of the tweezers **161** and **133** complexes with lysine- or arginine-containing guests obtained by the isothermal titration calorimetry (ITC) in phosphate buffer (10 mM, pH 7.6).

host@guest	K_d [μM]	n	ΔH[kcal/mol]	-TΔS[kcal/mol]	ΔG[kcal/mol]
161@AcLysOMe	28 ± 4 %	0.82	-8.17	1.96	-6.21
161@AcArgOMe	88 ± 9 %	0.90	-5.92	0.39	-5.53
133@AcLysOMe	14 ± 5 %	0.68	-5.55	-1.05	-6.60
133@AcArgOMe	31 ± 3 %	0.62	-6.80	0.67	-6.14
133@KLVFF	15 ± 4 %	1.02	-6.29	-0.28	-6.57
133@IAPP(1-7)	7 ± 3 %	1.16	-6.37	-0.70	-7.07
133@IAPP(2-14)	157 ± 40%	1.00	-5.38	0.19	-5.19
133@AcLysOMe[a]	172 ± 17%	1.25	10.15	-15.31	-5.16

[a] measured in methanol

The entropies determined for the complexes of the tweezer **133** with all the lysine-containing guests are favorable, whereas, for all the arginine-containing guests are unfavorable. Interestingly, the tweezer **133** binds AcArgOMe enthalpically more tightly than any other guests, but entropy compensation lowers the overall affinity for the complex **133**@AcArgOMe. More surprisingly, the complex **161**@AcLysOMe has highest negative enthalpy among all the complexes of the two tweezers, but high unfavorable entropy (-TΔS = 2.1 kcal/mole) cause substantial decrease in the overall affinity of this complex. Surprisingly, the complex **133**@AcLysOMe is entropy driven (-TΔS = -15.31 kcal/mole) in methanol. The positive enthalpy (ΔH = 10.15 kcal/mole) indicate lack of the hydrophobic interactions.

From the ITC data, it is observed that enthalpically lysine is bound much tighter to the tweezer **161,** whereas, arginine is bound much tighter to the tweezer **133** and, it is the entropy which play crucial role in deciding the net affinity the complex. The ITC results suggest that phosphate and sulfate anions are responsible for the difference in the enthalpy and the entropy of the complexes formed by the tweezers **133** and **161** with the same guest. Further, our results of large negative enthalpies of the complexes formed by the tweezers support the results obtained for host-guest complex formation in aqueous solutions that rely on the aromatic interactions, called the non-classical hydrophobic effects.[123,124,125,126]

3.2.1.2.5 Molecular modeling of the sulfate tweezer 161 complexes

In order to get structural information, the corresponding host-guest complexes were optimized by Monte-Carlo Simulations using the program Maestro 9.2. The resulted minimum energy structures for lysine and arginine guests are given in Figure 3.10. In the calculated structures of the sulfate tweezer **161** complexes with lysine and arginine, a combination of the hydrogen bonding interactions, the electrostatic interactions and the hydrophobic interactions is apparent. The ammonium cation of lysine and the guanidinium cation of arginine side-chains make hydrogen bonds and electrostatic interactions with one anionic sulfate group of the tweezer **161**. In case of lysine, a cation-л interaction between the ammonium cation and electron rich aromatic cavity of tweezer **161** also likely occurs. Apart from these clearly observable interactions, close inspection of the complex structures suggest that two S=O···C=O dipolar interaction can also exist. All together these complex structures are in good agreements with ^{1}H-NMR chemical shifts data.

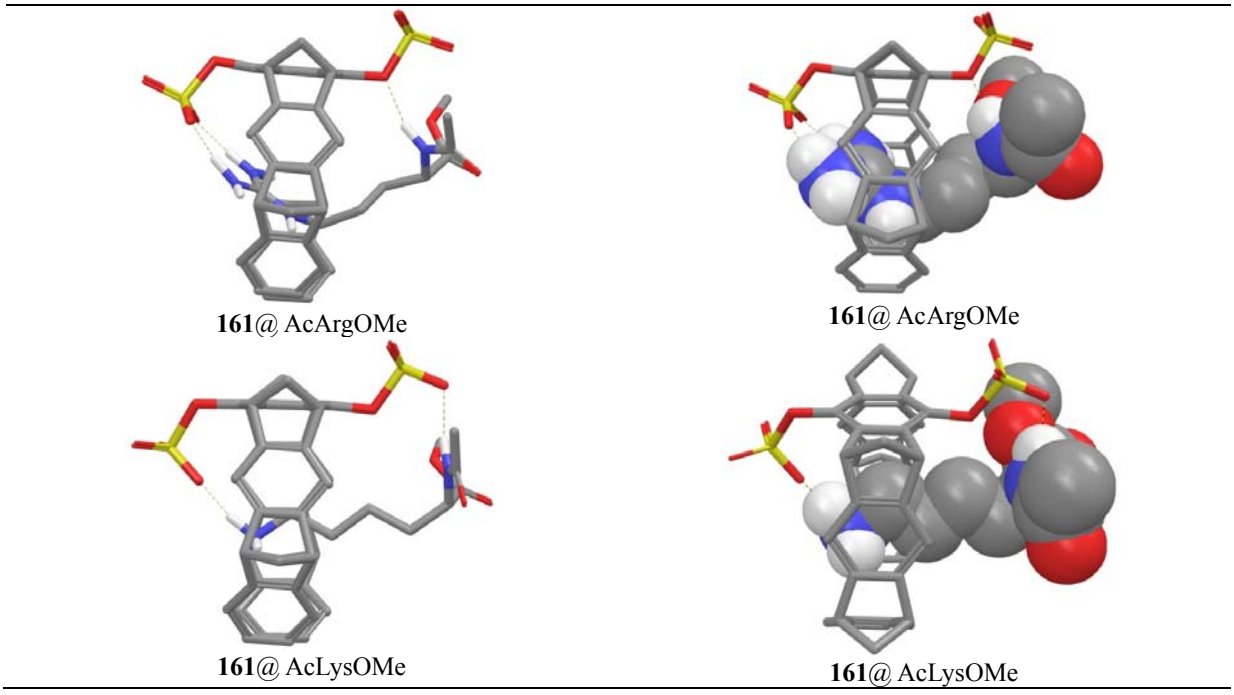

Figure 3.10 Molecular modeling structures of the sulfate tweezer **161** complexes with AcLysOMe and AcArgOMe obtained by Monte-Carlo Simulation (Maestro 9.2, OPLS_2005, water, 5000 steps).

Structural insights by molecular modeling were also investigated in case of low affinity guests HLysOH, HArgOH and KAA. The calculated minimum energy structures are listed in Figure 3.11. Hydrogen bonding seems to be involved between tweezer's sulfate anion and all the

protonated ammonium group of the guests. However, the anionic carboxylate group keeps apart from the anionic sulfate group. Moreover, calculated structure with unprotonated amine of the peptide KAA eliminated the possibility of any hydrogen bonding between the sulfate group and the peptide backbone. These structures indicate high repulsive interactions between the peptide and the sulfate group of the tweezer **161.** Obviously, such repulsive interactions can be the dominating factor for the decrease affinities of these complexes. The lack of strong electrostatic and hydrogen bonding interactions probably do not allow the guest to bind tightly inside the tweezer's cavity. Definitely, these results highlight the importance of strong cooperative hydrogen bonding between a tweezer and the backbone of a peptide guest in order to form a strong complex.

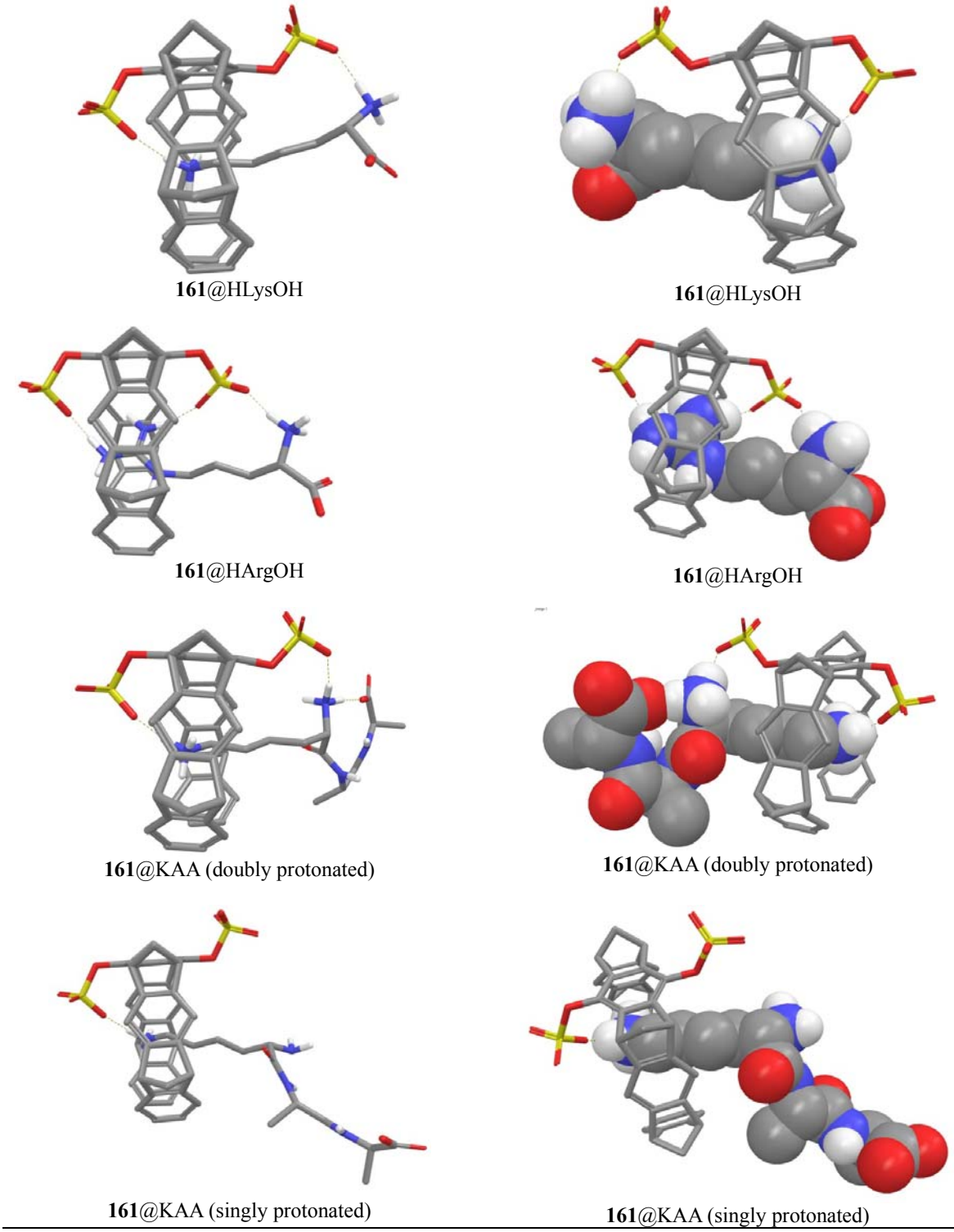

Figure 3.11 Calculated structures of the sulfate tweezer **161** with HLysOH, HArgOH, KAA (doubly protonated) and KAA (singly protonated) obtained by Monte-Carlo Simulation (Maestro 9.2, OPLS_2005, water, 5000 steps).

The Fluorescence emission spectra of the sulfate tweezer **161** on titration with KLVFF are surprising and unusual as shown in Figure 3.12 The fluorescence of the tweezer **161** is decreased

intiallly for ~ 5 equivalents of guest addition but thereafter slowly starts increasing with blue shift of the emission band. The exact reasons for the above mentioned effect are not clear, however, the resulted emission spectra indicates the presence of other strong interactions between the tweezer's hydrophobic surface and peptide's hydrophobic residues (Leu and Phe). A molecular modeling structure in different representation and from different angles is shown in Figure 3.13. It shows that the whole peptide adopts a concave conformation with the alignment of its amide –NH groups at the inner surface and making a cluster of three hydrogen bonds with the sulfate group of the tweezer **161**. Additionally, it shows the hydrophobic interactions between the hydrophobic phenyalanine and leucine residues of the peptide and the outer surface of the tweezer with lysine side-chain imbedded into the tweezer's cavity. It is known that the presence of aromatic interactions (π-stacking, T-shaped orientation, partial displaced orientation) in a complex or excimer can change the fluorescence properties of the fluorophore.[127,128] Obviously, either these additional aromatic interactions have modified or changed the fluorescence properties of the tweezer **161** or the new emission band have developed due to the aromatic interactions among the three aromatic ring (two from the guest and one from the tweezer).

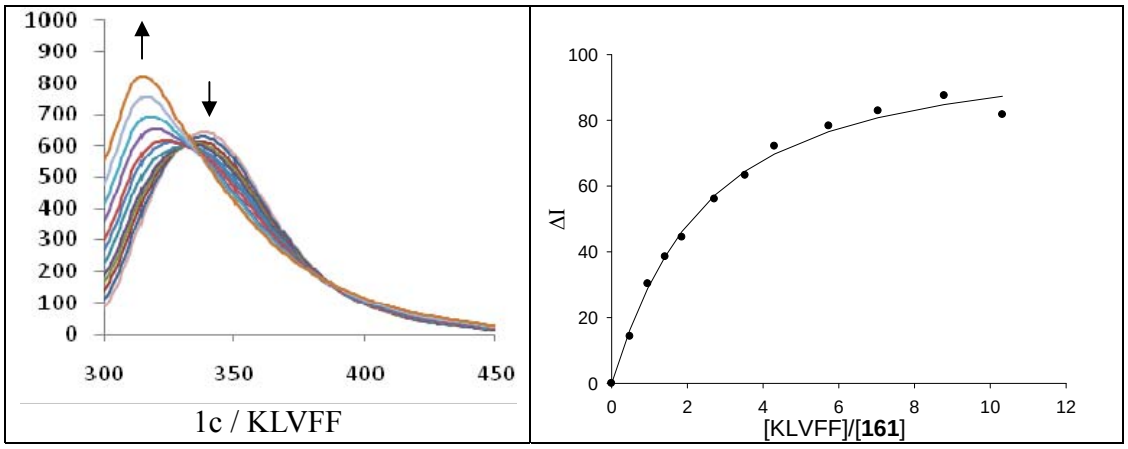

Figure 3.12 Left: peptide KLVFF concentration dependent emission spectra of the tweezer **161** (left) in aqueous phosphate buffer (10 mM, pH = 7.6), right: non linear binding isotherms obtained by the SigmaPlot (right).

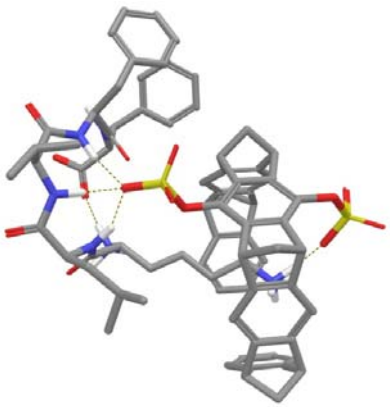

161 and KLVFF in stick model

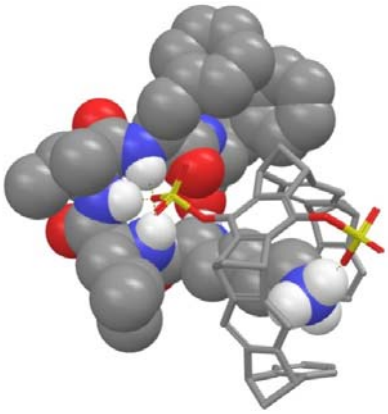

161 in stick and KLVFF in CPK model

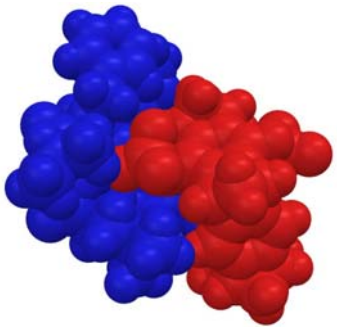

161 (red) and KLVFF (blue) in CPK model

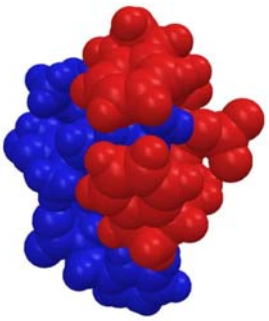

161 (red) and KLVFF (blue) in CPK model

Figure 3.13 Calculated structure of the complex **161**@KLVFF in different views and model obtained by Monte-Carlo Simulation (Maestro 9.2, OPLS_2005, water, 5000 steps).

3.2.2 Binding comparisons among the four anionic tweezers

The comparative study of the binding of anionic tweezers with lysine- and arginine-containing guests was made to understand and generalize the roles of different anions in the tweezers binding. The dissociation constants of the phosphate, phosphonate, sulfate and carboxylate tweezers for different guests measured by fluorometric titration experiments are summarized in Table 3.6. Surprisingly, there are substantial differences in the binding of all the four tweezers with respect to a particular guest. The phosphate tweezer **133** forms more stable complexes than the sulfate tweezer **161** followed by the phosphonate **734** and the carboxymethyl **150** tweezers. Surprisingly, the binding affinities of the tweezer **161** determined for the unprotected amino acids or peptides are about 10-fold lower than for the N/C-protected lysine and arginine guests. These are contrary to the very similar binding affinities of the tweezer **133** determined for these guests. The tweezer **734** also shows similar trends like sulfate tweezer **161** and binds strongly only to

AcLysOMe, but four times weaker than the tweezer **133** and two times weaker than the tweezer **161**.

Table 3.6 Comparisons among the guest binding (K_d value in μM) of different anionic tweezers measured by fluorescence spectrometry.

Guest	Phosphate	Phosphonate	Sulfate	Carboxymethyl
AcLysOMe	17 ± 6 % [a, [90,83]]	68 ± 1% [a, [90]]	28 ± 2 % [a]	226 ± 14 % [a, [113]]
	9 ± 6 % [b]		19 ± 3 % [c]	643 ± 7% [c, [113]]
HLysOH	21 ± 4 % [a, [90,83]]	874 ± 1% [a, [90]]	227 ± 6 % [b]	1170 ± 20 % [b, [113]]
KAA	30 ± 3 % [a, [90]]	905 ± 1% [a, [90]]	303 ± 5 % [b]	n.d. [c, [113]]
KLVFF	20 ± 5 % [a, [90]]		38 ± 11 % [b, *]	n.d. [c, [113]]
KKLVFF	4 ± 1 % [a, [90]]	71 ± 1% [a, [90]]		
IAPP(1-7)	9 ± 6 % [b]		110 ± 6 % [b]	
AcArgOMe	60 ± 2 % [a]		178 ± 4 % [a]	880 ± 26 % [a, [113]]
	20 ± 5 % [b]		77 ± 5 % [c]	281 ± 18% [c, [113]]
HArgOH			699 ± 15 % [b]	609 ± 27 % [c, [113]]
HArgOMe			160 ± 6 % [b]	

[a] Phosphate buffer, 200 mM, pH=7.6; [b] phosphate buffer, 10 mM pH=7.6; [c] phosphate buffer, 10 mM, pH=7.2.
n.d.: Not Determined or with the error of more than 30%.
[*] Strong shift of the fluorescence emission maxima (~ 20 nm blue shift) and intensity of new maximum increase after adding about 5 equivalent guests.

The carboxymethyl tweezer **150** is also superior to AcLysOMe among all the guests examined, but surprisingly, with 13-fold lower affinity compared to the tweezer **133**. From these data we have observed that the host-guest complex with high ^{1}H-NMR chemical shift changes in the guest protons (Table 3.7) also showed strong complex formation by means of ^{1}H-NMR and fluorometric titration experiments. On the other hand, where no significant chemical shift changes in the guest protons were observed, there the binding affinities measured by any method were also poor as in case of the tweezer **150.**

Table 3.7 Dissociation constants K_d [μM] and complexation-induced maximum ^{1}H-NMR chemical shifts ($\Delta\delta_{max}$[ppm]) of the guest protons determined for the host-guest complexes of the phosphate-, phosphonate-, sulfate-, and OCH_2-carboxylate-substituted tweezers **133**, **734**, **161**, and **150** with lysine- or arginine-containing amino acid and peptides derivatives by ^{1}H NMR titration experiments in aqueous phosphate buffer at pH = 7.2.

Host-Guest Complex	K_d [μM]	$\Delta\delta_{max}$ [ppm]
133 • Ac Lys OMe	17 ± 0 % [89]	3.91 (6-H), 0.51 (2-H), -0.32 (NCOCH_3)
133 • H Lys OH	40 ± 7 % [89]	4.51 (6-H), 4.47 (5-H), 0.24 (2-H)
133 • KAA	11 ± 9 % [89]	5.82, 5.92 (9-H)[a], 3.22 (8-H), 2.28 (7-H)
133 • Ac Arg OMe	22 ± 4 %	3.75 (5-H), 2.54 (4-H), 1.23 (3-H), 0.63 (2-H)
734 • Ac Lys OMe	227 ± 22 % [87]	> 4 (6-H)[b], 1.45, 1.57 (5-H)[a], 0.57 2-H)
734 • H Lys OH	714 ± 8 % [87]	> 4 (6-H)[b]
734 • KAA	833 ± 14 % [87]	2.80 (6-H), 1.03 (5-H), 0.29 (2-H)
161 • Ac Lys OMe	12 ± 11 %	3.75 (6-H), 4.41 (5-H), 2.64 (4-H), 1.29 (3-H), 0.37 (2-H)
161 • Ac Arg OMe	88 ± 5 %	3.86 (5-H), 2.51 (4-H), 1.32 (3-H), 0.42 (2-H)
150 • Ac Lys OMe	1164 ± 11% [113]	0.94 (6-H), 0.54 (5-H), 0.40 (4-H), 0.77, 0.52 (3-H)[a]
150 • Ac Arg OMe	1393 ± 18% [113]	0.96 (5-H), 0.62, 0.48 (4-H)[a], 0.52 (3-H)

[a] The diastereotopic methylene protons show two separate signals in the complex. [b] The signal broadening does not allow the exact ^{1}H NMR chemical shift determination of the complex.

In case of the strong complex formation, the chemical shift changes in the guest protons are very high (~ 3.5 – 5 ppm) which indicate that the stable complex is formed by the guest side-chain inclusion into the tweezer's hydrophobic cavity. The inclusion of a guest into the tweezer's cavity is a result of hydrophobic dispersive interactions between the CH_2-groups of the guest side-chain and π-electron rich tweezer's cavity. In a similar way, the fluorescence of the tweezer is partially quenched when a complex is formed by the inclusion of a guest into the tweezers's cavity. The quenching in the tweezer's fluorescence is higher when the tight complex is formed. So, combining the fluorescence and NMR data, it can be generalized that when the chemical shift changes in guest protons are smaller, the fluorescence quenching are also smaller and resulted binding affinities are also lower and vice versa. Now, the obvious question arise that though the cavity of all the tweezers are same and all the four anions are capable to interact strongly with ammonium or guanidinium cations of guest molecules, why there are very much differences in the binding of different tweezers, and how can we understand them?

In literature, several groups have investigated the complex formation of the calixarenes substituted by these anionic groups with lysine or arginine guests, however, comparative binding studies have not been made among them. Desrorsies and coworkers showed that in phosphate buffer solution the calix[4]arenesulphonate binds 2-fold strongly to the free arginine (K_d = 667 μM) compared to the free lysine.[129] Other report from Rachoń *et al* showed that the calix[4]arenephosphonate binds almost with the same affinity (K_d = 1667 μM) to these amino acids in the phosphate buffer.[130] In both calixarenes, the inclusion of the side-chains of both the amino acid were observed by ^{1}H-NMR chemical shifts which indicate that the complex was formed by the hydrophobic and electrostatic interactions. In case of arginine, a π-π interaction between the guanidinium moiety of arginine and the aromatic rings of calixarene is expected responsible for the higher affinity for arginine compared to lysine. Noticeably, our first three tweezers are more superior to the lysine or arginine compared to the above mentioned calixarenes.

Nilsson and coworker[102] synthesized and investigated several galactopyranoside sugar derivatives substituted with the phosphate, phosphonate and sulfate moiety for the binding to arginine rich galectin proteins. In their study they found that the sulfated ligands bound stronger to most of the galectins compared to the phosphate and phosphonate analogs. The dissociation constants for galectin-1, 3 and 9N correlated negatively with the calculated partial charge {PO_3^{2-} >$P(OMe)O_2^-$ >SO_3^-} of the anionic oxygens of the ligands. These results suggested the role of the desolvation penalty that depends on the magnitude of charge of anions. Contrary to the above examples our results partially correlate with them but in an inverse order.

When the two molecular species interact to form complex there are substantial modification in the degree of freedom of host and/or guest, the hydrophobic interactions, the electrostatic interactions, hydrogen bonding interactions, the π-π interactions etc. In a complex formation some of these interactions could be favorable and some unfavorable. Therefore, the net result of these contributions decides the stability of a complex. Understanding each single contribution would be very demanding, but this is not possible to evaluate them in our case, however, the general nature of these forces towards enthalpy and entropy of a host-guest complex formation in water are known (Table 3.8).

Table 3.8 Different factors involved in a host-guest complex formation and their contributions to the enthalpy or entropy in aqueous solution.

Interaction	Contribution to ΔH	Contribution to TΔS
Electrostatic interactions	Negative	
Hydrophobic interactions		positive
π-π interactions	Negative	
Desolvation of ionic groups	Positive	positive
Loss of degree of freedom		negative

All the above listed interactions are likely to be involved in our receptor-guest complexes. To understand the effects of electrostatic interactions on the stability of a complex of a tweezer and a guest, the Lewis structures of the different anions and their partial charge at about neutral pH in aqueous buffer solution are drawn below-

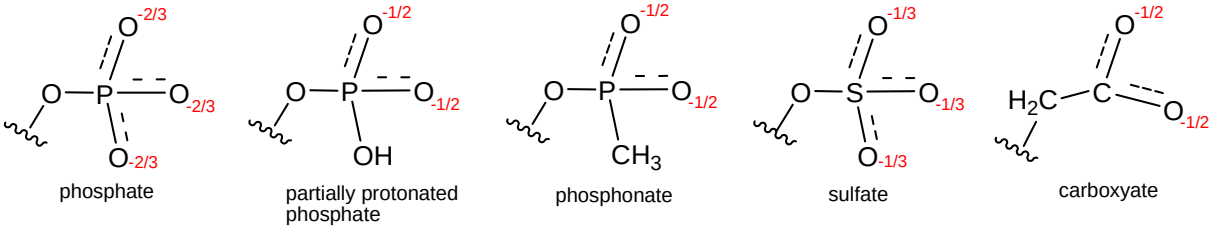

The phosphate group (in tweezer **133**) can have both fully deprotonated and partially protonated forms with -2 and -1 charge respectively and distributed over three oxygen atoms with the partial charges of -2/3 and -1/2. The phosphonate group (in tweezer **734**) and the carboxylate group (in tweezer **150**) have one negative charge distributed over two oxygen atoms and therefore -1/2 partial charges. Sulfate group has -1 charge distributed over three oxygen atoms and therefore -1/3 partial charges (in tweezer **161**). Therefore, the statistical partial charge of these anions are in the order: $-OPO_3^{2-} > -OP(OMe)O_2^- \geq -OCH_2CO_2^- > -OSO_3^-$. Based on the partial charge, the phosphate tweezer **133** can be expected to make the strongest electrostatic interaction among all the tweezers. Indeed, the phosphate tweezer **133** has the highest affinity among the four tweezers for any guest, supporting the role of the electrostatic interactions. But, the other three tweezers do not show correlation between their partial charge and binding affinity, as the sulfate tweezer **161** has the lowest partial charge but shows higher affinities than the phosphonate tweezer **734** and carboxymethyl tweezer **150**. These results indicate that only the electrostatic interactions do not decide the affinity of a tweezer for any guest.

Analyzing the hydrogen bonding features, the phosphate tweezer **133** again benefits more with the guest binding due to the hydrogen bond acceptor and donor nature of its partially protonated phosphate groups. On the other hand, the other tweezers can be expected completely deprotonated at the used pH values and therefore, they can benefit the guest binding only by accepting the hydrogen bonds from the guest molecules. Further, hydrogen bonding can be more prominent in bigger peptide guests that can form multiple hydrogen bonds with the tweezer's anions. A decrease in the affinity of a tweezer for the bigger guest molecules can be expected due to the steric hindrance around the lysine or arginine residues, unless more additional interactions, i.e. the hydrogen bonding occurs between a tweezer and a guest. This effect can be observed as the binding of the phosphate tweezer **133** to AcLysOMe and $IAPP_{1-7}$ are similar, while the binding of the sulfate tweezer **161** for $IAPP_{1-7}$ is decreased about 5-fold compared to AcLysOMe. Noticeably, hydrogen bonding play substantial role in the tweezer binding to a guest, but as the tweezer **161**, **734** and **150** can have similar tendency to form hydrogen bonds, this factor alone does not explain the big difference in the tweezers bindings.

Speaking about the hydrophobic interactions, since all the tweezers have same size and structures of their cavity therefore all of them must provide almost similar hydrophobic environment to a particular guest. Though, due to the different basicity of the four anionic groups, the electrostatic potential of the tweezer's cavity could be changed, and more basic anion can induce more electronegative potential on the tweezer's cavity. The decreasing order of basicity of tweezer's anions and thereby, the electrostatic potential of the respective tweezers can be listed as-
$\{-OPO_3^{2-} > -OCH_2CO_2^- > -OP(OMe)O_2^- > -OP(OH)O_2^- > -OSO_3^-\}$

Clearly, this factor does not correlate with the obtained experimental data indicating no substantial role of these anions on the hydrophobic cavity. Therefore, similar hydrophobic dispersive interactions can be expected from different tweezers towards a particular guest.

The π-π interactions are also found in chemical and biological recognitions. If an arginine guest form complex with a tweezer by the inclusion of its side-chain into the tweezer's cavity, the planer guanidinium group of arginine can make π-π interactions with the aromatic rings of the tweezer. When this force comes into existence then this will contribute to the negative enthalpy of the complex and therefore, strong affinity for arginine can be expected compared to lysine. But, all the tweezers are atleast 2-fold weaker to arginine compared to lysine. These data either eliminate the possibility of π-π interactions or indicate the overcompensation by the other factors.

Interestingly, the enthalpy determined by the ITC experiments for complex **133**@AcArgOMe (ΔH = -6.8 kcal/mol) is higher than that of complex **133**@AcLysOMe (ΔH = -5.5 kcal/mol). This indicates that arginine is bound enthaplically much tighter than lysine inside the tweezer **133,** and most probably due to the additional π-π interactions. But due to the unfavorable entropy (-TΔS = 0.67 kcal/mole) of the complex **133**@AcArgOMe, it is less stable compared to the complex **133**@AcLysOMe, for which the entropy (-TΔS = -1.05 kcal/mole) is favorable. These results indicates that though π-π interactions are apparent in the tweezer **133** binding to arginine, but there are also other factors that affects the overall stability of the complexes.

The interactions of ions or molecules with the solvent molecules also play crucial roles in the stability of molecular complexes. The ionic groups are highly solvated in water and their desolvation is always enthalpically unfavorable. Therefore, in complex formation, gain in enthalpy by the ion pair formation should be greater than the desolvation penalty of the ions. Several reports are published in the literature about the ions in water, dealing with the ions solvation and their interactions with water and other ions.[131,132] With the help of neutron diffraction, gas phase infrared vibrational spectroscopy, X-ray absorption spectroscopy, and *ab initio* molecular orbital studies, it has been shown that water interacts with the ions via a chemical bond that is affected over only a short distance (< 5 Å). This chemical interaction involves substantial charge transfer from strongly solvated ions to the solvent to delocalize the charge. Further, ions with more surface charge density are strongly solvated and can form strong ion pair with other counter charged ions that are also strongly solvated. The phosphate, sulfate and carboxylate anions are strongly solvated in water, while the ammonium or guanidinium cations of amino acids are weakly solvated. Therefore, on highly water exposure weak ion pair interactions could be expected among them however, given the less exposure to water these ions can make strong ion pair interactions. Considering the partial charge calculated from Nilsson, the desolvation penalty of the three anions will be in the order: $-OPO_3^{2-} > -OP(OMe)O_2^- > -OSO_3^-$. It is not certain if the desolvation of the phosphonate tweezer **734** would be higher or lower than the carboxymethyl tweezer **150** because of the similar partial charge of their anions. The entropy determined for the complex **133**@AcLysOMe is favorable, while for **133**@AcArgOMe is unfavorable. Obviously, in the later complex, the loss in entropy by the desolvation of guanidinium group is more than the gain in entropy by the release of bound water molecules in the bulk solution. Due to the lower charge density, the sulfate group will be less strongly solvated than the phosphate group. As discussed before, negative entropies are determined in case of the complexes of the tweezer **161** with AcLysOMe and AcArgOMe. The lower enthalpy for the

complex **161**@AcArgOMe compared to complex **161**@AcLysOMe indicates that the tweezer **161** binds lysine more tightly than arginine. It is apparent that the tweezers, due to even small differences in their anions, behave very distinctly in the guest binding.

Another factor affecting the complex stability is the modulation of degree of freedom of host and/or guest. In a complex formation, atomic motions and conformational flexibility of atleast one species become restricted that result in the unfavorable entropy of the system. This factor should obviously play a significant role in the complexes with guests that are included in the tweezer's cavity and locked by the ion pairs and hydrogen bonding. But, his factor can not be easily distinguished among the four tweezers; we can only say that when the entropy loss is over compensated by the enthalpy gain, complex is formed, and the net gain in enthalpy after compensating the entropy decide the strength of the complex.

All together, we found that there is no direct relationship between the anionic group characteristics and the binding affinities of their respective tweezers towards any guest. Further, it is also evident that no single force decides the overall stability of the complex, and only collective effects of all kind of favorable and unfavorable interactions govern the final stability of the complex. However, some points about the relative binding affinities of the tweezers can be made. For example, in the tweezer **734**, partial inclusion of the methyl group on the phosphonate group inside the tweezer's cavity, lower partial charge and only the hydrogen bond acceptor nature of the phosphonate anion may be the main factor for the decline in affinity of the phosphonate tweezer **734** compared to the phosphate tweezer **133**. In case of the carboxymethyl tweezer **150,** the partial inclusion of an amino acid guest inside the cavity and low binding affinities are far beyond than our expectation. The factors, like more solvation penalty and high flexibility of the carboxymethyl groups may diminish the ion pair interactions between the carboxylate anion of the tweezer and ammonium or guanidinium cations of the guests. Other factors could also be that the ion pairs of the receptor-guest cannot reach in close contacts and in a favorable arrangement. The ^{1}H-NMR of the pure receptor and molecular modeling structure suggest that the methylcarboxylate group stay away from the cavity and parallel to the central benzene ring that guarantee an open cavity of the tweezer **150**. Therefore, any guest must not have steric hindrance for the cavity inclusion. The calculated structures of the tweezer **150** with lysine and arginine suggest the presence of hydrogen bonds between the tweezer and the guests, but the conformation of the carboxymethyl moiety is twisted. Since moderate to strong electrostatic and hydrogen bonding interactions are known between carboxylate group and

ammonium or guanidinium groups in water, and tweezer's cavity is not sterically shielded, therefore, the poor affinities of the carboxymethyl tweezer **150** towards any guest reflect the absence of the proper electrostatic and hydrogen bonding interactions.

Comparisons between the phosphate tweezer **133** and the sulfate tweezer **161** have been more interesting because of the similar size and geometry of the two anions. Three differences can provide good arguments for the different behavior of these two tweezers. First, partially and fully deprotonated phosphate groups have more partial charge on its oxygen atoms than the sulfate groups and this factor can be one possible reason for the higher affinities of the tweezer **133** compared to the tweezer **161.** Second**,** partially protonated phosphate can accept and donate hydrogen bonds, while completely deprotonated sulfate only can accept hydrogen bonds. This difference leads the tweezer **133** to interact effectively with hydrogen bond acceptor and donor guest, while the tweezer **161** can be effective in complexing the guest with only hydrogen bond donor nature. As already discussed, that there are good tendency for ion pair interactions and hydrogen bonding between the sulfate and ammonium cation, but the anionic sulfate make strong repulsion with the anionic carboxylate of the unprotected amino acids backbone. This repulsive interaction can be the most probable reason for the drastic loss (about 10-fold) in affinities of tweezer **161** for HLysOH, HArgOH and KAA compared to the respective N/C protected amino acids (for modeling structures see Figure 3.11). All the data and above discussion about the phosphate and the sulfate tweezers highlight the importance of hydrogen bonding in their complex stability. As shown before, the NMR chemical shift changes of the protected lysine and arginine guests in complex with the tweezers **133** and **161** are almost similar, therefore, the difference in the tweezer's binding affinities must arise by the differences in the electrostatic and hydrogen bonding capabilities of the tweezer's anions that can lock the guest inside the tweezer's cavity in conjunction with the hydrophobic interactions.

A good example to support our results and assumptions is the selective uptake and transportation of inorganic phosphate by the phosphate binding protein (PBP) and inorganic sulfate by the sulfate binding protein (SBP) into the cells. In the PBP-phosphate complex structure, the phosphate ion is completely desolvated and forms extensive hydrogen bonds with 11 donor group and 1 acceptor group. On the other hand, in SBP-sulfate complex structure, the sulfate ion receives 7 hydrogen bonds from polar groups. Studies revealed that in T141D mutation which provides additional negative charge at the binding site; the affinity was not affected at pH below the second pK_2 of phosphate (where $H_2PO_4^-$ exists exclusively), but it diminished the affinity at

pH well above the pK_2 where HPO_4^{2-} species dominates. The loss in affinity is attributed to charge-charge repulsion between Asp-HPO_4^{2-}. This is the same mechanism that fully ionized sulfate does not bind to the PBP. The importance of complete hydrogen bonding is again reflected by no affinity of SBP towards phosphate. This is because SBP do not contain any hydrogen bond acceptor in its binding site. Therefore, we can say that hydrogen bonding can be crucial and highly specific. These examples provide strong support for the varied affinities of the phosphate tweezer **133** and the sulfate tweezer **161** towards the different guests.

So, all together in this chapter we have investigated distinct supramolecular properties of the closely related four anionic tweezers and their recognition abilities of basic amino acids and biologically relevant peptides taken from such as amyloid-β, IAPP etc. The phosphate tweezer **133** and the sulfate tweezer **161** are quite similar but exhibit the remarkable differences in their bindings. These tweezers, up to some extent, correlate or imitate the binding of phosphate and sulfate ions through the natural proteins PBP and SBP respectively. We are surprised that the carboxymethyl tweezer **150** does not bind any guest with a reasonable affinity. Our findings also suggest that replacement of one anionic group by other similar anionic groups in an artificial receptor molecule have a great impact on the molecular recognition properties. The phosphate and the sulfate tweezers can be used up to some extent as specific receptors. The tweezer **133** can be expected a strong receptor for a protein target if it has hydrogen bond acceptor and donor groups near the binding site (lysine or arginine residue). On the other hand, the tweezer **161** can only bind strongly to a protein that can furnish hydrogen bond donor groups near the binding sites (lysine or arginine residue).

3.2.3 Biological evaluation of the anionic tweezers against aggregation and toxicity of Aβ42 and IAPP

The biological evaluations of all these anionic tweezers were carried out in collaboration with Prof. Gal Bitan at neurology department, UCLA. I contributed the sulfate tweezer **161** and Constanze Wilch contributed the carboxymethyl tweezer **150** for the biological studies. In the figures, different names were given to the tweezers as listed in the brackets: the phosphate tweezer **133** (CLR01), the phosphonate tweezer **734** (CLR02), the sulfate tweezer **161** (CLR04) and the carboxymethyl tweezer **150** (CLR05). Biophysical and cell culture assays suggest that the phosphate tweezer **133** is the best inhibitor of aggregation and toxicity of amyloid proteins. The other three tweezers are little less effective against the aggregation and also proved to be

slightly toxic at the higher concentrations. Results on the phosphate tweezer **133** are published elsewhere[88] and the results obtained for the tweezers **161** and **150** are summarized here. The data for the phosphonate tweezer **734** are not presented here.

Inhibition of protein aggregation was performed by using the Thioflavin T (ThT) assays. For this, Aβ42 and IAPP were incubated with ThT in the absence and presence of molecular tweezers. The β-sheet formation was measured by monitoring the fluorescence change of ThT. Both the tweezers partially inhibit the aggregation processes at 1:1 Aβ42:tweezer ratio. Not completely, but substantial inhibition is achieved at the 10-fold excess of the tweezers. CLR04 is slightly superior to CLR05 (Figure 3.14). Inhibition effects of CLR04 are even stronger against IAPP aggregation and at 1:1 ratio almost complete inhibition of aggregation is observed. CLR05 shows complete inhibition of IAPP fibrils at the 10-fold excess.

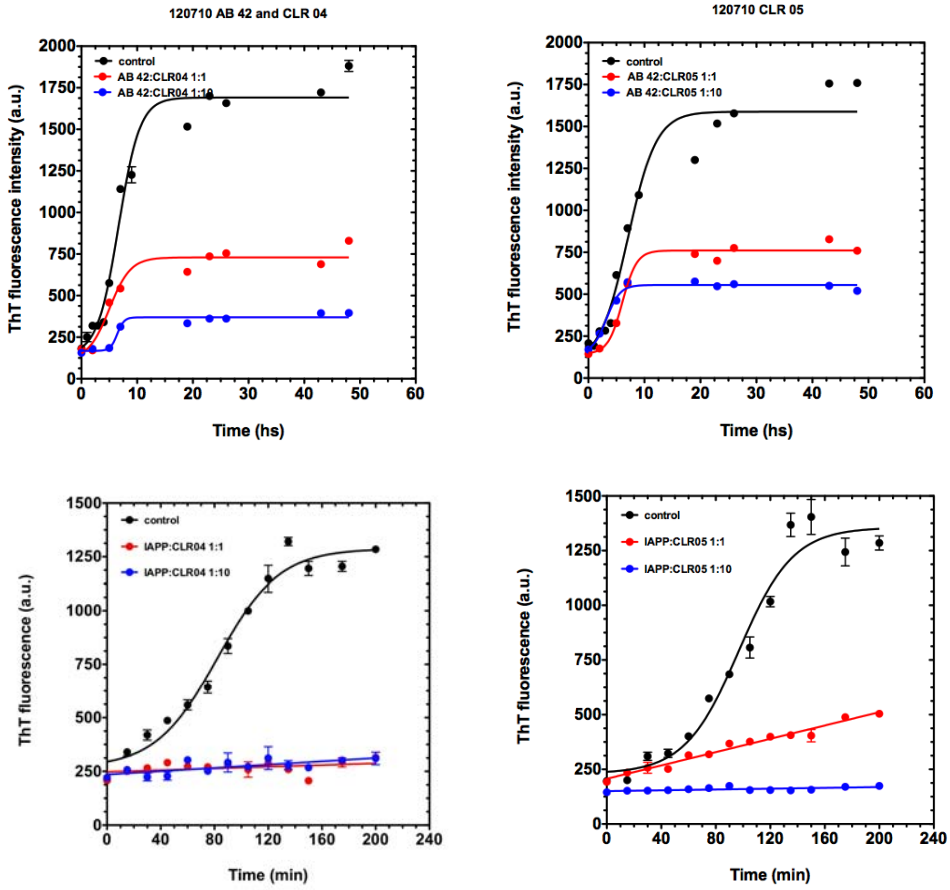

Figure 3.14 Inhibition of β-sheet formation by the molecular tweezers CLR04 and CLR05 as measured by ThT assay.

When the samples incubated in the absence of the tweezers were measured by electron

microscope, abundant thread like fibrils were observed (Figure 3.15). Aβ42 samples at the equimolar ratio of the tweezers, showed less fibrils together with other amorphous structures. At the 10-fold excess of CLR04 almost amorphous structures were dominant, while at the 10-fold excess of CLR05 substantial amount of fibrils were still observed. At 1:1 ratio of IAPP:CLR04, only amorphous structures were observed, as also observed by ThT assays. On the other hand, CLR05 also reduce the burden of IAPP fibrils at 1:1 and more at 1:10 ratio, but complete inhibition is not observed. All these data correlate with the ThT results and are in good agreements with the observed affinities of these tweezers towards the basic amino acids.

To examine whether these tweezers can also protect the cultured cells against the toxicity of amyloid and IAPP proteins, MTT (3-(4,5-dimethylthiazol-2-yl)-2,5-diphenyltetrazolium bromide) reduction assays were performed. Both the tweezers **161** and **150** did not rescue the cells from Aβ42 and IAPP toxicity upto 30 μM (3-fold access) concentrations. Moreover, both the tweezers are found slightly toxic to the cells at 100 μM concentrations.

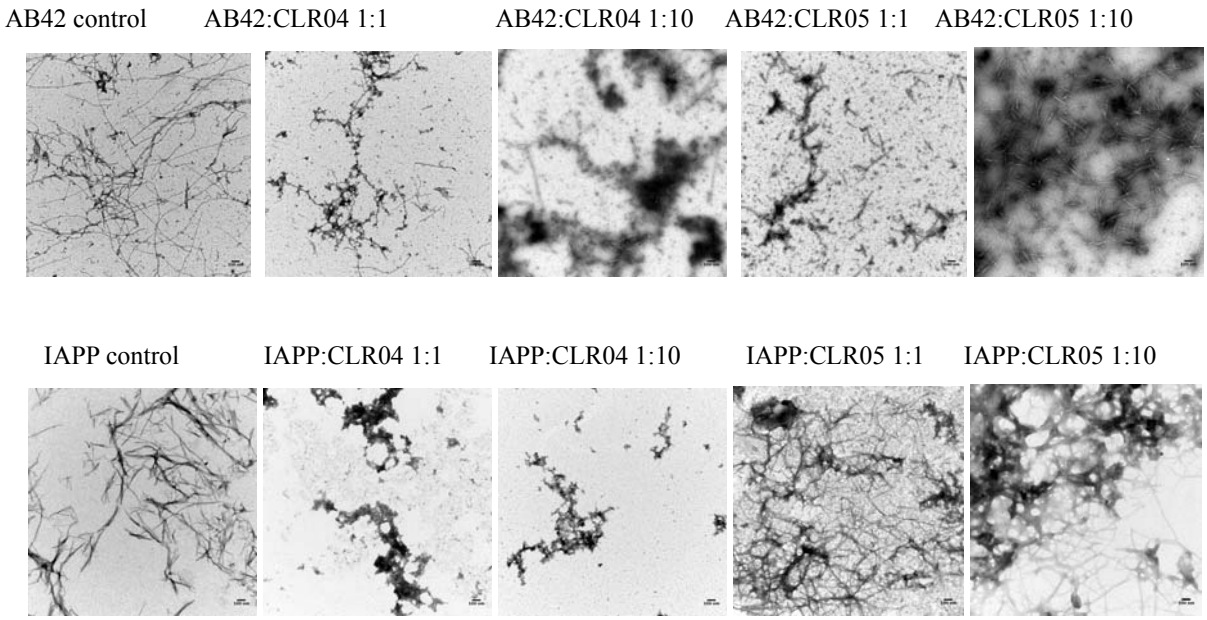

Figure 3.15 Electron microscope images of the aggregation reaction of Aβ42 (first row) and IAPP (second row) in the absence or presence of CLR04 and CLR05.

The biophysical assays have shown that the new sulfate tweezer **161** and carboxymethyl tweezer **150** can effectively interfere in the abnormal aggregation process of amyloid-β and IAPP. The sulfate tweezer **161** appears to be effective almost similar to the tweezer **133**. Less aggregation inhibition by the tweezer **150** compared to the phosphate tweezer **133** can be expected due to the

lower affinity of the tweezer **150** for lysine and arginine derivatives. The tweezers **161**, **150** and **734** are slightly toxic in cell culture assays at relatively high concentrations. Only the phosphate tweezer **133** prove to be the precious tweezer candidate in inhibiting the aggregation process as well as recovering the cell viability without showing any significant toxicity until 200 μM concentration.

3.2.4 Studies of the 1st generation unsymmetrical linker tweezers

In the second part of the work, unsymmetrical molecular tweezers that carry a phosphate group on one side and a linker or additional recognition unit on the other side of the tweezer's central benzene ring were synthesized and studied. The structures of these unsymmetrical linker tweezers are shown in Figure 3.16.

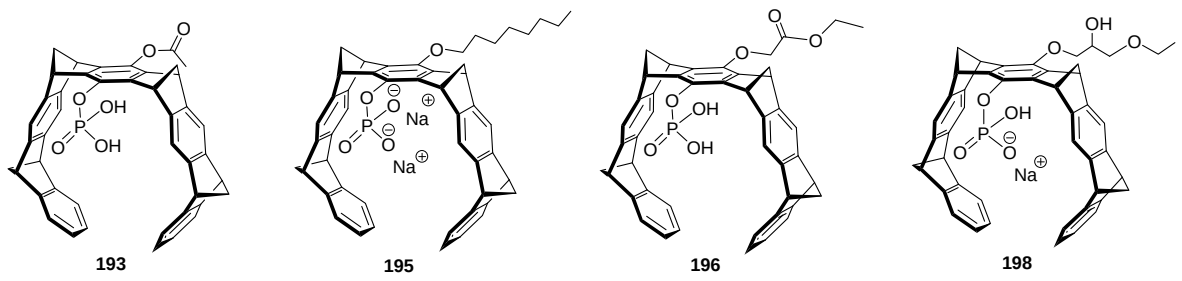

Figure 3.16 Structures of the 1st generation unsymmetrical phosphate tweezers.

3.2.4.1 Characteristics of the unsymmetrical linker tweezers

Inspection of ^{1}H-NMR spectra of the pure tweezers in methanol and mixture of methanol and buffer revealed that the short acetyl tether in tweezer **193** does not undergo self-inclusion in the tweezer's cavity. However, the highly flexible ether moieties in tweezer **196** ($\Delta\delta \sim 2.0$ ppm in methanol/buffer 2:1) as well as in tweezer **198** ($\Delta\delta \sim 1.0$ ppm in methanol/buffer 2:1) displayed significant upfield-shifts compared with their isolated counterparts. These chemical shifts indicate that especially the terminal methyl groups of the linkers point inside the open cavity. The size of this effect depends on the polarity of the solvent and increases from methanol to water – obviously a hydrophobic interaction. Interestingly, the octyl derivative does not include its alkyl chain inside the cavity – a counterintuitive observation. The aromatic tweezer signals do not show any concentration-dependent upfield-shifts and thus confirm the absence of entangled dimers; in addition, no experimental evidence was found for intermolecular self-association.

For the tweezer **195** in the free phosphate form and for its protected dimethyl phosphate precursor, crystals could be grown whose X-ray diffraction gave rise to 3D structures with intriguing properties. Due to severe disorders, the crystals of the free phosphate tweezer **190** diffracted rather poorly and for this reason the resolution of the electron density is too low to obtain a well refined structure model. Nonetheless, the connectivity and the general morphology of the molecule can be taken for granting bond length and angles however are not reliable. In accordance with the NMR evidence, no intramolecular alkyl inclusion takes place, but the n-octyl chain is instead engaged in numerous van-der-Waals contacts to aromatic CH-groups as well as CH-л interactions with its own and other aromatic tweezer moieties. Only the crystal packing (Figure 3.17) brings forward some intermolecular inclusion effects for dimethyl phosphate precursor **182**. In this case, methyl group of phosphate pointed inside the cavity of the next molecule while dispersed the octyl chain over the top surface of another molecule.

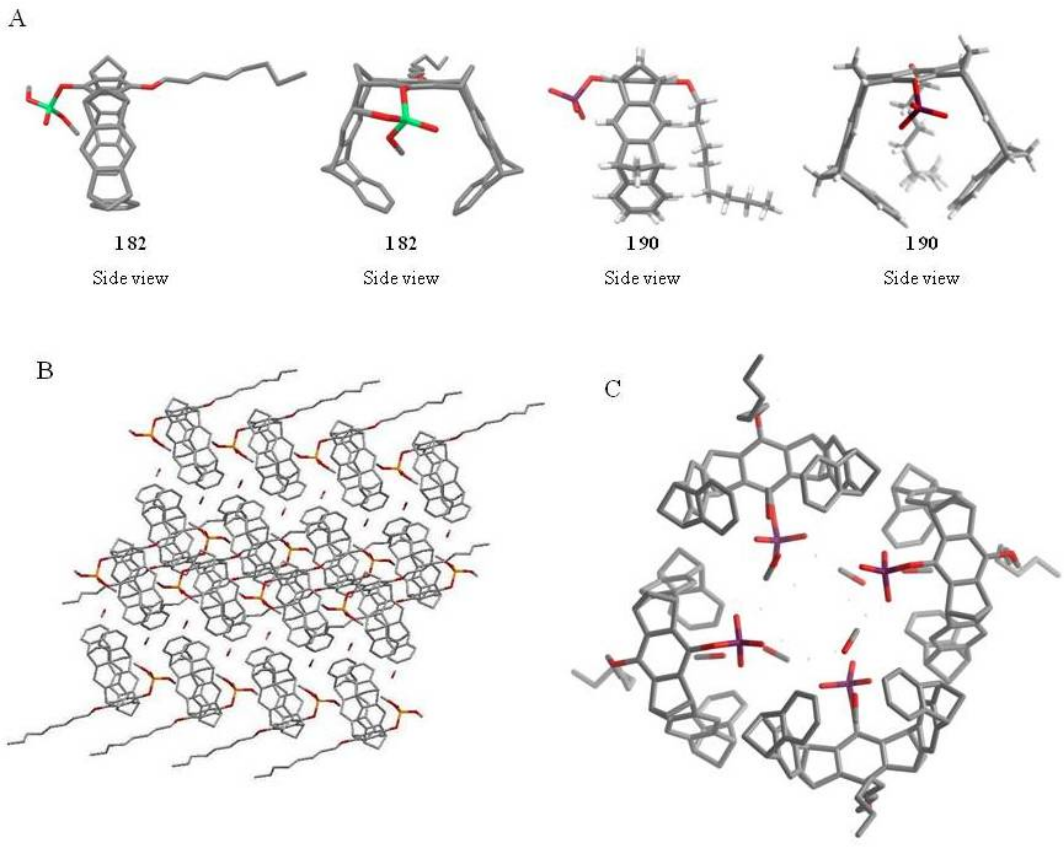

Figure 3.17 (A) crystal structures of the octyl dimethylphosphate tweezer **182** and the octyl phosphate tweezer **190** obtained in methanol-pentane mixture. (B) Crystal packing of the tweezer **182**; (C) crystal packing of the tweezer **190**. A molecule of methanol is inserted inside the cavity and makes a hydrogen bond with the phosphate group. Non polar hydrogen atoms are omitted for clarity.

The packing of free phosphate tweezer **190** showed assembly of four molecules where the phosphate groups head in the interior and the rest of the hydrophobic tweezer and octyl chain make the exterior surface that is exposed to the less polar solvent (Figure 3.17C) Interestingly, a molecule of methanol was found in the cavity and locked by hydrophobic and hydrogen bonding interactions.

Molecular mechanics calculations followed by extensive Monte-Carlo simulations were carried out for all the tweezer derivatives **193-198**, and the best final structures (Figure 3.22,first row) which were confined to a narrow energy window of 10 kJ/mol were analyzed with respect to their conformational preference (Maestro 9.2, OPLS_2005, water, 5000 steps). The results beautifully confirmed the NMR-spectroscopic evidence: Open conformations prevail for monoacetoxy tweezer **193**, with its carbonyl group always pointing away from the cavity. By contrast, the octyl chain in tweezer **195** remains in close van-der-Waals contact with the CH groups flanking the cavity opening, precisely as depicted in the crystal structure. The flexible ester and ether tethers in tweezers **195** and **196**, finally both insert their terminal ethyl group into the tweezer cavity, in perfect agreement with the observed upfield-shifts in the ^{1}H NMR spectrum. It may be hence expected, that tweezer **193** with its open cavity is superior in binding of amino acid and peptide guests, whereas the octyl group in tweezer **195** blocks the cavity entrance and in tweezers **196/198**, the cavity is already occupied, leading to lowered guest affinities.

3.2.4.2 Guest binding of unsymmetrical tweezers with amino acids and peptides

For a reliable determination of affinities of new unsymmetrical tweezers towards the *N/C*-protected amino acids and peptides fluorescence titrations were carried out in aqueous phosphate buffer. The high fluorescence emission intensity of the tweezer skeleton is efficiently quenched by guest binding, if the guest is included inside the cavity (vide infra). Dissociation constants (K_d) cover a relatively broad range from the low millimolar to the low μM regime.

Affinities of linkers with ester moieties (**193** and **196**) are substantially higher than those for tethers with ethers and alcohols (**195** and **198**). Thus, the octyl and the self-included glycerol side chain represent the most critical obstacle for guest inclusion.

Table 3.9 Dissociation constants K_d [μM] of the unsymmetrical tweezers with lysine- and arginine-containing guests measured in phosphate buffer (10 mM, pH 7.6) by the fluorescence titration experiments.

Substrate	**K_d [μM]**		
	193	**196**	**198**
AcLysOMe	34 ± 10 %	44 ± 4 %	362 ± 23 %
KAA	100 ± 7 %	-	-
KLVFF	44 ± 8 %	114 ± 14 %	-
IAPP (1-7)	41 ± 12 %	118 ± 6 %	-
AcArgOMe	44 ± 13 %	92 ± 7 %	617 ± 42 %
IAPP (2-14)	82 ± 17 %	96 ± 36 %	-

As usually observed, affinities for lysine are 2-3 times higher than those for arginine, with one interesting exception: The short acetyl derivative **193** binds arginine as well as lysine with comparable affinities (K_d < 50 μM). Its K_d value is the second lowest among the reported tweezers to date for an arginine derivative in aqueous buffer and holds promise for specific interference with biological processes which critically depend on strategic arginine residues.

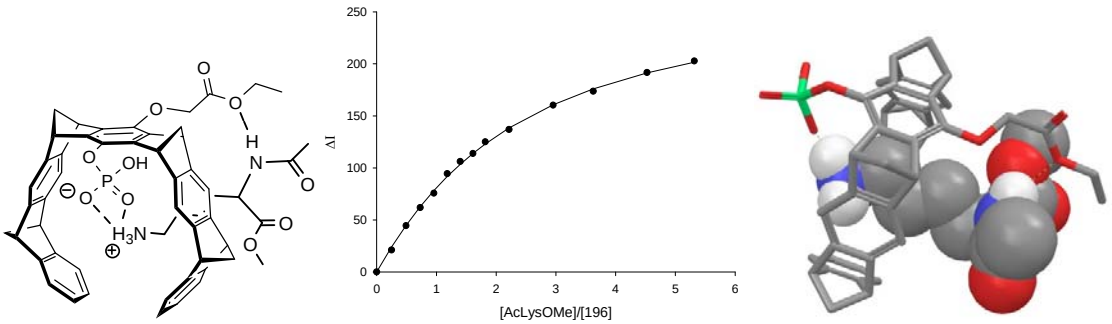

Figure 3.18 Left: Schematic representation of the preferred complexation mode for Ac-Lys-OMe by the tweezer **196**; center: fluorescence titration binding isotherm; right: Monte-Carlo simulation.

Comparisons with reference monophosphate tweezer **130** reveal that the simple linkers in **193** and **196** render these superior to the unsubstituted monophosphate tweezer **130** and comparable in affinity to an elaborate specialized tweezer. Hence, the acetyl group in **193** as well as the ethoxycarboxylmethyl group in **196** must take part in molecular recognition of their amino acid guests in a positively cooperative manner. A schematic representation of interactions between the tweezer **196** and lysine guest AcLysOMe, the binding isotherm obtained by the nonlinear regression fitting and a molecular modeling structure are shown in Figure 3.18.

NMR experiments offer more structural information than fluorescence titrations, if chemical shift changes of sensor protons occur during the addition of the host to its amino acid guest. All new tweezer derivatives were therefore first measured alone and then their complexes with AcLysOMe and AcArgOMe in methanol:buffer (2:1). In all cases, lysine methylene signals become broadened and shifted upfields, indicating specific inclusion of its ammonium butyl side chain. These chemical shift changes are accompanied by sizeable downfield shifts of the self-included receptor tethers of **196** and **198**. With increasing excess of the lysine guest, the receptor molecule releases its unpolar arm from its own cavity to accommodate the amino acid side chain – a beautiful illustration of two competing inclusion processes, one of which benefits not only from hydrophobic, but also from electrostatic interactions.

Table 3.10 NMR chemical shifts of the side-chain protons of AcLysOMe in the different ratio with the different tweezers in the methanol/buffer (2:1).

Tweezer	ratio (TW/AAs)	6-H	5-H	4-H	3-H	2-H
193	2:1	a	a	a	a	0.09
	1:1	a	0.28	0.66	0.33	0.07
	1:2	a	0.16	0.46	0.22	0.05
	1:4	0.45	0.08	0.28	0.14	0.03
198	3:1	a	a	a	a	0.06
	1:2	>0.40	0.08	0.24	0.13	0.03
	1:4	0.26	0.02	0.10	0.08	0.02
196/203	2:1	a	0.13	0.40	0.21	0.06
	1:2	>0.50	0.09	0.29	0.15	0.04
	1:4	0.30				
195	2:1	a	0.11	a	0.17	0.05
	1:2	0.20	0.00	0.00	0.06	0.02

a: signal was not detected or identified.

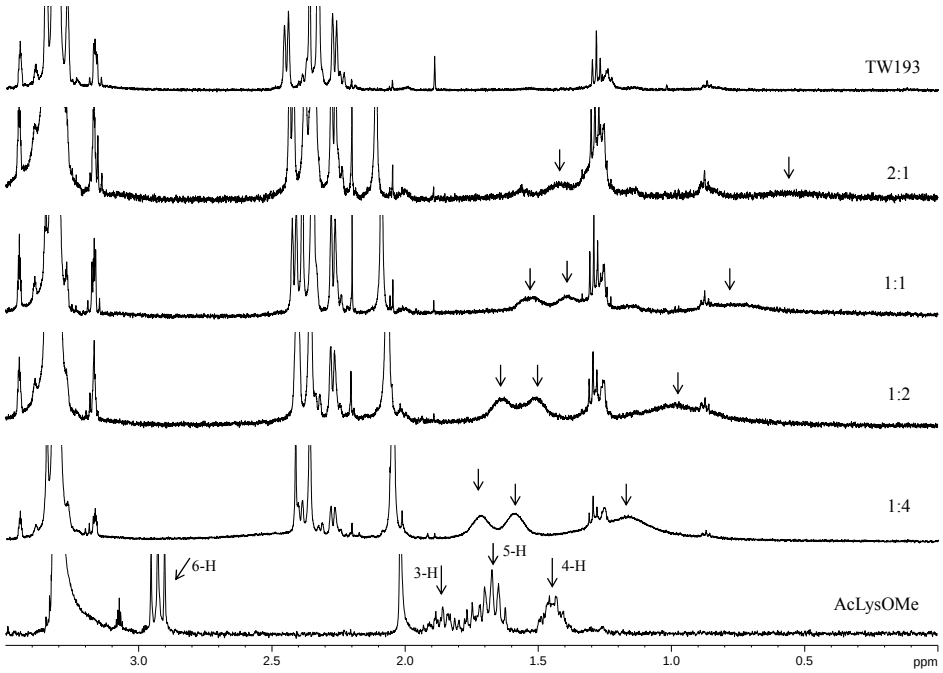

Figure 3.19 NMR spectra of the tweezer **193**, AcLysOMe and **193**:AcLysOMe (2:1, 1:1, 1:2 and 1:4) in CD_3OD/D_2O buffer (2:1). All the side-chain protons and particularly, 6-H protons of Lys at 2.9 ppm become very broad and shifted upfield.

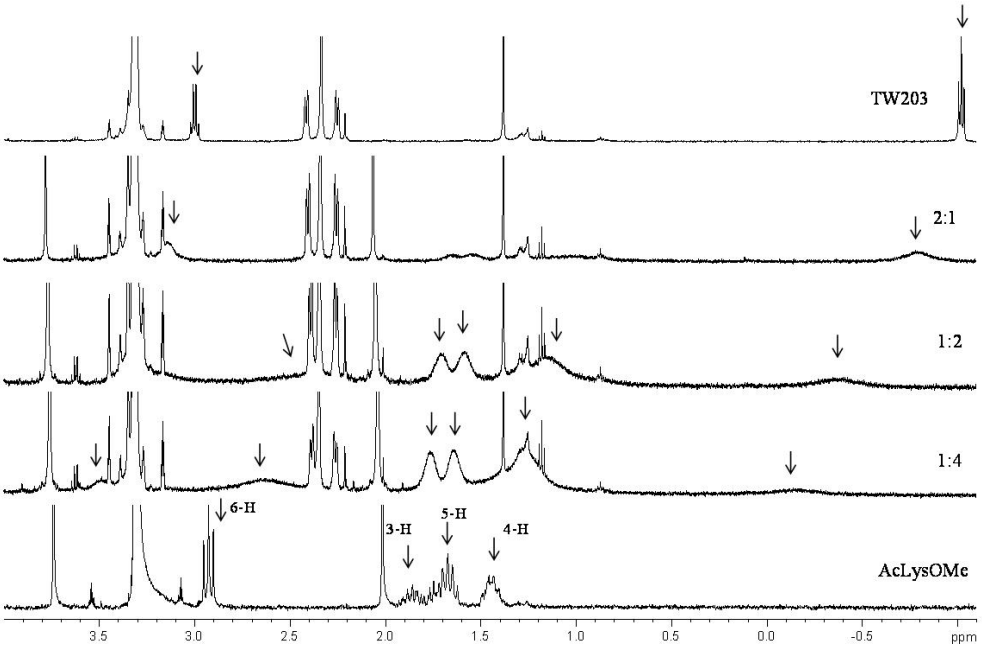

Figure 3.20 NMR spectra of the tweezer **203(196)**, AcLysOMe and **203**(**196**):AcLysOMe (2:1, 1:2 and 1:4) in CD_3OD/D_2O buffer (2:1).

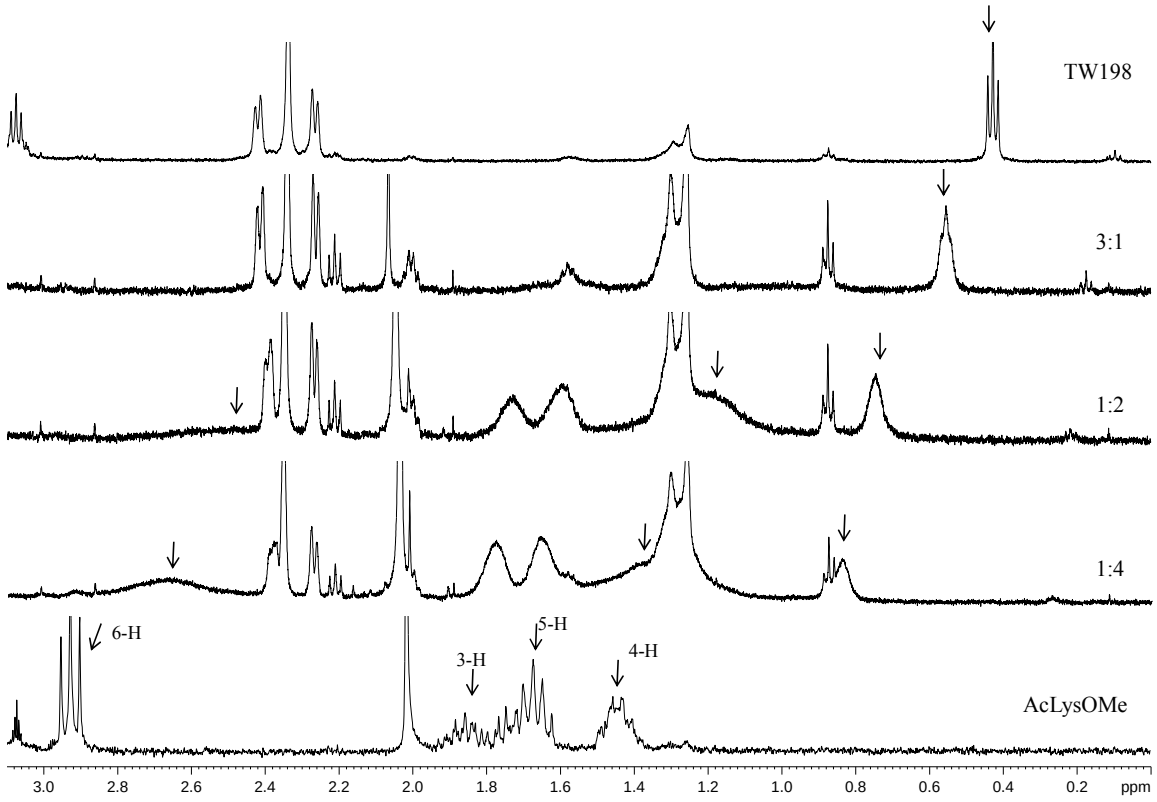

Figure 3.21 NMR spectra of the tweezer **198**, AcLysOMe and **198**/AcLysOMe (3:1, 1:2 and 1:4) in CD_3OD/D_2O buffer (2:1).

The structural informations available from NMR and fluorescence experiments were feed into starting geometries for molecular mechanics calculations of all lysine and arginine complexes with the unsymmetrical phosphate tweezers. Minimizations were followed by Monte-Carlo and subsequent Molecular Dynamics simulations. In all lysine complexes the C-4 side-chain is easily threaded through the tweezer cavity and locks its ammonium cation into a strong ion pair with the phosphate anion, without the need to pay the penalty for phosphate desolvation.

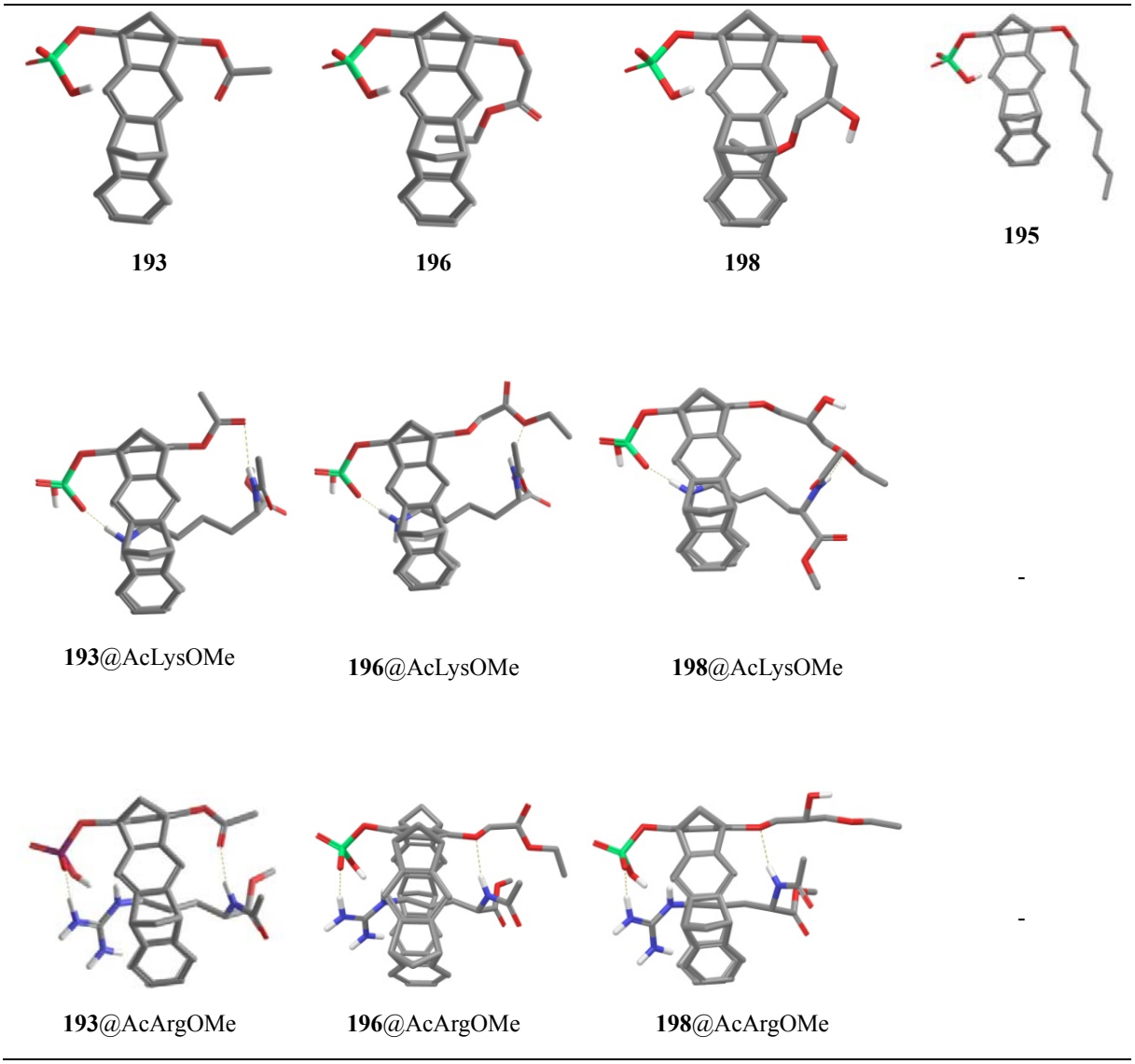

Figure 3.22 Side views of molecular modeling structures of the unsymmetrical linker tweezers (**193-198**) and their complexes with amino acid AcLysOMe and AcArgOMe.

Arginine derivatives can in principle also be drawn into the tweezer's cavity. Now cation-л interactions must replace the polar interaction with the solvent shell, but these are much weaker: according to seminal work by the Dougherty (and Schneider) group, cation- л attraction for a guanidinium cation and one benzene ring amounts to 1 kcal/mol. But this case does not seems to be dominant in unsymmetrical tweezers, as in the calculated minimum energy structures, the side chain of arginine penetrates more deeper into the cavity and guanidinium group stay out where it can be solvated in solution and make ion pair with the phosphate group.

Additional attractive interactions occur between oxygen atoms of the tethers and -NH proton of guest amide. These backbone hydrogen bonds are especially effective in complexes with tweezers **193** and **196** as reflected by their greater affinities compared to the hydroxyl monophosphate tweezer **130** which lack the additional interactions of linker with amino acid backbone –NH protons.

Interestingly, molecular dynamics calculations of the two best complexes **193**@AcArgOMe and **196**@AcLysOMe show intact complexes even after more than 50 ns of simulation time. A small difference occurs in the complex **196**@AcLysOMe**,** where linker flips vertically at 180^{o} and exchanged the hydrogen bond between its two ester oxygen to the same guest amide NH group.

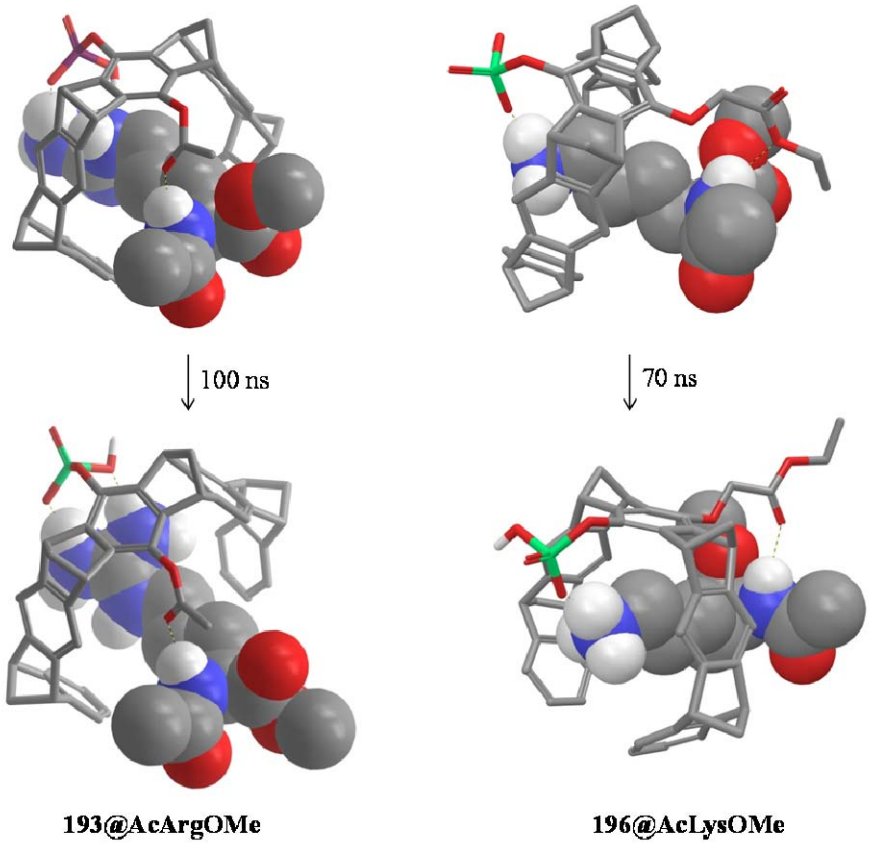

Figure 3.23 Molecular dynamic simulation structures of the complex **193**@AcArgOMe after 100 ns and the complex **196**@AcLysOMe after 70 ns (Maestro 9.2, OPLS_2005, H_2O). Starting structures are minimum energy conformations from Monte-Carlo simulations.

In summary, new unsymmetrical monophosphate tweezers have been synthesized, which carry ester or ether linkers on the opposite side. From fluorescence and NMR binding studies with N/C-protected basic amino acids the following lessons can be learnt: 1) Long alkoxyalkyl tethers

lower tweezer affinities for basic amino acids by competing self-inclusion (**196, 198**); 2) long alkyl chains form multiple van-der-Waals contacts with the tweezers' aromatic side walls (dispersive and CH-л interactions) and thus sterically block the entrance to the cavity; 3) short esters seem to keep the cavity open; 4) for a potential unsymmetrical tweezer, its linker must be able to interact a guest and involve cooperatively in molecular recognition. The acetyl tweezer **193** binds with similar affinities to lysine and arginine which now opens the door for specific interaction with biological processes which rely on critical arginine residues.

From the above-discussed, ester links seem to guarantee an open tweezer cavity for both lysine and arginine derivatives. However, for their use, hydrolysis at lower or higher pH or by enzymes must be prevented by all means. For this reason, slim ester types with pronounced stability towards pH changes must be found; alternatively, the OH group of the hydroxymonophosphate tweezer **130** could be replaced by a primary amine via Smiles rearrangement.[133,134] Its connection to secondary binding sites could then be smoothly effected with carboxylic acid derivatives.

3.2.5 Solvent polarity effects on complexation

In the above section we have seen that the stoichiometric ratios were varied from host excess over 1:1 ratio to guest excess in methanol/buffer (2:1), but only small chemical shifts were observed in guest protons. The observed small chemical shifts do not correlate with the fluorescence results obtained in buffer solution. We assumed that complex formation may not be very strong in the presence of methanol. This can be due to less solvent polarity and risk of methanol to accommodate into the tweezer's cavity as seen in the crystal structure. So, we investigated the polarity effects on complex formation of selected host/guest by varying the ratio of methanol/buffer from pure methanol to 1:9 methanol:buffer. Chemical shift changes of the most shifted protons of the guests in the 1:1 ratio of host/guest are listed in the Table 3.11. The data indicate that the difference in chemical shifts increases with the increased solvent polarity. The data also reflect that even the small amount of methanol (10%) influence the guest inclusion into the tweezer's cavity. For example, chemical shift change for the complex **133**@AcArgOMe in 10% methanol ($\Delta\delta_{obs}$ = 2.16 ppm for 5-H) decreased more than 1 ppm compared to complex in pure buffer solution ($\Delta\delta_{obs}$ = 3.30 ppm for 5-H). Due to the low solubility it was not possible to use pure buffer solution in case of the unsymmetrical tweezer **193**. Two observations in pure methanol were surprising: first, complex **133**@AcLysOMe showed two sets of lysine signals,

though not significantly upfield shifted; second, the chemical shifts of complex **161**@AcLysOMe were similar to those in pure buffer, but the chemical shift difference decreased substantially (~ 2 ppm) for **161**@AcArgOMe. The ITC data together with the negligible NMR chemical shifts of lysine protons for the complex **133**@AcLysOMe in methanol indicate that the binding of lysine does not occur inside the tweezer's cavity but occurs outside. Therefore, the observed binding affinity (172 μM) is purely based on the electrostatic and hydrogen bonding interactions between the phosphate anions of the tweezer and the lysine.

Next, the important question arises whether under the same conditions the change in chemical shifts can be correlated with the fluorescence changes and the dissociation constants obtained by the fluorescence spectroscopy. To find out some correlations among these parameters, fluorescence titrations were carried out in the different polarity medium of methanol-buffer mixture (Table 3.12). In methanol, lysine form similar complex with the sulfate tweezer **161**, while 6 times weaker complex with the phosphate tweezer **133** compared to the respective complexes in buffer solution. These data suggest that the phosphate and the sulfate groups behave significantly different in the two solvents. Therefore, different solvation or different interactions of these anions with the solvent molecules are responsible for the difference in their guest binding. As observed in most of the cases, changes in the fluorescence and the binding affinities (Table 3.12) depend on solvent polarity and increase with the more buffer content and correlate with the changes in chemical shifts (Table 3.11). From the data obtained, we can draw a conclusion as:

More polar solvent ~ large chemical shift difference ~ large fluorescence change ~ strong complex formation.

Table 3.11 Observed chemical shift changes [in ppm] of guest protons in 1:1 ratio with the tweezers **133**, **161**, **193** in increasing polarity solvents. In mixtures of solvents, the chemical shifts in pure methanol were used as reference and changes in the chemical shifts of the lysine/arginine protons were measured relative to reference shifts.

Receptor	**Substrate** (concentration)	**solvent**	$\Delta\delta_{obs}$(6-H)	$\Delta\delta_{obs}$ (5-H)	$\Delta\delta_{obs}$ (4-H)
Phosphate tweezer **133**	AcLysOMe (1.0 mM)	CD_3OD	0.09, 0.24[b]	0.0, 0.28	-0.04, 0.26
		CD_3OD:PB (1:2)	2.80	2.30	0.74
		PB	3.60	3.40	1.60
	AcArgOMe (1.0 mM)	CD_3OD		0.76	0.44
		CD_3OD:PB (2:1)		0.72	0.46
		CD_3OD:PB (1:2)		1.45	0.96
		CD_3OD:PB (1:9)[a]		2.16	1.47
		PB		3.30	2.19
Sulfate tweezer **161**	AcLysOMe (1.0 mM)	CD_3OD	2.96	3.25	1.75
		PB	3.40	3.30	1.30
	AcArgOMe (1.0 mM)	CD_3OD		0.67	0.30
		PB		2.67	1.70
Acetoxy tweezer **193**	AcArgOMe (0.4 mM)	CD_3OD		0.0	0.0
		CD_3OD:PB(2:1)		0.09	0.06
		CD_3OD:PB(1:4)		0.27	0.18
		CD_3OD:PB(1:9)		0.60	0.38

a: Concentrations for this measurement were 0.5 mM for both host/guest. b: the signal for these protons were split into two different signals. PB: phosphate buffer (10 mM, pH 7.2).

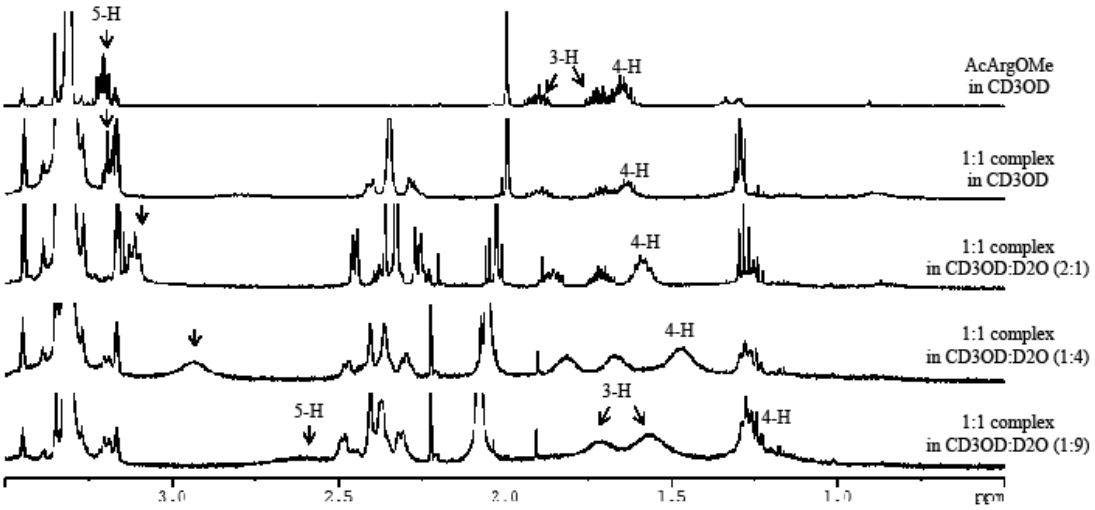

Figure 3.24 ^{1}H-NMR spectra of 1:1 complexes of **193**@AcArgOMe in methanol-buffer (10 mM, pH 7.6) mixtures. With the increasing water content, the spectra shows gradual upfield shifts of arginine protons assigned by numbers.

Table 3.12 Dissociation constant K_d [μM] and (ΔI_{max} [%] = 100 • (I_0-I_{max}) / I_0) fluorescence change of tweezer **133**, **161**, **193** and **196** with lysine and arginine in the varying polarity solvent (methanol - buffer, 10 mM, pH 7.6) measured by fluorescence titrations.

Receptor	Guest	Medium	K_d [μM]	ΔI_{max} [%]
Phosphate tweezer **133**	AcLysOMe	MeOH	66 ± 11 %	-6
		PB	9 ± 6 %	40
	AcArgOMe	MeOH	-	-
		MeOH:PB (2:1)	-	-
		MeOH:PB (1:9)	± 8 %	27
		PB	20 ± 5 %	47
Sulfate tweezer **161**	AcLysOMe	MeOH	20 ± 6 %	-44
		PB	19 ± 3 %	44
	AcArgOMe	MeOH	276 ± 7 %	-22
		PB	77 ± 5 %	30
Acetoxy phosphate tweezer **193**	AcLysOMe	MeOH	641 ± 11 %	-50
		MeOH:PB (1:4)	192 ± 35%	-10
		MeOH:PB (1:9)	-	-
		PB	34 ± 10 %	34
	AcArgOMe	MeOH	-	-
		MeOH:PB (1:4)	n.d.	3
		MeOH:PB (1:9)	167 ± 41%	6
		PB	44 ± 13 %	31
Ethoxycarboxylmethyl phosphate tweezer **196**	AcLysOMe	MeOH	-	-
		MeOH:PB (2:1)	-	-
		MeOH:PB (1:9)	n.d.	2
		PB	44 ± 4%	46
	AcArgOMe	MeOH	-	-
		MeOH:PB (2:1)	-	-
		MeOH:PB (1:9)	n.d.	4
		PB	92 ± 7%	40

PB: phosphate buffer (10 mM, pH 7.6); F. L.: Fluorescence; n.d.: not determined

In conclusion, the above data indicate that the complex formation is very sensitive to the solvent and solvent polarity. Most of the tweezers either do not bind to any guest in methanol or bind very weakly. Inclusion of methanol into the tweezer's cavity lowers the affinity of any guest. Also, the large hydrophobic tweezers and side-chain of lysine or arginine guests can separately be more solvated in methanol compared to aqueous solution, and therefore, host and guest do not interact in methanol as strongly as in buffer solution. Complex **161**@AcLysOMe is an exception case which has similar affinities in both the methanol and buffer. The molecular tweezers operate best in aqueous solutions that make them best suitable to use under the physiological conditions in biological systems. High affinity complexes in aqueous solution are formed due to the hydrophobic association of a tweezer and alkyl side-chain of a guest which are otherwise poorly solvated in aqueous solution. Remarkably, a correlation could be established in the chemical shift

changes, fluorescence change and binding affinity as: more polar solvent ~ large chemical shift difference ~ large fluorescence change ~ strong complex formation.

3.2.6 Study of the phosphate tweezer 133 binding to IAPP

All the biophysical and cell culture experiments (ThT assays, EM, CD and MTT assays) were performed in collaboration with Prof. Gal Bitan at neurology department, university of California, LA, USA. The molecular dynamics (MD) simulations of the tweezer **133** and IAPP were performed in collaboration with Prof. Elsa Sanchez at MPI Mulheim, Germany. I contributed the tweezer **133**(CLR01) for the above studies and investigated the binding sites of the tweezer **133** on IAPP fragments by using the ^{1}H-NMR and fluorescence titration experiments.

Type 2 diabetes mellitus (T2DM) is the most common amyloid-related disease affecting hundreds of millions of people worldwide[135]. It is closely associated with obesity and elevated blood glucose levels. T2DM abnormality include ocular, renal, cardiovascular, and neurologic complications[136], increasing morbidity and mortality[137] and causing substantial economic and public health burden[138].

In T2DM, Islet amyloid polypeptide (IAPP) self-assembles into toxic oligomers that cause β-cell-membrane damage and apoptosis, and later precipitates as extracellular pancreatic amyloid. Therefore, preventing IAPP self-assembly is a promising strategy for developing disease-modifying therapy for T2DM. IAPP is a 37-residue polypeptide pancreatic hormone synthesized and secreted with insulin.[139] Since IAPP has one Lys residue at position 1, therefore, inhibition of aggregation and toxicity of IAPP by the molecular tweezer **133** can be expected. The mechanism of the tweezer **133** inhibition of IAPP assembly and toxicity is investigated using a combination of cell viability assays, biophysical methods, spectroscopic and computer modeling. Since there is only one Lys and that too at position 1, the tweezer **133** was not expected to inhibit aggregation and toxicity of IAPP very effectively. However, using ThT fluorescence and electron microscopy (EM), Bitan group showed that the tweezer **133** inhibits IAPP to β-sheet and fibril formation at 1:1 ratio. Even more surprisingly, the tweezer **133** inhibits IAPP aggregation at low sub-stoichiometric concentrations, whereas inhibition of toxicity required excess of the tweezer **133**. Circular dichroism (CD) studies showed different conformations adopted by IAPP alone (α-helix) and IAPP in the presence of the tweezer **133** (α-helix and β-sheet), which are in good agreements with ThT and EM. IAPP is known to cause β-cell death predominantly by inducing

apoptosis.[140] At 10-fold excess, the tweezer **133** inhibits IAPP-induced apoptosis in RIN5fm cells completely.

To find out whether binding to only Lys1 mediated the tweezer **133** inhibition of IAPP aggregation and/or toxicity or is there other binding sites of the tweezer **133** in IAPP, Bitan group investigated the effect of the tweezer **133** on the truncated $IAPP_{2–37}$. Surprisingly, in the presence of equimolar ratio of the tweezer **133**, no increase in ThT fluorescence was observed and only amorphous structures were detected. These results suggest that the tweezer **133** completely inhibit the β-sheet and fibril formation of $IAPP_{2–37}$. The cell viability measured by MTT assay in ArgIN5fm β-cells and $IAPP_{2–37}$ showed that the tweezer **133** protected the cells against $IAPP_{2–37}$ induced toxicity even in the absence of the Lys1 binding site. Taken together, the data obtained with $IAPP_{2–37}$ strongly supported the existence of an additional binding-site on IAPP for the tweezer **133**.

Using the solution-state ^{1}H-NMR experiments, we investigated the binding of the tweezer **133** to unlabeled N-terminal fragments of IAPP. To explore the tweezer **133** binding to Lys1, ^{1}H-NMR of $IAPP_{1-7}$ at different ratios with the tweezer **133** were measured. Already at 1:1 concentration ratio of the peptide and the tweezer **133**, all the Lys side chain methylene signals shift drastically upfield into the negative-ppm range (Figure 3.25), indicating inclusion of the Lys1 side chain inside the tweezer's cavity. No further change occurred at 3-fold excess of the tweezer **133**. The Lys1 side-chain protons are assigned by ^{1}H-^{1}H COSY spectrum (Figure 3.26) which led to determine the $\Delta\delta_{obs}$ values (4.4 and 4.5 ppm for the δ and ε protons, respectively). To identify whether the tweezer **133** binds to the disulfide bridge present between the residues Cys2 and Cys7, we measured the NMR of $IAPP_{2–7}$ and the tweezer **133**. In contrast to $IAPP_{1–7}$, no change was observed in the spectrum of $IAPP_{2–7}$ even in the presence of 3-fold excess of the tweezer **133** (Figure 3.27) indicating that the presence of Lys1 was essential for the tweezer **133** binding to $IAPP_{1–7}$.

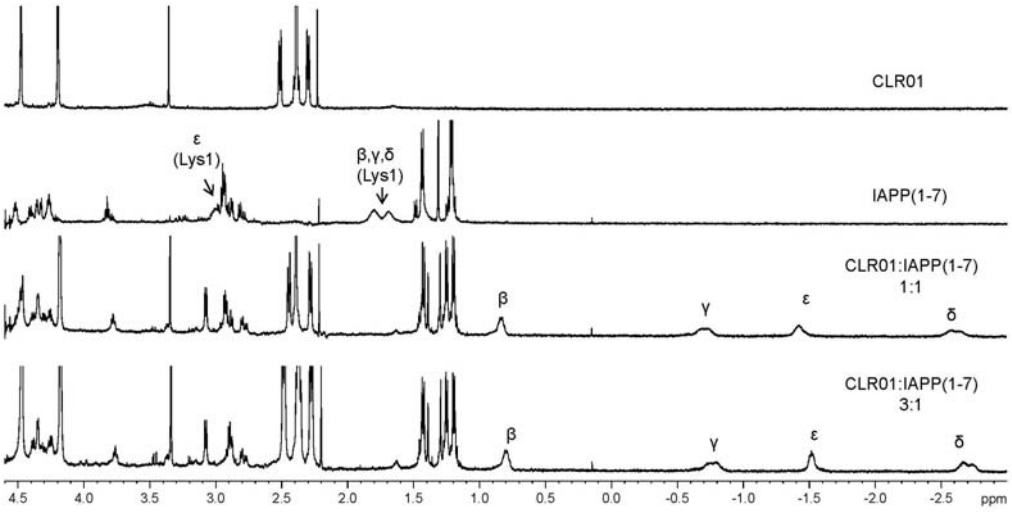

Figure 3.25 $IAPP_{1-7}$, tweezer **133**, and their 1:1 or 1:3 complexes in 10 mM phosphate-buffered D_2O, pH 7.2. The Lys1 side-chain methylene signals are assigned as α, β, γ, δ and ε from COSY. All the methylene resonances, most notably the δ- and ε-protons, are shifted upfield by 4.4 and 4.5 ppm, respectively, indicating strong binding of tweezer **133** to Lys1.

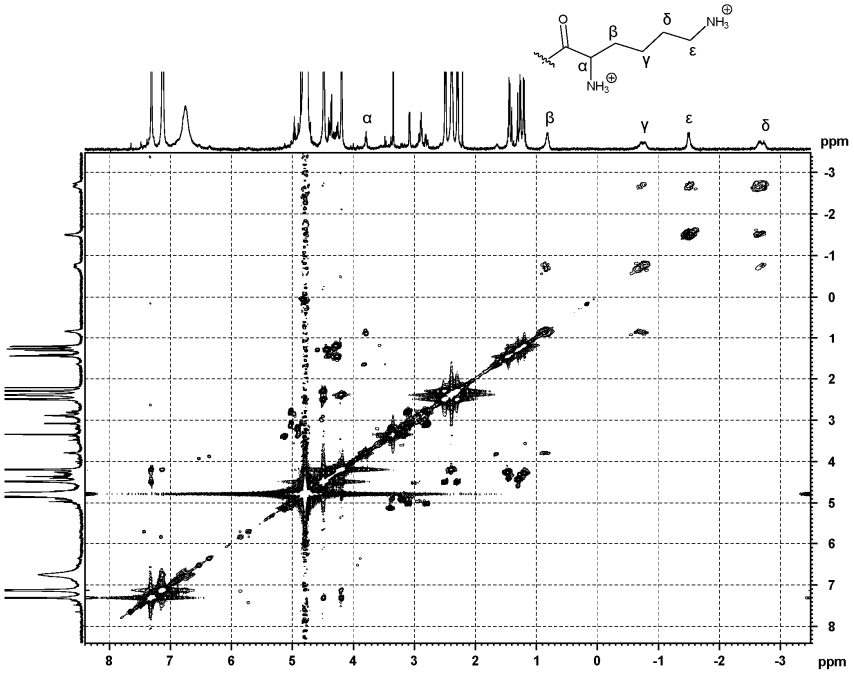

Figure 3.26 gs-H,H-COSY NMR of 3:1 molar ratio of tweezer **133**:$IAPP_{1-7}$, respectively, in D_2O phosphate buffer. Lys1 side chain protons in the complex are assigned as α, β, γ, δ and ε.

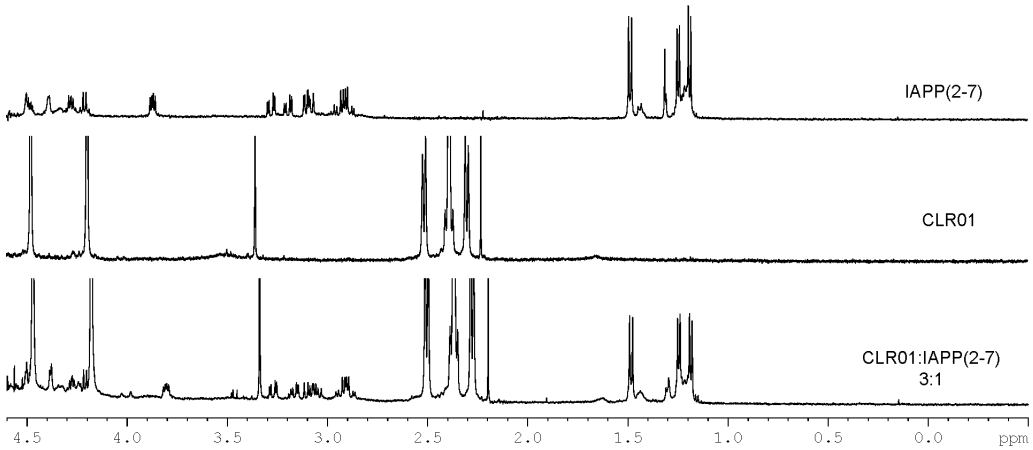

Figure 3.27 1H-NMR spectra of 1.0 mM $IAPP_{2–7}$, 3.0 mM tweezer **133**, and a 1:3 mixture of the two in 10 mM sodium phosphate, pH 7.2. No interaction is seen between tweezer **133** and peptide fragment.

We have already shown that the tweezer **133** binds to N/C-protected arginine (Kd = 20 μM) about 2 times weaker than to N/C-protected lysine. Therefore, to test whether the tweezer **133** also bind to Arg11, similar experiments are performed with $IAPP_{1–14}$. In the presence of 3-fold excess of the tweezer **133**, the side-chain protons of both Lys1 and Arg11 show an upfield shift (Figure 3.28), indicating binding at both sites. The shift of Arg11 protons resonances appeared weaker than that of Lys1 protons in the spectrum of $IAPP_{1–14}$. The peak overlap made analysis of the spectrum difficult. Therefore, we examined the tweezer **133**'s affinity for Arg11 in $IAPP_{2–14}$, where unambiguous binding of the tweezer **133** to Arg11 was confirmed (Figure 3.29). The chemical shifts of the complexed side-chain protons of Arg11 were confirmed by ^{1}H-^{1}H COSY (Figure 3.30).

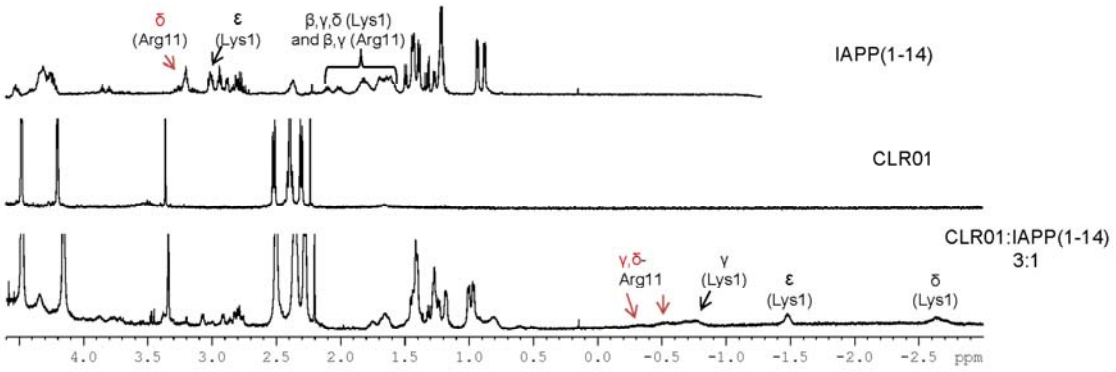

Figure 3.28 ^{1}H-NMR spectra of 1.0 mM $IAPP_{1–14}$, 3.0 mM tweezer **133**, and a 1:3 mixture of the two in phosphate buffer(10 mM, pH 7.2). The tweezer **133** is involved in complex formation with both, Lys1 and Arg11 (Lys1 signals marked in black, Arg11 signals in red). Complexed Lys1 signals show almost the same upfield shift as in the complex with $IAPP_{1-7}$. By contrast, Arg11 signals are broadened and significantly less upfield-shifted.

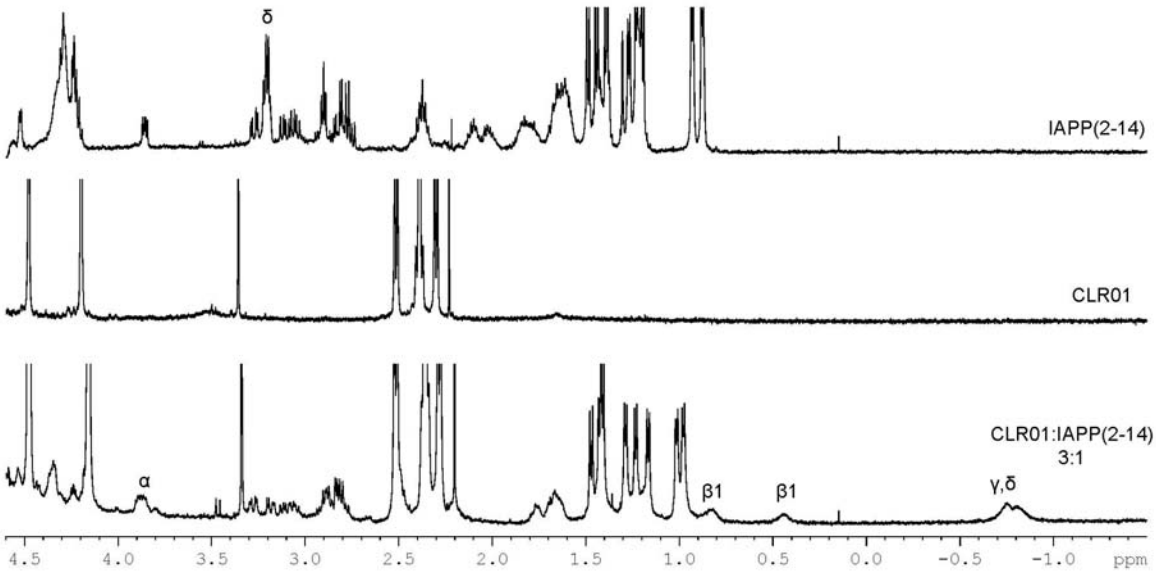

Figure 3.29 ^{1}H-NMR of $IAPP_{2\text{-}14}$, tweezer **133**, and their 1:3 complex in 10 mM phosphate-buffered D_2O, pH 7.2. The Arg11 side-chain methylene signals are assigned as α, β, γ, and δ (COSY). The δ-protons are shifted upfield by ~ 4 ppm indicating strong binding of tweezer **133** to Arg11.

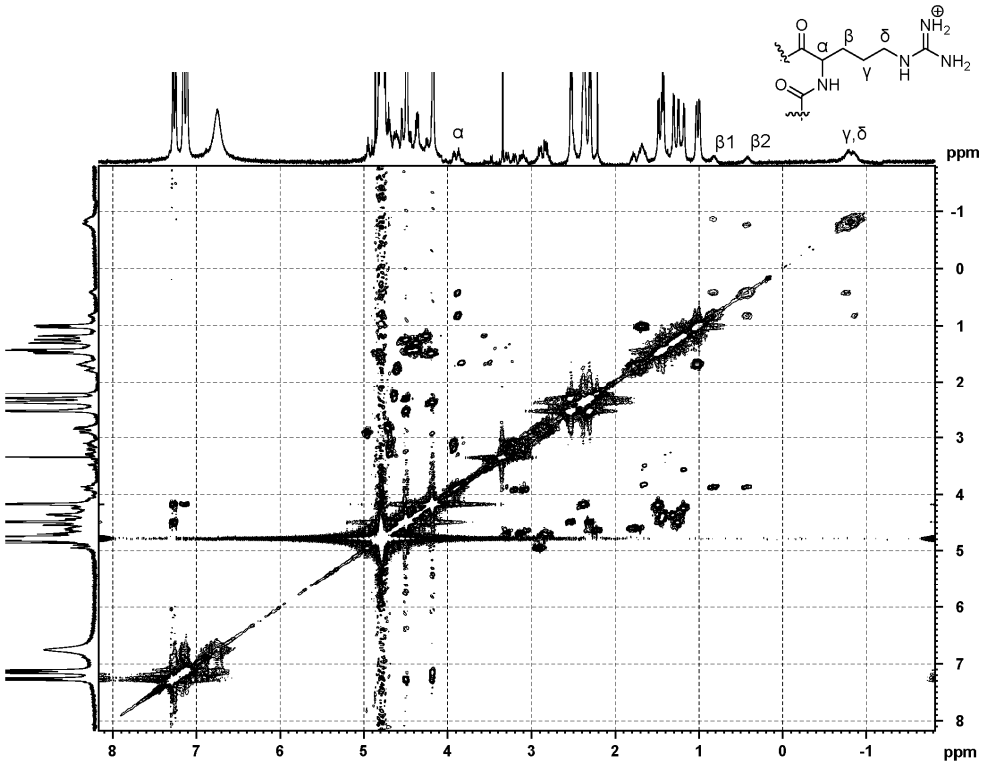

Figure 3.30 gs-H,H-COSY NMR of 3:1 molar ratio of tweezer **133**:$IAPP_{2–14}$, respectively, in D_2O phosphate buffer. Arg11 protons in the complex are assigned α, β, γ and δ.

In earlier discussions, we have shown that dissociation constants obtained by ^{1}H-NMR titration and fluorescence titration experiments are in good agreements. So, fluorescence titration experiments were performed to determine the binding affinities of the tweezer **133** to the lysine- and arginine- containing IAPP peptide fragments. Tight binding of the tweezer **133** to Lys1 of $IAPP_{1-7}$ is confirmed with the K_d = 9 μM (Figure 3.31) which is similar to value obtained for AcLysOMe (K_d = 9 μM) under the same conditions. Fluorescence titration experiments also reveals that the tweezer **133** bind to Arg11 with K_d = 104 μM, an order of magnitude weaker than at Lys1 and 5-fold weaker than the arginine derivative AcArgOMe. The decline in tweezer's affinity for Arg 11 in $IAPP_{2-14}$ can be attributed to steric hindrance around the arginine residue. Taken together, the NMR and fluorescence data strongly support that the tweezer **133** predominantly binds to Lys1 and weakly to a second binding site at Arg11. The latter observation provided a plausible explanation for the inhibition of $IAPP_{2–37}$ aggregation and toxicity by the tweezer **133**. However, these results do not reveal how the tweezer **133** affected IAPP assembly at fM concentrations.

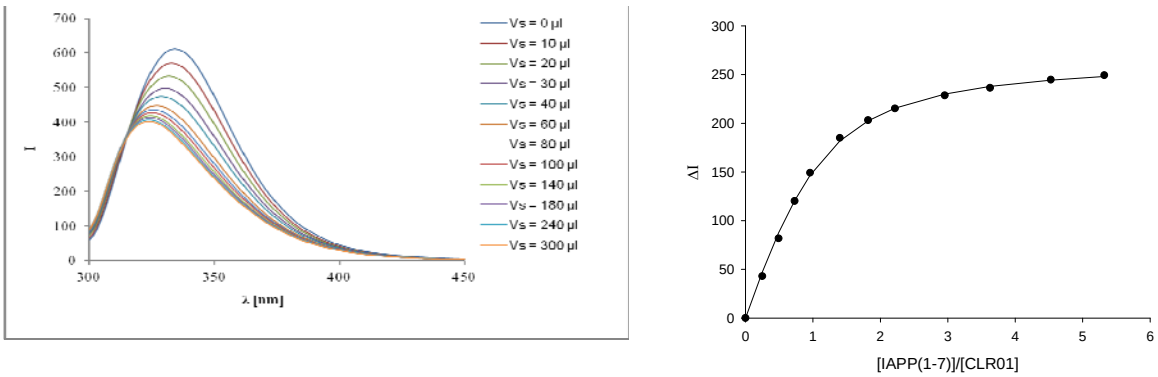

Figure 3.31 left: fluorescence emission spectra of the tweezer **133** on titration with $IAPP_{1–7}$ in 10 mM sodium phosphate buffer, pH 7.6 and, right: binding isotherm obtained by non linear curve fitting using SigmaPlot.

MD simulations performed in the Sanchez group showed that the tweezer **133** preferentially binds at Lys1 in $IAPP_{1–37}$. When MD simulations were performed by docking the tweezer **133** on Arg11 of IAPP, it was found that the Lys1 side chain competed effectively for the tweezer **133**. Lys1 pulled the tweezer off of the Arg11 side chain and slipped itself into the tweezer's cavity. The binding of the tweezer **133** to Lys1 resulted in a thermodynamically favourable complex in which the C- and N-termini of IAPP come into close proximity leading to a "wrapped" conformation that is stabilized by several intramolecular hydrogen bonds and ion pair interactions. It was speculated that most probably this structure serves as a template that can recruit other IAPP monomers into non-fibrillar assemblies. These results provided a possible

explanation for the catalytic effect of fM concentrations of the tweezer **133** on IAPP aggregation. Interestingly, when the tweezer **133** was removed from this complex, it was found that the prolonged MD simulations of IAPP have maintained this compact conformation.

In summary, in conjunction to the biophysical and MD simulations experiments we have shown that the tweezer **133** preferred complexation with Lys1 in IAPP. The strong complex formation between the tweezer **133** and IAPP was confirmed by NMR and fluorescence titrations of IAPP fragments with the tweezer **133**. The resulting dissociation constant (K_d) value by the fluorescence experiments corresponded well with that of isolated lysine derivatives. Further, the drastic upfield shifts of Lys1 side-chain signals provided the evidence that the tweezer´s binding occurs by the insertion of the Lys1 side-chain inside the tweezer's cavity.

4 Summary and outlook

4.1 Summary

4.1.1 Symmetrical anionic tweezers

The molecular tweezer **161** substituted with sulfate anion at the central benzene ring was synthesized starting from the dihydroxy tweezer **121**. The sulfate tweezer **161** is soluble in methanol and water. Chemical shifts observed by the ^{1}H-NMR dilution experiment in aqueous solution and calculated structures suggest that the tweezer **161** weakly self-assemble into the dimer (K_{dm} = 370 M^{-1}). In contrast, such dimer formation is absent in methanol, indicating that a hydrophobic effect operate in water. Among all the anionic tweezers, the tweezer **161** aggregates more efficiently than the tweezer **133**, whereas, the tweezers **734** and **150** do not self-assembled at all. The structures of all the four anionic tweezers are shown in figure 4.1.

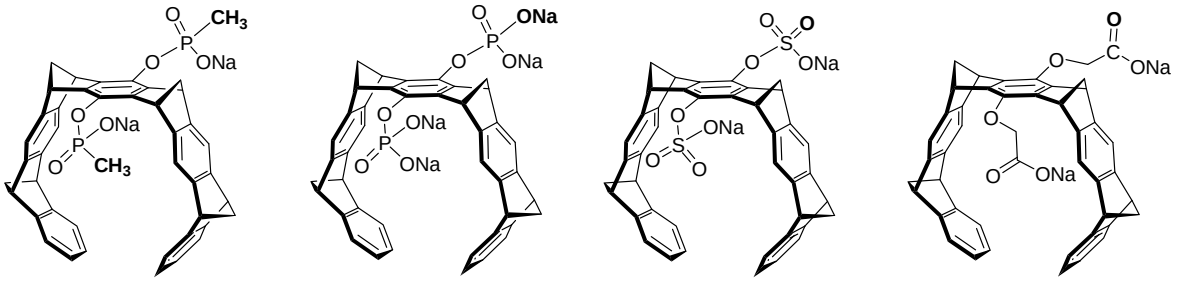

Figure 4.1 Structures of the four anionic tweezers substituted with phosphonate, phosphate, sulfate and carboxylate anions.

Binding affinities of the tweezer **161** were evaluated with lysine and arginine derivatives, and peptide guests. The tweezer **161** binds to protected lysine about 13-fold stronger compared to free lysine. Also, it shows about fourfold decreased affinity to the N/C free arginine compared to N/C protected arginine. The lower affinities to the free amino acids are expected due to the electrostatic repulsion between the sulfate anion of the tweezer and the carboxylate anion of the guest amino acids. The KLVFF case was interesting as some additional interactions between the guest's aromatic residues and tweezer's aromatic rings likely occur that alter the fluorescence emission band of the complex.

Comparative studies among the tweezers **161, 133**, **734** and **150** were carried out based on NMR, fluorescence and ITC titration experiments, and molecular modeling to investigate roles of the

anionic groups on the different tweezers in binding to the lysine and arginine amino acid derivatives and peptide guests. All the studies suggest that the tweezer **133** is the most potential receptor. The tweezer **161** proved to be the second best anionic tweezer followed by the tweezer **734** and the tweezer **150** respectively. Usually, all the anionic tweezers bind to lysine about 2-3 times stronger than arginine. The tweezer **133** binds to all the guests almost in the low micromolar affinities (< 30 μM). The tweezer **161** is quite selective to N/C protected lysine among all the amino acid derivatives. Remarkably, the tweezer **133** binds to the free and protected lysine with similar affinities, while, the tweezers **161**, **734** and **150** bind to the free lysine about one order of magnitude weaker than to the protected lysine. The strong upfield chemical shifts of 3-5 ppm for the guest protons obtained by the ^{1}H-NMR titration experiments strongly support the guest binding by the inclusion of lysine or arginine side-chain into the tweezer's cavity. The chemical shifts of < 1 ppm of guest protons of the complexes of the tweezer **150** with lysine or arginine derivatives indicate very week stability of the complex formed by the inclusion of any guest inside the tweezer's cavity.

The ITC studies of the complexes of the tweezers **133** and **161** bring forward the individual enthalpy and entropy of the complex formation. The tweezer **133** binds to AcArgOMe enthalpically more tightly than AcLysOMe but due the favorable entropy of the complex **133**@AcLysOMe, it is 2-fold stronger than the complex **133**@AcArgOMe. The enthalpy and entropy contributions of the complexes of the tweezer **161** are somewhat contrary to those of the complexes of the tweezer **133**. Surprisingly, the complex **133**@AcLysOMe is entropy driven in methanol. The ITC data together with the negligible NMR chemical shifts of lysine protons of the complex **133**@AcLysOMe in methanol indicate that the binding of lysine does not occur inside the tweezer's cavity but outside. These results imply that the observed binding affinity in methanol is purely based on the electrostatic and hydrogen bonding interactions between the phosphate anions of the tweezer **133** and the lysine. Surprisingly, in methanol and aqueous buffer solution the tweezer **161** binds to lysine with the similar affinity and by the lysine side-chain inclusion into the tweezer's cavity. This is contrary to the external binding of the tweezer **133** to lysine in methanol. These results point towards very different characteristics of the phosphate and the sulfate groups in methanol and water.

In neutral aqueous buffer, partial protonated form and the highest negative partial charge on the oxygen atoms of the phosphate group in the tweezer **133** are expected to be responsible for the higher affinities of this tweezer compared to the other tweezers. The tweezers **161**, **734** and **150**

due to their fully deprotonated anions can only act as hydrogen bond acceptor. Therefore, these tweezers lack hydrogen bond donor sites and experience strong electrostatic repulsive interactions from the carboxylate anion of the free amino acids or peptides backbone. The lower affinities of the tweezer **734** compared to the tweezer **161** are attributed to the partial steric hindrance of the tweezer **734**'s cavity by the methyl group on its phosphate group. On the other hand, the much lower affinities of the tweezer **150** are believed due to the absence of proper hydrogen bonding and electrostatic interactions between the carboxylate anion of the tweezer and the ammonium or guanidinium groups of the guests. Longer length and high flexibility of the carboxymethyl groups of the tweezer **150** are supposed to reduce the suitable hydrogen bonding and ion pair interactions between the tweezer and the guests. Our studies suggest that no single force (i.e. hydrophobic or electrostatic) decides the overall stability of the complex, and only collective effects of all kind of favorable and unfavorable interactions govern the final stability of the complex.

Biological studies performed in the collaboration with Prof. Bitan suggest that all these anionic tweezers interfere in the aggregation process of several pathological amyloid proteins like Aβ and IAPP etc. The inhibition effects are usually in the order of the tweezers affinities to the isolated amino acid derivatives. Surprisingly, the tweezer **161**, **734** and **150** are found slightly toxic to the cells and only the tweezer **133** is the most prominent tweezer candidate.

4.1.2 Unsymmetrical phosphate tweezers

In the second part of the work, effects of replacing one phosphate group of the tweezer **133** by other substitutions were investigated. For this purpose, the unsymmetrical molecular tweezers that carry a phosphate group on one side and a linker or additional recognition unit on the other side of the tweezer's central benzene ring were synthesized and studied. The structures of these unsymmetrical linker tweezers are shown in Figure 4.2. The unsymmetrical tweezers are soluble in aqueous buffer (1-50 μM).

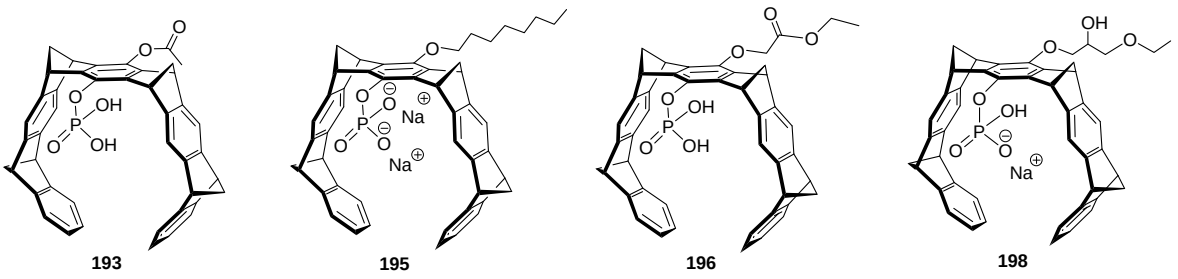

Figure 4.2 Structures of the four unsymmetrical phosphate tweezers synthesized and studied.

^{1}H-NMR and molecular modeling structures suggest that the tweezer **193** keeps the cavity open and accessible for the guest molecules. From the crystal structures, ^{1}H-NMR and molecular modeling structures, the tweezer **195** is found to completely block the cavity entrance by engaging its n-octyl chain in numerous van-der-Waals contacts to aromatic CH-groups as well as CH-л interactions with its own and other aromatic tweezer moieties. Unexpectedly, the tweezer **196** and **198** insert the ethyl group of their linkers into the tweezer's cavity that suggest an intramolecular hydrophobic effect.

The dissociation constants of these tweezers cover relatively broad range of affinities ranging from 30 μM to 600 μM in aqueous phosphate buffer. The tweezers with ester groups (tweezers **193** and **196**) are better tweezer candidate for complexing the guests compared to the tweezers with ether tethers (tweezers **195** and **198**). Additionally, the tweezers **193** and **196** binds N/C-protected lysine or arginine more strongly compared to the unsubstituted hydroxy monophosphate tweezer **130** which indicate that the acetyl group and the ethoxycarboxymethyl group take part in molecular recognition of their guests in a positive cooperative manner. Interestingly, the guest molecules compete with self-included linker units in the tweezers **196** and **198**. The tweezer **193** binds to lysine and arginine derivatives with almost similar affinities. This tweezer also binds to $IAPP_{2\text{-}14}$ slightly stronger compared to the tweezer **133**.

The effects of solvent polarity were also evaluated on the guest binding of all the tweezers by using the methanol-buffer mixtures. A correlation is found among the solvent polarity, chemical shifts of the guest protons, fluorescence change of the tweezer and binding affinity as: more polar solvent ~ large chemical shift difference ~ large fluorescence change ~ strong complex formation.

The results that the carbonyl group takes part in the guest binding of the tweezers **193** and **196**, and that the affinities of these tweezers are still lower than the tweezer **133**, render both the

phosphate groups essential for the optimum affinity of a tweezer. For this reason it is realized that both the phosphate groups must be installed in the new unsymmetrical bisphosphate tweezers and the additional recognition site should be attached to one or both the phosphates. Therefore, to synthesize more elaborative unsymmetrical molecular tweezers, we have synthesized 2nd generation linker tweezers that contain an alkyne or ester linker on one phosphate group (Figure 4.3).

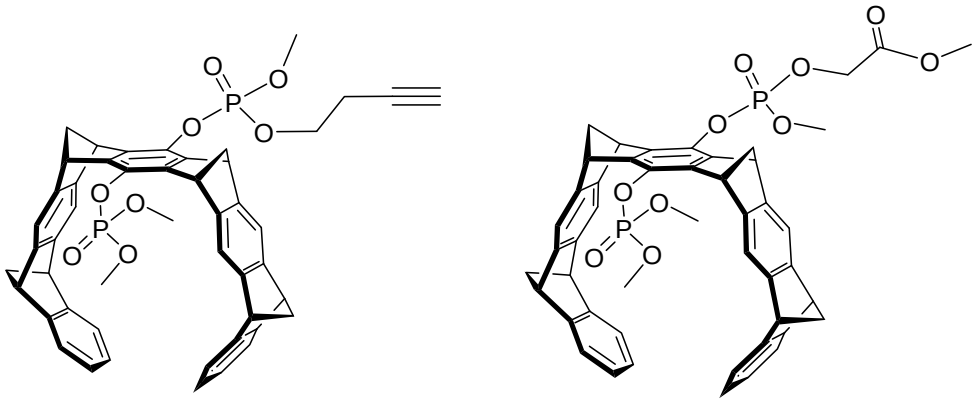

248 **247**

Figure 4.3 Structures of the synthesized 2nd generation alkyne and ester containing linker tweezers **248** and **247**.

4.2 Outlook

All the anionic tweezers can be used in solutions which have the pH values well above the pK_a values of the tweezer's anionic groups. Therefore, the tweezers **133**, **734** and **150** can not be used at acidic pH (< 4) due to the protonation of their anionic groups.[141] On the other hand, the sulfate group can be readily deprotonated in acidic medium (pK_a < 0), therefore, the tweezer **161** holds the promise of a potential receptor for the proteins that are used at acidic pH. For that reason, the tweezer **161** will be tested to modulate the structure and function of lysozyme in acidic medium (pH < 2) in collaboration with Prof. Bitan.

In order to achieve protein selectivity, several protein specific recognition units could be designed and synthesized for various protein targets and then can be coupled with the alkyne or ester containing tweezers **248** or **247** to synthesize 2nd generation unsymmetrical bisphosphate tweezers. The new unsymmetrical tweezers thus obtained shall be evaluated for their binding to the required guests. Finally, biological studies of the new tweezers shall be performed in collaboration with Prof. Bitan.

4.2.1 2nd generation unsymmetrical tweezers

The tweezer **248** can be coupled with an azide containing recognition unit through cupper catalyzed click reaction and then the protecting groups can be cleaved to obtain the final tweezer (Scheme 4.1). If a recognition site does not have protecting groups then the methyl groups of the tweezer **248** can be cleaved prior to couple the tweezer with protecting group free azide containing recognition sites.

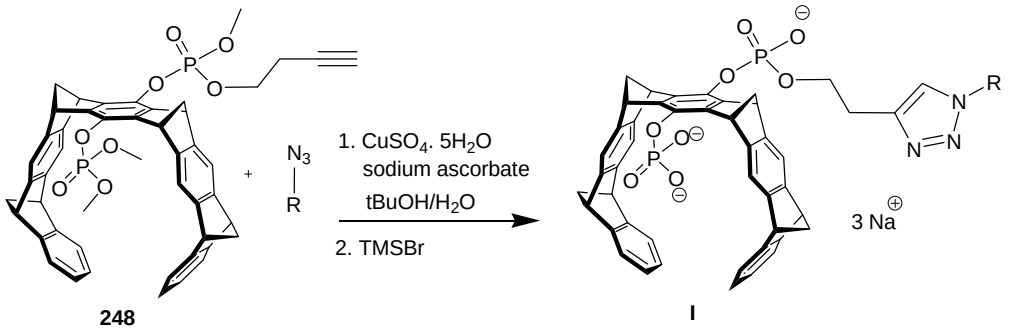

Scheme 4.1 General synthetic route for the unsymmetrical tweezer **I** starting from tweezer **248**.

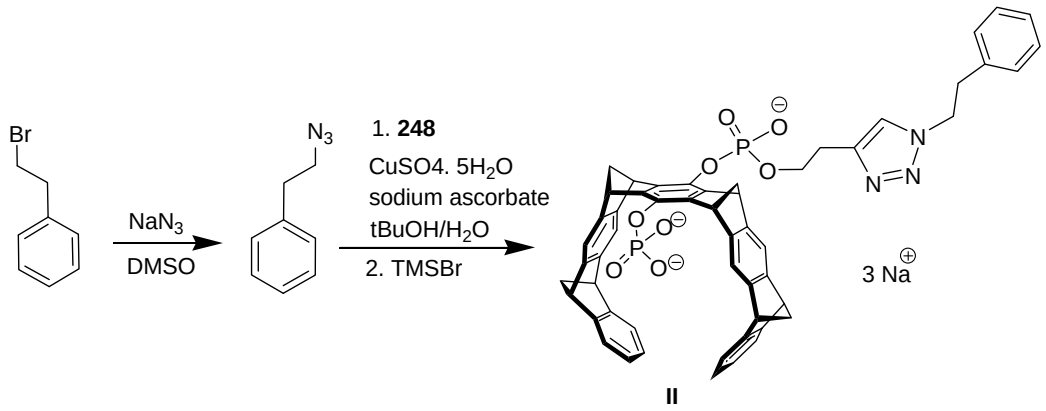

Scheme 4.2 Synthesis plan of the simple unsymmetrical tweezer **II** starting from the tweezer **248**.

The tweezer 247 is the another potential linker tweezer that provides the opportunity to couple the ester group with an amine containing recognition unit as shown in Scheme 4.3.

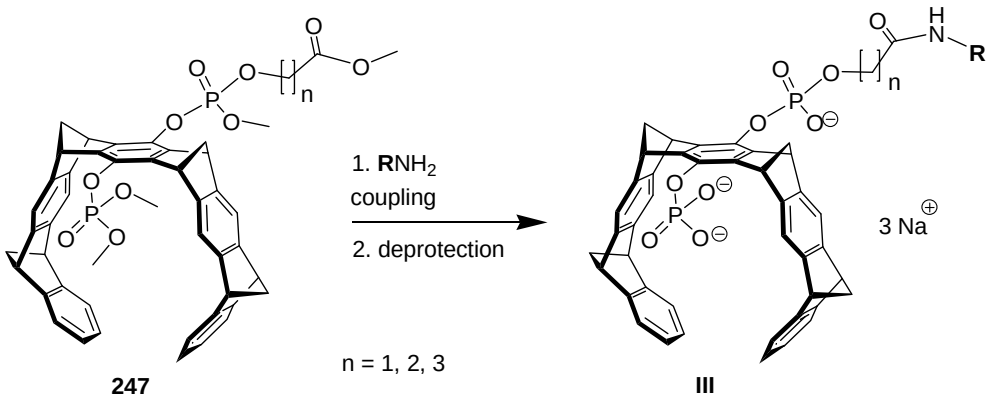

Scheme 4.3 General synthetic route for the unsymmetrical tweezer **III** starting from the tweezer **247**.

4.2.2 Structure based design of the molecular tweezers for Aβ peptide

The tweezer **IV** is designed to bind specifically at Lys16 in Aβ (10-42). The calculated structures obtained by means of Conformational Search (Maestro 9.2, OPLS_2005, water, 5000 steps) suggest that this tweezer might complex to Aβ with nanomolar affinity compared to the micromolar affinity of the phosphate tweezer **133**. The tweezer **IV** can be synthesized according to the synthesis plan shown in Scheme 4.4.

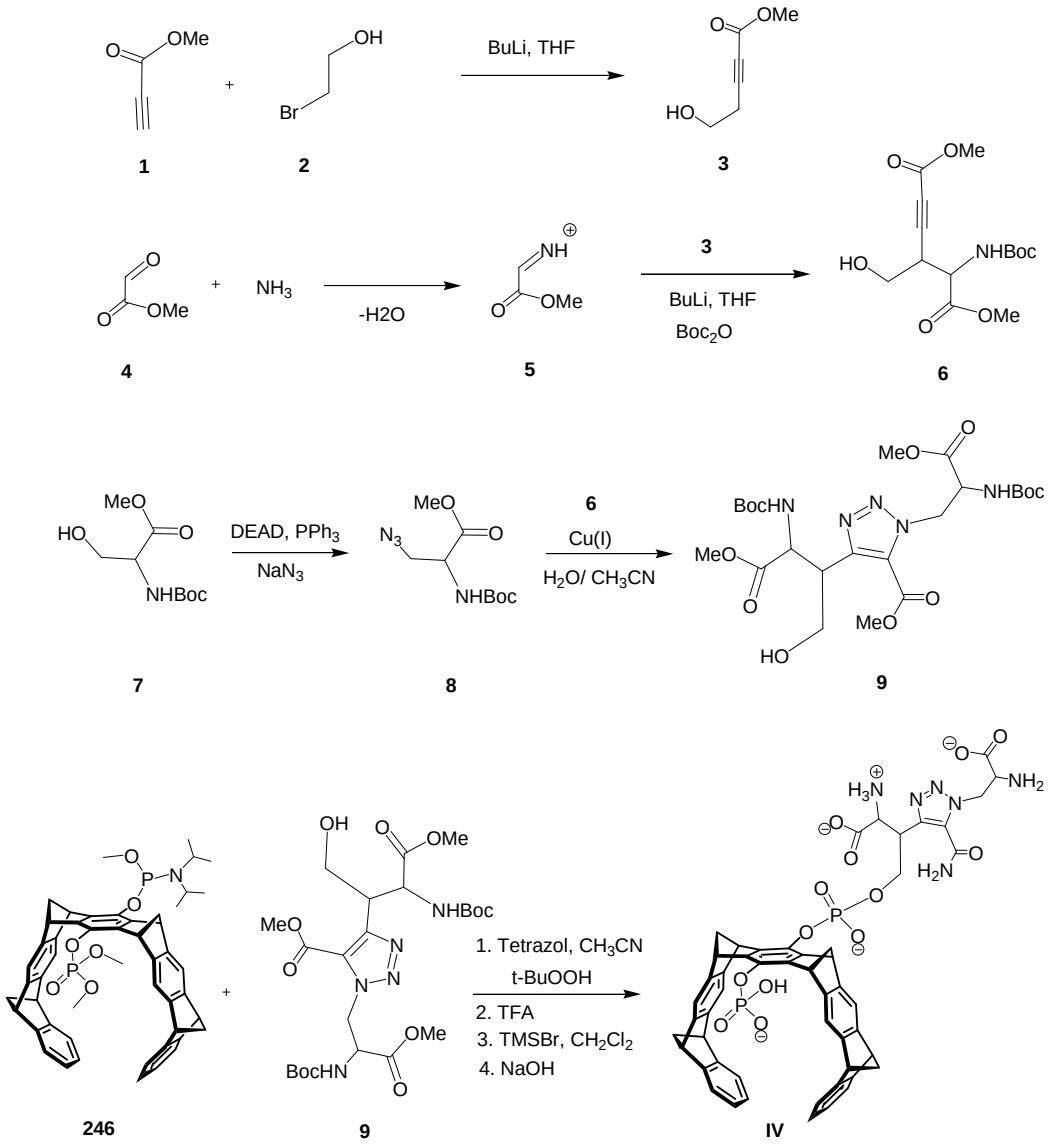

Scheme 4.4 A possible synthesis scheme for the unsymmetrical tweezer **IV**.

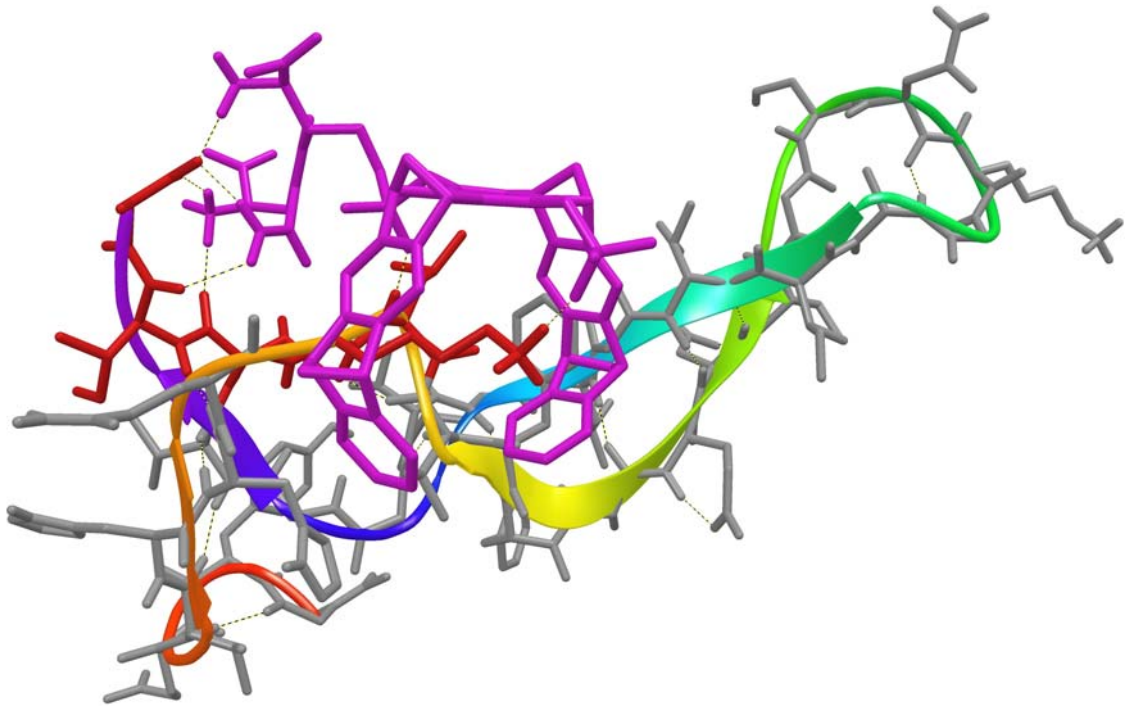

Figure 4.4 Calculated structure of the tweezer **IV** (shown in pink) docked on Lys16 in Aβ (10-42) (Maestro 9.2, conformational search, OPLS_2005, water, 5000 steps). The peptide residues involved in the interactions with the tweezer are shown in red color and the rest peptide in gray. All the hydrogen bonds are shown by doted lines.

The following tweezers **V** and **VI** substituted with serine or serine derivatives could also be synthesized and tested.

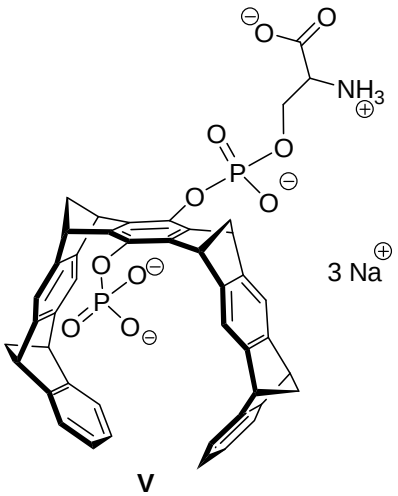

V

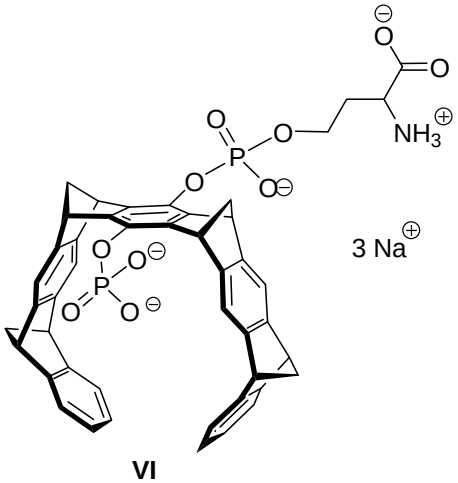

VI

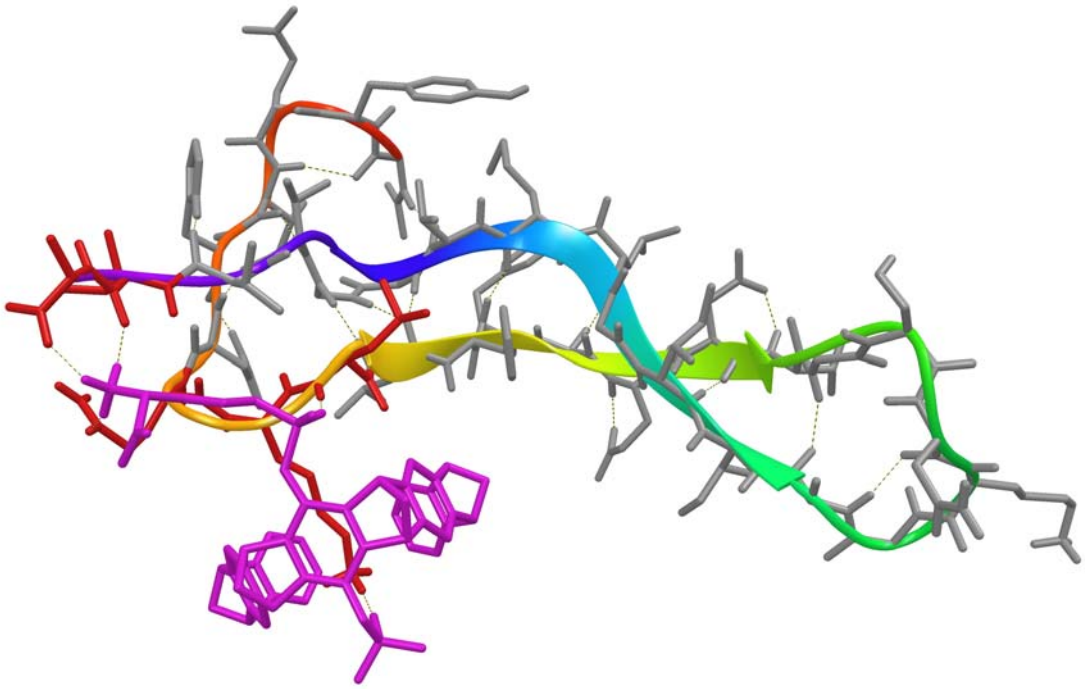

Figure 4.5 Calculated structure of the tweezer **VI** docked on Lys16 of Aβ (10-42) (Maestro 9.2, Conformational Search, OPLS_2005, water, 5000 steps). The peptide residues involved in the interactions with the tweezer are shown in red color and the rest peptide in gray. All the hydrogen bonds are shown by doted lines.

5 Experimental part

5.1 Material and method

Chemicals

All the chemicals required for this work were purchased from Sigma-Aldrich, Fluka, Acros Organics, Bachem and Merck in high commercial grade. The technical grade solvents were distilled/dried prior to use by standard literature methodology.[142]

Chromatography

Thin Layer Chromatography (TLC) plates from Merck with silica gel-60 were used to monitor the reactions. Silica gel-60 (200-400 mesh) from Merck was used for the column chromatography purification of compounds.[143]

UV-Vis spectroscopy

UV/Vis- Spectrum were measured on a Jasco V-550 Spectrometer. Quartz cuvette of 10 mm was used for solution.

Mass spectroscopy

High-resolution electron spray ionization (ESI) mass spectra were measured on a Bruker BioTOF III spectrometer by Mr. Werner Karow.

Crystallography

Single crystal analyses were carried out on an X-ray diffractometer by Dr. Christoph Wölper in the research group of Prof. Schulz at University of Duisburg-Essen.

Buffer preparation for fluorescence titration and ITC measurements

PB, 10 mM, pH 7.2: 109 mg (0.7 mmol) of $NaH_2PO_4 \cdot 2H_2O$ and 170 mg (1.2 mmol) Na_2HPO_4 were dissolved in 200 ml bidist water and the pH was adjusted to 7.2 by dropwise adding an aqueous solution of 0.1M NaOH or 0.1 M solution of phosphoric acid.

Following buffers were also prepared using the same procedure.

PB, 10 mM, pH 6.2

PB, 10 mM, pH 7.6

PB, 10 mM, pH 8.5

PB, 200 mM, pH 7.6

PBS: 10 mM phosphate buffer + 150 mM NaCl, pH 7.6.

Buffer preparation for NMR titration

(PB, 10 mM, pH 7.2): 28 mg (0.10 mmol) KH_2PO_4 were dissolved in 20 ml D_2O and pH was adjusted to 7.2 with 0.1 M NaOH solution in D_2O. Phosphate buffer for IAPP measurements was also prepared in D_2O:H_2O (1:9) in the same way.

Fluorescence spectroscopy

Fluorescence measurements were performed at 25 ^oC on a Jasco FP-6500 spectrofluorometer. Solutions were measured in a round quartz cuvette of 1 cm diameter.

Isothermal titration calorimetry (ITC)

ITC measurements were performed on a VP-ITC instrument from MicroCal Inc. All the measurements were carried out with the help of Mr. Kowski.

NMR spectroscopy

NMR spectra were recorded on Bruker AMX 300 or Bruker DRX 500. Chemical shifts were reported in ppm relative to tetramethylsilane (δ = 0 ppm). NMR signals of commonly used solvents were taken from literature.[144] Multiplicities were indicated by s (singlet), d (doublet), t (triplet), m (multiplet) and br (broad). ^{13}C spectra were broadband decoupled and calibrated on the particular solvent signal. All the spectra at 500 MHz were measured by Mr. Bandmann or Dr. Schaller, whereas, NMR titrations were performed by myself.

NMR experiments examining the interactions between CLR01 and unlabeled IAPP fragments were carried out at 25 °C using a Bruker DRX-500 MHz spectrometer equipped with a 5 mm QNP-Probe (^1H) or a 5 mm TBI-Probe (^1H, X, ^{13}C) with Z-Gradient (gs-COSY90 and gs-NOESY). ^1H-NMR of CLR01 alone was measured by dissolving CLR01 at 1.0 mM in 10 mM phosphate-buffered D_2O, pH 7.2. Solutions of IAPP fragments in the absence or presence of 3 equivalents of CLR01 were prepared in 10 mM sodium phosphate in 9:1 – H_2O:D_2O, pH 7.2, at peptide concentration of 1.0 mM in all cases. ^1H-NMR was measured with water suppression using presaturation and composite pulses (zgcppr). For COSY experiments, samples of $IAPP_{1–7}$ or $IAPP_{2–14}$ were prepared in phosphate-buffered D_2O, pH 7.2, in the absence or presence of 3 equivalents of CLR01 and gs-COSY90 (cosygpqf) spectra were measured. For NOESY experiments, a 1:1 mixture of $IAPP_{2–14}$:CLR01 was prepared in sodium phosphate in 9:1 –

H_2O:D_2O, pH 7.2, degassed and sealed under argon. A gs-NOESY (noesyesgpph) spectrum was measured with water suppression using excitation sculpting with gradient.

Molecular modeling

Molecular modeling was performed on Maestro 9.2 using OPLS_2005 force field. Minimized structures were calculated by Monte-Carlo Simulations for 5000 steps with 5000 iterations using Mixed Torsional/Low-Mode Sampling method. Minimum energy structures obtained from Monte-Carlo Simulations were used for Molecular Dynamics Simulations.

Measuring the association constant K_a by 1H-NMR titration spectroscopy

All the NMR titration experiments were performed by the standard ^{1}H-NMR titration method or the dilution titration method. In a standard titration method, guest is kept at constant concentration while the receptor concentration varies. In a typical experiment, a tweezer is dissolved in a guest solution at about 3:1 ratio of tweezer:guest in an NMR tube. Guest solution is added in several aliquots of 50-100 µl and the ^{1}H-NMR is recorded after each addition. Guest is added until the guest stoichiometry reached above the tweezer stoichiometry. In the dilution titration method, a tweezer and a guest are dissolved in 1:1 ratio and at different overall concentrations. Usually, six samples which differ in concentration by a factor of ~ 2 are required and the observed chemical shifts of guest protons at each concentration are recorded. Association constants of complex are determined by standard non linear regression analysis of the data using program Table Curve.[145]

Measuring the association constant K_a by fluorescence titration spectroscopy

A tweezer was dissolved in a solvent of choice (buffer or methanol or mixture of two solvent) and at a given concentration (10-50 µM). A guest was dissolved (0.2-3.0 mM) in the tweezer solution to keep the tweezer concentration constant over the entire titration. Seven-hundred µl of tweezer solution were placed in a quartz cuvette of 1-cm path length and fluorescence spectra were measured on a FP-6500 spectrophotometer (JASCO). Aliquots of guest solution were added to the tube and fluorescence spectra were recorded following each addition. Binding isotherms for a 1:1 complex were obtained from fluorescence of maximum emission intensities and converted into binding constants by standard, non-linear regression fitting[146] using SigmaPlot 10.0 (Systat, San Jose, CA) [147].

Measuring the association constant K_a by isothermal titration calorimetry (ITC)

ITC measurements were performed on an isothermal titration calorimeter from MicroCal.[121] In a typical experiment, 0.1 mM tweezer solution is placed in the calorimetry cell. 1.0 mM solution of a guest is mixed to the tweezer solution by a syringe in 5 µl aliquots at an interval of 300 s. A total 120 µl guest solution is added to the tweezer solution in 120 min. The solution was continuously stirred and maintained at a fix temperature of 25 ^{o}C throughout the experiment. Association constants and enthalpy (ΔH) of complex formation are calculated from the non linear least square regression method using the Origin software. Entropy (ΔS) of complex formation is determined by the formula $\Delta G = \Delta H - T\Delta S$.

5.2 Synthesis

5.2.1 Synthesis of the sulfate tweezer 161

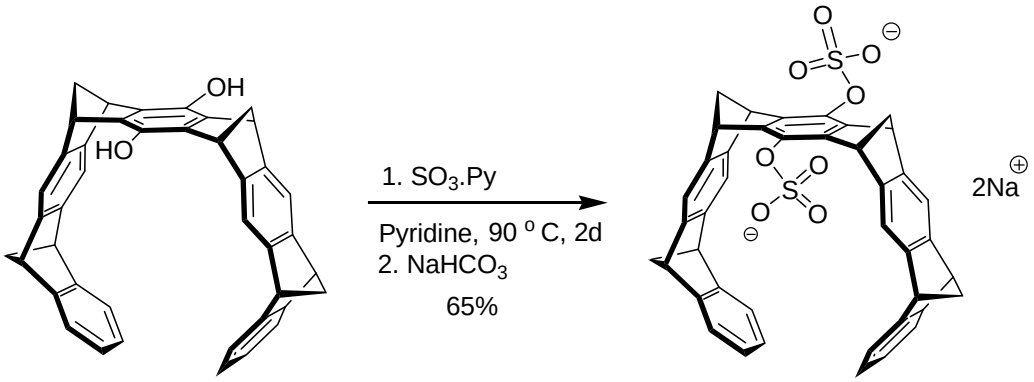

121
$C_{42}H_{30}O_2$
566,69 g/mol

161
$C_{42}H_{28}Na_2O_8S_2$
770,78 g/mol

75 mg (0.1325 mmol) of the hydroxy tweezer **121** and 85 mg (0.53 mmol) sulfur trioxide pyridinium complex were dissolved in 7 ml dry pyridine and refluxed at 90 ^{o} C for 24 h. After that additional 63 mg (0.397 mmol) of SO_3·Py complex were added to this solution and stirred the mixture for another 36 h. The mixture was cooled to RT and quenched with sat. $NaHCO_3$ solution. The excess of inorganic salts was filtered off by a glass filter (D4) and the filtrate aqueous solution was extracted with diethyl ether (3×50 ml). The aqueous phase was dried on rotary evaporator and solid residue suspended in ethanol and filtered. Solvent removed on *vacuo* and 70 mg of white solid product were collected.

Yield: 70 mg. 68%

Melting Point: > 229 ^{o}C, brown coloration, decomposition.

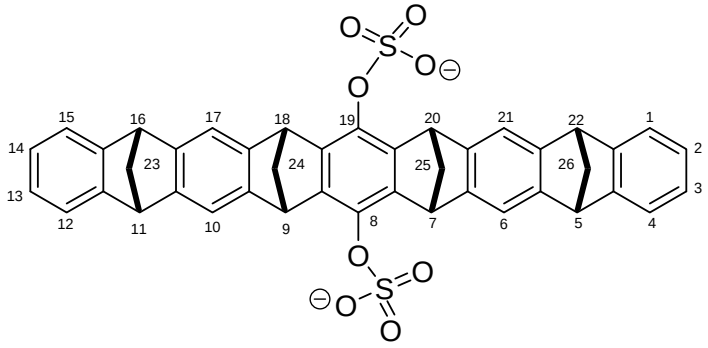

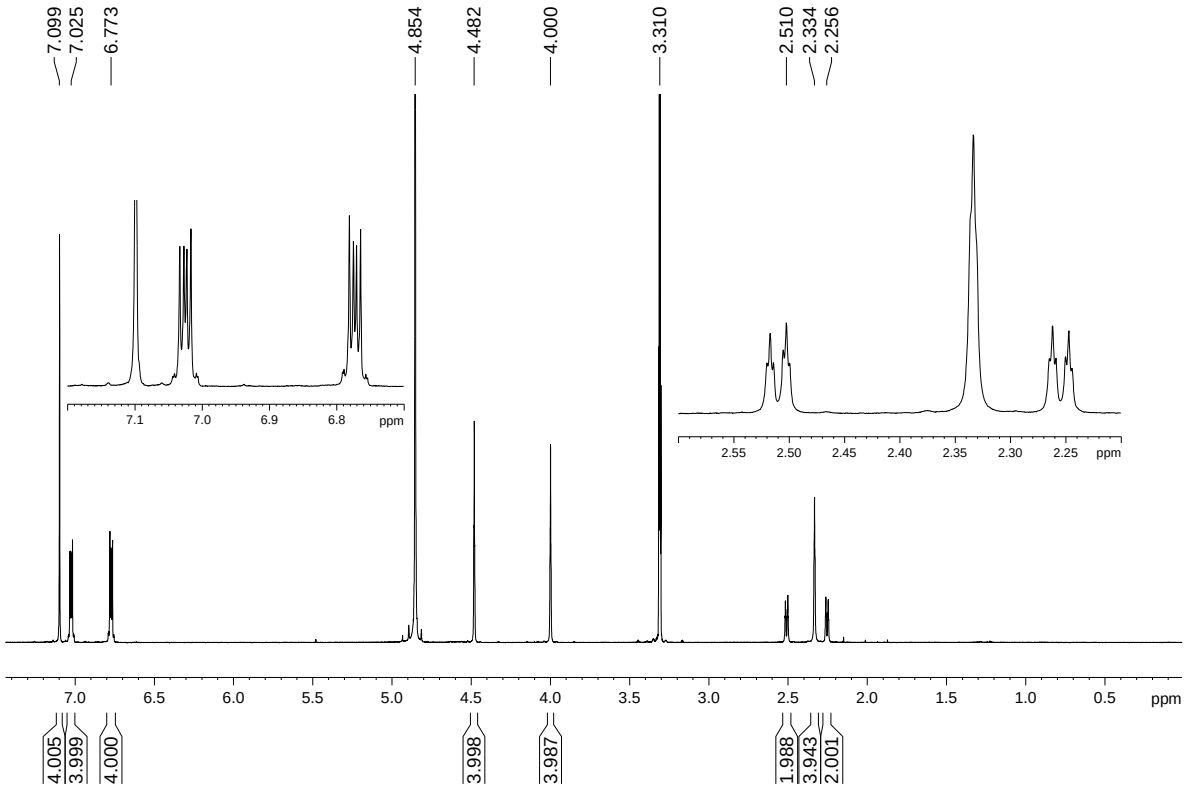

^{1}H-NMR in CD_3OD

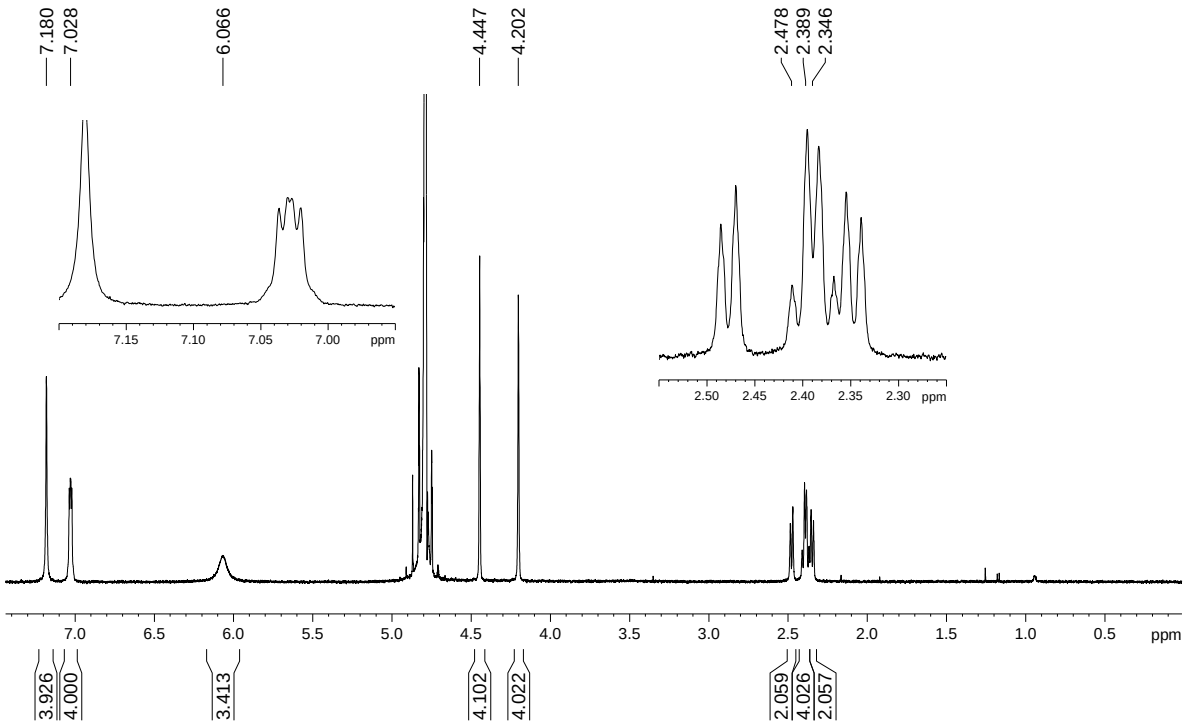

^{1}H-NMR in D_2O

^{1}H-NMR (500 MHz, CD_3OD): δ [ppm] = 2.26 (td, 2H, H-24a, H-25a), 2.33 (s, 4H, H-23, H-26), 2.51 (td, 2H, H-24i, H-25i), 4.00 (4H, H-5, H-11, H-16, H-22), 4.48 (s, 4H, H-7, H-9,

H-18, H-20), 6.78 (m, 4H, 4H, H-2, H-3, H-13, H-14), 7.02 (m, 4H, H-4, H-12, H-1, H-15), 7.10 (s, 4H, H-6, H-10, H-17, H-21).

^{1}H-NMR (500 MHz, D_2O): δ [ppm] = 2.34 (d, 2H, H-24a, H-25a), 2.39 (m, 4H, H-23, H-26), 2.48 (d, 2H, H-24i, H-25i), 4.20 (4H, H-5, H-11, H-16, H-22), 4.45 (s, 4H, H-7, H-9, H-18, H-20), 6.06 (br, s, 4H, 4H, H-2, H-3, H-13, H-14), 7.03 (m, 4H, H-4, H-12, H-1, H-15), 7.18 (s, 4H, H-6, H-10, H-17, H-21).

^{13}C-NMR (125,7 MHz, CD_3OD): δ [ppm] = 50.0 (C-7, C-9, C-18, C-20), 52.4 (C-5, C-11, C-16, C-22), 69.0, 69.4 (C-23, C-24, C-25, C-26), 117.3 (C-6, C-10, C-17, C-21), 122.1 (C-4, C-12, C-1, C-15), 125.8 (C-2, C-3, C13, C-14), 139.3 (C-8, C-19) 144.8 (C-7a, C-8a, C-18a, C-19a), 148.6 (C-6a, C-9a, C-17a, C-20a), 149.2 (C-5a, C-10a, C-16a, C-21a), 151.9 (C-4a, C-11a, C-15a, C-22a).

HR-MS (**ESI**, pos., neg., MeOH):

m/z $[M+Na]^+$: cal. : 793.0913

obs.: 793.0944

m/z $[M-Na]^-$: cal. : 747.1129

obs.: 747.1131

m/z $[M-2Na]^{2-}$: cal.: 362.0618

obs.: 362.0635

5.2.2 Synthesis of the unsymmetrical linker tweezers

5.2.2.1 Synthesis of the acetoxy tweezer 193

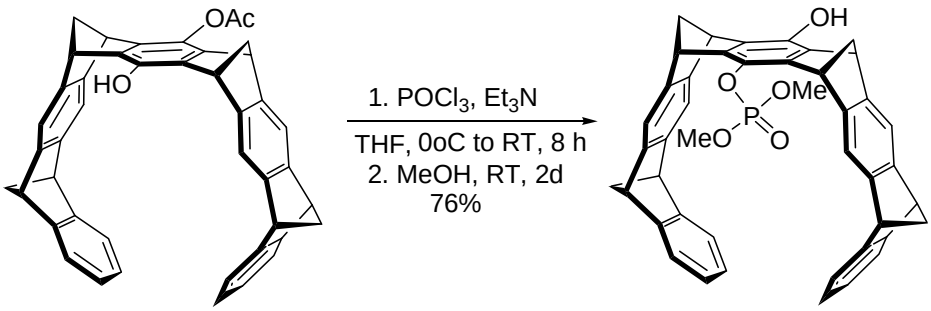

120
$C_{44}H_{32}O_3$
608,72 g/mol

189
$C_{44}H_{35}O_5P$
674,72 g/mol

Under argon atmosphere, 300 mg (0.493 mmol) tweezer **120** was dissolved in 40 ml anhydrous THF and cooled the solution to 0 ^oC. To this cooled solution 90 µl (0.987 mmol) $POCl_3$ and after 10 min. 137 µl (0.987 mmol) Et_3N were added. The reaction mixture is stirred from 0^oC to RT for 8 h and then 8 ml dry methanol were added and stirred again at RT for 2 days. The solvent was removed on rotary evaporator and to the crude 50 ml sat.NH_4Cl solution were added and extracted with CH_2Cl_2 (3×100 ml). The organic layer was washed the with brine solution. Solvent was removed on rotary evaporator and solid purified by column chromatography using EtOAc//cyclohexane (1:3) eluent.

Yield: 250 mg, white solid, 76 %.

Melting Point: > 240 ^oC brown coloration.

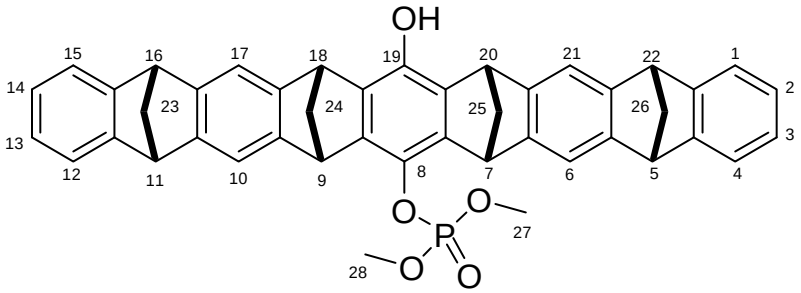

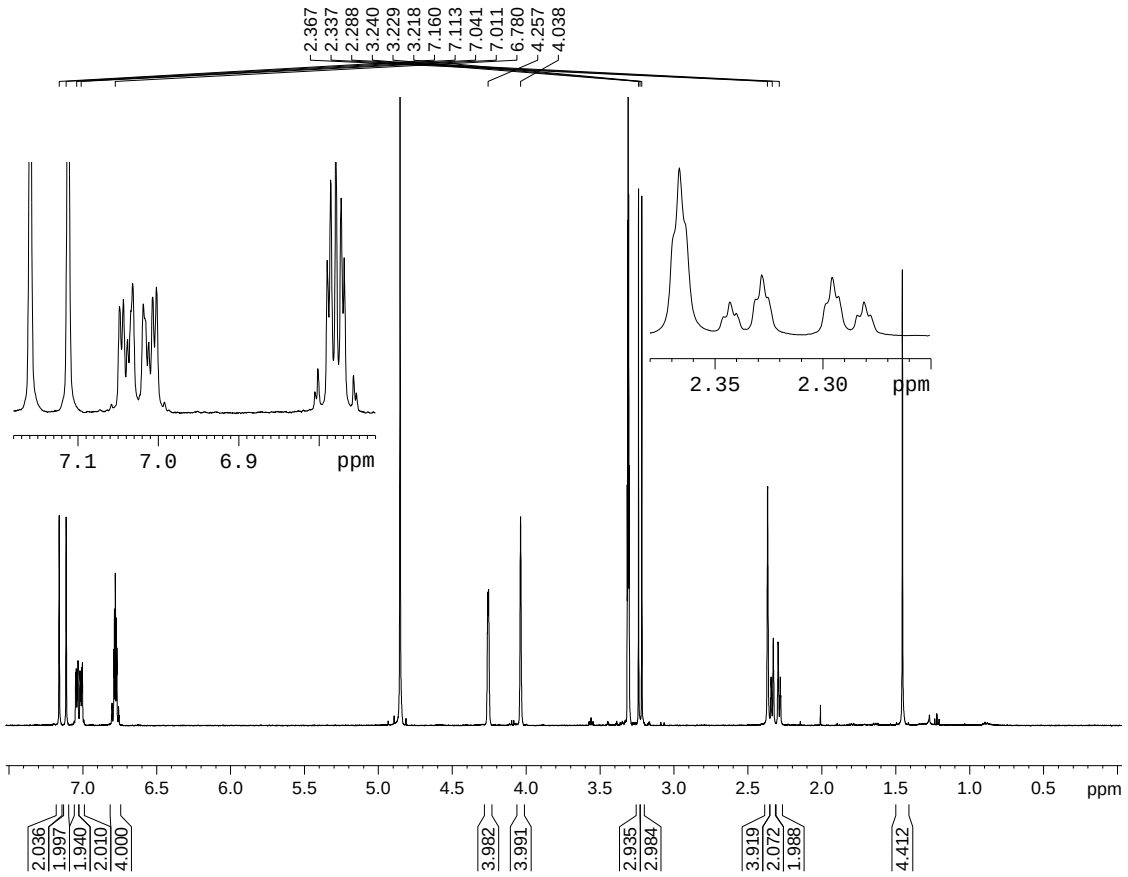

^{1}H-NMR

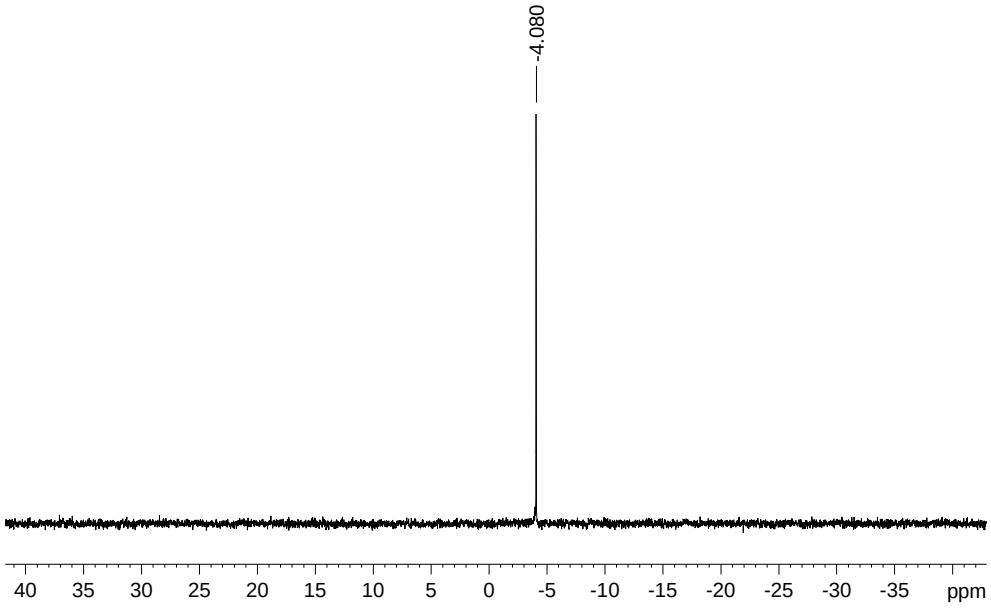

^{31}P-NMR

^{1}H-NMR (500MHz, CD_3OD): δ [ppm] = 2.28 (dt, 2H, H-24a, H-25a), 2.33 (dt, 2H, H-24i, H-25i), 2.36 (s, 4H, H-23, H-26), 3.99 (s, 2H), 3.22 (d, $^{3}J_{\text{H-27/P, H-28/P}}$ = 11.00, 6H, H-27, H-28), 4.03

(s, 4H, H-5, H-11, H-16, H-22), 4.25 (s, 4 H, H-7, H-9, H-18, H-20), 6.78 (m, 4H, H-2, H-3, H-13, H-14), 7.01 (m, 2H, H-1, H-15), 7.04 (m, 2H, H-4, H-12), 7.11 (s, 2H, H-17, H-21), 7.15 (s, 2H, H-6, H-10).

^{13}C-NMR (125.7MHz, CD_3OD): δ [ppm] = 48.6-49.3 (C-7, C-9, C-18, C-20), 52.4(d, C-5, C-11, C-16, C-22), 55.8(d, C-27, C-28), 68.8, 69.2 (C-23, C-24, C-25, C-26), 117.0 (C-17, C-21), 117.8 (C-6, C-10), 121.8 (C-1, C-15), 122.3 (C-4, C-12), 126.0 (d, C-2, C-3, C13, C-14), 138.4, 141.7, 144.0 (C-5a, C-16a, C-21a, C-10a,C-7a, C-8a, C-18a, C-19a), 148.4, 148.9, 149.2 (C-6a, C-9a, C-17a, C-20a, C-8, C-9), 152.2 (d, C-4a, C-11a, C-15a, C-22a).

^{31}P-NMR (202MHz, CD_3OD): δ [ppm] = -4.08

HR-MS (ESI pos., MeOH): m/z $[M+Na]^+$: cal. 697.2114, obs. 697.2133.

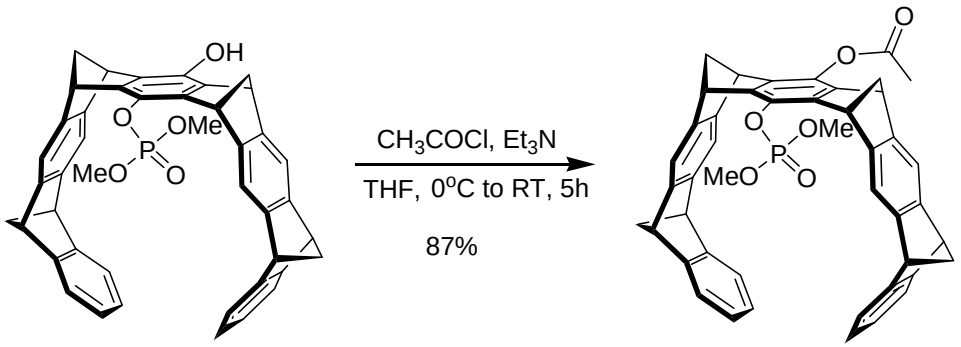

189
$C_{44}H_{35}O_5P$
674,72 g/mol

192
$C_{46}H_{37}O_6P$
716,76 g/mol

Under argon atmosphere, 30 mg (0.044 mmol) tweezer **189** were dissolved in 5 ml anhydrous THF and cooled to 0 °C. Then 9 µl (0.066 mmol) Et_3N were added by micro syringe. After 5 min. were added 5 µl (0.066 mmol) of acetyl chloride with subsequent formation of white precipitate of $Et_3N{\cdot}HCl$. The reaction stirred for 5 hour from 0 °C to rt and then added sat. $NaHCO_3$ solution and extracted three times with CH_2Cl_2. The combined organic phase is then washed with dist. water and dried over $MgSO_4$. Solvent removed on a *rota vap* and thus collected 27 mg pure white solid.

Yield: 27 mg, 87%

Melting Point: > 200 ^{o}C brown coloration.

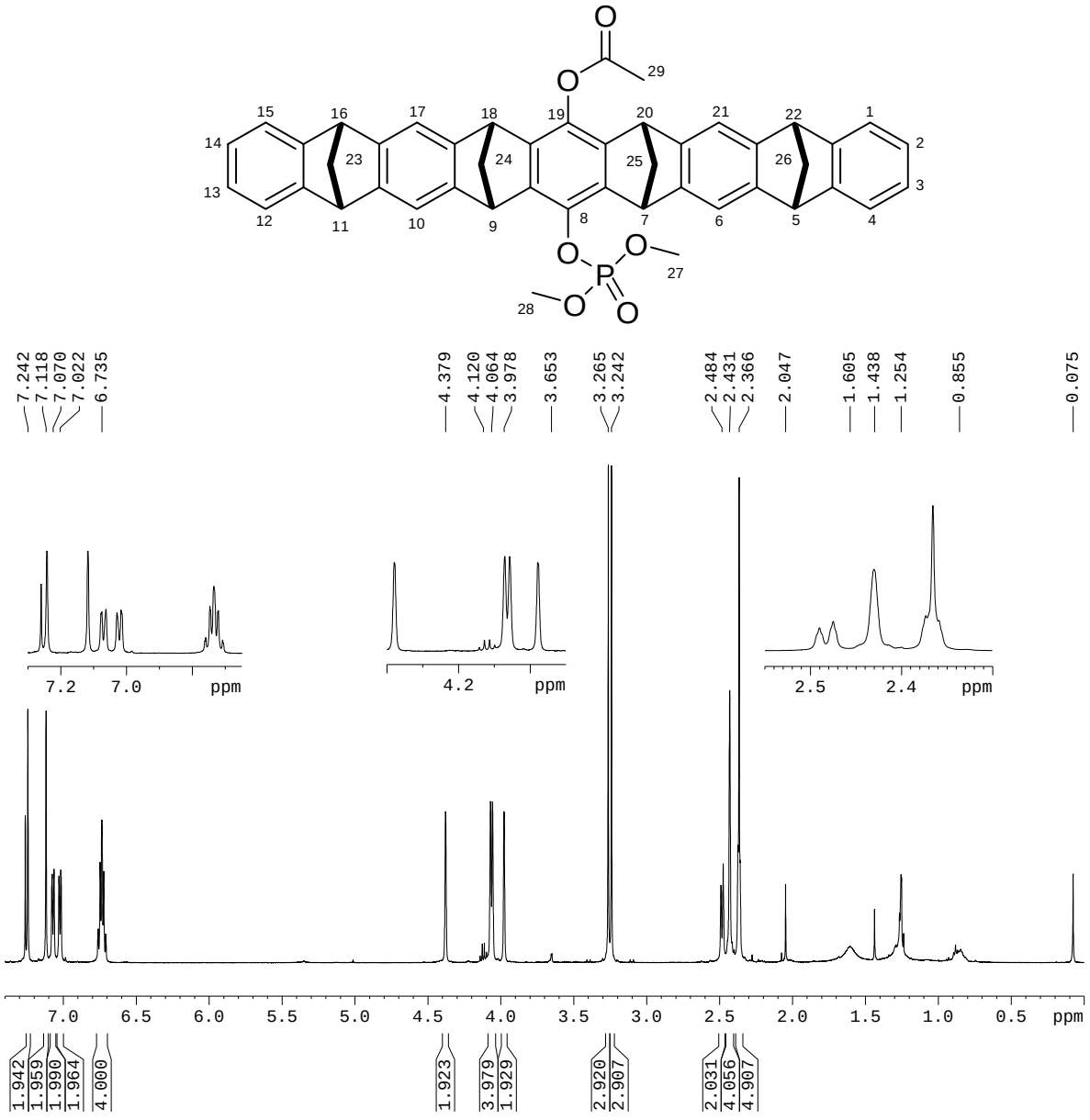

^{1}H-NMR

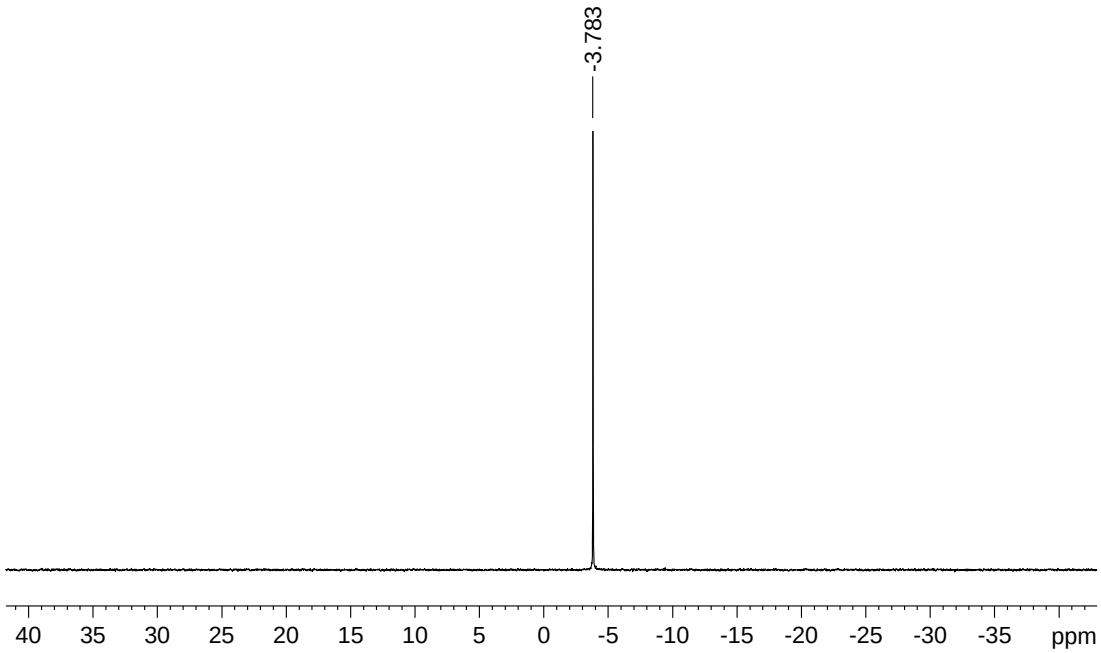

^{31}P-NMR

^{1}H-NMR (500MHz, $CDCl_3$): δ [ppm] = 2.36 (m, 5H, H-24a, H-25a, H-29), 2.43 (s, 4H, H-23, H-26), 2.48 (d, 4H, H-23, H-26), 3.25 (d, $^{3}J_{\text{H-27/P, H-28/P}}$ =1.00, 6H, H-27, H-28), 3.97 (s, 2H, H-7, H-9), 3.06 (d, 4H, H-5, H-11, H-16, H-22), 4.38 (s, 2H, H-18, H-20), 6.73 (m, 4H, H-2, H-3, H-13, H-14), 7.02 (d, 2H, H-4, H-12), 7.07 (d, 2H, H-1, H-15), 7.12 (s, 2H, H-6, H-10), 7.24 (s, 2H, H-17, H-21).

^{13}C-NMR (125.7MHz, $CDCl_3$): δ [ppm] = 20.9 (C-29), 48.7 (C-7, C-9, C-18, C-20), 51.3(d, C-5, C-11, C-16, C-22), 54.9(d, C-27, C-28), 68.5, 69.7 (C-23, C-24, C-25, C-26), 116.6 (C-17, C-21), 117.2 (C-6, C-10), 121.0 (C-1, C-15), 121.8 (C-4, C-12), 124.8 (d, C-2, C-3, C13, C-14), 136.7, 141.4, 142.3 (C-5a, C-16a, C-21a, C-10a,C-7a, C-8a, C-18a, C-19a), 146.4, 146.8, 147.8 (C-6a, C-9a, C-17a, C-20a, C-8, C-9), 150.6 (d, C-4a, C-11a, C-15a, C-22a), 169.0 (-CH_3CO).

^{31}P-NMR (202MHz, CD_3OD): δ [ppm] = -3.78

HR-MS (ESI pos., MeOH): m/z $[M+Na]^+$: cal. 739.2220, obs. 739.2281.

General procedure for methyl deprotection of phosphate ester of the tweezers

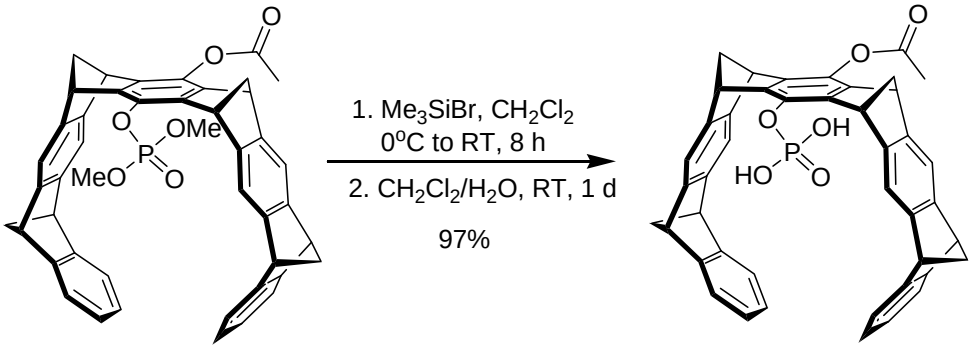

192
$C_{46}H_{37}O_6P$
716,76 g/mol

193
$C_{44}H_{33}O_6P$
688,7 g/mol

To a 0 ^oC cooled solution of 24 mg (0.0336 mmol) tweezer **192** in anhydrous CH_2Cl_2, 44 µl (0.336 mmol) trimethylsilyl bromides (TMSBr) were added dropwise and then stirred at RT for 8 hour. The excess of TMSBr and solvent were removed by condensation and remaining residue was dried on oil pump for 2-5 h. The solid residue was then dissolved in CH_2Cl_2/H_2O (1:1) and stirred at RT for 24 h. Two phases were separated, and after drying organic phase on *rota vap,* 22 mg of white solid were collected. The crude was washed with n-hexane or acetonitrile to remove the trace amount of grease from the product. This procedure is used as a general procedure for the methyl group deprotection of all the other tweezers.

Yield: 22 mg, 97 %.

Melting Point: > 221 ^oC brown coloration.

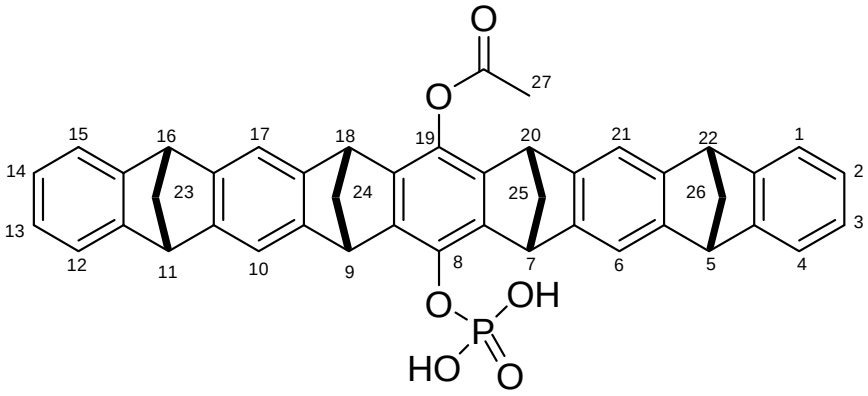

193

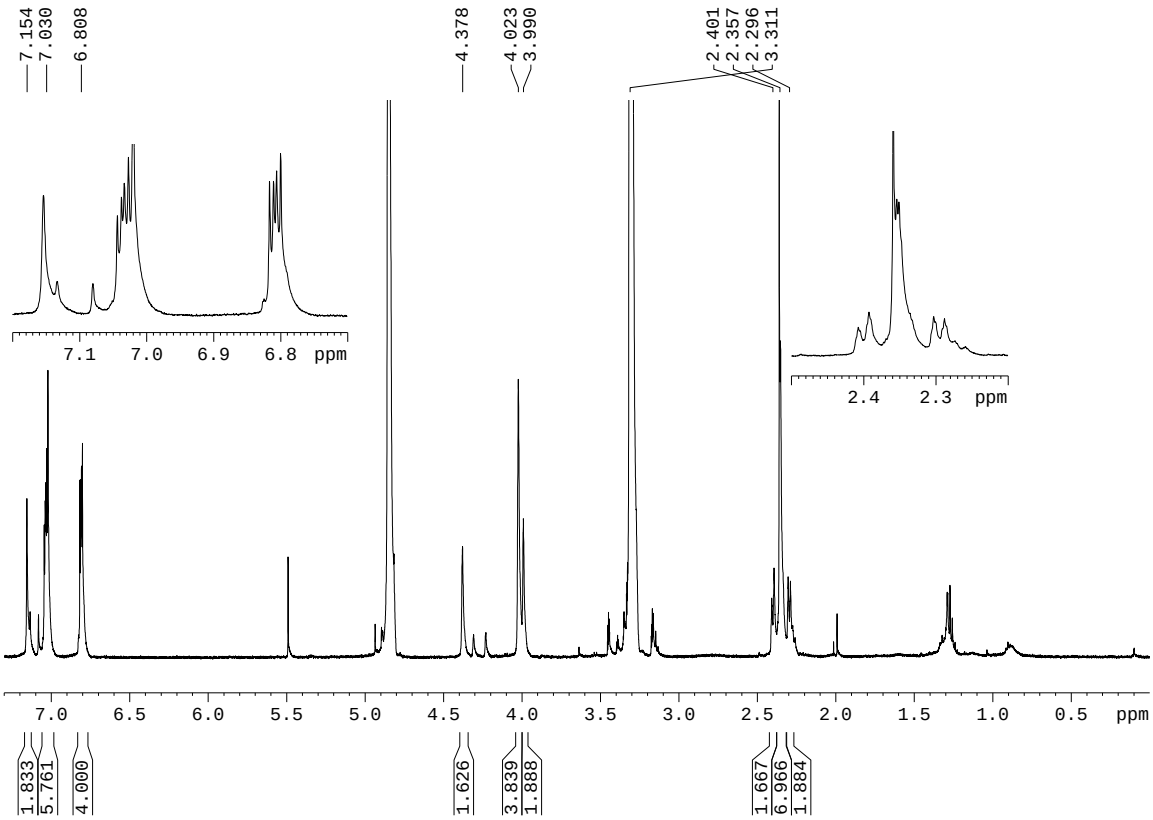

^{1}H-NMR

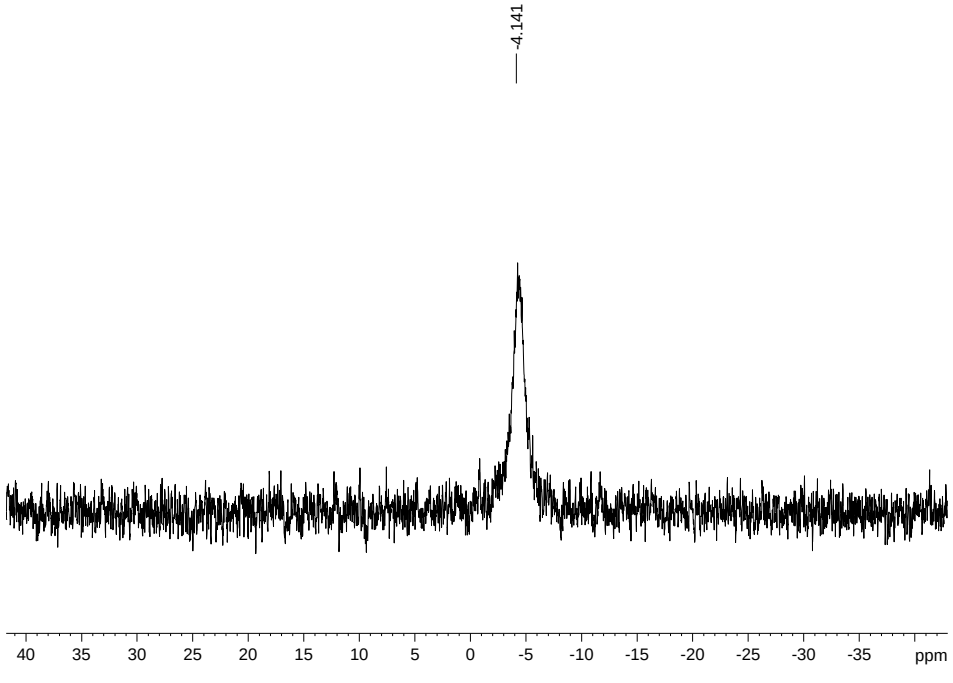

^{31}P-NMR

^{1}H-NMR (500 MHz, CD3OD): δ [ppm] = 2.29 (d, 2H, H-24a, H-25a), 2.35 (m, 7H, H-23, H-26, H-27), 2.40 (d, 2H, H-24i, H-25i), 3.99 (2H, H-7, H-9), 4.02 (s, 4H, H-5, H-11, H-16,

H-22), 4.38 (s, 2H, H-18, H-20), 6.81 (m, 4H, 4H, H-2, H-3, H-13, H-14), 7.03 (m, 6H, H-6, H-10, H-4, H-12, H-1, H-15), 7.15 (s, 2H, H-17, H-21).

^{13}C-NMR (125.7 MHz, CD_3OD): δ [ppm] = 20.6 (C-27), 49.4 (C-7, C-9, C-18, C-20), 52.5(C-5, C-11, C-16, C-22), 69.2, 69.4 (C-23, C-24, C-25, C-26), 117.2 (C-6, C-10), 118.3 (C-17, C-21), 122.3 (d, C-4, C-12, C-1, C-15), 126.1 (d, C-2, C-3, C13, C-14), 137.7, 138.9, 143.4 (C-5a, C-16a, C-21a, C-10a,C-7a, C-8a, C-18a, C-19a), 148.2, 148.7, 149.2 (C-6a, C-9a, C-17a, C-20a, C-8, C-9), 150.2 (d, C-4a, C-11a, C-15a, C-22a), 170.9 (-CH_3CO).

^{31}P-NMR (202MHz, CD_3OD): δ [ppm] = -4.14

HR-MS (ESI pos., neg., MeOH): m/z $[M+Na]^+$: cal. 711.1907, obs. 711.2030, m/z $[M-H]^-$: cal. 687.1942, obs. 687.2061.

5.2.2.2 Synthesis of the octyl phosphate tweezer 195

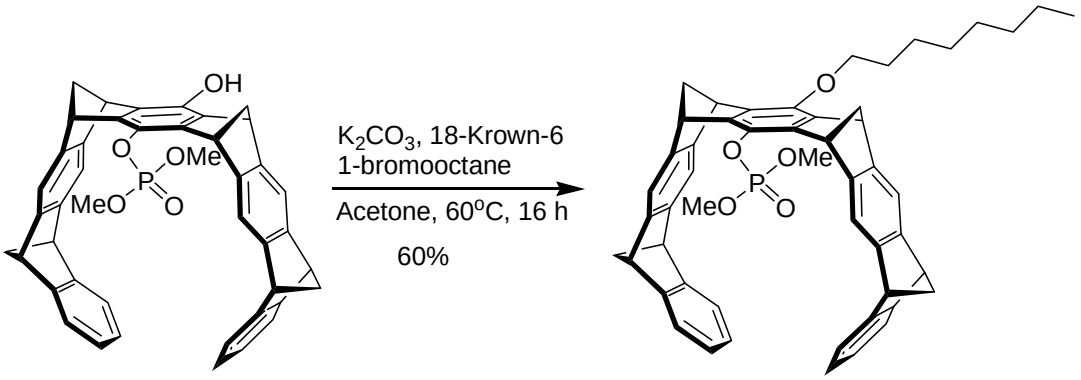

189
$C_{44}H_{35}O_5P$
674,72 g/mol

182
$C_{52}H_{51}O_5P$
786,93 g/mol

In a suspension of 22 mg (0.0326 mmol) tweezer **189** and 5.0 mg (0.0326 mmol) K_2CO_3 in abs acetone, 9 µl (0.0489 mmol) 1-bromooctane were added. A catalytic amount of 18-Krown-6 was also added and the reaction mixture was stirred at 60 °C for 24 h. The mixture was then cooled to RT and transferred into a separating funnel. After adding sat $NaHCO_3$, the mixture was extracted three times with dichloromethane. The combined organic layer was washed once with sat NH_4Cl and once with brine solution. Organic phase was dried over Na_2SO_4 and the solvent was removed by reduced pressure. Product was purified by column chromatography using 1:3 (EtOAc/ Cyclohexane) as eluent. Compound **182** also crystallized in methanol.

Yield: 15 mg, 60%

Melting Point: 188 ^{o}C

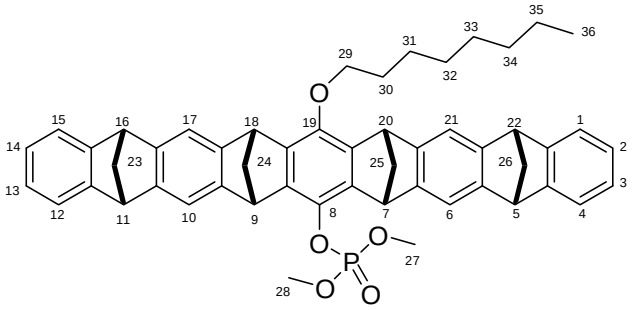

182

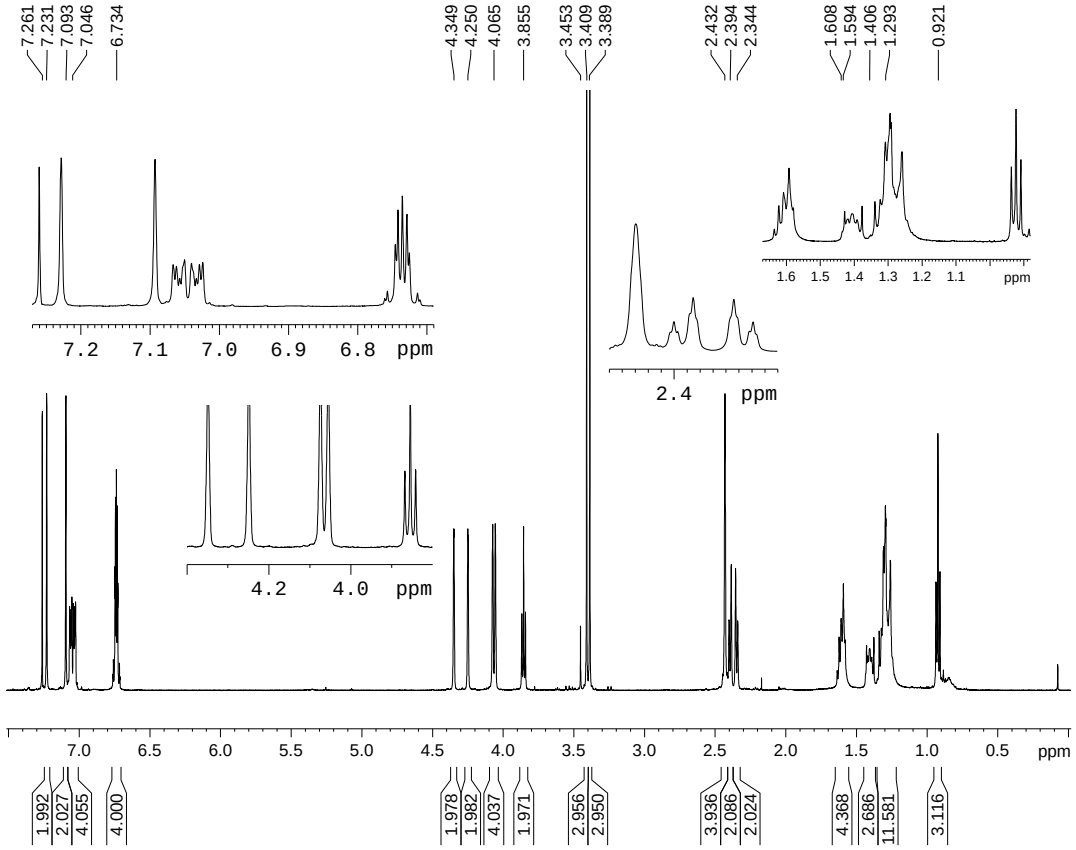

^{1}H-NMR

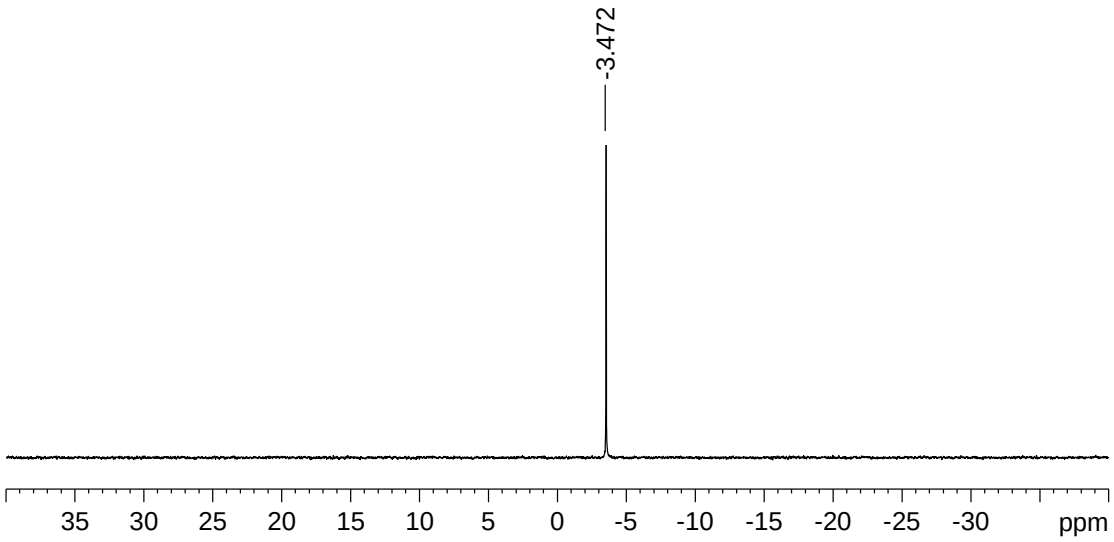

^{31}P-NMR

^{1}H-NMR (500MHz, $CDCl_3$): δ [ppm] = 0.92 (t, 3H, H-36), 1.29 (m, 8H, H-32, H-33, H-34, H-35), 1.40 (m, 2H, H-31), 1.59 (m, 2H, H-30), 2.35 (d, 2H, H-24a, H-25a), 2.39 (d, 2H, H-24i, H-25i), 2.43 (s, 4H, H-23, H-26), 3.39 (d, $^{3}J_{\text{H-27/P, H-28/P}}$ = 11.00, 6H, H-27, H-28), 3.85 (t, 2H, H-29), 4.06 (d, 4H, H-5, H-11, H-16, H-22), 4.25 (s, 2 H, H-18, H-20), 4.35 (s, 2H, H-7, H-9), 6.73 (m, 4H, H-2, H-3, H-13, H-14), 7.05 (dm, 4H, H-1, H-15, H-4, H-12), 7.09 (s, 2H, H-17, H-21), 7.23 (s, 2H, H-6, H-10).

^{13}C-NMR (125.7MHz, $CDCl_3$): δ [ppm] = 14.3 (C-36), 22.9 (C-35), 26.2 (C-34), 29.5 (C-32, C-33), 30.4 (C-31), 31.9 (C-30), 48.6, 51.4 (d, C-7, C-9, C-18, C-20, C-5, C-11, C-16, C-22), 68.8, 69.7 (C-23, C-26, C-24, C-25), 74.1 (C-29), 116.1, 117.2 (C-17, C-21, C-6, C-10), 121.2, 121.6 (C-1, C-15, C-4, C-12), 124.7 (d, C-2, C-3, C13, C-14), 134.9, 140.8, 141.2, 145.8 (C-5a, C-16a, C-21a, C-10a,C-7a, C-8a, C-18a, C-19a), 147.1, 147.7 (C-6a, C-9a, C-17a, C-20a, C-8, C-9), 150.6 (d, C-4a, C-11a, C-15a, C-22a).

^{31}P-NMR (202MHz, $CDCl_3$): δ [ppm] = -3.47

HR-MS (ESI pos., MeOH): m/z $[M+Na]^+$: cal. 809.3366, obs. 809.3442.

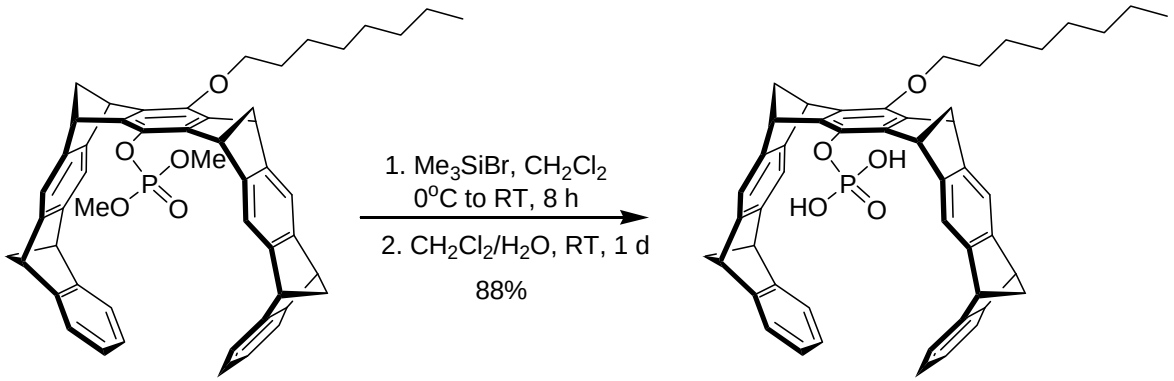

182
$C_{52}H_{51}O_5P$
786,93 g/mol

190
$C_{50}H_{47}O_5P$
758,88 g/mol

13 mg (0.0165mmol) of **182** were treated with 22 µl (0.165mmol) of TMSBr in 5 ml CH_2Cl_2 by using the general procedure.

Yield: 11 mg, 88 %.

Melting Point: > 185 °C brown coloration.

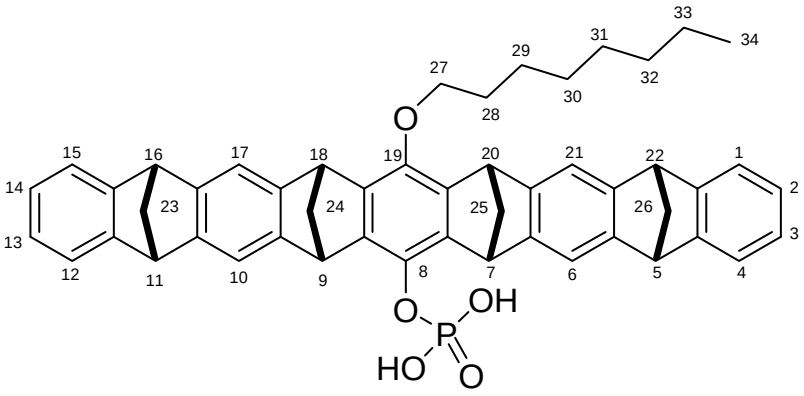

190

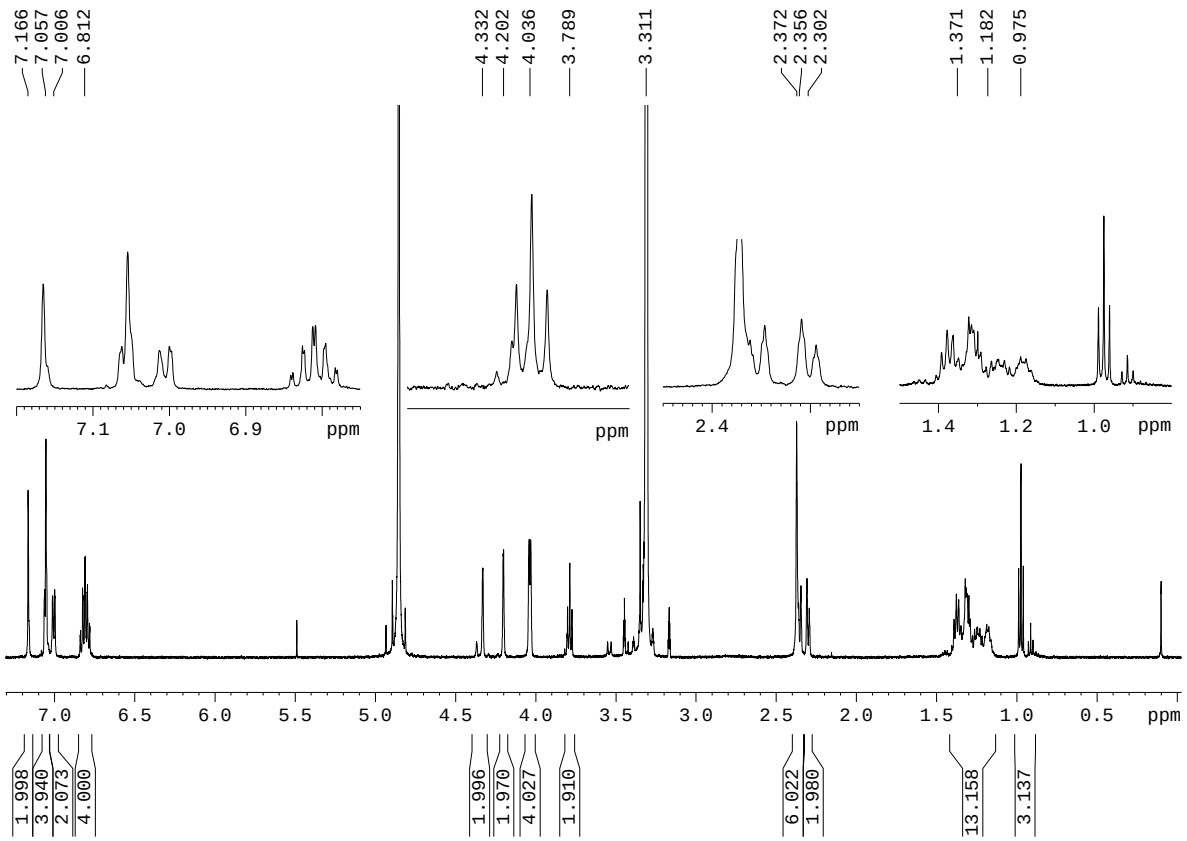

^{1}H-NMR

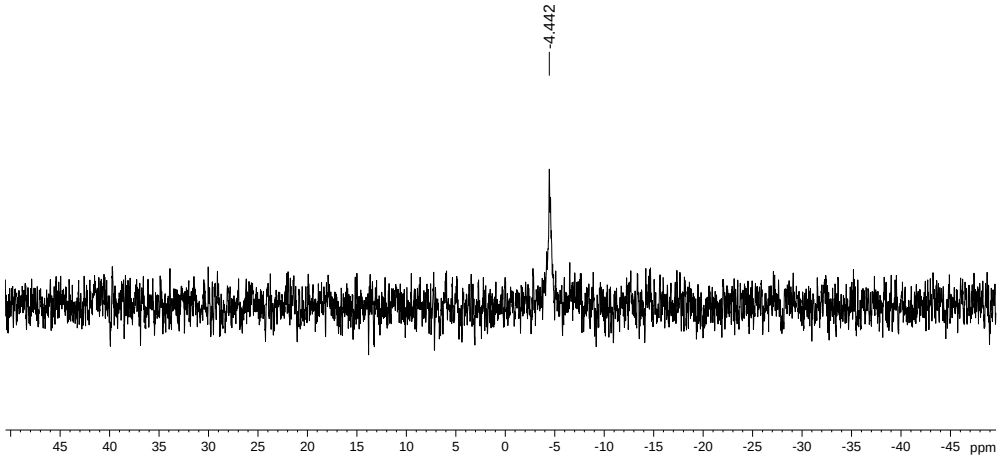

^{31}P-NMR

^{1}H-NMR (500MHz, CD_3OD): δ [ppm] = 0.97 (t, 3H, H-34), 1.18-1.37 (m, 12H, H-28, H-29, H-30, H-31, H-32, H-33), 2.30 (d), 2.35 (d), 2.37(s) (8H, H-24, H-25, H-23, H-26), 3.79 (t, 2H, H-27), 4.04 (ds, 4H, H-5, H-11, H-16, H-22), 4.20 (s, 2 H, H-18, H-20), 4.33 (s, 2H, H-7, H-9), 6.81 (m, 4H, H-2, H-3, H-13, H-14), 7.00 (d, 2H, H-1, H-15), 7.06 (m, 4H, H-4, H-12, H-17, H-21), 7.17 (s, 2H, H-6, H-10).

^{31}P-NMR (202MHz, CD_3OD): δ [ppm] = -4.44.

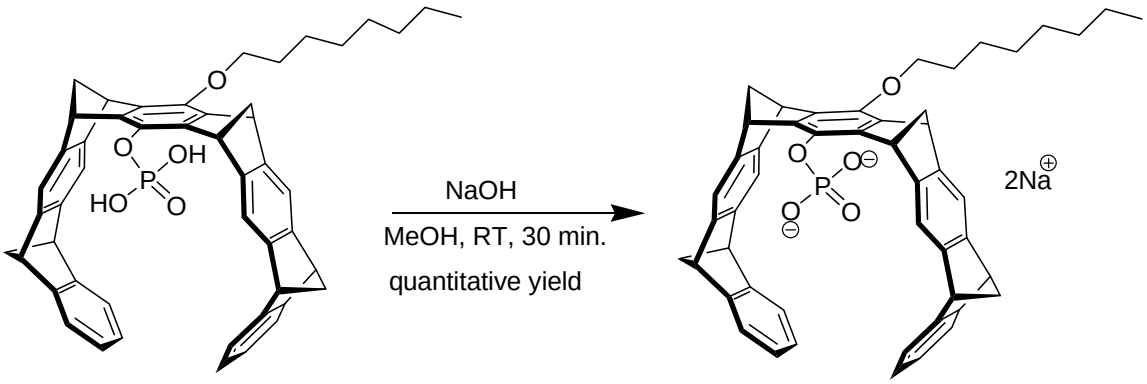

190
$C_{50}H_{47}O_5P$
758,88

195
$C_{50}H_{46}Na_2O_5P$
802,84 g/mol

In a solution of 9.0 mg (0.0118 mmol) tweezer **190,** 0.316 mg (0.948 mmol) sodium hydroxide was added and stirred the solution for 30 min. at RT. The solvent was removed on a *rota vap* and white solid product was obtained in quantitative yield.

Melting Point: > 220 °C, decomposition.

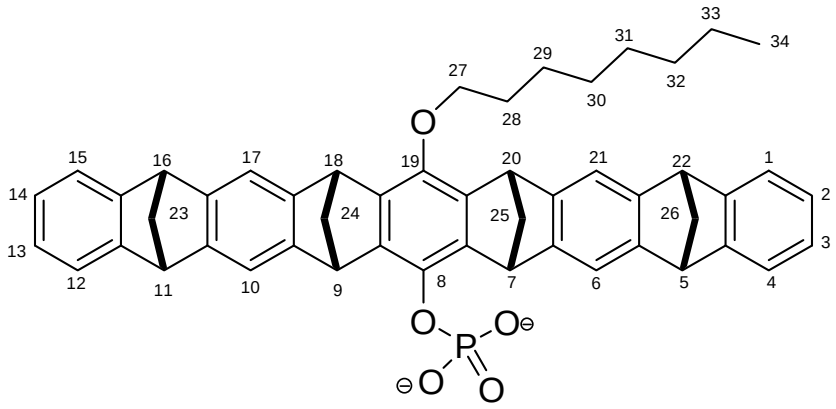

3

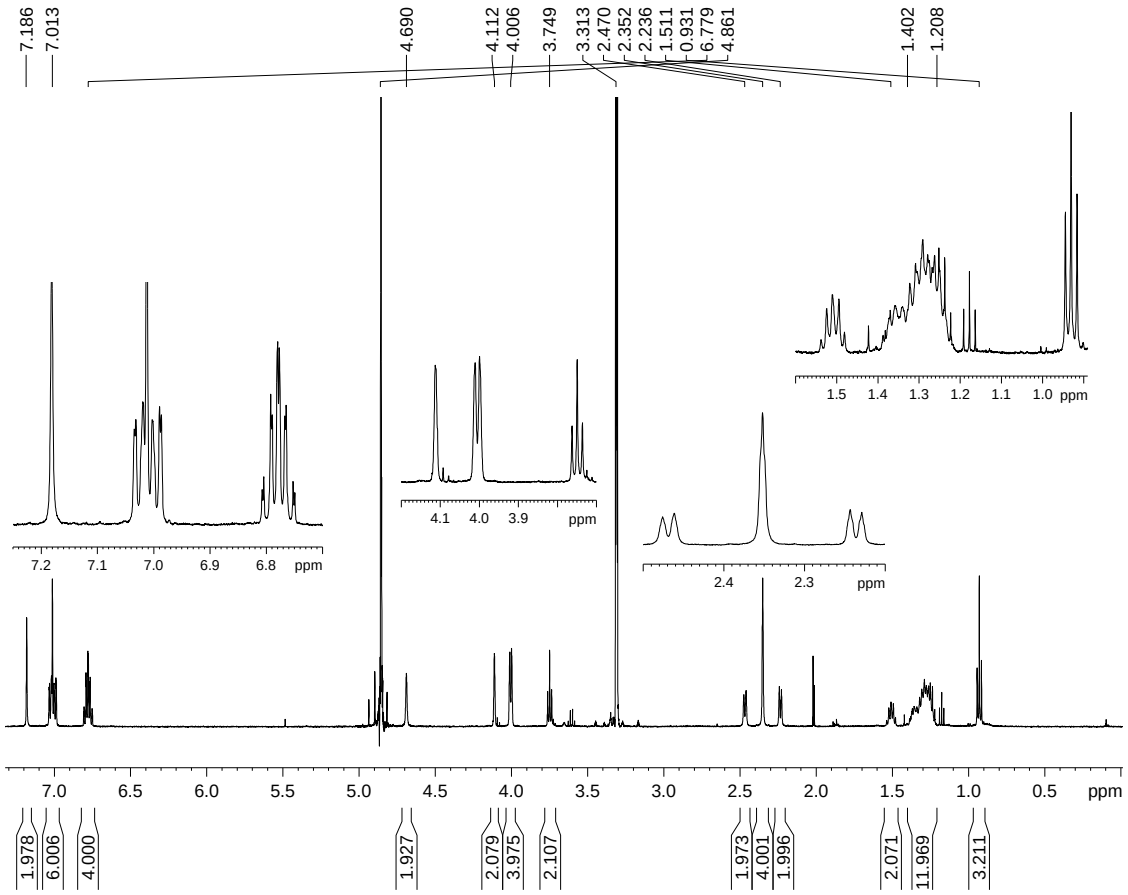

^{1}H-NMR

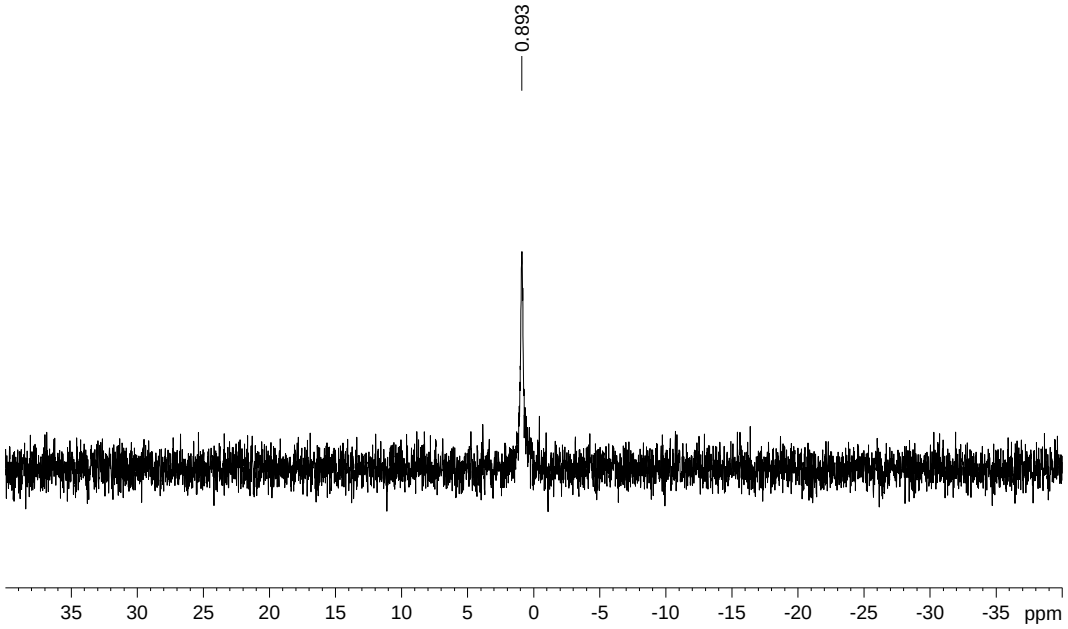

^{31}P-NMR

^{1}H-NMR (500MHz, CD_3OD): δ [ppm] = 0.93 (t, 3H, H-34), 1.23-1.38 (m, 10H, H-29, H-30, H-31, H-32, H-33), 1.51 (m, 2H, H-28), 2.24 (d, 2H, H-24a, H-25a), 2.35 (s, 4H, H-23, H-26), 2.47

(d, 2H, H-24i, H-25i), 3.75 (t, 2H, H-27), 4.00 (ds, 4H, H-5, H-11, H-16, H-22), 4.11 (s, 2 H, H-18, H-20), 4.69 (s, 2H, H-7, H-9), 6.78 (m, 4H, H-2, H-3, H-13, H-14), 7.01 (m, 6H, H-1, H-15, H-4, H-12, H-17, H-21), 7.18 (s, 2H, H-6, H-10).

^{13}C-NMR (125.7MHz, CD_3OD): δ [ppm] = 14.6 (C-34), 23.8 (C-33), 27.1 (C-32), 30.5 (d, C-31, C-30), 31.2 (C-29), 32.9 (C-28), 49.3-49.6 (C-7, C-9, C-18, C-20), 52.4 (C-5, C-11, C-16, C-22), 69.1 (d, C-23, C-26, C-24, C-25), 74.9 (C-27), 116.3, 117.6 (C-17, C-21, C-6, C-10), 122.0 (d, C-1, C-15, C-4, C-12), 125.9 (d, C-2, C-3, C13, C-14), 141.3, 143.2, 144.6 (C-5a, C-16a, C-21a, C-10a,C-7a, C-8a, C-18a, C-19a), 148.5(d), 149.6, 150.1 (C-6a, C-9a, C-17a, C-20a, C-8, C-9), 152.1 (d, C-4a, C-11a, C-15a, C-22a).

^{31}P-NMR (202MHz, CD_3OD): δ [ppm] = 0.893

HR-MS (ESI pos., MeOH): m/z $[M+H]^+$: cal. 803.2873, obs. 803.2904.

5.2.2.3 Synthesis of the ethoxycarboxymethyl phosphate tweezer 196

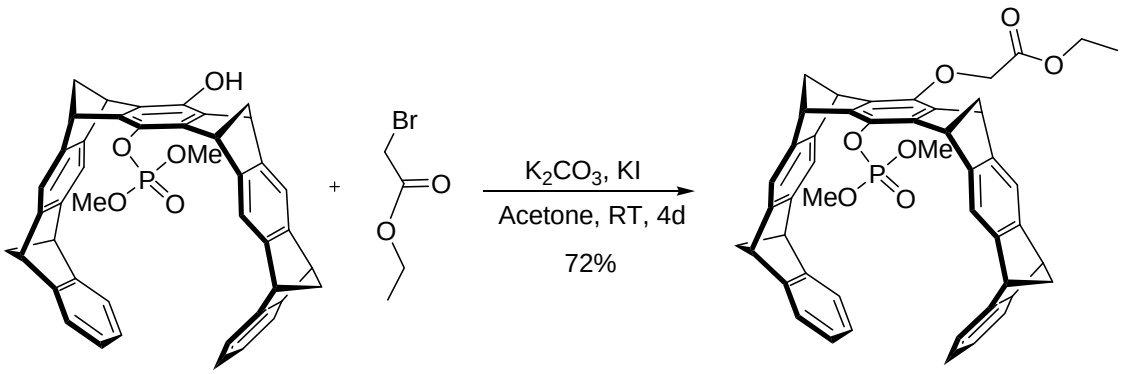

189
$C_{44}H_{35}O_5P$
674,72 g/mol

191
$C_{48}H_{41}O_7P$
760,81 g/mol

Under argon atmosphere, in a solution of 30 mg (0.044 mmol) tweezer **189** in 5 ml absolute acetone 9.0 mg (0.066 mmol) K_2CO_3, 7.0 µl (0.066 mmol) ethylbromoacetate and a few granules of KI were added and then the reaction mixture is stirred at RT for 4 days. The reaction mixture was diluted with CH_2Cl_2 and washed with sat NH_4Cl and finally with dist water. Organic phase was dried over Na_2SO_4. Solvent removed on a rotary evaporator and crude was purified by column chromatography using EtOAc/cyclohexane (1:3) eluent.

Yield: 24 mg, 72%

Melting Point: > 170 ^{o}C brown coloration.

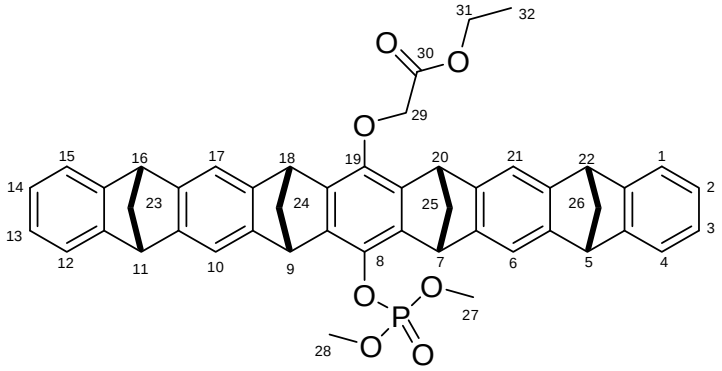

191

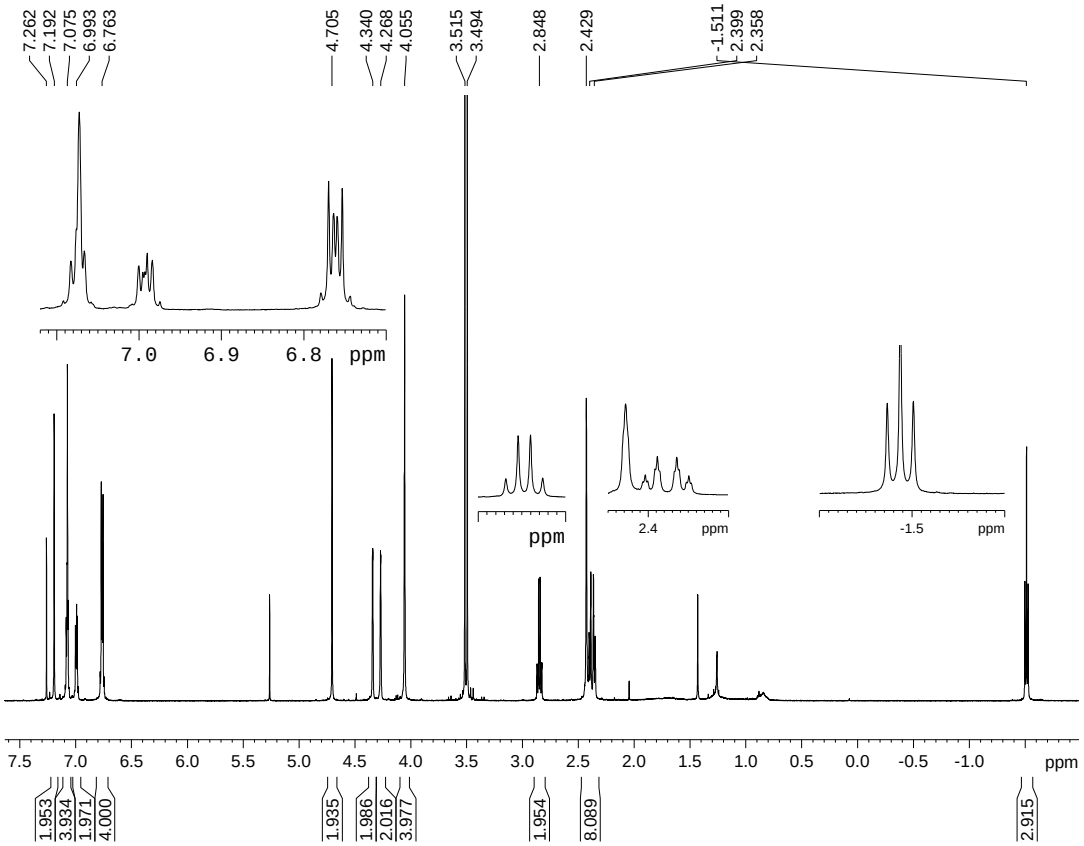

^{1}H-NMR

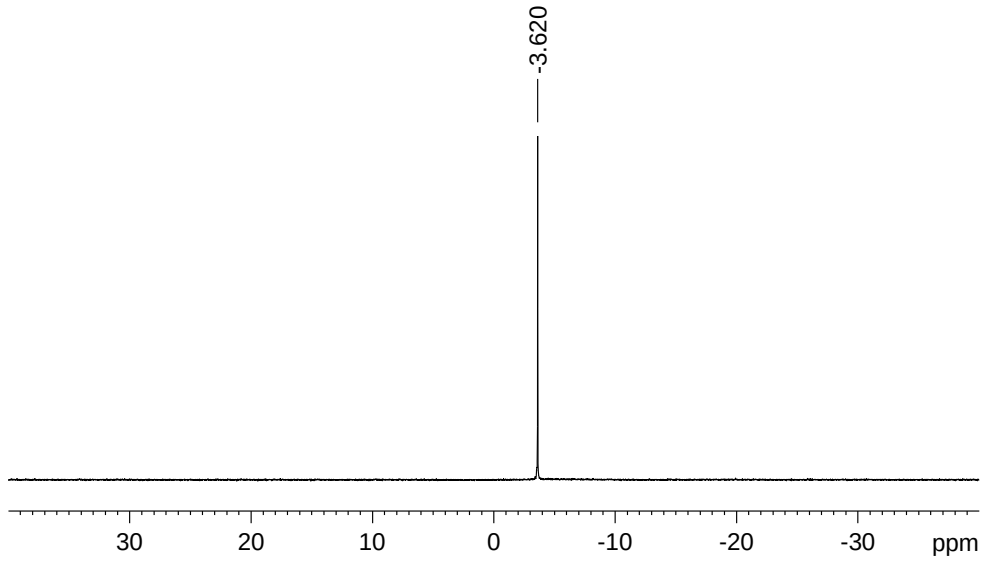

^{31}P-NMR

^{1}H-NMR (500MHz, $CDCl_3$): δ [ppm] = -1.51 (t, 3H, H-32), 2.37 (tm, 4H, 24a, H-25a, H-24i, H-25i), 2.43 (s, 4H, H-23, H-26), 2.85 (m, 2H, H-31), 3.50 (d, $^{3}J_{\text{H-27/P, H-28/P}}$ = 11.00, 6H, H-27, H-28), 4.05 (s, 4H, H-5, H-11, H-16, H-22), 4.27 (s, 2 H, H-18, H-20), 4.34 (s, 2H, H-7, H-9), 4.70 (s, 2H, H-29), 6.76 (m, 4H, H-2, H-3, H-13, H-14), 6.99 (m, 2H, H-1, H-15), 7.07 (m, 4H, H-4, H-12, H-17, H-21), 7.19 (s, 2H, H-6, H-10).

^{13}C-NMR (125.7MHz, $CDCl_3$): δ [ppm] = 10.9 (C-32), 48.1, 48.8 (C-7, C-9, C-18, C-20), 51.2(C-5, C-11, C-16, C-22), 54.9 (d, C-27, C-28), 61.1 (C-31), 68.5 (C-23, C-26, C-24, C-25), 69.1 (C-29), 116.3, 117.0 (C-17, C-21, C-6, C-10), 120.9, 121.5 (C-1, C-15, C-4, C-12), 124.8 (d, C-2, C-3, C13, C-14), 134.7(d), 139.8, 141.1(d), 145.0 (C-5a, C-16a, C-21a, C-10a,C-7a, C-8a, C-18a, C-19a), 146.9, 147.2, 147.5, 147.7 (C-6a, C-9a, C-17a, C-20a, C-8, C-9), 150.8, 151.0 (C-4a, C-11a, C-15a, C-22a), 169.1 (C-30).

^{31}P-NMR (202MHz, $CDCl_3$): δ [ppm] = -3.62

HR-MS (ESI pos., MeOH): m/z $[M+Na]^+$: cal. 783.2482, obs. 783.2550.

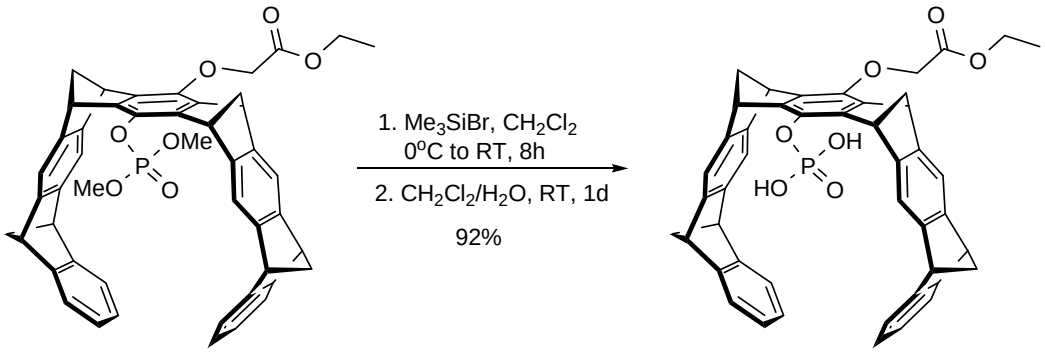

191
$C_{48}H_{41}O_7P$
760,81 g/mol

196
$C_{46}H_{37}O_7P$
732,76 g/mol

28 mg (0.0368 mmol) **191** were treated with 48 µl (0.368 mmol) TMSBr using the general procedure.

Yield: 24 mg, 92%.

Melting Point: > 282 °C brown coloration.

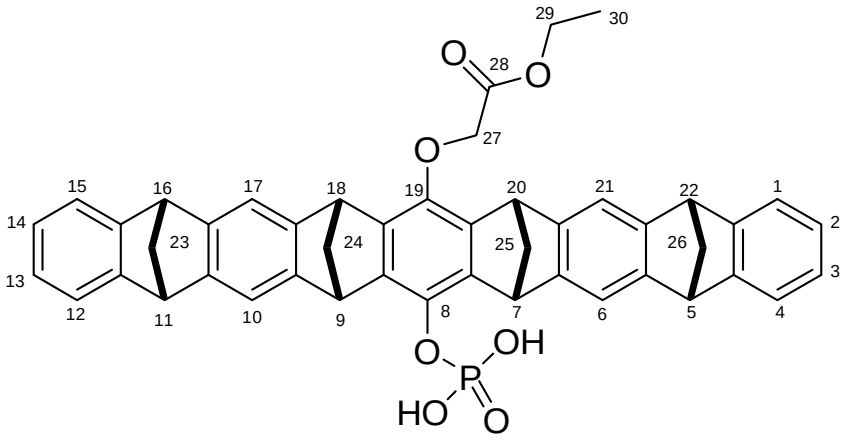

196

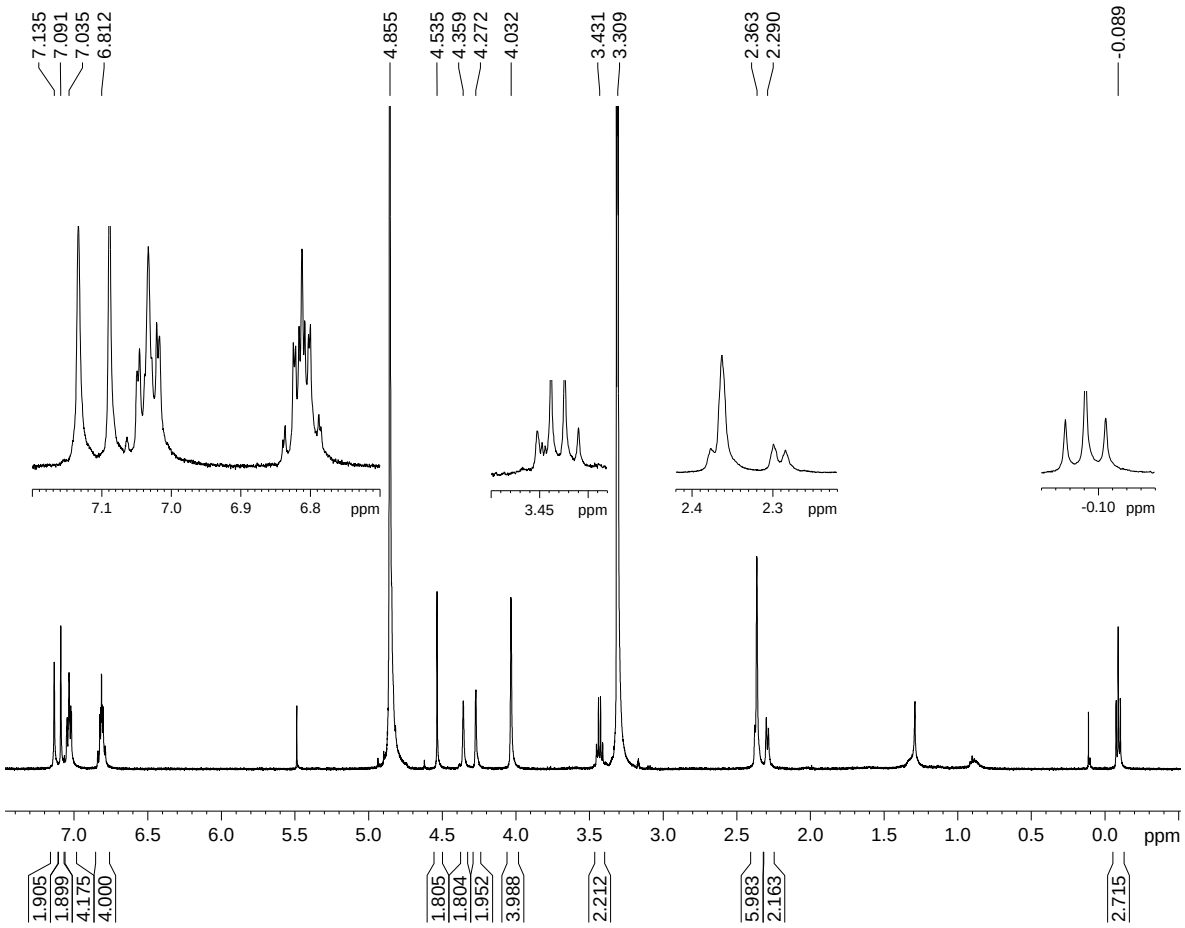

^{1}H-NMR

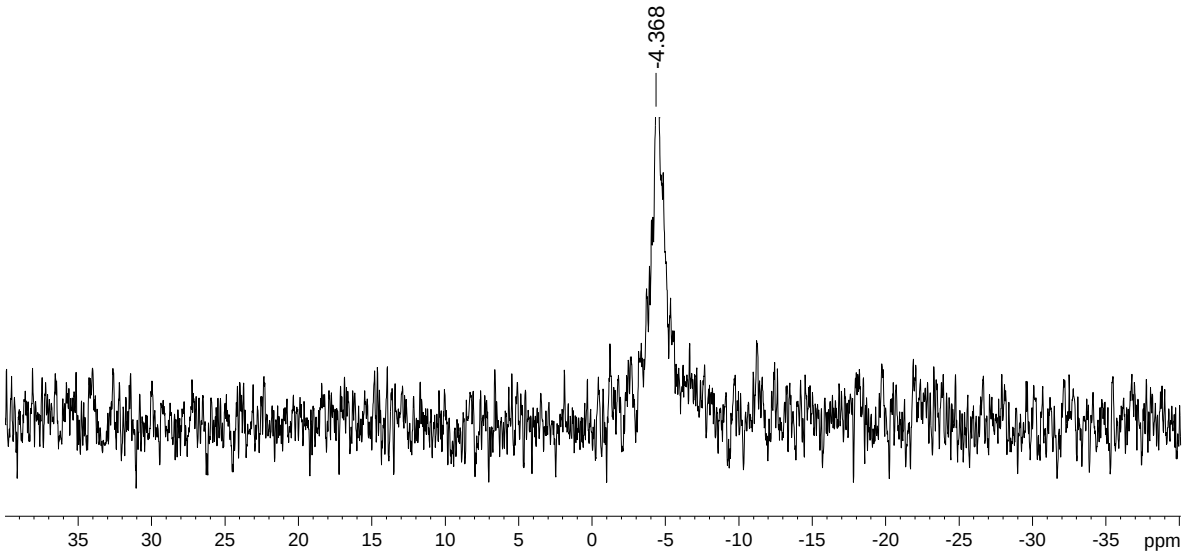

^{31}P-NMR

^{1}H-NMR (500MHz, CD_3OD): δ [ppm] = -0.089 (t, 3H, H-30), 2.29 (d, 2H, 24a, H-25a), 2.36 (m, 6H, H-23, H-26, H-24i, H-25i), 3.43 (m, 2H, H-29), 4.03 (s, 4H, H-5, H-11, H-16, H-22),

4.27 (s, 2 H, H-18, H-20), 4.36 (s, 2H, H-7, H-9), 4.53 (2H, H-27), 6.81 (m, 4H, H-2, H-3, H-13, H-14), 7.03 (m, 4H, H-1, H-15, H-4, H-12), 7.09 (s, 2H, H-17, H-21), 7.13 (s, 2H, H-6, H-10).

^{13}C-NMR (125.7MHz, CD_3OD): δ [ppm] = 13.4 (C-30), 49.4 (m, C-7, C-9, C-18, C-20), 52.5 (C-5, C-11, C-16, C-22), 62.4 (C-29), 69.1 (C-23, C-26, C-24, C-25), 70.8 (C-27), 117.1, 118.1 (C-17, C-21, C-6, C-10), 122.3 (d, C-1, C-15, C-4, C-12), 126.1 (d, C-2, C-3, C13, C-14), 141.8, 143.1 (C-5a, C-16a, C-21a, C-10a,C-7a, C-8a, C-18a, C-19a), 148.7, 148.9, 149.1(d) (C-6a, C-9a, C-17a, C-20a, C-8, C-9), 152.3 (C-4a, C-11a, C-15a, C-22a), 171.1 (C-28).

^{31}P-NMR (202MHz, CD_3OD): δ [ppm] = -4.37

HR-MS (ESI pos., neg., MeOH): m/z $[M+Na]^+$: cal. 755.2169, obs. 755.2237. m/z $[M-H]^-$: cal. 731.2204, obs. 731.2301.

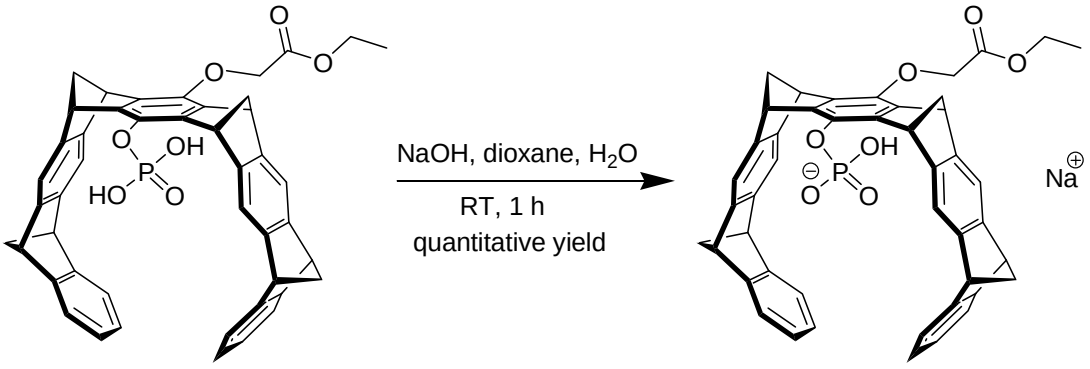

196
C46H37O7P
732,76 g/mol

203
C46H36O7PNa
754,74 g/mol

To a solution of 16 mg (0.022 mmol) **196** in 10 ml dioxane, 0.813 mg (0.022 mmol) NaOH in 1.0 ml water was added and stirred for 1 h at RT. Solvent removed in *vacuo* and solid was supended in 5 ml water and dried on lyophilization apparatus.

Yield: quantitative.

Melting Point: > 225 °C brown coloration.

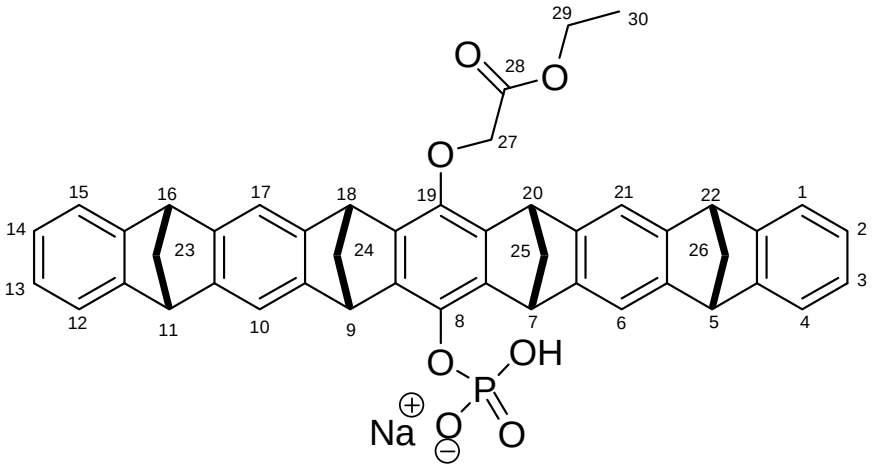

203

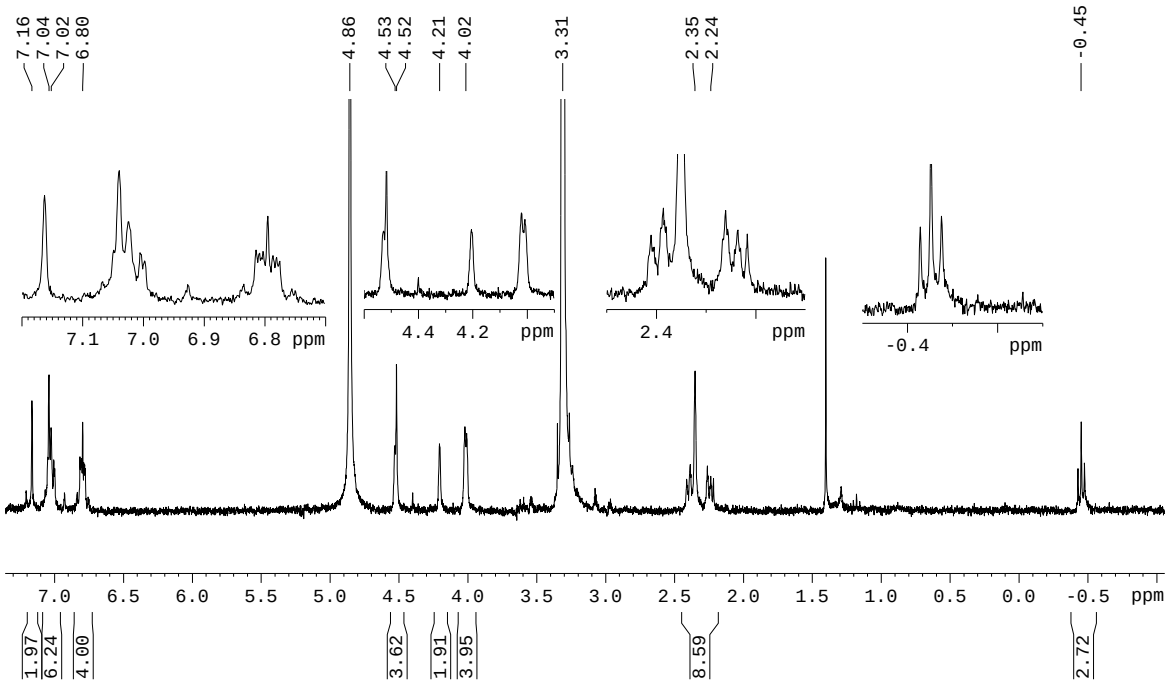

^{1}H-NMR in CD_3OD

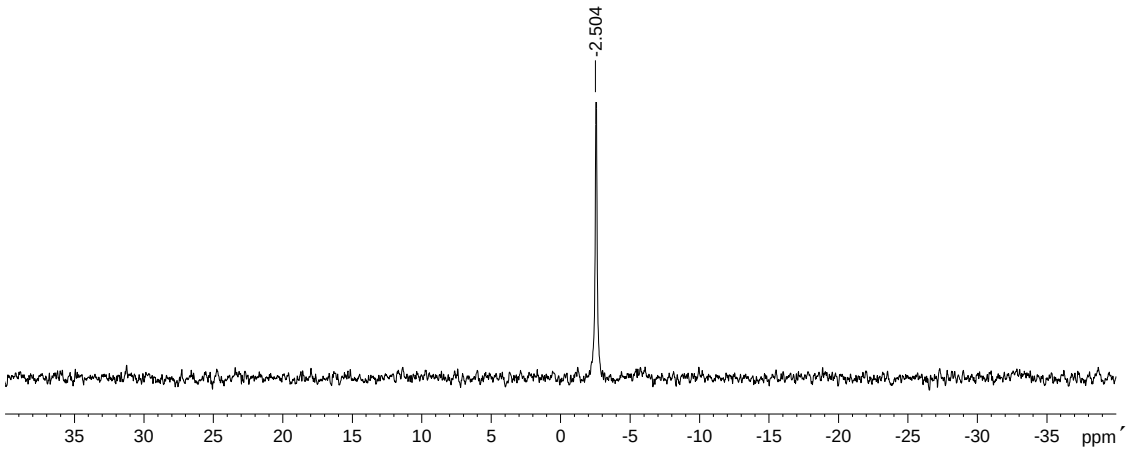

^{31}P-NMR in CD_3OD

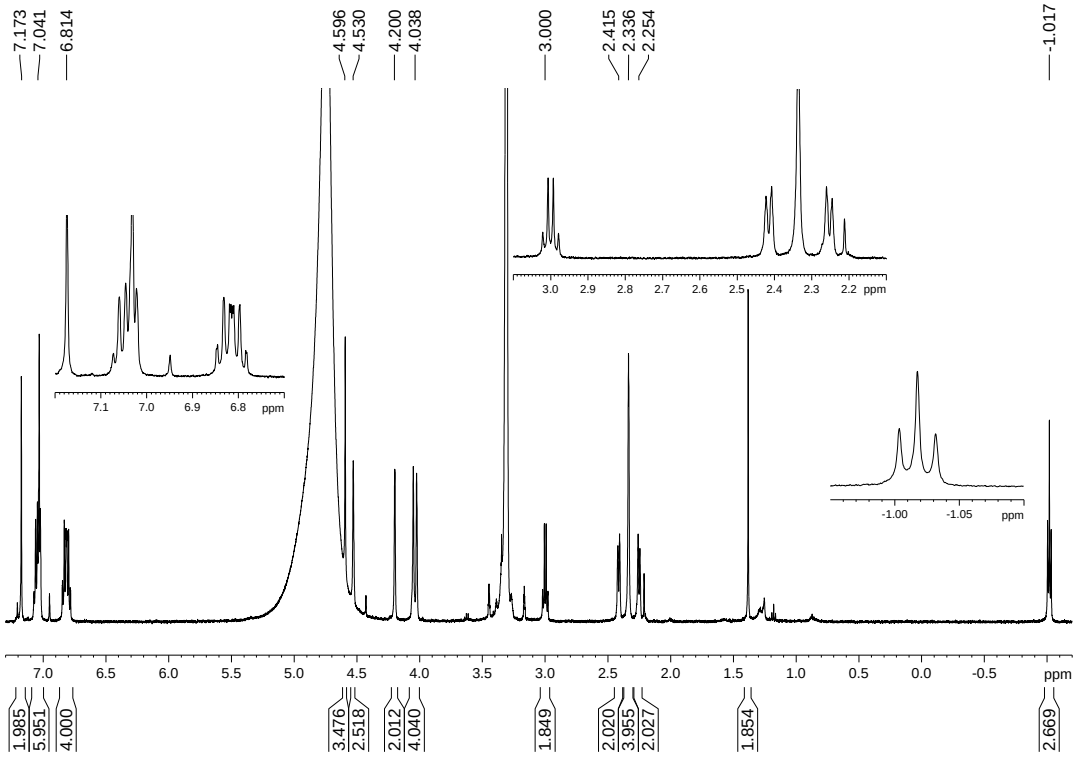

^{1}H-NMR in CD_3OD/D_2O buffer 10 mM, pH 7.2 (2:1)

^{1}H-NMR (300 MHz, CD_3OD): δ [ppm] = -0.45 (2H, H-30), 2.24 (d, 2H, 24a, H-25a), 2.35 (s, 4H, H-23, H-26), 2.39 (d, 2H, H-24i, H-25i), 3.30 (m, 2H, H-29), 4.02 (ds, 4H, H-5, H-11, H-16, H-22), 4.21 (s, 2H, H-18, H-20), 4.52 (s, 2H, H-27), 4.53 (s, 2H, H-7, H-9), 6.80 (m, 4H, H-2, H-3, H-13, H-14), 7.02, 7.04 (m, 6H, H-1, H-15, H-4, H-12, H-17, H-21), 7.16 (s, 2H, H-6, H-10).

^{1}H-NMR {500MHz, CD_3OD/D_2O buffer (2:1)}: δ [ppm] = -1.01 (3H, H-30), 2.25 (d, 2H, 24a, H-25a), 2.34 (s, 4H, H-23, H-26), 2.41 (d, 2H, H-24i, H-25i), 3.00 (m, 2H, H-29), 4.04 (d, 4H, H-5, H-11, H-16, H-22), 4.20 (s, 2H, H-18, H-20), 4.53 (s, 2H, H-7, H-9), 4.59 (s, 2H, H-27),

6.81 (m, 4H, H-2, H-3, H-13, H-14), 7.04 (m, 6H, H-1, H-15, H-4, H-12, H-17, H-21), 7.17 (s, 2H, H-6, H-10).

^{31}P-NMR (202MHz, CD_3OD): δ [ppm] = -2.50

HR-MS (ESI pos., neg., MeOH): m/z $[M+H]^+$: cal. 755.2169, obs. 755.2289, m/z $[M+Na]^+$: cal. 777.1989, obs. 777.2096, m/z $[M-Na]^-$: cal. 731.2204, obs. 731.2329.

5.2.2.4 Synthesis of the glycerol phosphate tweezer 198

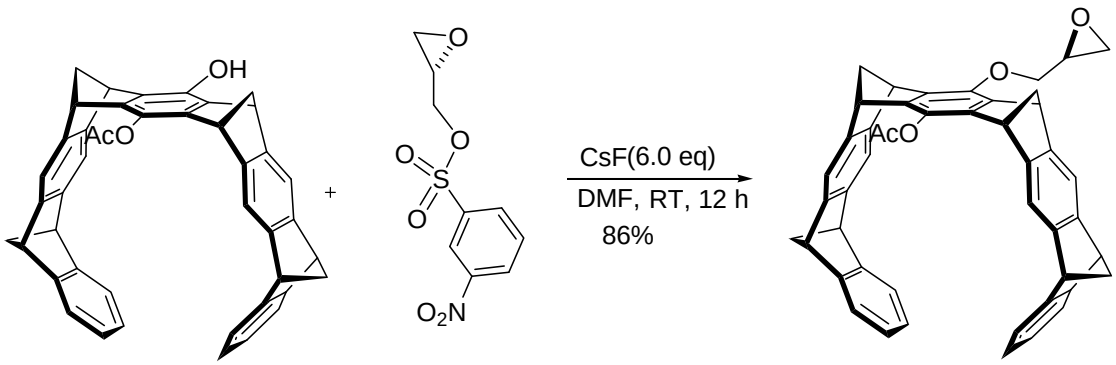

120
$C_{44}H_{32}O_3$
608,72 g/mol

164
$C_{47}H_{36}O_4$
664,79 g/mol

Under argon atmosphere, to a solution of 165 mg (0.271 mmol) tweezer **120** in 5 ml anhydrous DMF, 124 mg (0.814 mmol) CsF were added. The reaction mixture was stirred at RT for 1 h and 84 mg (0.325 mmol) glycidyl nosylate were added and stirred the mixture at 40 °C for 24 h. After cooling to RT, water was added and extracted three times with EtOAc. Organic phase was dried over $MgSO_4$ and solvent was removed by reduced pressure. The residue was purified by column chromatography over silica gel (1:5, EtOAc/cyclohexane).

Yield: 155 mg, 86%.

Melting Point: > 230 °C, brown coloration.

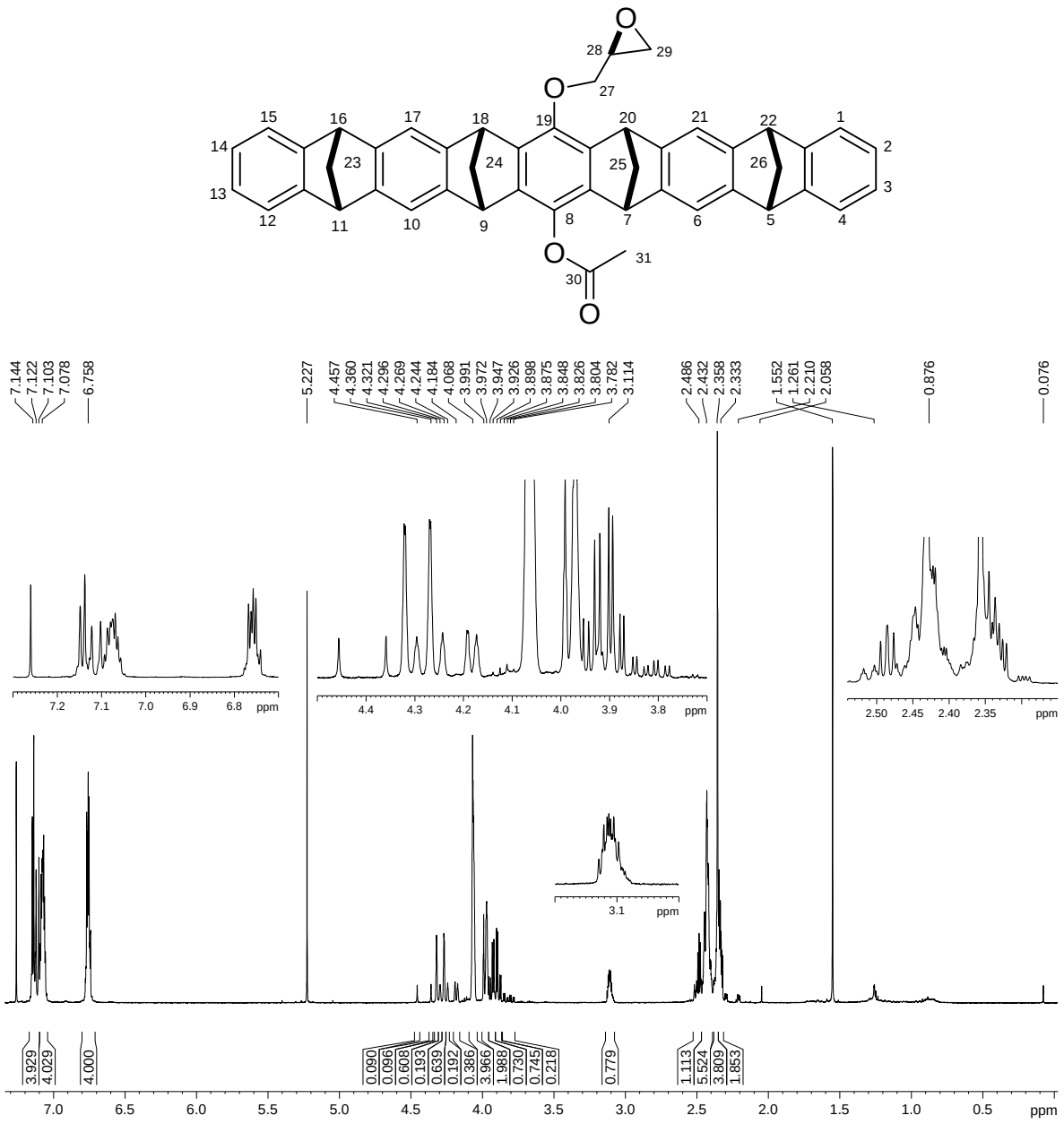

^{1}H-NMR (500MHz, $CDCl_3$): δ [ppm] = 2.33-2.48 (m, 13H, H-29a, H-29i, H-31, 24a, H-25a, H-24i, H-25i, H-23, H-26), 3.11 (m, 1H, H-28), 3.88, 3.94 (m, 2H, H-27a, H-27i), 3.98 (ds, H-7, H-9), 4.07 (s, 4H, H-5, H-11, H-16, H-22), 4.26, 4.31 (dd, 2 H, H-18, H-20), 6.76 (m, 4H, H-2, H-3, H-13, H-14), 7.08 (m, 4H, H-1, H-15, H-4, H-12), 7.10-7.15 (m, 4H, H-17, H-21, H-6, H-10).

^{13}C-NMR (125.7MHz, $CDCl_3$): δ [ppm] = 21.0 (C-31), 44.9 (C-29), 48.7 (m, C-7, C-9, C-18, C-20), 50.4 (C-28), 51.4(C-5, C-11, C-16, C-22), 69.1, 70.1 (C-23, C-26, C-24, C-25), 74.4 (C-27), 116.1, 116.8 (m, C-17, C-21, C-6, C-10), 121.6 (m, C-1, C-15, C-4, C-12), 124.8 (m, C-2, C-

3, C13, C-14), 135.7, 141.0 (C-5a, C-16a, C-21a, C-10a,C-7a, C-8a, C-18a, C-19a), 145.7, 146.4, 146.7, 147.0 (C-6a, C-9a, C-17a, C-20a, C-8, C-9), 150.4 (C-4a, C-11a, C-15a, C-22a), 169.2 (C-30).

HR-MS (ESI pos., MeOH): m/z $[M+Na]^+$: cal. 687.2506, obs. 687.2607.

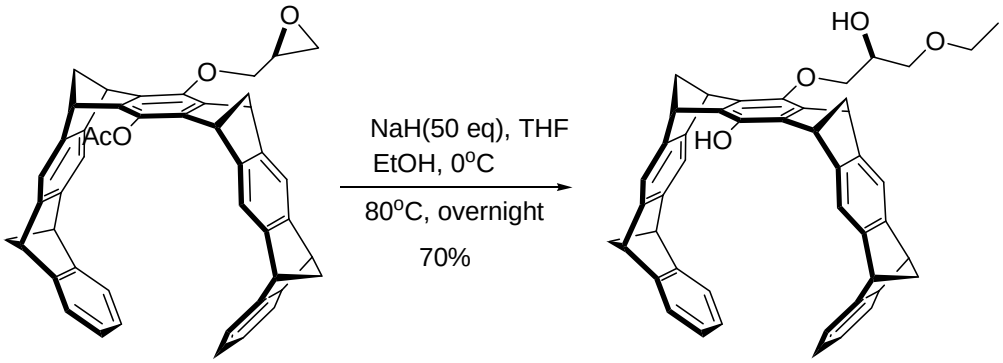

164
$C_{47}H_{36}O_4$
664,79 g/mol

172
C47H40O4
668,82 g/mol

120 mg (3.0 mmol) NaH (60%) were suspended in 2 ml anhydrous THF and cooled to 0°C. To this suspension, 1.0 ml dry ethanol was added dropwise and stirred for 10 min. This solution was transferred with the syringe to a solution of 40 mg (0.06 mmol) **164** in 7 ml dry ethanol and stirred the reaction mixture at 80 °C for 12 h. After cooling the mixture to RT, 5% aq. HCl were added and extracted with EtOAc for three times. The organic phase was washed with sat. NH_4Cl and brine and the solvent were evaporated. The product was purified by column chromatography over silica gel (1:3, EtOAc/cyclohexane).

Yield: 25 mg, 62%.

Melting Point: >160 °C, brown coloration

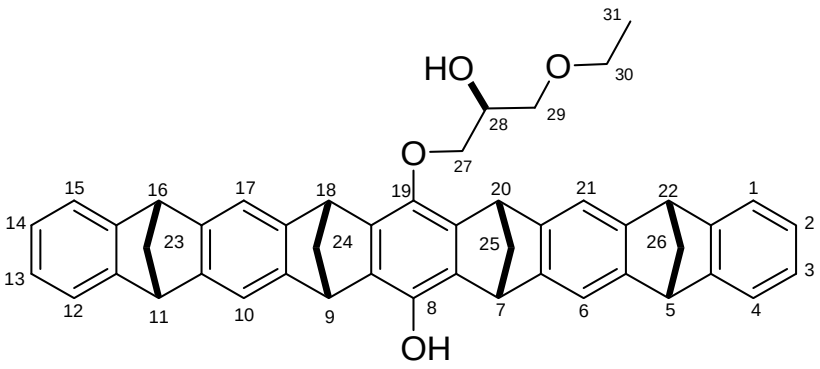

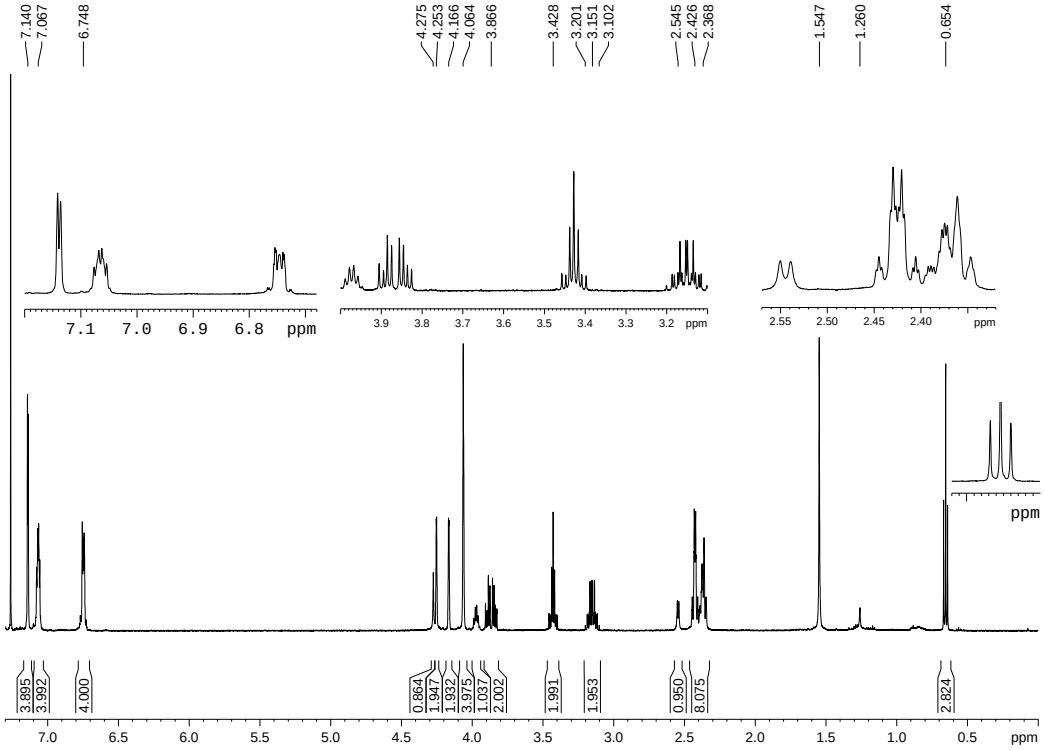

^{1}H-NMR in $CDCl_3$

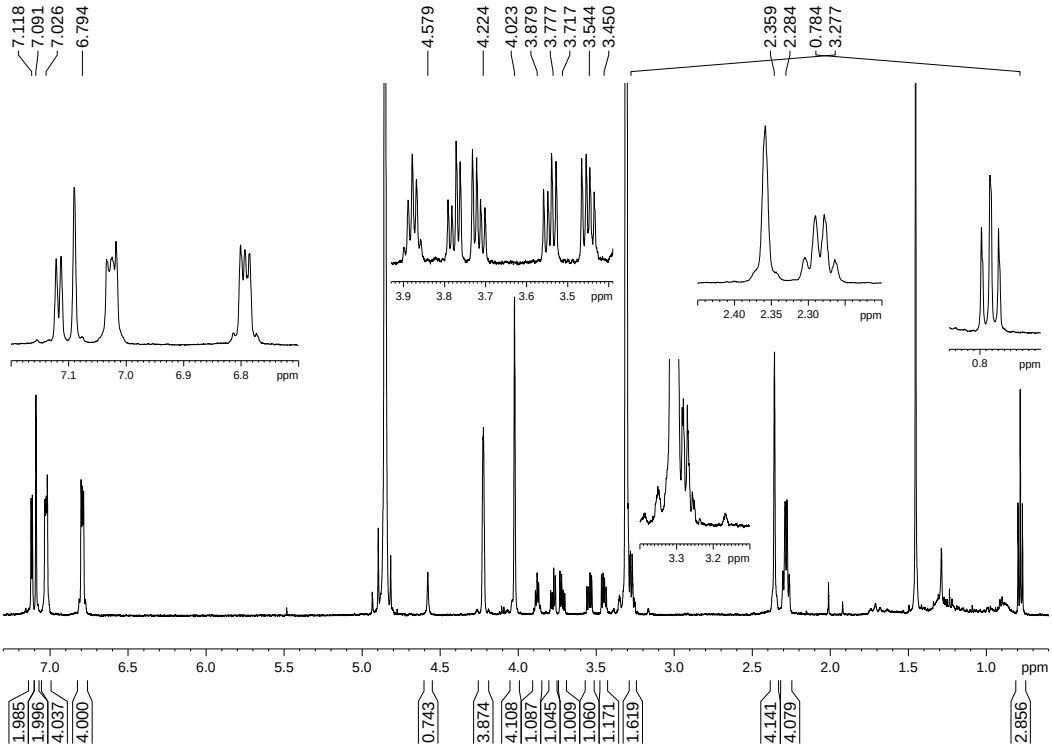

^{1}H-NMR in CD_3OD

^{1}H-NMR (500MHz, $CDCl_3$): δ [ppm] = 0.65 (t, 3H, H-31), 2.37, 2.43 (m, 8H, 24, H-25, H-23,

H-26), 2.54 (d, 1H, OH), 3.15 (m, 2H, H-30), 3.43 (m, 2H, H-29a, H-29i), 3.84, 3.89 (m, 2H, H-27a, H-27i), 3.97 (m, 1H, H-28), 4.06 (s, 4H, H-5, H-11, H-16, H-22), 4.17 (s, 2 H, H-7, H-9), 4.25 (s, 2H, H-18, H-20), 4.27 (s, 1H, OH), 6.75 (m, 4H, H-2, H-3, H-13, H-14), 7.07 (m, 4H, H-1, H-15, H-4, H-12), 7.14 (d, 4H, H-17, H-21, H-6, H-10).

^{1}H-NMR (500MHz, CD_3OD): δ [ppm] = 0.78 (t, 3H, H-31), 2.28 (m, 4H, H-24, H-25), 2.36 (s, 4H, H-23, H-26), 3.28 (m, 2H, H-30), 3.45, 3.54 (m, 2H, H-29a, H-29i), 3.72, 3.78 (m, 2H, H-27a, H-27i), 3.88 (m, 1H, H-28), 4.02 (s, 4H, H-5, H-11, H-16, H-22), 4.22 (s, 4H, H-7, H-9, H-18, H-20), 4.57 (s, 1H, OH), 6.79 (m, 4H, H-2, H-3, H-13, H-14), 7.03 (m, 4H, H-1, H-15, H-4, H-12), 7.09 (s, 2H, H-6, H-10), 7.12 (d, 2H, H-17, H-21).

^{13}C-NMR (125.7MHz, CD_3OD): δ [ppm] = 15.3 (C-31), 28.1, 49.4, 52.6, 67.9, 69.1, 69.3, 70.9, 72.5, 76.2, 117.1 (t), 122.3 (d), 126.1(d), 137.3, 141.5, 142.5, 143.6, 148.9, 149.2, 149.5, 152.2 (d).

HR-MS (ESI pos., MeOH): m/z $[M+Na]^+$: cal. 691.2819, obs. 691.2930.

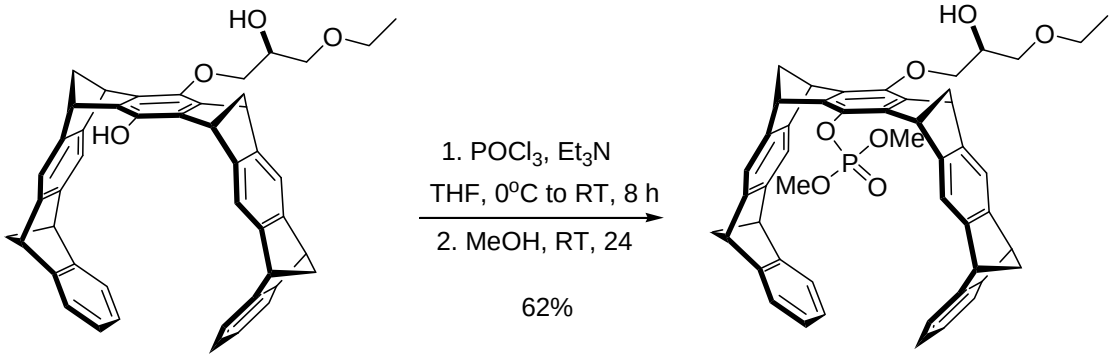

172
$C_{47}H_{40}O_4$
668,82 g/mol

194
$C_{49}H_{45}O_7P$
776,85 g/mol

A solution of 21 mg (0.0313 mmol) **172** in 5 ml anhydrous THF was cooled to 0 °C. To the stirred solution under inert atmosphere, 26 µl (0.1878 mmol) Et_3N were added. After 10 min 57 µl (0.627 mmol) $POCl_3$ were added and the reaction mixture stirred from 0 °C to RT for 8 h. Thereafter, 4 ml dry methanol was added and stirred again for 24 h at RT. Solvent was removed on rotary evaporator and after adding 30 ml Dist. H_2O, the crude is extracted with CH_2Cl_2 (3×20 ml). Organic layer is dried on rotary evaporator and residue is purified by column chromatography on silica gel (1:3, EtOAc/cyclohexane).

Yield: 15 mg, 62%, white solid.

Melting Point: 195 °C.

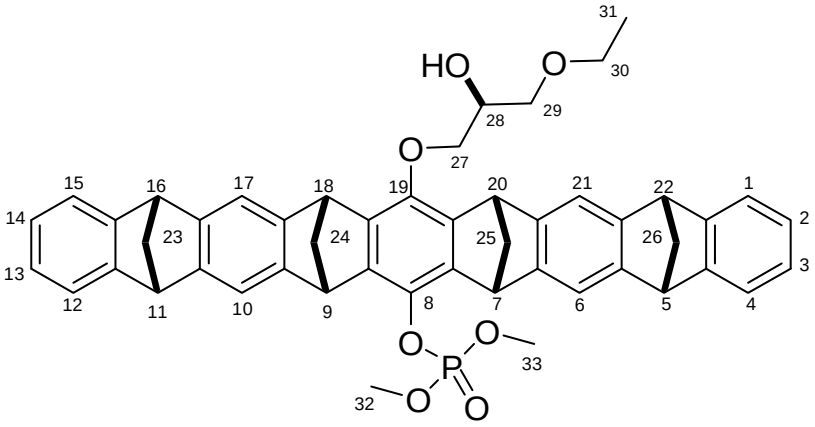

^{1}H-NMR (500MHz, $CDCl_3$): δ [ppm] = 0.30 (t, 3H, H-31), 2.38 (m, 4H, H-24, H-25), 2.43 (s, 4H, H-23, H-26), 3.02 (m, 2H, H-30), 3.40 (m, 2H, H-29), 3.42 (d, 6H, $^{3}J_{\text{H-32/P, H-33/P}}$ = 11.3 Hz, H-32, H-33), 3.98 (m, 3H, H-27, H-28), 4.07 (s, 4H, H-5, H-11, H-16, H-22), 4.27 (s, 2H, H-18, H-20), 4.36 (s, 2H, H-7, H-9), 6.73 (m, 4H, H-2, H-3, H-13, H-14), 7.04 (dd, 4H, H-1, H-15, H-4, H-12), 7.13 (d, 2H, H-17, H-21), 7.23 (s, 2H, H-6, H-10).

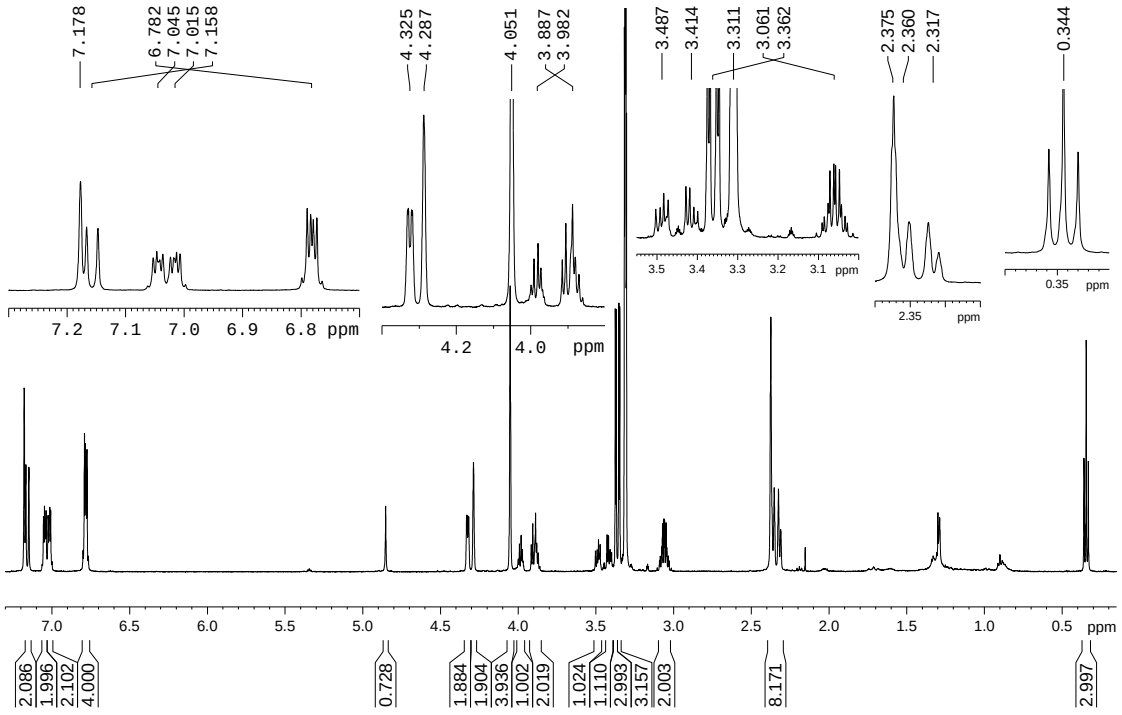

^{1}H-NMR in CD_3OD

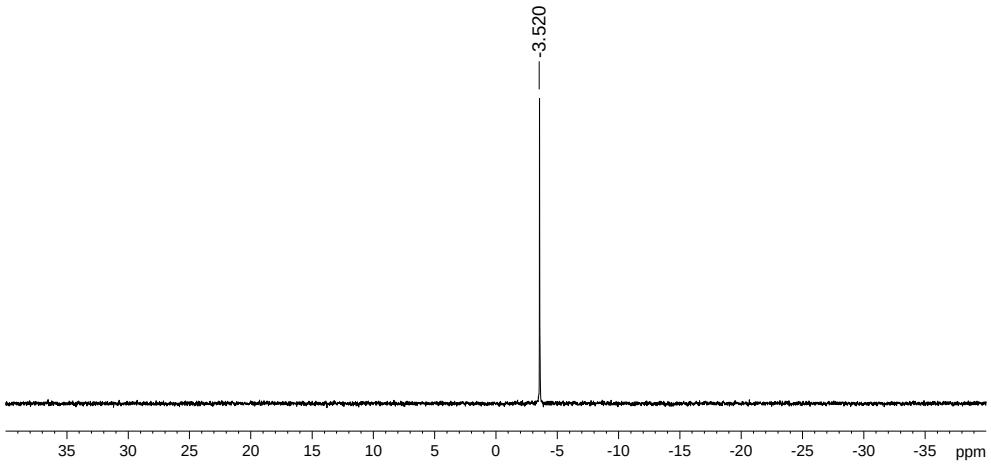

^{31}P-NMR in $CDCl_3$

^{1}H-NMR (500MHz, CD_3OD): δ [ppm] = 0.34 (t, 3H, H-31), 2.32, 2.36 (d, 4H, H-24, H-25), 2.37 (s, 4H, H-23, H-26), 3.06 (m, 2H, H-30), 3.36 (dd, 6H, $^{3}J_{\text{H-32/P, H-33/P}}$ = 11.3 Hz, H-32, H-33), 3.41, 3.49 (m, 2H, H-29a, H-29i), 3.89 (m, 2H, H-27a, H-27i), 3.98 (m, 1H, H-28), 4.05 (s, 4H, H-5, H-11, H-16, H-22), 4.29(s), 4.32(d) (4H, H-7, H-9, H-18, H-20), 6.78 (m, 4H, H-2, H-3, H-13, H-14), 7.01, 7.04 (m, 4H, H-1, H-15, H-4, H-12), 7.16 (d, 2H, H-17, H-21), 7.18 (s, 2H, H-6, H-10).

^{13}C-NMR (125.7MHz, $CDCl_3$): δ [ppm] = 14.1 (C-31), 48.5-48.8 (m, C-7, C-9, C-18, C-20), 50.4 (C-28), 51.3 (C-5, C-11, C-16, C-22), 54.9 (d, C-32, C-33), 66.6 (C-30), 68.8, 69.4 (d, C-23, C-26, C-24, C-25), 69.7 (C-28), 70.3 (C-29), 74.0 (C-27), 116.2, 117.2 (C-17, C-21, C-6, C-10), 121.1, 121.7 (C-1, C-15, C-4, C-12), 124.7 (d, C-2, C-3, C13, C-14), 134.9, 140.5, 141.1, 145.7(s) (d, C-5a, C-16a, C-21a, C-10a,C-7a, C-8a, C-18a, C-19a), 146.8, 147.1, 147.7 (d, C-6a, C-9a, C-17a, C-20a, C-8, C-9), 150.6, 150.8 (C-4a, C-11a, C-15a, C-22a).

^{31}P-NMR (202MHz, $CDCl_3$): δ [ppm] = -3.52 ppm.

HR-MS (ESI pos., MeOH): m/z $[M+Na]^+$: cal. 799.2795, obs. 799.2860.

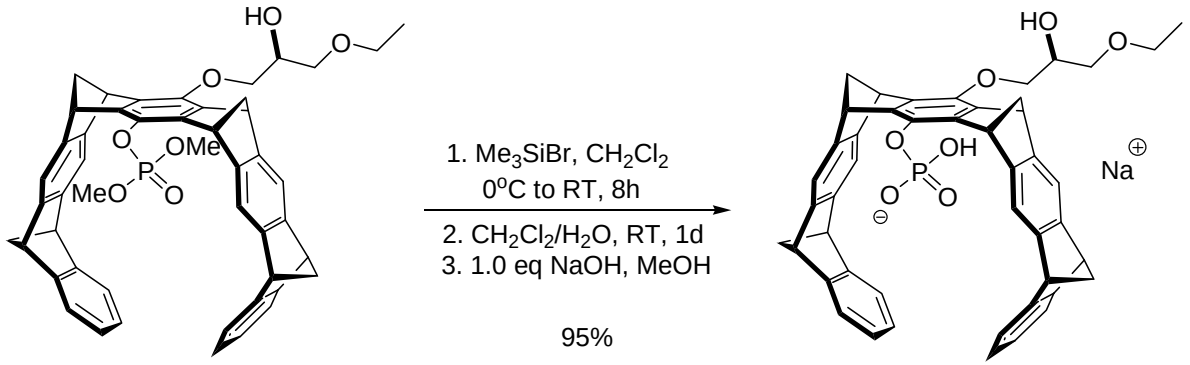

194
$C_{49}H_{45}O_7P$
776,85 g/mol

198
$C_{47}H_{40}NaO_7P$
770,78 g/mol

To a 0°C cooled solution of 13 mg (0.0167 mmol) **194** in anhydrous CH_2Cl_2, 22 µl (0.167 mmol) TMSBr were added dropwise and solution was stirred at RT for 8 hour. The excess of TMSBr and solvent were removed by condensation and remaining residue dried on oil pump for 4 h. The solid residue was dissolved in 10 ml CH_2Cl_2/H_2O (1:1) and stirred at RT for 24 h. Two phases were separated, and from organic phase collected 12 mg (95%) of white solid. For the neutralization of phosphate, to a solution of 5.0 mg (0.0067 mmol) of phosphoric acid tweezers in 5 ml methanol 0.27 mg (0.0067 mmol) NaOH were added and stirred at RT for 30 min., dried the solvent and collected white solid in quantitative yield.

Melting Point: > 215 °C, brown coloration.

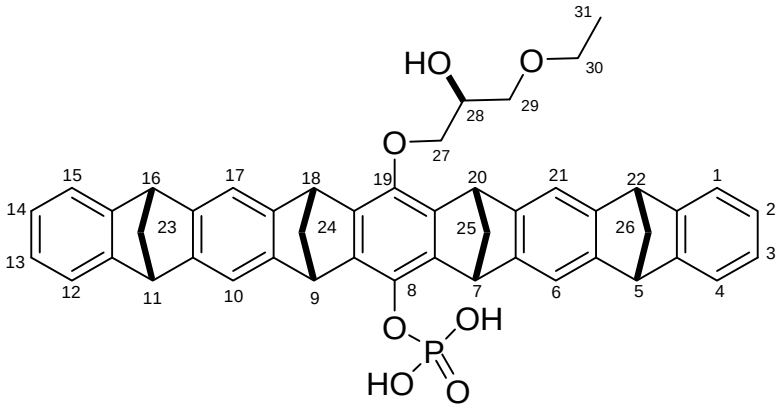

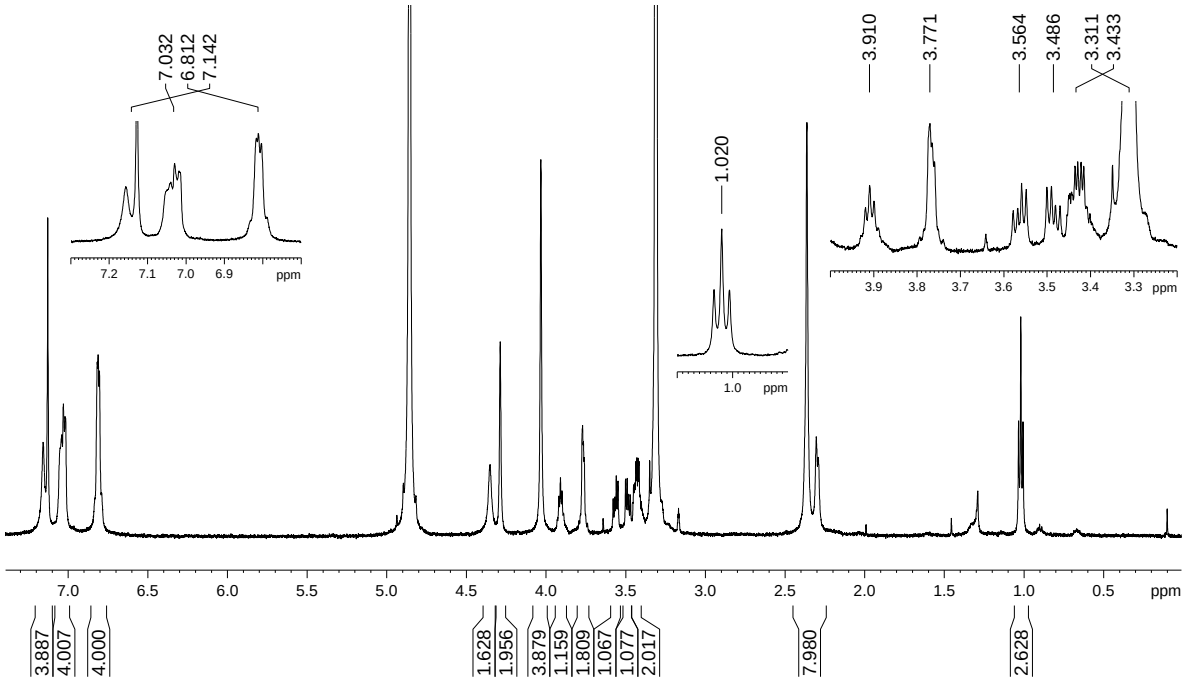

^{1}H-NMR in CD_3OD

^{1}H-NMR (500MHz, CD_3OD): δ [ppm] = 1.02 (t, 3H, H-31), 2.29-2.36 (m, 8H, H-24, H-25, H-23, H-26), 3.43 (m, 2H, H-30), 3.48, 3.56 (m, 2H, H-29a, H-29i), 3.77 (m, 2H, H-27), 3.91 (m, 1H, H-28), 4.03 (s, 4H, H-5, H-11, H-16, H-22), 4.29, 4.35 (s, 4H, H-7, H-9, H-18, H-20), 6.81 (m, 4H, H-2, H-3, H-13, H-14), 7.03 (m, 4H, H-1, H-15, H-4, H-12), 7.14 (d, 4H, H-17, H-21, H-6, H-10).

^{13}C-NMR (125.7MHz, CD_3OD): δ [ppm] = 15.5 (C-31), 49.0 (m, C-7, C-9, C-18, C-20), 52.4 (C-5, C-11, C-16, C-22), 67.9 (C-30), 69.0 (d, C-23, C-26, C-24, C-25), 70.7 (C-28), 72.4 (C-29), 75.9 (C-27), 116.6(d), 118.2 (C-17, C-21, C-6, C-10), 122.0, 122.2 (C-1, C-15, C-4, C-12), 125.9 (d, C-2, C-3, C13, C-14), 142.4, 142.9, 146.3 (C-5a, C-16a, C-21a, C-10a,C-7a, C-8a, C-18a, C-19a), 148.8, 149.1 (m, C-6a, C-9a, C-17a, C-20a, C-8, C-9), 152.1 (C-4a, C-11a, C-15a, C-22a).

^{31}P-NMR (202MHz, $CDCl_3$): δ [ppm] = -4.16 ppm.

HR-MS (ESI pos., neg., MeOH): m/z $[M+Na]^+$: cal. 771.2482, obs. 771.2538, m/z $[M-H]^-$: cal. 747.2517, obs. 747.2591.

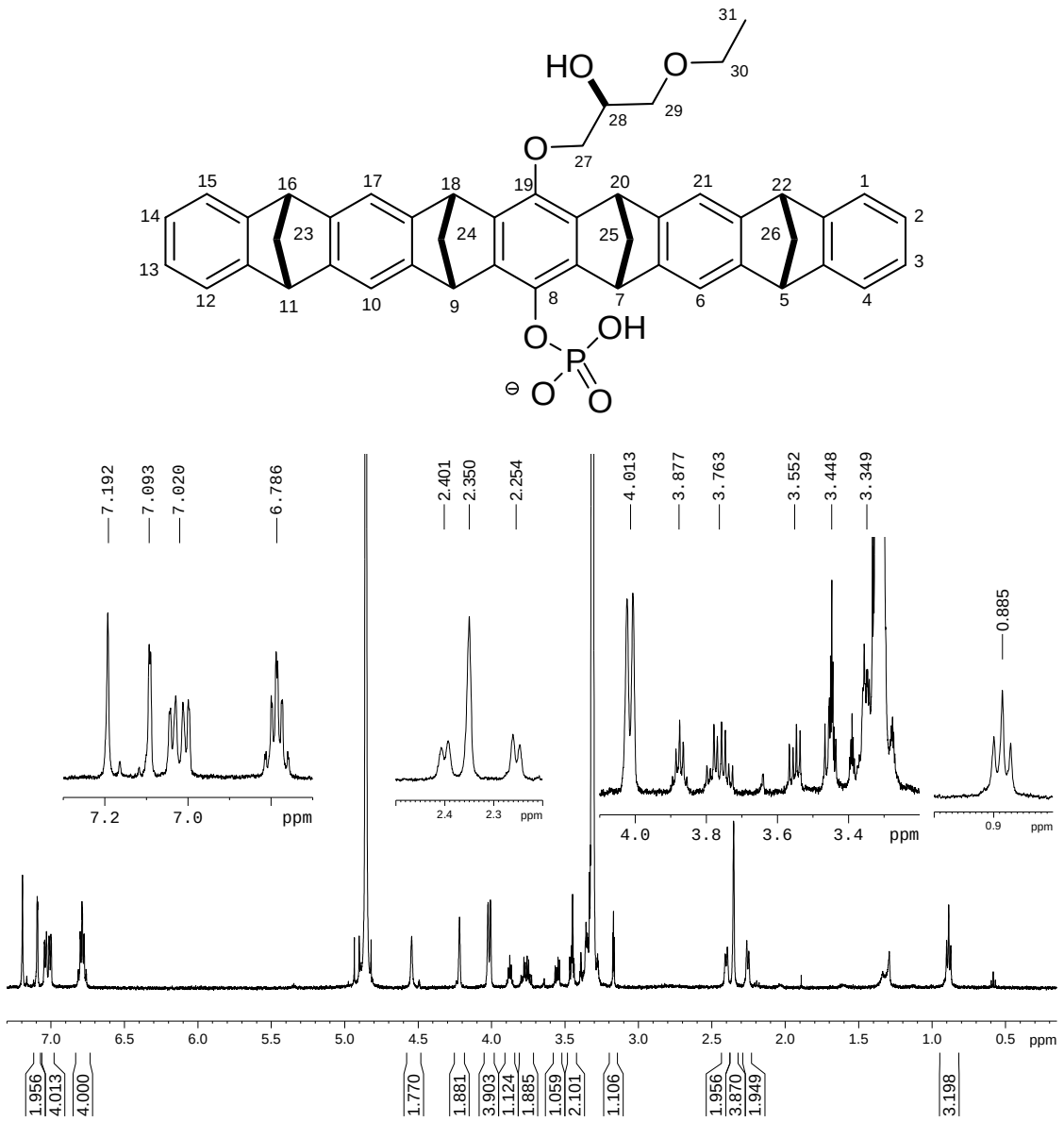

^{1}H-NMR in CD_3OD

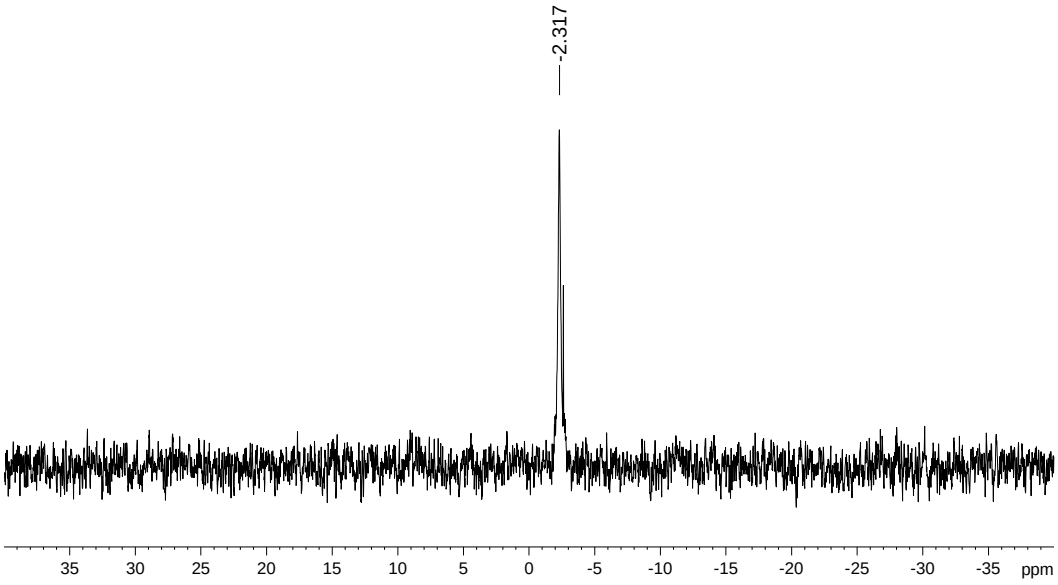

^{31}P-NMR in CD_3OD

^{1}H-NMR (500MHz, CD_3OD): δ [ppm] = 0.88 (t, 3H, H-31), 2.25 (d, 2H, H-24a, H-25a), 2.35 (s, 4H, H-23, H-26), 2.40 (d, 2H, H-24i, H-25i), 3.35 (m, 2H, H-30), 3.45, 3.55 (m, 2H, H-29a, H-29i), 3.76 (m, 2H, H-27), 3.88 (m, 1H, H-28), 4.01 (d, 4H, H-5, H-11, H-16, H-22), 4.22 (s, 4H, H-18, H-20), 4.54 (s, 2H, H-7, H-9), 6.78 (m, 4H, H-2, H-3, H-13, H-14), 7.02 (m, 4H, H-1, H-15, H-4, H-12), 7.09 (s, 2H, H-17, H-21), 7.19 (d, 2H, H-6, H-10).

^{31}P-NMR (202MHz, CD_3OD): δ [ppm] = -2.32 ppm.

5.2.3 Synthesis of 2nd generation unsymmetrical bis phosphate tweezers

5.2.3.1 Synthesis of the phosphoramidite tweezer 246

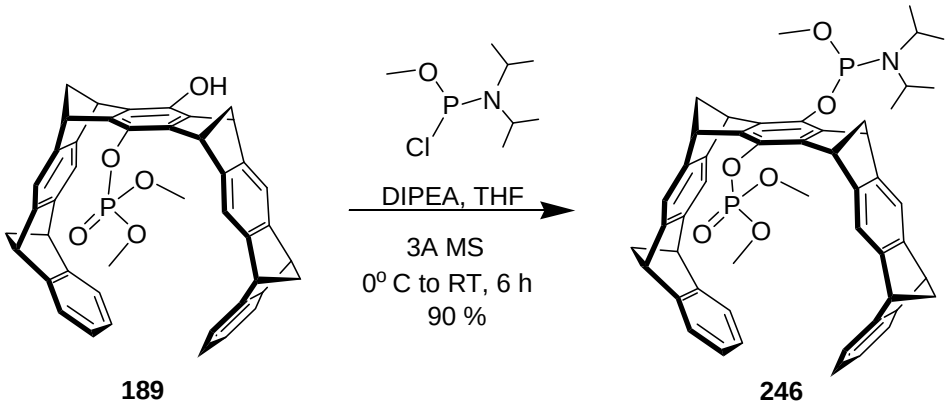

189 **246**

Prior to use, tweezer **189** was dried at 60-80°C on an oil pump. A solution of 165 mg (0.244

mmol) of **189** in 15 ml dry THF was transferred to well dried argon fluxed flask containing 10 beads of 3Å molecular sieves. To the 0°C cooled solution, 340 µl (1.956 mmol) of diisopropylethylamine (DIPEA) and 190 µl (0.978 mmol) of chloro-*N, N*-disopropyl methyl phosphoramidite were added. After 6 hour, TLC showed the complete conversion. The mixture was diluted with 10 ml ethyl acetate and transferred to the separating funnel. After adding 20 ml saturated $NaHCO_3$, the organic phase was separated and aqueous layer was washed twice with EtOAc. The combined organic layer was washed with 20 ml brine solution and dried over Na_2SO_4. After removing the solvent on rotory evaporator, the resulting yellowish residue was purified by column chromatography using EtOAc/cyclohexane (1:4) eluent. Thus 204 mg pure white solid of **246** were obtained.

R_f: 0.30 (1:3, EtOAc/cyclohexane)
Yield: 90%, white solid
MP: 108 °C

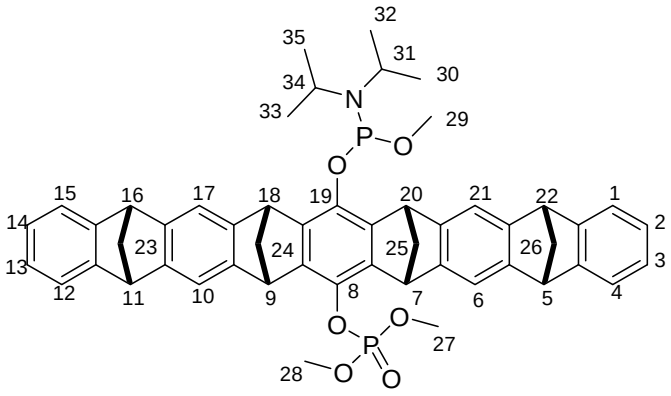

246

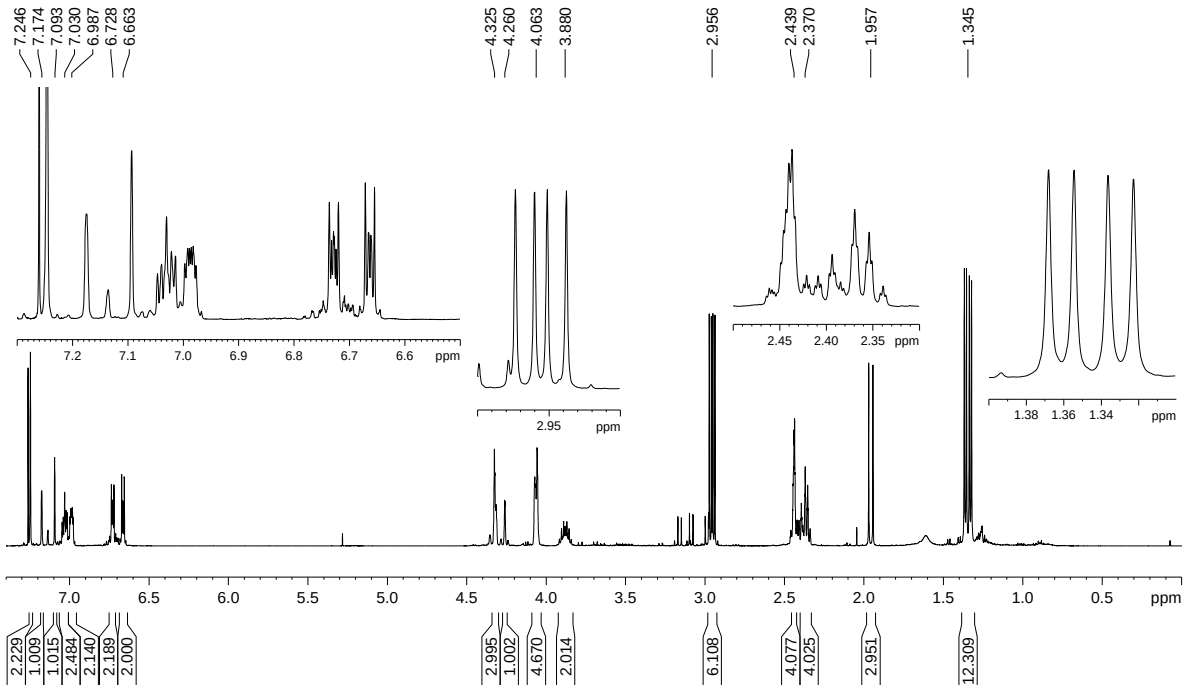

^{1}H-NMR spectra of **TW 246** in $CDCl_3$

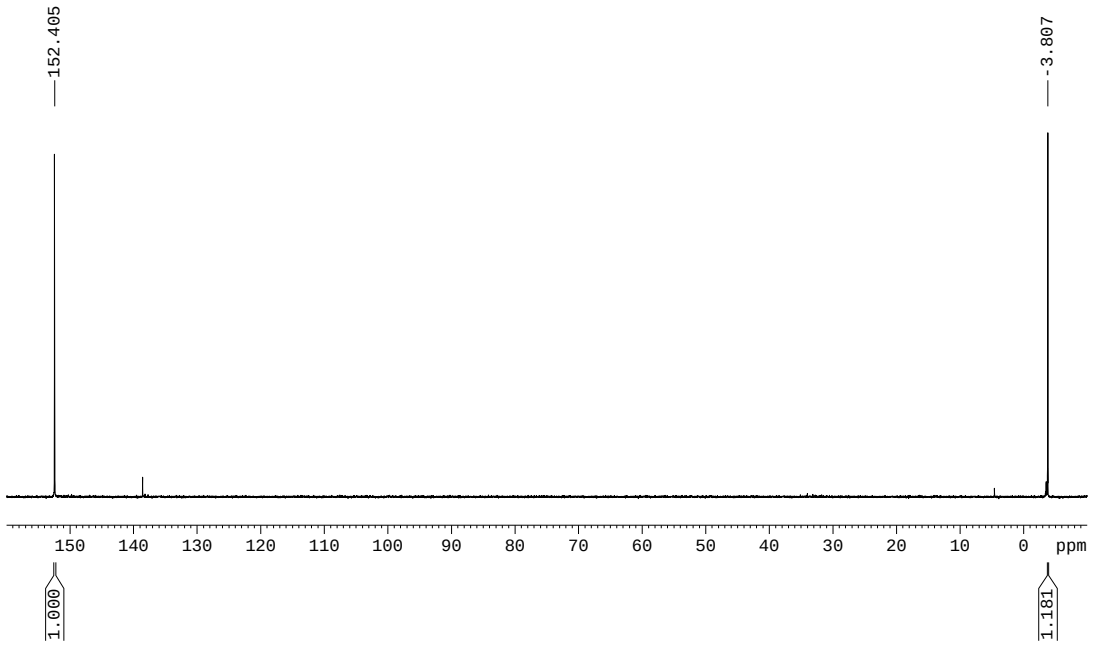

^{31}P-NMR spectra of **TW 246** in $CDCl_3$

^{1}H-NMR (500MHz, $CDCl_3$): δ [ppm] = 1.34 (m, 12H, H-30, H-32, H-33, H-35), 1.95 (d, 3H, H-29), 2.37, 2.44 (m, 8H, H-23, H-26, H-24, H-25), 2.96 (m, 6H, H-27, H-28), 3.88 (m, 2H, H-31, H-34), 4.06 (m, 4H, H-5, H-11, H-16, H-22), 4.26, 4.32 (m, 4H, H-7, H-9, H-18, H-20), 6.66, 6.72 (m, 4H, H-2, H-3, H-13, H-14), 6.98, 7.03 (m, 4H, H-1, H-15, H-4, H-12), 7.09, 7.17 (s, 2H, H-17, H-21), 7.24 (s, 2H, H-6, H-10).

^{13}C-NMR (125.7MHz, $CDCl_3$): δ [ppm] = 24.9, 43.9, 48.5, 48.8, 49.2, 51.2, 54.7, 67.6, 68.0, 68.5, 68.7, 116.8, 117.0, 117.2, 120.9, 121.1, 124.6, 134.7, 140.4, 140.9, 141.7, 142.5, 147.4, 151.

^{31}P-NMR (202MHz, $CDCl_3$): δ [ppm] = -3.80 and 152.4.

HR-MS (ESI pos., MeOH): m/z $[M+Na]^+$: cal. 858.3084, obs. 858.3082.

5.2.3.2 Synthesis of the ester linker tweezer 247

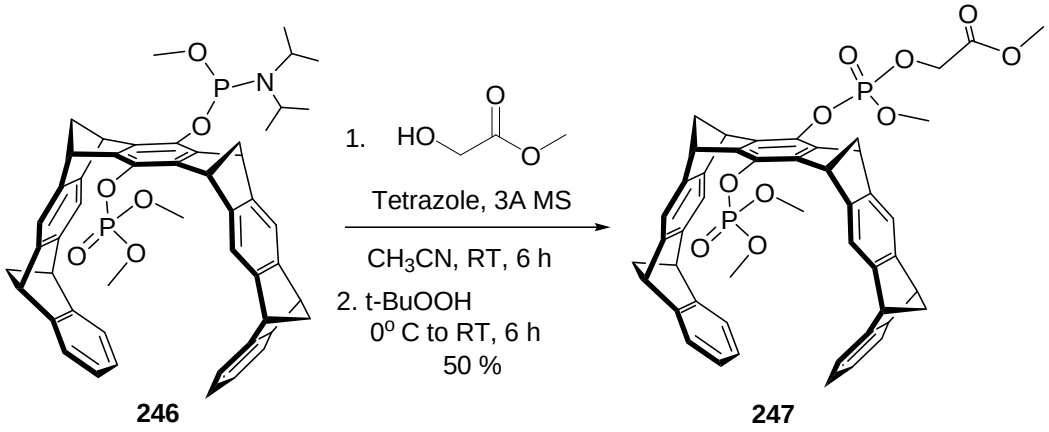

246 **247**

85 mg (0.101 mmol) of intermediate phosphoramidite **246** were dissolved in 6.0 ml dry acetonitrile and 5-10 beads of 3Å molecular sieves were added to the solution. To this clear solution 46 µl (0.61 mmol) of methyl glycolate and 610 µl (0.305 mmol) of tetrazole solution (0.45 M solution in CH_3CN) were added and the reaction mixture stirred at RT. After 2 hour, TLC indicated conversion of starting material; however, the new spot appears at the same R_f value as tweezer **189**. Therefore, the formation of product was monitored by oxidizing a small fraction of the reaction mixture with tert-butylhydroperoxide (TBHP). After 6 hour the reaction mixture was cooled to 0°C and 92 µl (0.508 mmol) of anhydrous TBHP solution (5.5 M in octane) were added. The reaction stirred from 0°C to RT for 12 hour and then saturated $NaHCO_3$ solution was added and extracted three times with dichloromethane. The resulting organic phase was washed with dist water and dried over NaSO4. The solvent removed on rotory evaporator and residue purified by column chromatography using EtOAc/cyclohexane (1:1) eluent. Thus 42 mg pure white solid of **247** were obtained.

R_f: 0.25 (1:1, EtOAc/cyclohexane)

Yield: 50%, white solid.

Smp > 130 °C

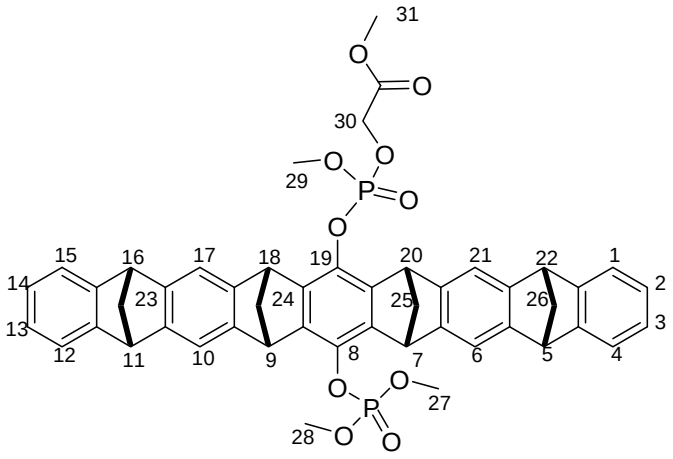

247

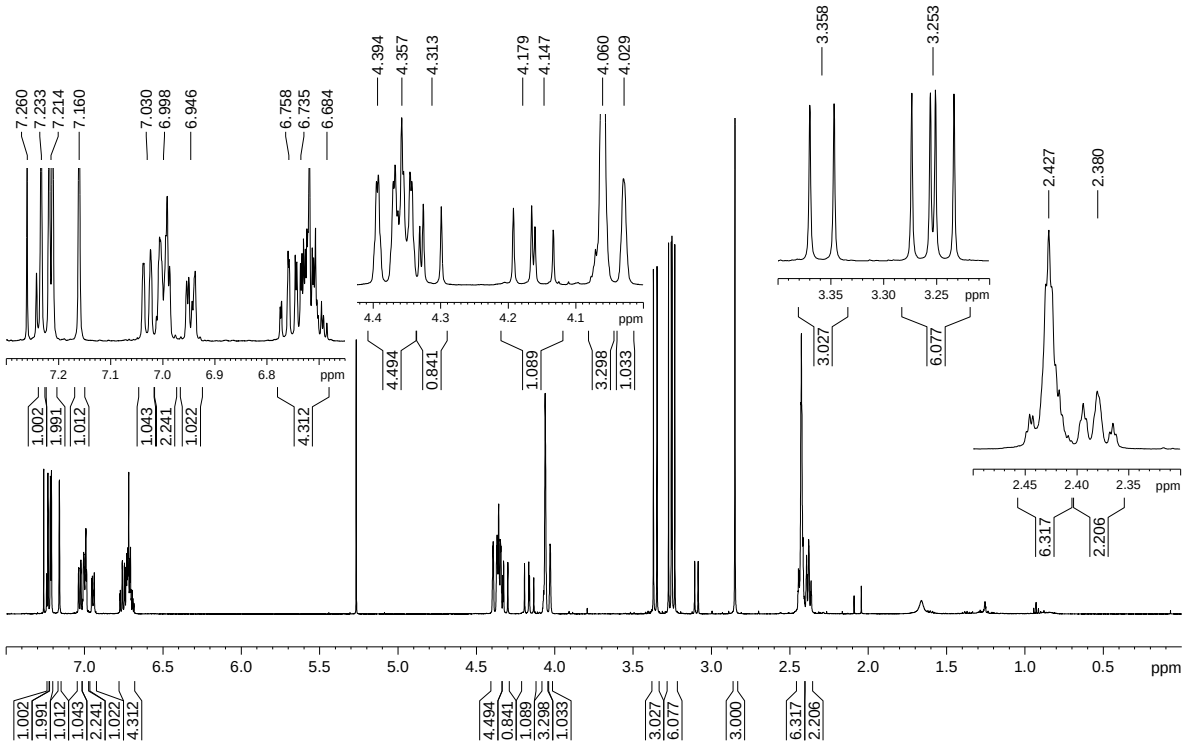

^{1}H-NMR spectra of tweezer **247** in $CDCl_3$

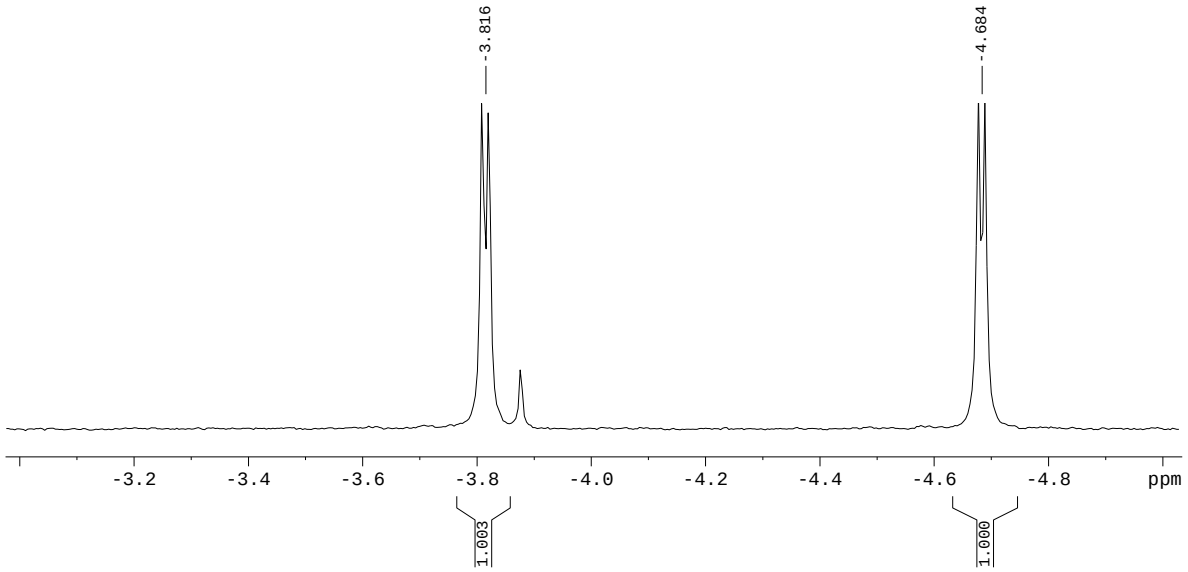

^{31}P-NMR spectra of tweezer **247** in $CDCl_3$

^{1}H-NMR (500MHz, $CDCl_3$): δ [ppm] = 2.38, 2.43 (m, 8H, H-23, H-26, H-24, H-25), 2.85 (s, 3H, H-31), 3.25 (dd, 6H, H-27, H-28), 3.36 (d, 3H, H-29), 4.03, 4.06 (s, 1H, 3H, H-5, H-11, H-16, H-22), 4.16, 4.33 (m, 2H, H-30), 4.36 (m, 4H, H-7, H-9, H-18, H-20), 6.72 (m, 4H, H-2, H-3, H-13, H-14), 6.94-7.03 (m, 4H, H-1, H-15, H-4, H-12), 7.16, 7.21, 7.23 (s, d, s, 1H, 2H, 1H, H-6, H-10, H-17, H-21).

^{13}C-NMR (125.7MHz, $CDCl_3$): δ [ppm] = 48.6, 51.1, 51.5, 54.8, 55.2, 64.1, 68.0, 69.0, 116.9, 117.2, 120.8, 121.3, 124.6, 124.9, 136.2, 142.1, 146.7, 146.9, 147.8, 150.8, 167.6.

^{31}P-NMR (202MHz, $CDCl_3$): δ [ppm] = -4.68 ppm and -3.81 ppm.

HR-MS (ESI pos., MeOH): m/z $[M+Na]^+$: cal. 863.2145, obs. 863.2146.

5.2.3.3 Synthesis of the tweezer 248

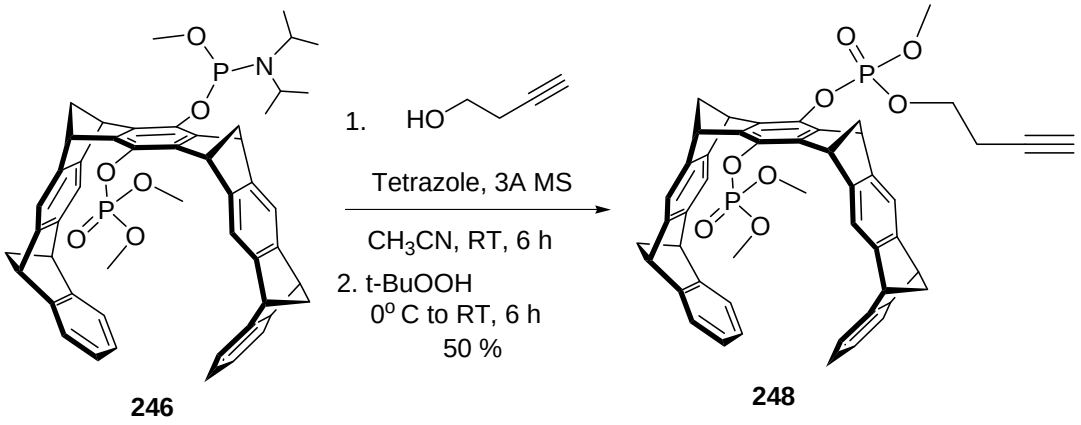

246 **248**

25 mg (0.0299 mmol) of intermediate phosphoramidite **246** were dissolved in 3.0 ml dry acetonitrile and 5 beads of 3Å molecular sieves were added to the solution. To this clear solution 7 µl (0.0897 mmol) of 3-butyn-1-ol and 332 µl (0.149 mmol) of tetrazole solution (0.45 M solution in CH_3CN) were added and the reaction mixture stirred at RT. After 3 hour, TLC indicated conversion of starting material. The reaction mixture was cooled to 0^oC and 11 µl (0.0598 mmol) of anhydrous TBHP solution (5.5 M in octane) was added. The resulting reaction mixture was stirred from 0^oC to RT for 6 hour and then 10 ml saturated $NaHCO_3$ solution were added and extracted with dichloromethane (3×10 ml). The resulting organic phase was washed with dist water and dried over Na_2SO4. The solvent removed on rotary evaporator and residue purified by column chromatography using EtOAc/cyclohexane (1:1) eluent. Thus 12 mg pure white solid of the tweezer **248** were obtained.

R_f: 0.22 (1:1, EtOAc/cyclohexane)
Yield: 48 %
Smp > 130 ^oC

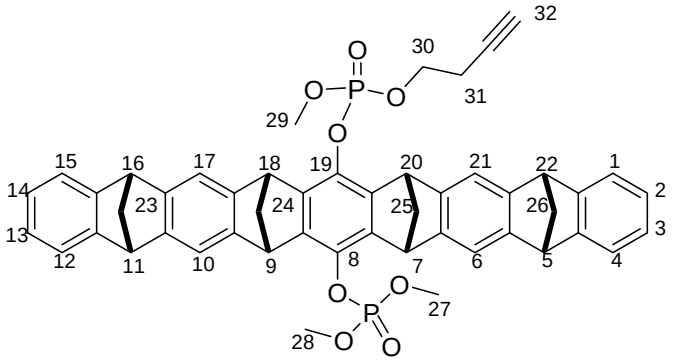

248

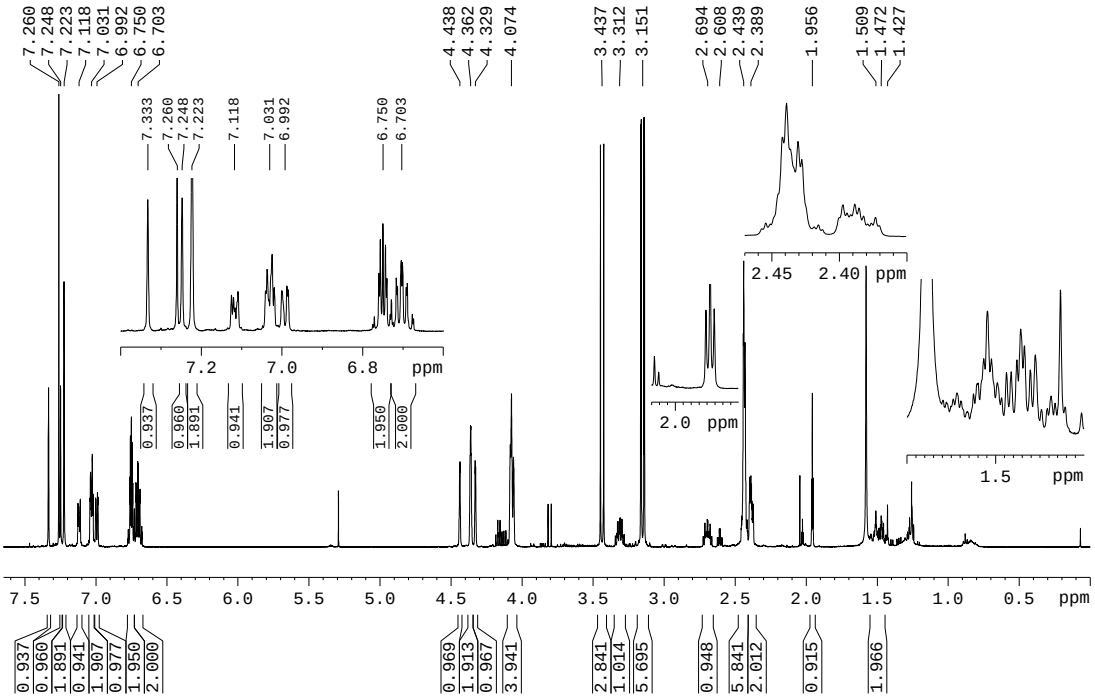

^{1}H-NMR spectra of tweezer **248** in $CDCl_3$

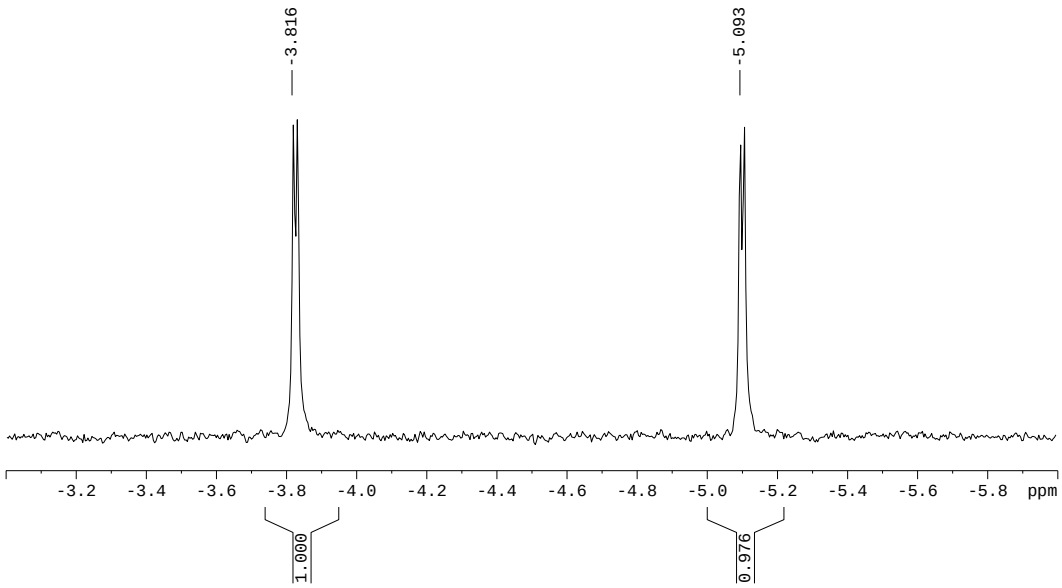

^{31}P-NMR spectra of tweezer **248** in $CDCl_3$

^{1}H-NMR (500MHz, $CDCl_3$): δ [ppm] = 1.47-1.50 (m, 2H, H-31), 1.96 (t, 1H, H-32), 2.39, 2.44 (m, 8H, H-23, H-26, H-24, H-25), 2.69, 3.31 (m, 2H, H-30), 3.15 (dd, 6H, H-27, H-28), 3.44 (d, 3H, H-29), 4.07 (m, 4H, H-5, H-11, H-16, H-22), 4.33, 4.36, 4.44 (m, 1H, 2H, 1H, H-7, H-9, H-18, H-20), 6.70, 6.75 (m, 2H, 2H, H-2, H-3, H-13, H-14), 6.99, 7.03, 7.12 (m, 1H, 2H, 1H, H-1, H-15, H-4, H-12), 7.22, 7.25, 7.33 (s, 2H, 1H, 1H, H-6, H-10, H-17, H-21).

^{13}C-NMR (125.7MHz, $CDCl_3$): δ [ppm] = 20.4, 48.6, 51.2, 54.9, 66.0, 67.9, 68.5, 70.2, 117.1, 117.5, 120.9, 121.1, 121.6, 124.7, 136.4, 142.2, 146.8, 147.8, 150.9.

^{31}P-NMR (202MHz, $CDCl_3$): δ [ppm] = -5.09 ppm and -3.81 ppm.

HR-MS (ESI pos., MeOH): m/z $[M+Na]^+$: cal. 843.2247, obs. 843.2237.

5.3 NMR titration

Receptor	**161**	M_R [g/mol]	770.78
Solvent	Phosphate buffer	m_R [mg]	1.13
T[°C]	25	V_0 [ml]	2.3
Substrate	**Itself**	$[R]_0$ [mM]	1.13

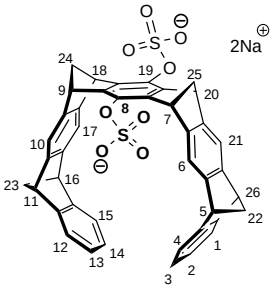

161

[R][mM]	**δ_{obs}[ppm]**	**$\delta_{monomer-calc} - \delta_{obs} = \Delta\delta_{calc}$[ppm]**
1.13	6.212	0.707
0.565	6.419	0.500
0.282	6.624	0.295
0.141	6.733	0.186
0.0706	6.836	0.083
0.0353	6.858	0.061

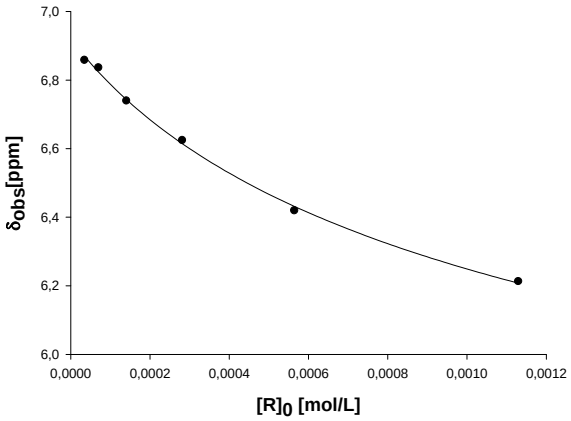

$K_{dm}[M^{-1}] = 370 \pm 80$

$\Delta\delta_{max}$ [ppm] = 2.0219

$\delta_{monomer-calc}$ [ppm] = 6.919

Receptor	**161**	M_R [g/mol	770.78
Solvent	Phosphate buffer	M_S [g/mol]	238.7
T[°C]	25	m_R [mg]	0.672
Substrate	**AcLysOMe**	m_S [mg]	0.410
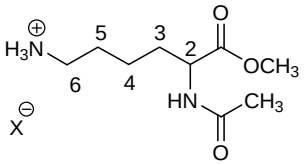	δ_0 (2-H) [ppm] = 4.398	V_0 [ml]	3.0
	δ_0 (6-H) [ppm] = 2.999	$[S_0]$[mM]	0.5725
	δ_0 (-*NAc*) [ppm] = 2.050		
	δ_0 (-CO_2Me) [ppm] = 3.770		

X^-: HPO_4^{2-}

V **[ml]**	**[R][mM]**	**δ (2-H) [ppm]**	**$\Delta\delta_{obs}$ [ppm]**	**$\Delta\delta_{calc}$ [ppm]**
0.60	1.4548	4.0313	0.3670	0.3667
0.66	1.3225	4.0332	0.3651	0.3658
0.72	1.2123	4.0340	0.3643	0.3648
0.78	1.1191	4.0340	0.3643	0.3637
0.84	1.0391	4.0359	0.3624	0.3624
0.90	0.9699	4.0367	0.3616	0.3609
0.96	0.9093	4.0374	0.3609	0.3592
1.02	0.8558	4.0405	0.3578	0.3572
1.08	0.8082	4.0443	0.3540	0.3549
1.18	0.7397	4.0501	0.3482	0.3500
1.28	0.6819	4.0570	0.3413	0.3436
1.40	0.6235	4.0689	0.3294	0.3337
1.50	0.5819	4.0761	0.3222	0.3235
1.70	0.5135	4.0898	0.3085	0.2997
0.00	0.0000	4.3983	0.0000	0.0000

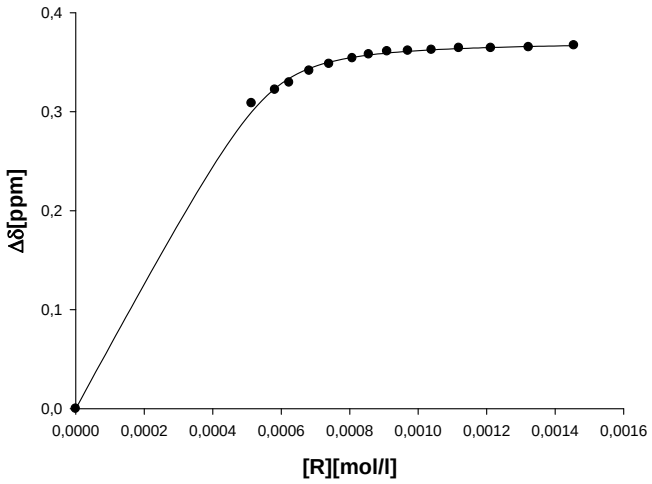

$K_a[M^{-1}]$ = 79536 ± 8889

K_d [μM] = 12 ± 11 %

$\Delta\delta_{max}$ (2-H) [ppm] = 0.3719

$\Delta\delta_{max}$ (6-H) [ppm] = 3.749

* Limit of 95% - confidence interval from the nonlinear regression of the signals of the Protons 2-H.

Receptor	**161**	M_R [g/mol]	770.78
Solvent	Phosphate buffer	M_S [g/mol]	266.7
T[°C]	25	m_R [mg]	0.800
Substrate	**AcArgOMe**	m_S [mg]	0.511
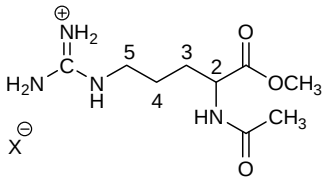	δ_0 (2-H) [ppm] = 4.421	V_0 [ml]	3.42
	δ_0 (5-H) [ppm] = 3.226	$[S]_0$ [mM]	0.5602
	δ_0 (4-H) [ppm] = 1.663		
	δ_0 (-NAc) [ppm] = 2.052		
X^-: HPO_4^{2-}	δ_0 (-CO_2Me) [ppm] = 3.775		

***V* [ml]**	**[R] [mM]**	**δ (5-H) [ppm]**	**$\Delta\delta_{obs}$ [ppm]**	**$\Delta\delta_{calc}$ [ppm]**
0.60	1.7298	-0.3837	3.6096	3.6009
0.65	1.5968	-0.3578	3.5837	3.5719
0.70	1.4827	-0.3216	3.5475	3.5416
0.75	1.3839	-0.2950	3.5209	3.5101
0.80	1.2974	-0.2534	3.4793	3.4773
0.85	1.2211	-0.2227	3.4486	3.4433
0.90	1.1532	-0.1865	3.4124	3.4079
0.95	1.0925	-0.1410	3.3669	3.3714
1.00	1.0379	-0.0926	3.3185	3.3338
1.10	0.9436	-0.0113	3.2372	3.2553
1.20	0.8649	0.0957	3.1302	3.1729
1.30	0.7984	0.1700	3.0559	3.0876
1.40	0.7414	0.2620	2.9639	3.0004
1.50	0.6919	0.2955	2.9304	2.9119
1.70	0.6105	0.4491	2.7768	2.7358
1.90	0.5463	0.6097	2.6162	2.5658
0.00	0.0000	3.2259	0.0000	0.0000

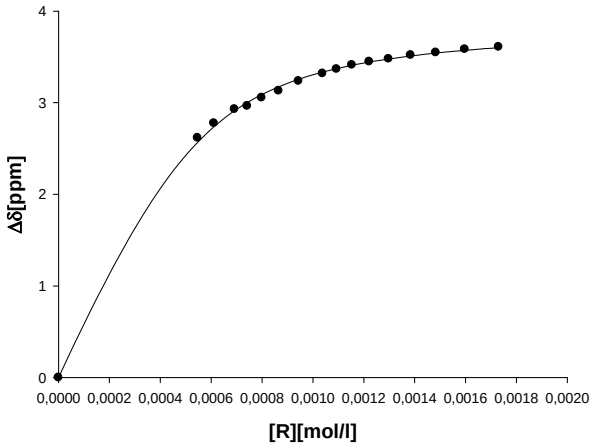

K_a [M^{-1}] = 11342 ± 561

$\Delta\delta_{max}$ (5-H) [ppm] = 3.86

$\Delta\delta_{max}$ (4-H) [ppm] = 2.51

* Limit of 95% - confidence interval from the nonlinear regression of the signals of the Protons 5-H.

Receptor	**133**	M_R [g/mol]	770.78
Solvent	Phosphate buffer	M_S [g/mol]	266.7
T[°C]	25	m_R [mg]	0.800
Substrate	**AcArgOMe**	m_S [mg]	0.511

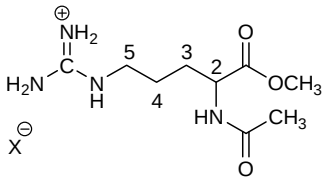

X^-: HPO_4^{2-}

δ_0 (2-H) [ppm] = 4.421

δ_0 (5-H) [ppm] = 3.226

δ_0 (4-H) [ppm] = 1.663

δ_0 (-NAc) [ppm] = 2.052

δ_0 (-CO_2Me) [ppm] = 3.775

$[R]_0$[mM]	$[S]_0$[mM]	δ (5-H) [ppm]	$\Delta\delta_{obs}$ [ppm]	$\Delta\delta_{calc}$ [ppm]
3.0	3.0	-0.198	3.424	3.442
1.5	1.5	-0.113	3.338	3.323
0.75	0.75	0.058	3.168	3.162
0.375	0.375	0.274	2.952	2.947
0.188	1.88	0.563	2.663	2.671

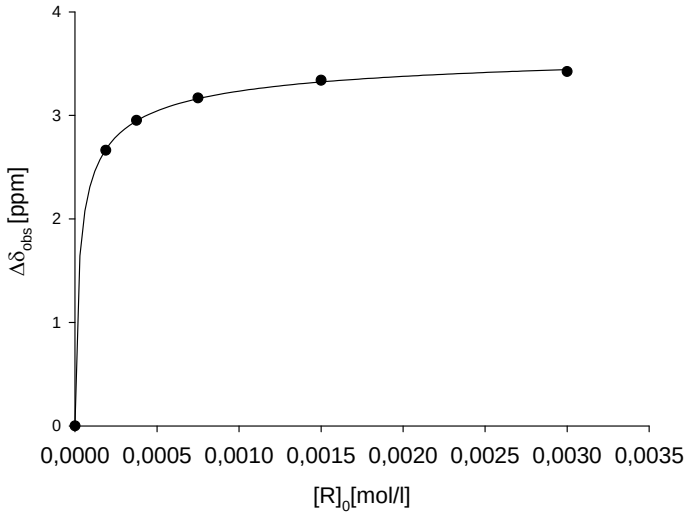

K_a [M^{-1}] = 45939 ± 2065

$\Delta\delta_{max}$ (5-H) [ppm] = 3.748 ± 0.16

$\Delta\delta_{max}$ (4-H) [ppm] = 2.540 ± 0.005

$\Delta\delta_{max}$ (3-H) [ppm] = 1.229 ± 0.007

$\Delta\delta_{max}$ (2-H) [ppm] = 0.630 ± 0.002

* Limit of 95% - confidence interval from the nonlinear regression of the signals of the Protons 5-H.

5.4 Fluorescence titrations

5.4.1 Fluorescence titrations of the phosphate tweezer 133

Fluorescence titration of the tweezer 133 with AcLysOMe in phosphate buffer (10mM, pH 7.6)

λ_{exc} = 285 nm λ_{em} = 334 nm	Receptor **133**	Guest AcLysOMe · HCl
Amount [mg]:	0.225	0.263
Volume [mL]:	10.710	0.780
Concentration [mol/L]:	$2.579 \cdot 10^{-05}$	$4.573 \cdot 10^{-04}$

Guest V (µL)	**Receptor V (µL)**	**[Receptor] [mol/L]**	**[Guest] [mol/L]**	**[Guest]/ [Receptor]**	**F.I. ($I_{334\ nm}$)**	**ΔI_{obs}**	**ΔI_{calc}**
0	700	2.58E-05	0.00E+00	0.00	594.451	0.000	0.000
10	710	2.58E-05	6.44E-06	0.25	550.838	43.613	42.321
20	720	2.58E-05	1.27E-05	0.49	515.279	79.172	78.336
30	730	2.58E-05	1.88E-05	0.73	483.590	110.861	107.795
40	740	2.58E-05	2.47E-05	0.96	459.677	134.774	131.058
60	760	2.58E-05	3.61E-05	1.40	433.532	160.919	162.749
80	780	2.58E-05	4.69E-05	1.82	416.212	178.239	181.512
100	800	2.58E-05	5.72E-05	2.22	403.594	190.857	193.191
140	840	2.58E-05	7.62E-05	2.95	389.476	204.975	206.378
180	880	2.58E-05	9.35E-05	3.63	382.237	212.214	213.434
240	940	2.58E-05	1.17E-04	4.53	373.044	221.407	219.364
300	1000	2.58E-05	1.37E-04	5.32	369.385	225.066	222.793

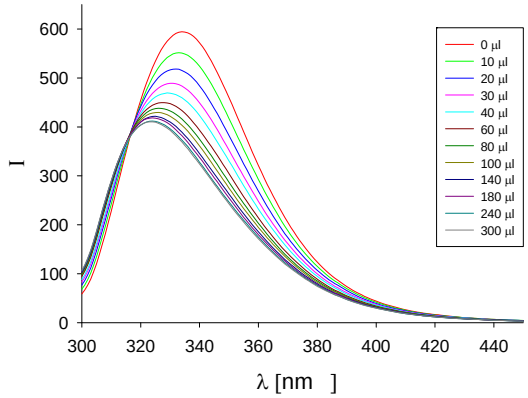

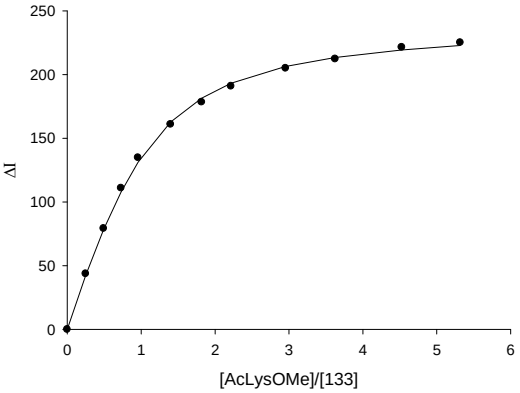

K_a [M^{-1}] = 113000 ± 6 %,

K_d[µM] = 9 ± 6 %,

ΔI_{max} = 240

Fluorescence titration of the tweezer 133 with AcArgOMe in phosphate buffer (10mM, pH 7.6)

λ_{exc} = 285 nm λ_{em} = 334 nm	Receptor **133**	Guest AcArgOMe · HCl
Amount [mg]:	0.225	0.101
Volume [mL]:	10.710	0.828
Concentration [mol/L]:	$2.579 \cdot 10^{-05}$	$4.573 \cdot 10^{-04}$

Guest V (µL)	**Receptor V (µL)**	**[Receptor] [mol/L]**	**[Guest] [mol/L]**	**[Guest]/ [Receptor]**	**F.I. ($I_{334\ nm}$)**	**ΔI_{obs}**	**ΔI_{calc}**
0	700	2.58E-05	0.00E+00	0.00	593.577	0.000	0.000
10	710	2.58E-05	6.44E-06	0.25	556.958	36.619	37.456
20	720	2.58E-05	1.27E-05	0.49	525.313	68.264	69.073
30	730	2.58E-05	1.88E-05	0.73	493.808	99.769	95.421
40	740	2.58E-05	2.47E-05	0.96	473.990	119.587	117.216
60	760	2.58E-05	3.61E-05	1.40	443.240	150.337	150.075
80	780	2.58E-05	4.69E-05	1.82	421.906	171.671	172.777
100	800	2.58E-05	5.72E-05	2.22	405.990	187.587	188.925
140	840	2.58E-05	7.62E-05	2.96	386.727	206.850	209.801
180	880	2.58E-05	9.35E-05	3.63	373.825	219.752	222.433
240	940	2.58E-05	1.17E-04	4.53	359.004	234.573	233.984
340	1040	2.58E-05	1.50E-04	5.80	345.525	248.052	244.467

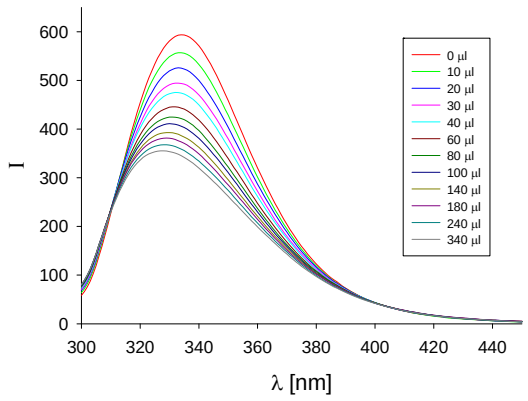

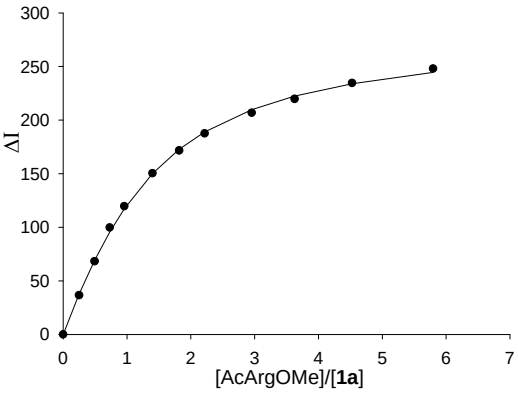

K_a [M^{-1}] = 50600 ± 5 %

K_d [µM] = 20 ± 5 %

ΔI_{max} = 282

Fluorescence titration of the tweezer 133 with AcArgOMe in phosphate buffer (200mM, pH 7.6)

λ_{exc} = 285 nm λ_{em} = 335 nm	Receptor **133**	Guest AcArgOMe · HCl
Amount [mg]:	0.170	0.364
Volume [mL]:	8.96	0.535
Concentration [mol/L]:	$2.33 \cdot 10^{-05}$	$2.55 \cdot 10^{-03}$

Guest V (µL)	**Receptor V (µL)**	**[Receptor] [mol/L]**	**[Guest] [mol/L]**	**[Guest]/ [Receptor]**	**F.I. ($I_{335\ nm}$)**	**ΔI_{obs}**	**ΔI_{calc}**
0	700	2.33E-05	0.00E+00	0.00	973.832	0.000	0.000
10	710	2.33E-05	3.59E-05	1.54	842.941	130.891	128.837
20	720	2.33E-05	7.09E-05	3.04	775.363	198.469	199.554
30	730	2.33E-05	1.05E-04	4.50	732.780	241.052	242.139
40	740	2.33E-05	1.38E-04	5.92	700.879	272.953	270.041
60	760	2.33E-05	2.01E-04	8.64	669.874	303.958	303.919
80	780	2.33E-05	2.62E-04	11.23	653.089	320.743	323.546
100	800	2.33E-05	3.19E-04	13.68	638.677	335.155	336.290
120	820	2.33E-05	3.73E-04	16.02	631.899	341.933	345.214
150	850	2.33E-05	4.50E-04	19.32	616.878	356.954	354.492
180	880	2.33E-05	5.22E-04	22.39	610.332	363.500	360.880
220	920	2.33E-05	6.10E-04	26.18	608.956	364.876	366.829
260	960	2.33E-05	6.91E-04	29.65	602.008	371.824	371.029
300	1000	2.33E-05	7.65E-04	32.84	598.502	375.330	374.151

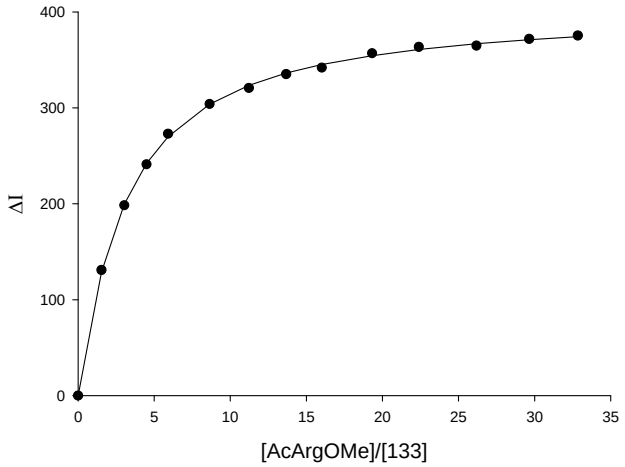

K_a [M^{-1}] = 16400 ± 2 %

K_d [µM] = 61 ± 2 %

ΔI_{max} = 405

Fluorescence titration of the tweezer 133 with AcLysOMe in methanol

λ_{exc} = 285 nm λ_{em} = 322 nm	Receptor **133**	Guest AcLysOMe · HCl
Amount [mg]:	0.120	0.382
Volume [mL]:	6.00	1.00
Concentration [mol/L]:	$2.46 \cdot 10^{-05}$	$1.60 \cdot 10^{-03}$

Guest V (µL)	**Receptor V (µL)**	**[Receptor] [mol/L]**	**[Guest] [mol/L]**	**[Guest]/ [Receptor]**	**F.I. (I_{322})**	**$-\Delta I_{obs}$**	**$-\Delta I_{calc}$**
0	700	2.46E-05	0.00E+00	0.00	608.731	0.000	0.000
10	710	2.46E-05	2.25E-05	0.92	615.971	7.240	7.651
20	720	2.46E-05	4.45E-05	1.81	621.386	12.655	12.889
30	730	2.46E-05	6.58E-05	2.68	625.740	17.009	16.594
40	740	2.46E-05	8.65E-05	3.52	626.250	17.519	19.308
60	760	2.46E-05	1.26E-04	5.15	632.937	24.206	22.964
100	800	2.46E-05	2.00E-04	8.15	636.981	28.250	26.873
180	880	2.46E-05	3.27E-04	13.33	639.343	30.612	30.135
220	920	2.46E-05	3.83E-04	15.59	638.661	29.930	30.962
260	960	2.46E-05	4.33E-04	17.65	639.838	31.107	31.555

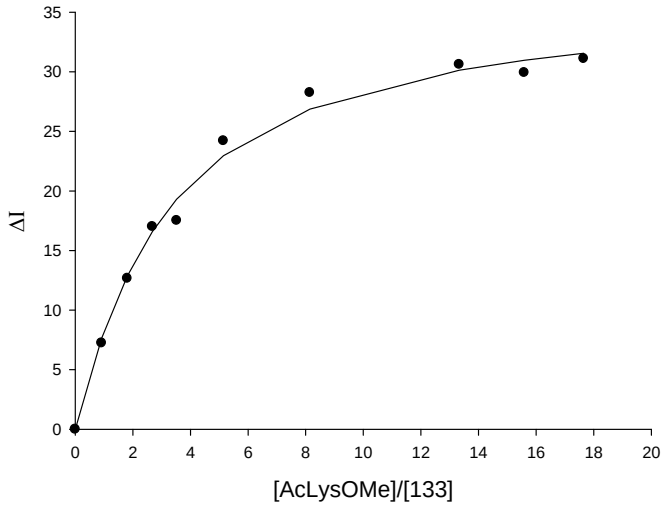

K_a [M^{-1}] = 15200 ± 11 %

K_d [µM] = 66 ± 11 %

ΔI_{max} = -37

Fluorescence titration of the tweezer 133 with IAPP (1-7) in phosphate buffer (10mM, pH 7.6)

λ_{exc} = 285 nm λ_{em} = 334 nm	Receptor **133**	Guest IAPP (1-7)
Amount [mg]:	0.225	0.263
Volume [mL]:	10.710	0.780
Concentration [mol/L]:	$2.579 \cdot 10^{-05}$	$4.573 \cdot 10^{-04}$

Guest V (µL)	**Receptor V (µL)**	**[Receptor] [mol/L]**	**[Guest] [mol/L]**	**[Guest]/ [Receptor]**	**F.I. ($I_{334\ nm}$)**	**ΔI_{obs}**	**ΔI_{calc}**
0	700	2.58E-05	0.00E+00	0.00	612.158	0.000	0.000
10	710	2.58E-05	6.44E-06	0.25	569.172	42.986	47.290
20	720	2.58E-05	1.27E-05	0.49	530.430	81.728	87.553
30	730	2.58E-05	1.88E-05	0.73	492.028	120.130	120.483
40	740	2.58E-05	2.47E-05	0.96	463.046	149.112	146.461
60	760	2.58E-05	3.61E-05	1.40	427.225	184.933	181.757
80	780	2.58E-05	4.69E-05	1.82	409.022	203.136	202.571
100	800	2.58E-05	5.72E-05	2.22	396.970	215.188	215.482
140	840	2.58E-05	7.62E-05	2.95	383.541	228.617	230.017
180	880	2.58E-05	9.35E-05	3.63	375.852	236.306	237.774
240	940	2.58E-05	1.17E-04	4.53	367.371	244.787	244.284
300	1000	2.58E-05	1.37E-04	5.32	362.955	249.203	248.044

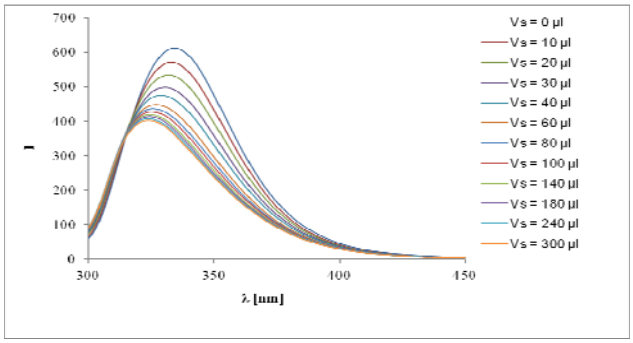

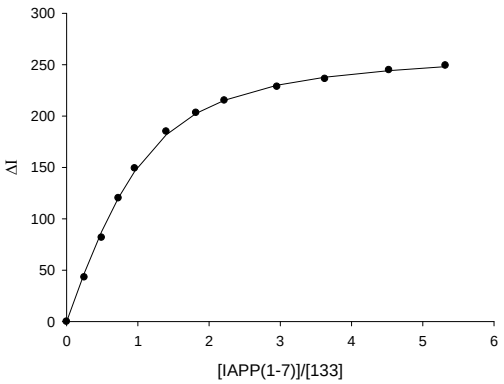

K_a [M^{-1}] = 115000 ± 6 %

K_d [µM] = 9 ± 6 %

Fluorescence titration of the tweezer 133 with IAPP (2-14) in phosphate buffer (10mM, pH 7.6)

λ_{exc} = 285 nm λ_{em} = 334 nm	Receptor **133**	Guest IAPP (2-14)
Amount [mg]:	0.225	0.549
Volume [mL]:	10.710	0.880
Concentration [mol/L]:	$2.579 \cdot 10^{-05}$	$4.575 \cdot 10^{-04}$

Guest V (µL)	**Receptor V (µL)**	**[Receptor] [mol/L]**	**[Guest] [mol/L]**	**[Guest]/ [Receptor]**	**F.I. ($I_{334\ nm}$)**	**ΔI_{obs}**	**ΔI_{calc}**
0	700	2.58E-05	0.00E+00	0.00	596.576	0.000	0.000
10	710	2.58E-05	6.44E-06	0.25	580.210	16.366	17.418
20	720	2.58E-05	1.27E-05	0.49	564.679	31.897	33.094
30	730	2.58E-05	1.88E-05	0.73	553.575	43.001	47.254
40	740	2.58E-05	2.47E-05	0.96	537.644	58.932	60.086
60	760	2.58E-05	3.61E-05	1.40	510.046	86.530	82.404
80	780	2.58E-05	4.69E-05	1.82	496.676	99.900	101.094
100	800	2.58E-05	5.72E-05	2.22	481.567	115.009	116.932
140	840	2.58E-05	7.63E-05	2.96	450.962	145.614	142.223
180	880	2.58E-05	9.36E-05	3.63	434.443	162.133	161.446
240	940	2.58E-05	1.17E-04	4.53	412.349	184.227	182.862
300	1000	2.58E-05	1.37E-04	5.32	398.538	198.038	198.498
400	1100	2.58E-05	1.66E-04	6.45	382.369	214.207	216.847
600	1300	2.58E-05	2.11E-04	8.19	359.076	237.500	238.599
700	1400	2.58E-05	2.29E-04	8.87	349.319	247.257	245.559

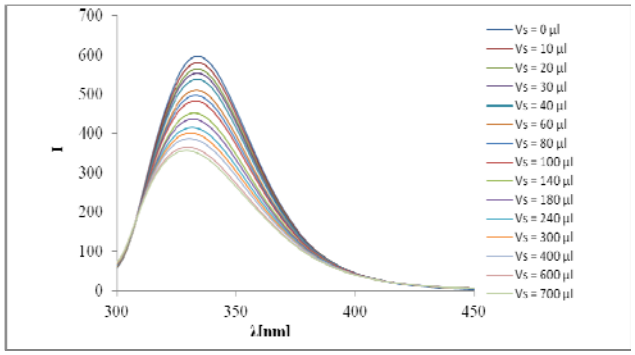

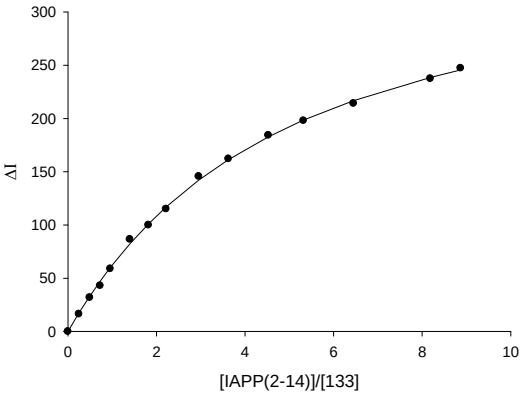

K_a [M^{-1}] = 9540 ± 4 %

K_d [µM] = 104 ± 4 %

5.4.2 Fluorescence titrations of the sulfate tweezer 161

Fluorescence titration of the tweezer 161 with AcLysOMe · HCl in phosphate buffer (200 mM, pH 7.6)

λ_{exc} = 285 nm	Receptor **161**	Guest AcLysOMe · HCl
Amount [mg]:	0.156	0.410
Volume [mL]:	8.69	0.673
Concentration [mol/L]:	$2.33 \cdot 10^{-05}$	$2.55 \cdot 10^{-03}$

Guest V (µL)	**Receptor V (µL)**	**[Receptor] [mol/L]**	**[Guest] [mol/L]**	**[Guest]/ [Receptor]**	**F.I. (I_{337})**	**ΔI_{obs}**	**ΔI_{calc}**
0	700	2.33E-05	0.00E+00	0.00	918.114	0.000	0
10	710	2.33E-05	3.59E-05	1.54	725.153	192.961	193.3159
20	720	2.33E-05	7.09E-05	3.04	642.548	275.566	272.2011
30	730	2.33E-05	1.05E-04	4.50	611.539	306.575	309.9996
40	740	2.33E-05	1.38E-04	5.92	584.480	333.634	331.4145
60	760	2.33E-05	2.01E-04	8.65	565.857	352.257	354.424
80	780	2.33E-05	2.62E-04	11.23	551.001	367.113	366.4685
100	800	2.33E-05	3.19E-04	13.69	548.189	369.925	373.8478
120	820	2.33E-05	3.73E-04	16.03	541.879	376.235	378.8253
150	850	2.33E-05	4.50E-04	19.33	532.487	385.627	383.8455
180	880	2.33E-05	5.22E-04	22.40	527.754	390.360	387.2144
220	920	2.33E-05	6.10E-04	26.19	526.147	391.967	390.2914
260	960	2.33E-05	6.91E-04	29.66	525.849	392.265	392.4293
300	1000	2.33E-05	7.66E-04	32.86	524.197	393.917	394.0008

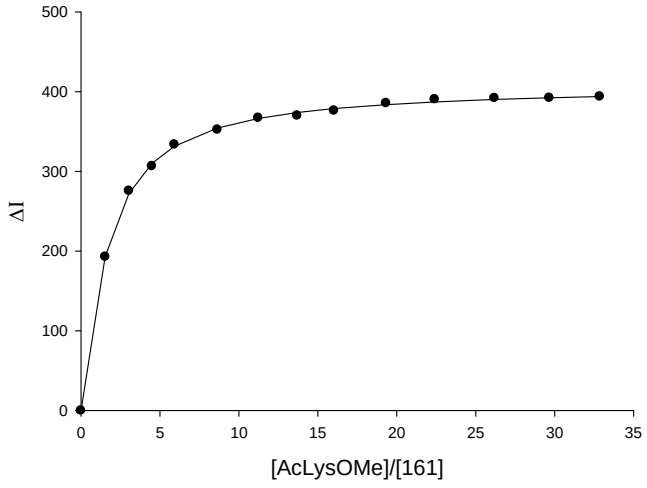

K_a [M^{-1}] = 36000 ± 2 %

K_d [µM] = 28 ± 2 %

ΔI_{max} = 409

Fluorescence titration of the tweezer 161 with AcArgOMe · HCl in phosphate buffer (200 mM, pH 7.6)

λ_{exc} = 285 nm	Receptor **161**	Guest AcArgOMe · HCl
Amount [mg]:	0.156	0.340
Volume [mL]:	8.69	0.499
Concentration [mol/L]:	$2.33 \cdot 10^{-05}$	$2.55 \cdot 10^{-03}$

Guest V (µL)	**Receptor V (µL)**	**[Receptor] [mol/L]**	**[Guest] [mol/L]**	**[Guest]/ [Receptor]**	**F.I. (I_{337})**	**ΔI_{obs}**	**ΔI_{calc}**
0	700	2.33E-05	0.00E+00	0.00	921.704	0.000	0.000
10	710	2.33E-05	3.60E-05	1.54	863.162	58.542	56.863
20	720	2.33E-05	7.10E-05	3.05	825.328	96.376	98.541
30	730	2.33E-05	1.05E-04	4.51	795.250	126.454	130.157
40	740	2.33E-05	1.38E-04	5.93	765.497	156.207	154.846
60	760	2.33E-05	2.02E-04	8.66	723.468	198.236	190.741
80	780	2.33E-05	2.62E-04	11.24	703.545	218.159	215.465
100	800	2.33E-05	3.19E-04	13.70	691.642	230.062	233.478
120	820	2.33E-05	3.74E-04	16.04	675.124	246.580	247.162
150	850	2.33E-05	4.51E-04	19.35	662.666	259.038	262.445
180	880	2.33E-05	5.23E-04	22.42	654.232	267.472	273.656
220	920	2.33E-05	6.11E-04	26.22	638.021	283.683	284.648
260	960	2.33E-05	6.92E-04	29.69	625.181	296.523	292.749
300	1000	2.33E-05	7.66E-04	32.89	619.139	302.565	298.964

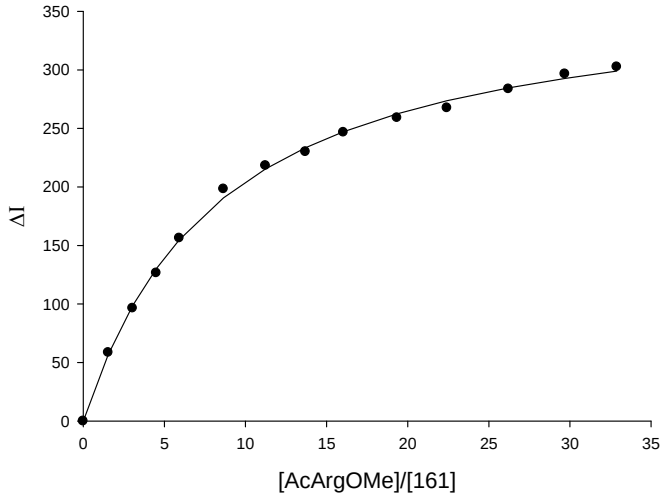

K_a [M^{-1}] = 5600 ± 4 %

K_d [µM] = 178 ± 4 %

ΔI_{max} = 370

Fluorescence titration of the tweezer 161 with AcLysOMe · HCl in phosphate buffer (10mM, pH 6.2)

λ_{exc} = 285 nm	Receptor **161**	Guest AcLysOMe · HCl
Amount [mg]:	0.109	0.372
Volume [mL]:	6.068	0.611
Concentration [mol/L]:	$2.33 \cdot 10^{-05}$	$2.55 \cdot 10^{-03}$

Guest V (µL)	**Receptor V (µL)**	**[Receptor] [mol/L]**	**[Guest] [mol/L]**	**[Guest]/ [Receptor]**	**F.I. (I_{338})**	**ΔI_{obs}**	**ΔI_{calc}**
0	700	2.33E-05	0.00E+00	0.00	909.488	0.000	0.000
10	710	2.33E-05	3.59E-05	1.54	712.669	196.819	195.357
20	720	2.33E-05	7.09E-05	3.04	653.965	255.523	258.245
30	730	2.33E-05	1.05E-04	4.50	626.159	283.329	283.571
40	740	2.33E-05	1.38E-04	5.92	610.490	298.998	296.686
60	760	2.33E-05	2.01E-04	8.64	599.700	309.788	309.904
80	780	2.33E-05	2.62E-04	11.23	596.310	313.178	316.500
100	800	2.33E-05	3.19E-04	13.68	587.791	321.697	320.442
120	820	2.33E-05	3.73E-04	16.02	582.066	327.422	323.060
150	850	2.33E-05	4.50E-04	19.31	584.337	325.151	325.669
180	880	2.33E-05	5.22E-04	22.39	582.969	326.519	327.403
220	920	2.33E-05	6.10E-04	26.17	581.129	328.359	328.975
260	960	2.33E-05	6.91E-04	29.64	581.089	328.399	330.061
300	1000	2.33E-05	7.65E-04	32.83	577.771	331.717	330.856

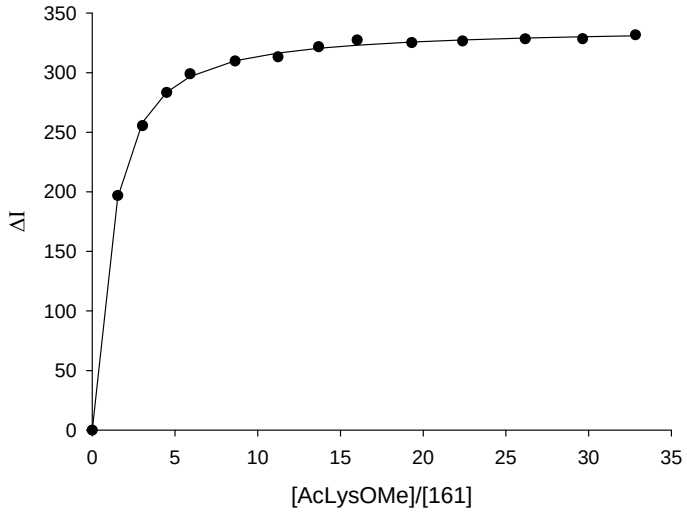

K_a [M^{-1}] = 60900 ± 3%

K_d [µM] = 16 ± 3 %

ΔI_{max} = 338

Fluorescence titration of the tweezer 161 with AcArgOMe · HCl in phosphate buffer (10mM, pH 6.2)

λ_{exc} = 285 nm	Receptor **161**	Guest AcArgOMe · HCl
Amount [mg]:	0.109	0.350
Volume [mL]:	6.068	0.514
Concentration [mol/L]:	$2.33 \cdot 10^{-05}$	$2.55 \cdot 10^{-03}$

Guest V (µL)	**Receptor V (µL)**	**[Receptor] [mol/L]**	**[Guest] [mol/L]**	**[Guest]/ [Receptor]**	**F.I. (I_{338})**	**ΔI_{obs}**	**ΔI_{calc}**
0	700	2.33E-05	0.00E+00	0.00	960.000	0.000	0.000
10	710	2.33E-05	3.60E-05	1.54	872.883	87.117	82.937
20	720	2.33E-05	7.09E-05	3.04	824.577	135.423	130.271
30	730	2.33E-05	1.05E-04	4.50	800.783	159.217	159.662
40	740	2.33E-05	1.38E-04	5.92	781.239	178.761	179.344
60	760	2.33E-05	2.02E-04	8.65	760.417	199.583	203.734
80	780	2.33E-05	2.62E-04	11.24	747.828	212.172	218.125
100	800	2.33E-05	3.19E-04	13.69	736.247	223.753	227.574
120	820	2.33E-05	3.74E-04	16.03	724.760	235.240	234.240
150	850	2.33E-05	4.51E-04	19.33	721.904	238.096	241.215
180	880	2.33E-05	5.22E-04	22.41	714.210	245.790	246.043
220	920	2.33E-05	6.10E-04	26.19	704.210	255.790	250.559
260	960	2.33E-05	6.91E-04	29.67	701.741	258.259	253.757
300	1000	2.33E-05	7.66E-04	32.86	702.693	257.307	256.141

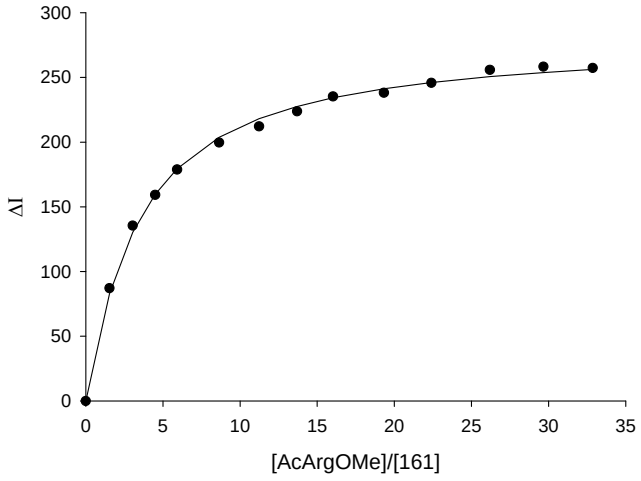

K_a [M^{-1}] = 14500 ± 4%
K_d [µM] = 69 ± 4 %

ΔI_{max} = 280

Fluorescence titration of the tweezer 161 with AcLysOMe · HCl in phosphate buffer (10mM, pH 7.2)

λ_{exc} = 285 nm	Receptor **161**	Guest AcLysOMe · HCl
Amount [mg]:	0.100	0.354
Volume [mL]:	5.568	0.581
Concentration [mol/L]:	$2.33 \cdot 10^{-05}$	$2.55 \cdot 10^{-03}$

Guest V (µL)	Receptor V (µL)	[Receptor] [mol/L]	[Guest] [mol/L]	[Guest]/ [Receptor]	F.I. (I_{338})	ΔI_{obs}	ΔI_{calc}
0	700	2.33E-05	0.00E+00	0.00	925.462	0.000	0.000
10	710	2.33E-05	3.60E-05	1.54	702.801	222.661	222.446
20	720	2.33E-05	7.09E-05	3.04	623.958	301.504	299.942
30	730	2.33E-05	1.05E-04	4.50	591.476	333.986	332.975
40	740	2.33E-05	1.38E-04	5.92	578.192	347.270	350.558
60	760	2.33E-05	2.02E-04	8.65	559.736	365.726	368.613
80	780	2.33E-05	2.62E-04	11.24	545.225	380.237	377.746
100	800	2.33E-05	3.19E-04	13.69	544.797	380.665	383.242
120	820	2.33E-05	3.74E-04	16.03	537.159	388.303	386.908
150	850	2.33E-05	4.50E-04	19.33	532.127	393.335	390.573
180	880	2.33E-05	5.22E-04	22.41	533.112	392.350	393.015
220	920	2.33E-05	6.10E-04	26.20	530.630	394.832	395.234
260	960	2.33E-05	6.91E-04	29.67	533.667	391.795	396.769
300	1000	2.33E-05	7.66E-04	32.86	522.077	403.385	397.893

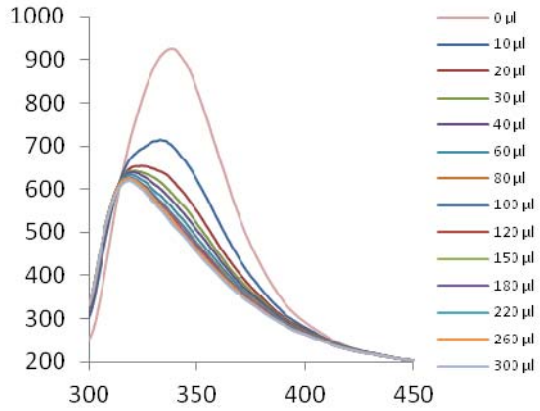

Δλ ~ 10 nm, blue shift

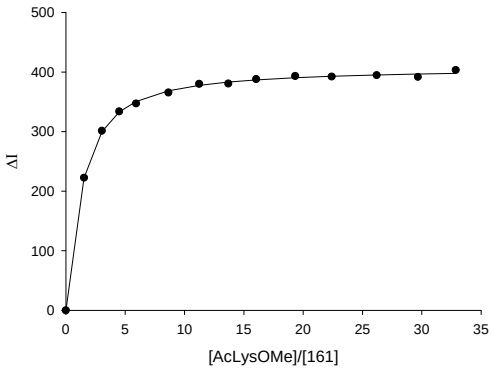

K_a [M^{-1}] = 51500 ± 3 %

K_d [µM] = 19 ± 3 %

ΔI_{max} = 408

Fluorescence titration of the tweezer 161 with AcArgOMe · HCl in phosphate buffer (10mM. pH 7.2)

λ_{exc} = 285 nm	Receptor **161**	Guest AcArgOMe · HCl
Amount [mg]:	0.100	0.354
Volume [mL]:	5.568	0.520
Concentration [mol/L]:	$2.33 \cdot 10^{-05}$	$2.55 \cdot 10^{-03}$

Guest V (µL)	**Receptor V (µL)**	**[Receptor] [mol/L]**	**[Guest] [mol/L]**	**[Guest]/ [Receptor]**	**F.I. (I_{338})**	**ΔI_{obs}**	**ΔI_{calc}**
0	700	2.33E-05	0.00E+00	0.00	906.244	0.000	0.000
10	710	2.33E-05	3.59E-05	1.54	827.374	78.870	76.058
20	720	2.33E-05	7.09E-05	3.04	782.379	123.865	120.955
30	730	2.33E-05	1.05E-04	4.50	753.140	153.104	149.585
40	740	2.33E-05	1.38E-04	5.92	739.276	166.968	169.129
60	760	2.33E-05	2.01E-04	8.65	713.500	192.744	193.803
80	780	2.33E-05	2.62E-04	11.23	700.130	206.114	208.608
100	800	2.33E-05	3.19E-04	13.69	691.374	214.870	218.432
120	820	2.33E-05	3.74E-04	16.03	684.805	221.439	225.413
150	850	2.33E-05	4.50E-04	19.33	679.489	226.755	232.761
180	880	2.33E-05	5.22E-04	22.41	668.375	237.869	237.873
220	920	2.33E-05	6.10E-04	26.19	662.402	243.842	242.675
260	960	2.33E-05	6.91E-04	29.67	656.113	250.131	246.088
300	1000	2.33E-05	7.66E-04	32.86	650.395	255.849	248.638

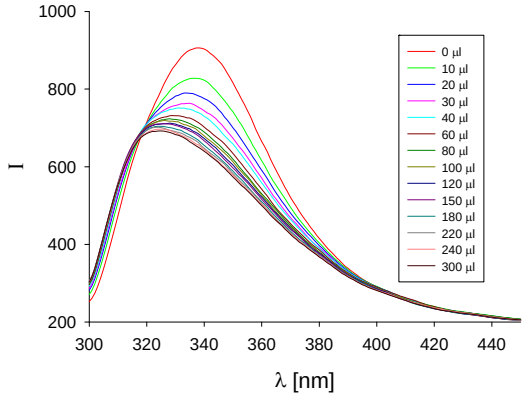

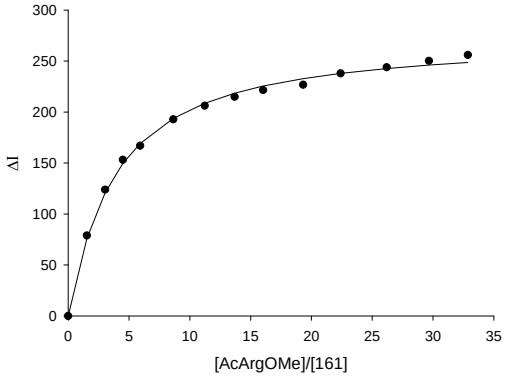

K_a [M^{-1}] = 13000 ± 5 %

K_d [µM] = 77 ± 5 %

ΔI_{max} = 274

Fluorescence titration of the tweezer 161 with AcLysOMe · HCl in phosphate buffer (10mM, pH 8.6)

λ_{exc} = 285 nm	Receptor **161**	Guest AcLysOMe · HCl
Amount [mg]:	0.092	0.380
Volume [mL]:	5.124	0.624
Concentration [mol/L]:	$2.33 \cdot 10^{-05}$	$2.55 \cdot 10^{-03}$

Guest V (µL)	**Receptor V (µL)**	**[Receptor] [mol/L]**	**[Guest] [mol/L]**	**[Guest]/ [Receptor]**	**F.I. (I_{338})**	**ΔI_{obs}**	**ΔI_{calc}**
0	700	2.33E-05	0.00E+00	0.00	647.758	0.000	0.000
10	710	2.33E-05	3.59E-05	1.54	453.457	194.301	185.303
20	720	2.33E-05	7.09E-05	3.04	400.921	246.837	248.519
30	730	2.33E-05	1.05E-04	4.50	377.422	270.336	275.058
40	740	2.33E-05	1.38E-04	5.92	363.845	283.913	289.077
60	760	2.33E-05	2.01E-04	8.65	347.507	300.251	303.399
80	780	2.33E-05	2.62E-04	11.23	341.385	306.373	310.616
100	800	2.33E-05	3.19E-04	13.69	331.055	316.703	314.950
120	820	2.33E-05	3.73E-04	16.03	332.507	315.251	317.838
150	850	2.33E-05	4.50E-04	19.33	327.646	320.112	320.723
180	880	2.33E-05	5.22E-04	22.40	322.389	325.369	322.643
220	920	2.33E-05	6.10E-04	26.19	320.437	327.321	324.387
260	960	2.33E-05	6.91E-04	29.66	317.721	330.037	325.592
300	1000	2.33E-05	7.65E-04	32.86	318.211	329.547	326.476

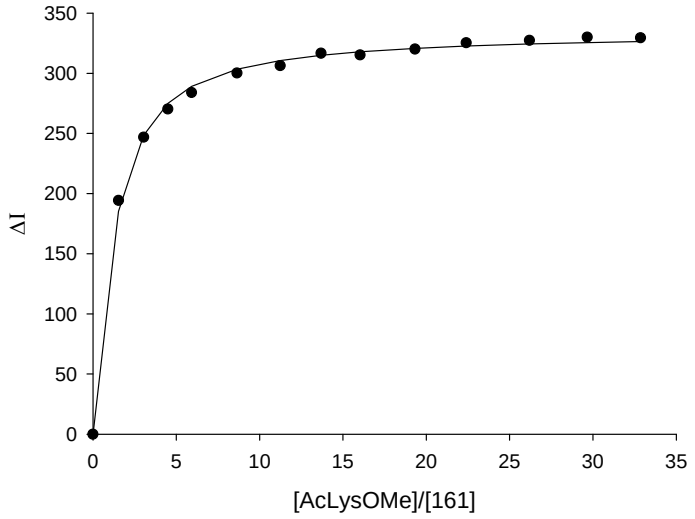

K_a [M^{-1}] = 53900 ± 5 %

K_d [µM] = 18 ± 5 %

ΔI_{max} = 335

Fluorescence titration of the tweezer 161 with AcArgOMe · HCl in phosphate buffer (10mM, pH 8.6)

λ_{exc} = 285 nm	Receptor **161**	Guest AcArgOMe · HCl
Amount [mg]:	0.092	0.382
Volume [mL]:	5.124	0.561
Concentration [mol/L]:	$2.33 \cdot 10^{-05}$	$2.55 \cdot 10^{-03}$

Guest V (µL)	**Receptor V (µL)**	**[Receptor] [mol/L]**	**[Guest] [mol/L]**	**[Guest]/ [Receptor]**	**F.I. (I_{338})**	**ΔI_{obs}**	**ΔI_{calc}**
0	700	2.33E-05	0.00E+00	0.00	620.606	0.000	0.000
10	710	2.33E-05	3.60E-05	1.54	558.129	62.477	59.765
20	720	2.33E-05	7.09E-05	3.04	519.910	100.696	96.577
30	730	2.33E-05	1.05E-04	4.50	498.401	122.205	120.855
40	740	2.33E-05	1.38E-04	5.92	482.759	137.847	137.847
60	760	2.33E-05	2.02E-04	8.65	464.441	156.165	159.832
80	780	2.33E-05	2.62E-04	11.24	450.309	170.297	173.329
100	800	2.33E-05	3.19E-04	13.70	438.258	182.348	182.417
120	820	2.33E-05	3.74E-04	16.04	434.110	186.496	188.940
150	850	2.33E-05	4.51E-04	19.34	428.968	191.638	195.865
180	880	2.33E-05	5.22E-04	22.42	423.093	197.513	200.719
220	920	2.33E-05	6.10E-04	26.21	414.712	205.894	205.306
260	960	2.33E-05	6.91E-04	29.68	409.409	211.197	208.581
300	1000	2.33E-05	7.66E-04	32.88	401.665	218.941	211.037

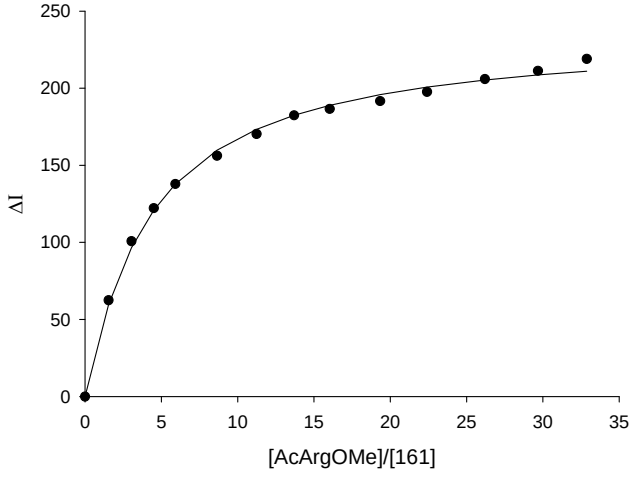

K_a [M^{-1}] = 11300 ± 5 %

K_d [µM] = 88 ± 5 %

ΔI_{max} = 236

Fluorescence titration of the tweezer 161 with HLysOH in phosphate buffer (10mM, pH 7.6)

λ_{exc} = 285 nm λ_{em} = 338 nm	Receptor **161**	Guest HLysOH · HCl
Amount [mg]:	0.154	0.282
Volume [mL]:	8.58	0.607
Concentration [mol/L]:	$2.33 \cdot 10^{-05}$	$2.54 \cdot 10^{-03}$

Guest V (µL)	**Receptor V (µL)**	**[Receptor] [mol/L]**	**[Guest] [mol/L]**	**[Guest]/ [Receptor]**	**F.I. (I_{338})**	**ΔI_{obs}**	**ΔI_{calc}**
0	700	2.33E-05	0.00E+00	0.00	668.101	0.000	0.000
10	710	2.33E-05	3.58E-05	1.54	624.460	43.641	37.471
20	720	2.33E-05	7.06E-05	3.03	600.417	67.684	66.272
30	730	2.33E-05	1.05E-04	4.49	571.074	97.027	88.995
40	740	2.33E-05	1.37E-04	5.90	565.345	102.756	107.324
60	760	2.33E-05	2.01E-04	8.62	539.165	128.936	134.979
80	780	2.33E-05	2.61E-04	11.19	516.322	151.779	154.784
100	800	2.33E-05	3.18E-04	13.64	495.840	172.261	169.631
140	840	2.33E-05	4.24E-04	18.19	478.098	190.003	190.359
180	880	2.33E-05	5.20E-04	22.32	465.560	202.541	204.114
240	940	2.33E-05	6.49E-04	27.86	451.082	217.019	217.799
300	1000	2.33E-05	7.63E-04	32.74	437.507	230.594	226.874

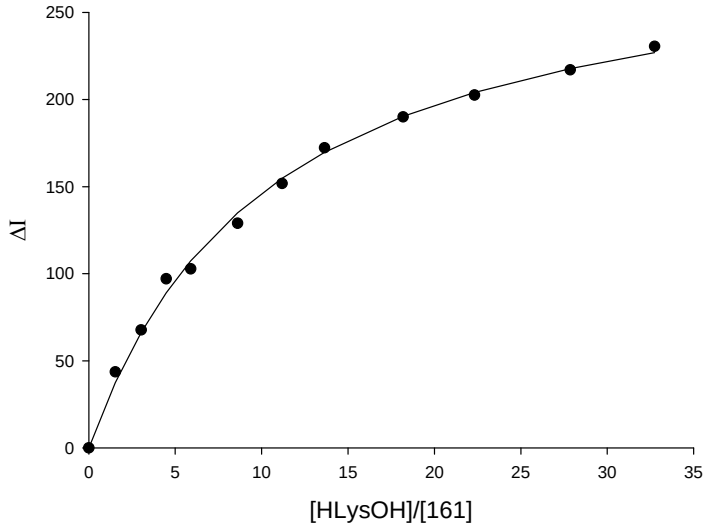

K_a [M^{-1}] = 4410 ± 6 %

K_d [µM] = 227 ± 6 %

ΔI_{max} =296

Fluorescence titration of the tweezer 161 with HLysOH in phosphate buffer (10mM. pH 6.2)

λ_{exc} = 285 nm λ_{em} = 336 nm	Receptor **161**	Guest HLysOH
Amount [mg]:	0.190	0.192
Volume [mL]:	11.310	1.400
Concentration [mol/L]:	$2.18 \cdot 10^{-05}$	$7.51 \cdot 10^{-04}$

Guest V (µL)	Receptor V (µL)	[Receptor] [mol/L]	[Guest] [mol/L]	[Guest]/ [Receptor]	F.I. ($I_{334\ nm}$)	ΔI_{obs}	ΔI_{calc}
0	700	2.18E-05	0.00E+00	0.00	615.594	0.000	0.000
10	710	2.18E-05	1.06E-05	0.49	606.248	9.346	13.338
20	720	2.18E-05	2.09E-05	0.96	591.587	24.007	25.074
30	730	2.18E-05	3.08E-05	1.42	577.498	38.096	35.465
40	740	2.18E-05	4.06E-05	1.86	565.311	50.283	44.718
60	760	2.18E-05	5.93E-05	2.72	558.092	57.502	60.453
80	780	2.18E-05	7.70E-05	3.53	544.148	71.446	73.303
100	800	2.18E-05	9.38E-05	4.31	529.922	85.672	83.973
140	840	2.18E-05	1.25E-04	5.74	514.226	101.368	100.631
180	880	2.18E-05	1.54E-04	7.04	509.955	105.639	113.005
240	940	2.18E-05	1.92E-04	8.79	482.395	133.199	126.529
300	1000	2.18E-05	2.25E-04	10.33	475.508	140.086	141.332

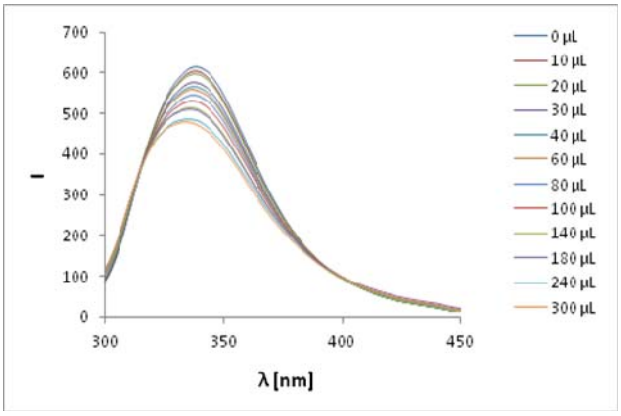

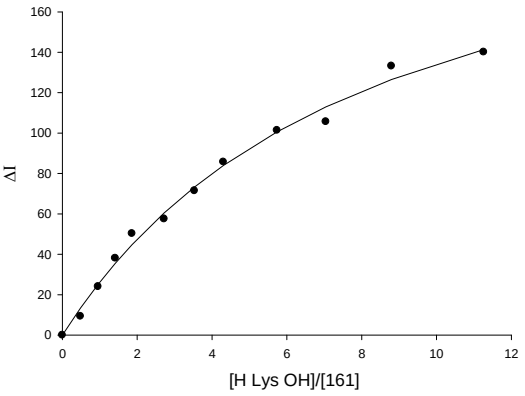

K_a [M^{-1}] = 5790 ± 15 %

K_d [µM] = 173 ± 15 %

Fluorescence titration of the tweezer 161 with HArgOH in phosphate buffer (10mM, pH 7.6)

λ_{exc} = 285 nm λ_{em} = 338 nm	Receptor **161**	Guest HArgOH · HCl
Amount [mg]:	0.154	0.282
Volume [mL]:	8.58	0.607
Concentration [mol/L]:	$2.33 \cdot 10^{-05}$	$2.54 \cdot 10^{-03}$

Guest V (µL)	**Receptor V (µL)**	**[Receptor] [mol/L]**	**[Guest] [mol/L]**	**[Guest]/ [Receptor]**	**F.I. (I_{338})**	**ΔI_{obs}**	**ΔI_{calc}**
0	700	2.33E-05	0.00E+00	0.00	663.928	0.000	0.000
10	710	2.33E-05	3.58E-05	1.54	651.777	12.151	10.660
20	720	2.33E-05	7.07E-05	3.03	640.915	23.013	20.121
30	730	2.33E-05	1.05E-04	4.49	633.350	30.578	28.573
40	740	2.33E-05	1.38E-04	5.90	629.736	34.192	36.168
60	760	2.33E-05	2.01E-04	8.62	609.553	54.375	49.252
80	780	2.33E-05	2.61E-04	11.20	602.310	61.618	60.118
100	800	2.33E-05	3.18E-04	13.65	595.105	68.823	69.282
140	840	2.33E-05	4.24E-04	18.20	587.086	76.842	83.879
180	880	2.33E-05	5.21E-04	22.34	573.167	90.761	94.982
240	940	2.33E-05	6.50E-04	27.88	555.393	108.535	107.403
300	1000	2.33E-05	7.63E-04	32.76	543.114	120.814	116.533

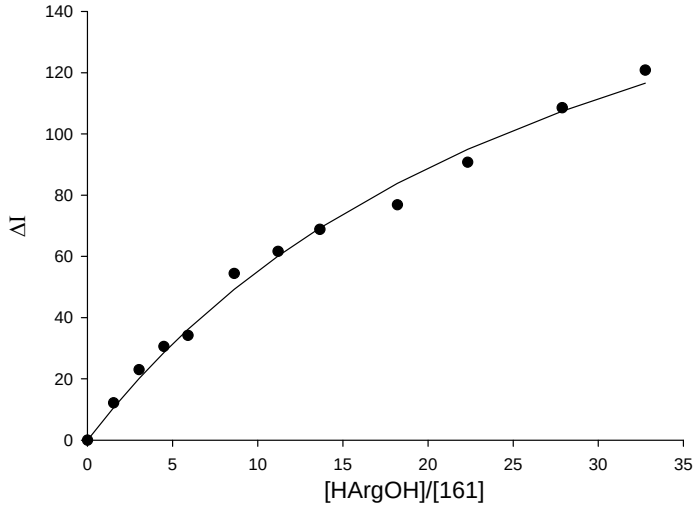

K_a [M^{-1}] = 1430 ± 15 %

K_d [µM] = 699 ± 2 %

ΔI_{max} =225

Fluorescence titration of the tweezer 161 with HArgOMe in phosphate buffer (10mM, pH 7.6)

λ_{exc} = 285 nm λ_{em} = 338 nm	Receptor **161**	Guest HArgOMe · 2HCl
Amount [mg]:	0.154	0.429
Volume [mL]:	8.575	0.644
Concentration [mol/L]:	$2.33 \cdot 10^{-05}$	$2.55 \cdot 10^{-03}$

Guest V (µL)	**Receptor V (µL)**	**[Receptor] [mol/L]**	**[Guest] [mol/L]**	**[Guest]/ [Receptor]**	**F.I. ($I_{338\ nm}$)**	**ΔI_{obs}**	**ΔI_{calc}**
0	700	2,33E-05	0,00E+00	0,00	668,334	0,000	0,000
10	710	2,33E-05	3,59E-05	1,54	608,912	59,422	51,408
20	720	2,33E-05	7,09E-05	3,04	571,524	96,810	88,201
30	730	2,33E-05	1,05E-04	4,50	552,344	115,990	115,571
40	740	2,33E-05	1,38E-04	5,92	536,594	131,740	136,610
60	760	2,33E-05	2,01E-04	8,64	505,163	163,171	166,659
80	780	2,33E-05	2,62E-04	11,23	482,611	185,723	186,984
100	800	2,33E-05	3,19E-04	13,68	470,043	198,291	201,600
140	840	2,33E-05	4,25E-04	18,25	451,324	217,010	221,160
180	880	2,33E-05	5,22E-04	22,39	435,475	232,859	233,623
240	940	2,33E-05	6,51E-04	27,95	418,363	249,971	245,633
300	1000	2,33E-05	7,65E-04	32,84	411,150	257,184	253,393

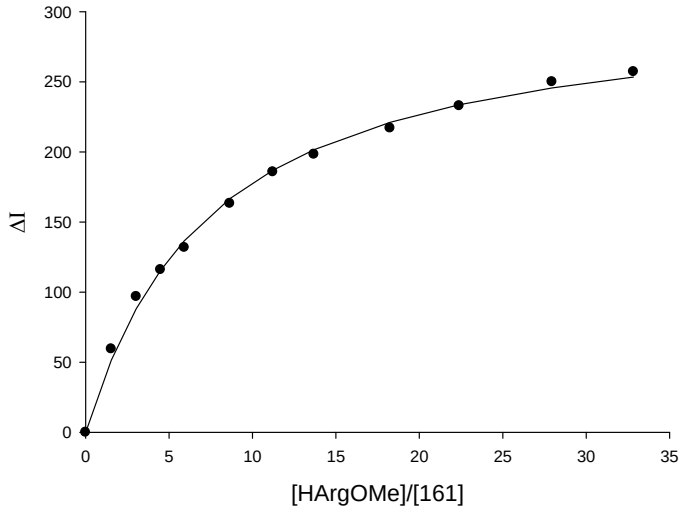

K_a [M^{-1}] = 6260 ± 6 %

K_d [µM] = 160 ± 6 %

ΔI_{max} = 308

Fluorescence titration of the tweezer 161 with peptide KAA in phosphate buffer (10mM, pH 7.6)

λ_{exc} = 285 nm λ_{em} = 338 nm	Receptor **161**	Guest KAA
Amount [mg]:	0.154	0.37
Volume [mL]:	8.58	0.503
Concentration [mol/L]:	$2.33 \cdot 10^{-05}$	$2.55 \cdot 10^{-03}$

Guest V (µL)	**Receptor V (µL)**	**[Receptor] [mol/L]**	**[Guest] [mol/L]**	**[Guest]/ [Receptor]**	**F.I. (I_{338})**	**ΔI_{obs}**	**ΔI_{calc}**
0	700	2.33E-05	0.00E+00	0.00	671.428	0.000	0.000
10	710	2.33E-05	3.59E-05	1.54	644.313	27.115	32.063
20	720	2.33E-05	7.09E-05	3.04	606.546	64.882	57.917
30	730	2.33E-05	1.05E-04	4.50	595.503	75.925	79.153
40	740	2.33E-05	1.38E-04	5.92	575.253	96.175	96.878
60	760	2.33E-05	2.01E-04	8.64	544.662	126.766	124.722
80	780	2.33E-05	2.62E-04	11.23	525.733	145.695	145.552
100	800	2.33E-05	3.19E-04	13.69	514.004	157.424	161.693
140	840	2.33E-05	4.25E-04	18.25	484.077	187.351	185.041
180	880	2.33E-05	5.22E-04	22.39	469.864	201.564	201.088
240	940	2.33E-05	6.51E-04	27.95	451.425	220.003	217.517
300	1000	2.33E-05	7.65E-04	32.85	445.244	226.184	228.679

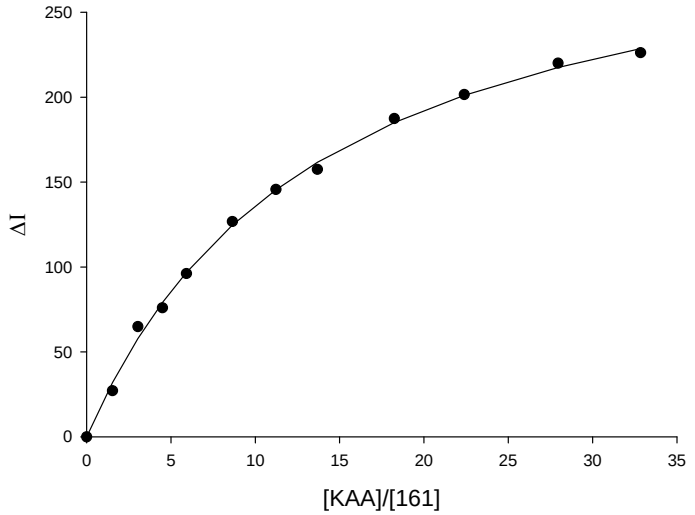

K_a [M^{-1}] = 3300 ± 5 %

K_d [µM] = 303 ± 5 %

ΔI_{max} =321

Fluorescence titration of the tweezer 161 with KAA in phosphate buffer (10mM. pH 6.2)

λ_{exc} = 285 nm λ_{em} = 336 nm	Receptor **161**	Guest KAA
Amount [mg]:	0.190	0.260
Volume [mL]:	11.310	1.202
Concentration [mol/L]:	$2.18 \cdot 10^{-05}$	$7.5 \cdot 10^{-04}$

Guest V (µL)	Receptor V (µL)	[Receptor] [mol/L]	[Guest] [mol/L]	[Guest]/ [Receptor]	F.I. ($I_{334\ nm}$)	ΔI_{obs}	ΔI_{calc}
0	700	2.18E-05	0.00E+00	0.00	618.074	0.000	0.000
10	710	2.18E-05	1.06E-05	0.48	607.968	10.106	12.009
20	720	2.18E-05	2.08E-05	0.96	598.678	19.396	22.630
30	730	2.18E-05	3.08E-05	1.41	581.431	36.643	32.080
40	740	2.18E-05	4.05E-05	1.86	576.712	41.362	40.533
60	760	2.18E-05	5.92E-05	2.72	559.753	58.321	54.994
80	780	2.18E-05	7.69E-05	3.53	550.712	67.362	66.889
100	800	2.18E-05	9.38E-05	4.30	543.848	74.226	76.827
140	840	2.18E-05	1.25E-04	5.74	528.168	89.906	92.459
180	880	2.18E-05	1.53E-04	7.04	514.292	103.782	104.167
240	940	2.18E-05	1.92E-04	8.79	501.664	116.410	117.060
300	1000	2.18E-05	2.25E-04	10.33	484.849	133.225	131.295

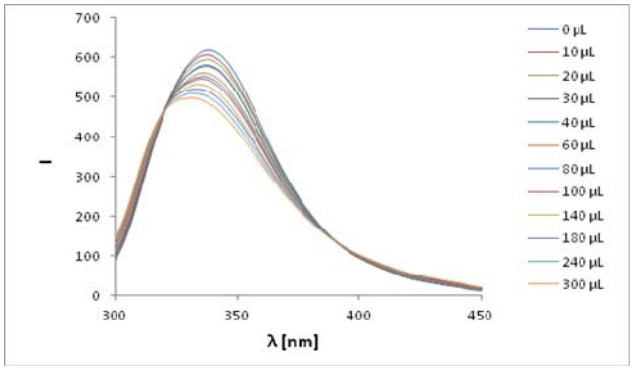

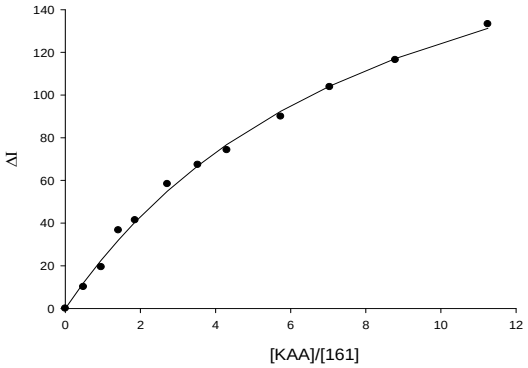

K_a [M^{-1}] = 5440 ± 12 %

K_d [µM] = 184 ± 12 %

Fluorescence titration of the tweezer 161 with peptide KLVFF in phosphate buffer (10mM, pH 7.6)

λ_{exc} = 285 nm λ_{em} = 338 nm	Receptor **161**	Guest KLVFF
Amount [mg]:	0.113	0.355
Volume [mL]:	6.724	0.725
Concentration [mol/L]:	$2.18 \cdot 10^{-05}$	$7.5 \cdot 10^{-04}$

Guest V (µL)	**Receptor V (µL)**	**[Receptor] [mol/L]**	**[Guest] [mol/L]**	**[Guest]/ [Receptor]**	**F.I. (I_{338})**	**ΔI_{obs}**	**ΔI_{calc}**
0	700	2.18E-05	0.00E+00	0.00	644.084	0.000	0.000
10	710	2.18E-05	1.06E-05	0.48	629.776	14.308	16.276
20	720	2.18E-05	2.08E-05	0.96	613.787	30.297	28.826
30	730	2.18E-05	3.08E-05	1.41	605.562	38.522	38.553
40	740	2.18E-05	4.05E-05	1.86	599.635	44.449	46.180
60	760	2.18E-05	5.92E-05	2.72	588.012	56.072	57.153
80	780	2.18E-05	7.69E-05	3.53	580.781	63.303	64.522
100	800	2.18E-05	9.38E-05	4.30	571.938	72.146	69.743
140	840	2.18E-05	1.25E-04	5.73	565.785	78.299	76.576
180	880	2.18E-05	1.53E-04	7.04	561.215	82.869	80.811
240	940	2.18E-05	1.92E-04	8.78	556.559	87.525	84.792
300	1000	2.18E-05	2.25E-04	10.32	562.350	81.734	87.306

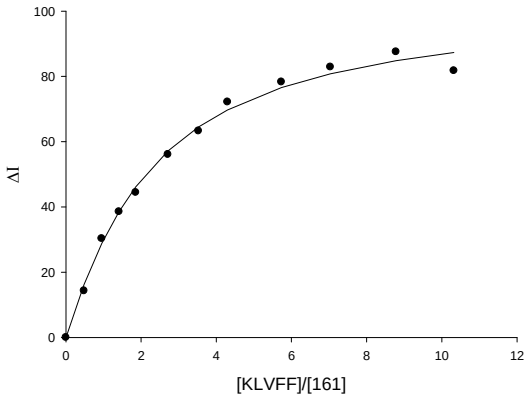

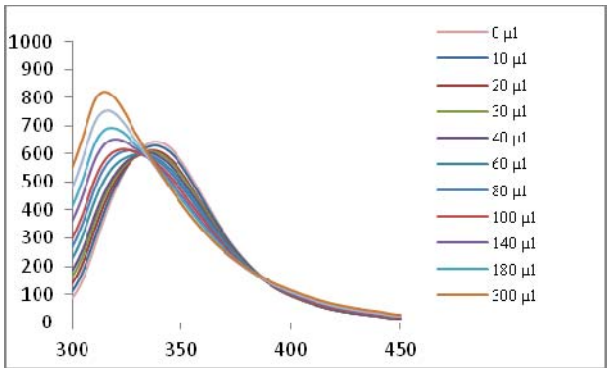

Δλ ~ 20 nm, blue shift

K_a [M^{-1}] = 26200 ± 11 %

K_d [µM] = 38 ± 11 %

ΔI_{max} =104

Fluorescence titration of the tweezer 161 with peptide IAPP (1-7) in phosphate buffer (10mM, pH 7.6)

λ_{exc} = 285 nm λ_{em} = 338 nm	Receptor **161**	Guest IAPP (1-7)
Amount [mg]:	0.113	0.400
Volume [mL]:	6.724	0.700
Concentration [mol/L]:	$2.18 \cdot 10^{-05}$	$7.75 \cdot 10^{-04}$

Guest V (µL)	**Receptor V (µL)**	**[Receptor] [mol/L]**	**[Guest] [mol/L]**	**[Guest]/ [Receptor]**	**F.I. (I_{338})**	**ΔI_{obs}**	**ΔI_{calc}**
0	700	2.18E-05	0.00E+00	0.00	580.391	0.000	0.000
10	710	2.18E-05	1.09E-05	0.50	563.471	16.920	18.683
20	720	2.18E-05	2.15E-05	0.99	540.767	39.624	34.598
30	730	2.18E-05	3.18E-05	1.46	531.674	48.717	48.268
40	740	2.18E-05	4.19E-05	1.92	520.234	60.157	60.104
60	760	2.18E-05	6.12E-05	2.81	500.379	80.012	79.501
80	780	2.18E-05	7.95E-05	3.65	486.185	94.206	94.662
100	800	2.18E-05	9.69E-05	4.44	473.604	106.787	106.792
140	840	2.18E-05	1.29E-04	5.92	458.300	122.091	124.916
180	880	2.18E-05	1.59E-04	7.27	444.470	135.921	137.757
240	940	2.18E-05	1.98E-04	9.08	429.102	151.289	151.210
300	1000	2.18E-05	2.32E-04	10.66	417.189	163.202	160.516

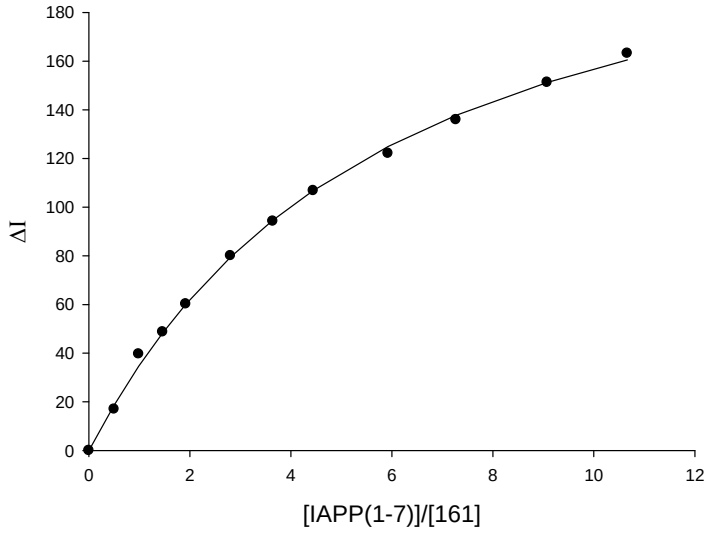

K_a [M^{-1}] = 9080 ± 6 %

K_d [µM] = 110 ± 6 %

ΔI_{max} =242

Fluorescence titration of the tweezer 161 with AcLysOMe in PBS buffer (10mM, pH 7.2, 150 mM NaCl)

λ_{exc} = 285 nm λ_{em} = 338 nm	Receptor **161**	Guest AcLysOMe · HCl
Amount [mg]:	0.133	0.435
Volume [mL]:	7.517	0.714
Concentration [mol/L]:	$2.30 \cdot 10^{-05}$	$2.55 \cdot 10^{-03}$

Guest V (µL)	**Receptor V (µL)**	**[Receptor] [mol/L]**	**[Guest] [mol/L]**	**[Guest]/ [Receptor]**	**F.I. ($I_{338\ nm}$)**	**ΔI_{obs}**	**ΔI_{calc}**
0	700	2.30E-05	0.00E+00	0.00	637.960	0.000	0.000
10	710	2.30E-05	3.59E-05	1.57	477.957	160.003	159.909
20	720	2.30E-05	7.09E-05	3.09	405.555	232.405	227.556
30	730	2.30E-05	1.05E-04	4.57	376.727	261.233	260.956
40	740	2.30E-05	1.38E-04	6.01	359.043	278.917	280.221
60	760	2.30E-05	2.02E-04	8.78	339.784	298.176	301.216
80	780	2.30E-05	2.62E-04	11.40	330.001	307.959	312.331
100	800	2.30E-05	3.19E-04	13.90	323.139	314.821	319.182
140	840	2.30E-05	4.25E-04	18.53	312.929	325.031	327.169
180	880	2.30E-05	5.22E-04	22.74	306.314	331.646	331.674
240	940	2.30E-05	6.52E-04	28.39	297.298	340.662	335.653
300	1000	2.30E-05	7.66E-04	33.36	294.357	343.603	338.056

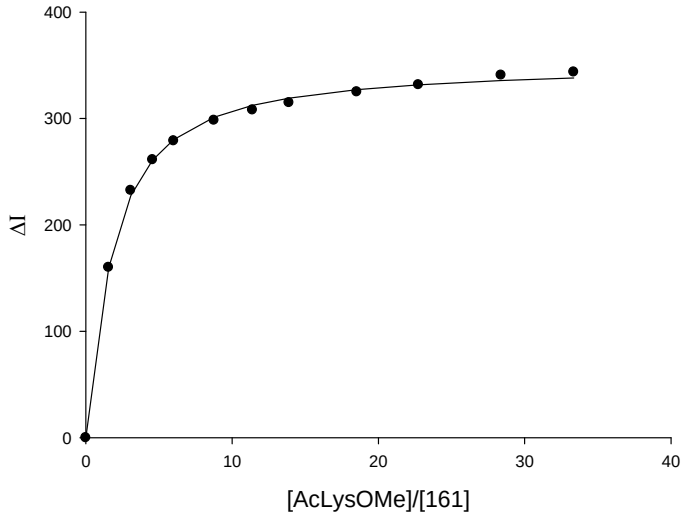

$K_a\ [M^{-1}] = 32600 \pm 4\ \%$

$K_d\ [\mu M] = 31 \pm 4\ \%$

$\Delta I_{max} = 352$

Fluorescence titration of the tweezer 161 with peptide KAA in PBS (10mM, pH 7.2, 150 mM NaCl)

λ_{exc} = 285 nm λ_{em} = 338 nm	Receptor **161**	Guest KAA · CH_3COOH
Amount [mg]:	0.133	0.643
Volume [mL]:	7.517	0.875
Concentration [mol/L]:	$2.30 \cdot 10^{-05}$	$2.55 \cdot 10^{-03}$

Guest V (µL)	**Receptor V (µL)**	**[Receptor] [mol/L]**	**[Guest] [mol/L]**	**[Guest]/ [Receptor]**	**F.I. ($I_{338\ nm}$)**	**ΔI_{obs}**	**ΔI_{calc}**
0	700	2.30E-05	0.00E+00	0.00	620.053	0.000	0.000
10	710	2.30E-05	3.59E-05	1.56	598.190	21.863	22.410
20	720	2.30E-05	7.08E-05	3.08	576.260	43.793	41.169
30	730	2.30E-05	1.05E-04	4.56	563.923	56.130	57.082
40	740	2.30E-05	1.38E-04	6.00	548.533	71.520	70.737
60	760	2.30E-05	2.01E-04	8.76	529.000	91.053	92.929
80	780	2.30E-05	2.61E-04	11.39	508.270	111.783	110.168
100	800	2.30E-05	3.19E-04	13.88	497.067	122.986	123.930
140	840	2.30E-05	4.25E-04	18.50	477.125	142.928	144.499
180	880	2.30E-05	5.21E-04	22.71	458.805	161.248	159.120
240	940	2.30E-05	6.51E-04	28.35	446.819	173.234	174.519
300	1000	2.30E-05	7.65E-04	33.31	434.113	185.940	185.242

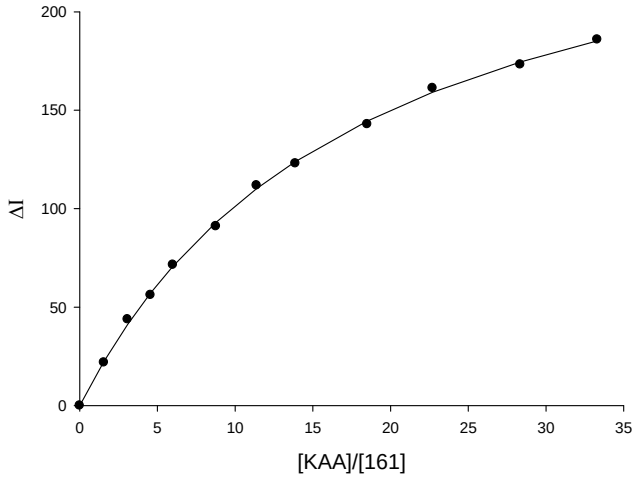

K_a [M^{-1}] = 2520 ± 3 %

K_d [µM] = 397 ± 3 %

ΔI_{max} = 283

Fluorescence titration of the tweezer 161 with AcLysOMe in methanol

λ_{exc} = 285 nm λ_{em} = 320 nm	Receptor **161**	Guest AcLysOMe
Amount [mg]:	0.118	0.459
Volume [mL]:	7.000	0.754
Concentration [mol/L]:	$2.19 \cdot 10^{-05}$	$2.55 \cdot 10^{-03}$

Guest V (µL)	**Receptor V (µL)**	**[Receptor] [mol/L]**	**[Guest] [mol/L]**	**[Guest]/ [Receptor]**	**F.I. (I_{320})**	**- ΔI_{obs}**	**- ΔI_{calc}**
0	700	2.19E-05	0.00E+00	0.00	341.665	0.000	0.000
10	710	2.19E-05	3.59E-05	1.64	491.668	150.003	147.138
20	720	2.19E-05	7.08E-05	3.24	541.670	200.005	197.765
30	730	2.19E-05	1.05E-04	4.79	558.559	216.894	219.535
40	740	2.19E-05	1.38E-04	6.30	572.238	230.573	231.212
60	760	2.19E-05	2.01E-04	9.21	580.712	239.047	243.285
80	780	2.19E-05	2.62E-04	11.96	586.192	244.527	249.429
100	800	2.19E-05	3.19E-04	14.58	593.864	252.199	253.137
140	840	2.19E-05	4.25E-04	19.43	599.100	257.435	257.390
180	880	2.19E-05	5.22E-04	23.85	604.290	262.625	259.757
240	940	2.19E-05	6.51E-04	29.77	601.297	259.632	261.830
300	1000	2.19E-05	7.65E-04	34.98	613.000	271.335	263.074

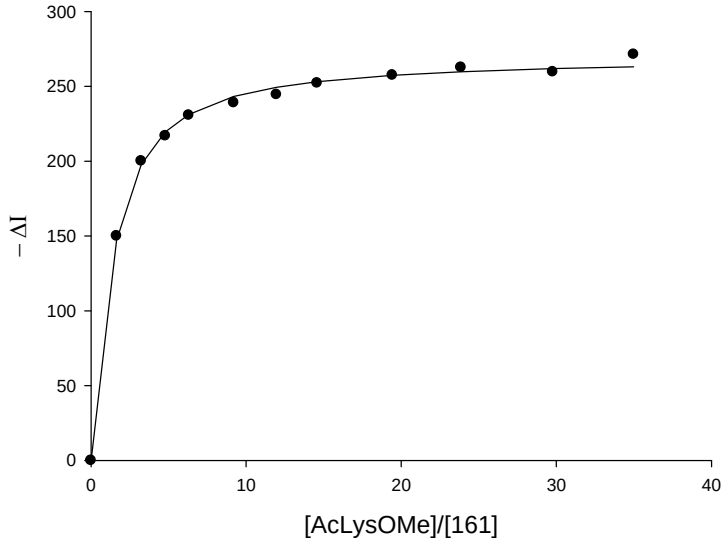

K_a [M^{-1}] = 49800 ± 6 %

K_d [µM] = 20 ± 6 %

ΔI_{max} = - 270

Fluorescence titration of the tweezer 161 with AcArgOMe in methanol

λ_{exc} = 285 nm λ_{em} = 320 nm	Receptor **161**	Guest AcArgOMe
Amount [mg]:	0.118	0.484
Volume [mL]:	7.000	0.711
Concentration [mol/L]:	$2.19 \cdot 10^{-05}$	$2.55 \cdot 10^{-03}$

Guest V (µL)	**Receptor V (µL)**	**[Receptor] [mol/L]**	**[Guest] [mol/L]**	**[Guest]/ [Receptor]**	**F.I. (I_{320})**	**- ΔI_{obs}**	**- ΔI_{calc}**
0	700	2.19E-05	0.00E+00	0.00	342.695	0.000	0.000
10	710	2.19E-05	3.59E-05	1.64	351.154	8.459	9.834
20	720	2.19E-05	7.09E-05	3.24	359.956	17.261	17.635
30	730	2.19E-05	1.05E-04	4.80	369.160	26.465	23.956
40	740	2.19E-05	1.38E-04	6.31	372.464	29.769	29.172
60	760	2.19E-05	2.02E-04	9.21	379.892	37.197	37.254
80	780	2.19E-05	2.62E-04	11.97	385.463	42.768	43.213
100	800	2.19E-05	3.19E-04	14.59	387.707	45.012	47.780
140	840	2.19E-05	4.25E-04	19.45	398.203	55.508	54.306
180	880	2.19E-05	5.22E-04	23.87	401.469	58.774	58.740
240	940	2.19E-05	6.52E-04	29.80	406.335	63.640	63.235
300	1000	2.19E-05	7.66E-04	35.01	409.009	66.314	66.264

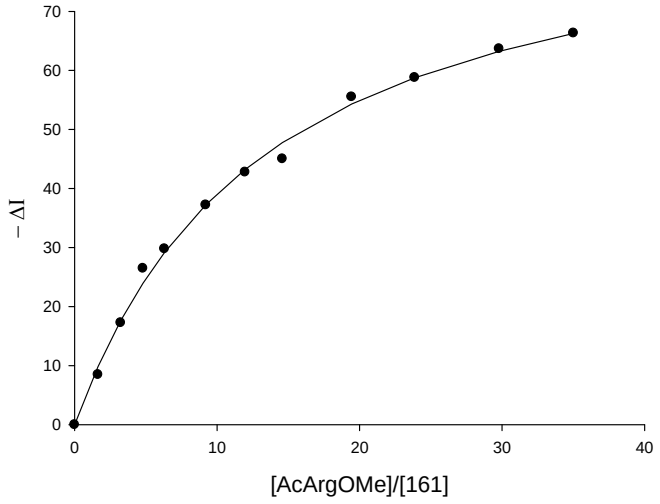

K_a [M^{-1}] = 3620 ± 7 %

K_d [µM] = 276 ± 7 %

ΔI_{max} = - 91

5.4.3 Fluorescence titration of the unsymmetrical tweezers

5.4.3.1 Fluorescence titration of the acetoxy phosphate tweezer 193

Fluorescence titration of the tweezer 193 with AcLysOMe in phosphate buffer (10mM, pH 7.6)

λ_{exc} = 285 nm λ_{em} = 336 nm	Receptor **193**	Guest AcLysOMe · HCl
Amount [mg]:	0.133	0.351
Volume [mL]:	8.858	1.0
Concentration [mol/L]:	$2.18 \cdot 10^{-05}$	$1.47 \cdot 10^{-03}$

Guest V (µL)	**Receptor V (µL)**	**[Receptor] [mol/L]**	**[Guest] [mol/L]**	**[Guest]/ [Receptor]**	**F.I. ($I_{336\ nm}$)**	**ΔI_{obs}**	**ΔI_{calc}**
0	700	2.180E-05	0.000E+00	0.00	590.348	0.000	0.000
5	705	2.180E-05	1.043E-05	0.48	549.331	41.017	33.753
10	710	2.180E-05	2.071E-05	0.95	523.016	67.332	59.898
20	720	2.180E-05	4.085E-05	1.87	495.942	94.406	95.925
40	740	2.180E-05	7.948E-05	3.65	459.793	130.555	133.326
60	760	2.180E-05	1.161E-04	5.32	442.974	147.374	151.413
80	780	2.180E-05	1.508E-04	6.92	431.023	159.325	161.809
100	800	2.180E-05	1.838E-04	8.43	424.652	165.696	168.502
140	840	2.180E-05	2.451E-04	11.24	416.324	174.024	176.568
180	880	2.180E-05	3.008E-04	13.80	404.437	185.911	181.239
240	940	2.180E-05	3.754E-04	17.22	399.988	190.360	185.434

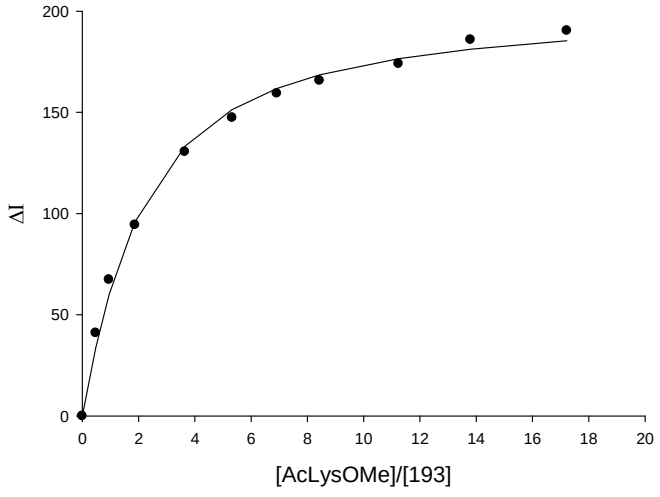

K_a [M^{-1}] = 29200 ± 10 %

K_d [µM] = 34 ± 10 %

ΔI_{max} = 203

Fluorescence titration of the tweezer 193 with Ac-Arg-OMe in phosphate buffer (10mM, pH 7.6)

λ_{exc} = 285 nm λ_{em} = 336 nm	Receptor **193**	Guest AcArgOMe · HCl
Amount [mg]:	0.133	0.375
Volume [mL]:	8.858	0.956
Concentration [mol/L]:	$2.18 \cdot 10^{-05}$	$1.471 \cdot 10^{-03}$

Guest V (µL)	**Receptor V (µL)**	**[Receptor] [mol/L]**	**[Guest] [mol/L]**	**[Guest]/ [Receptor]**	**F.I. ($I_{336\ nm}$)**	**ΔI_{obs}**	**ΔI_{calc}**
0	700	2.180E-05	0.000E+00	0.00	599.607	0.000	0.000
5	705	2.180E-05	1.043E-05	0.48	566.185	33.422	26.951
10	710	2.180E-05	2.072E-05	0.95	544.781	54.826	48.343
20	720	2.180E-05	4.086E-05	1.87	518.092	81.515	79.093
30	730	2.180E-05	6.044E-05	2.77	501.274	98.333	99.400
40	740	2.180E-05	7.950E-05	3.65	486.036	113.571	113.471
60	760	2.180E-05	1.161E-04	5.33	475.263	124.344	131.341
80	780	2.180E-05	1.509E-04	6.92	463.666	135.941	142.051
100	800	2.180E-05	1.838E-04	8.43	454.836	144.771	149.129
140	840	2.180E-05	2.451E-04	11.24	438.828	160.779	157.856
180	880	2.180E-05	3.008E-04	13.80	428.066	171.541	163.010

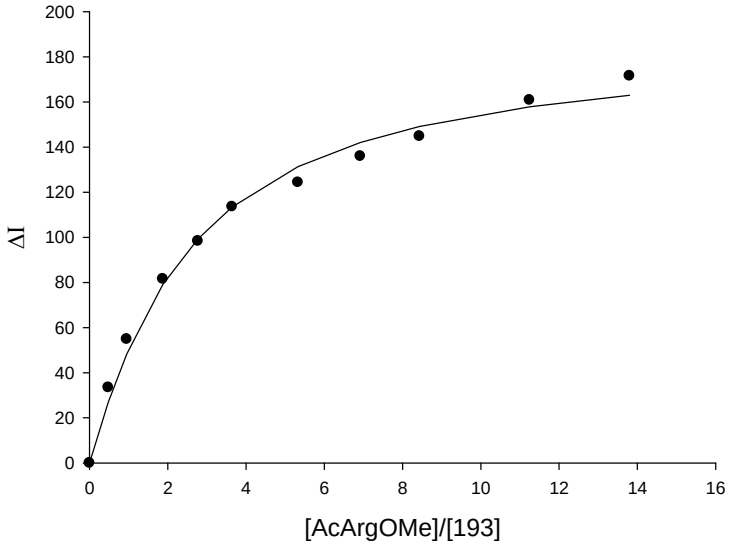

K_a [M^{-1}] = 22840 ± 13 %

K_d [µM] = 44 ± 13 %

ΔI_{max} = 188

Fluorescence titration of the tweezer 193 with KAA in phosphate buffer (10mM. pH 7.6)

λ_{exc} = 285 nm λ_{em} = 336 nm	Receptor **193**	Guest KAA
Amount [mg]:	0.143	0.232
Volume [mL]:	9.523	1.073
Concentration [mol/L]:	$2.18 \cdot 10^{-05}$	$7.50 \cdot 10^{-04}$

Guest V (µL)	Receptor V (µL)	[Receptor] [mol/L]	[Guest] [mol/L]	[Guest]/ [Receptor]	F.I. ($I_{334\ nm}$)	ΔI_{obs}	ΔI_{calc}
0	700	2.18E-05	0.00E+00	0.00	624.893	0.000	0.000
10	710	2.18E-05	1.06E-05	0.48	605.406	19.487	20.312
20	720	2.18E-05	2.08E-05	0.96	585.662	39.231	37.536
30	730	2.18E-05	3.08E-05	1.41	573.879	51.014	52.264
40	740	2.18E-05	4.05E-05	1.86	557.438	67.455	64.962
60	760	2.18E-05	5.92E-05	2.72	534.839	90.054	85.650
80	780	2.18E-05	7.69E-05	3.53	523.887	101.006	101.704
100	800	2.18E-05	9.37E-05	4.30	512.650	112.243	114.471
140	840	2.18E-05	1.25E-04	5.73	495.772	129.121	133.409
180	880	2.18E-05	1.53E-04	7.04	478.560	146.333	146.721
240	940	2.18E-05	1.91E-04	8.78	466.308	158.585	160.571
300	1000	2.18E-05	2.25E-04	10.32	450.371	174.522	170.093

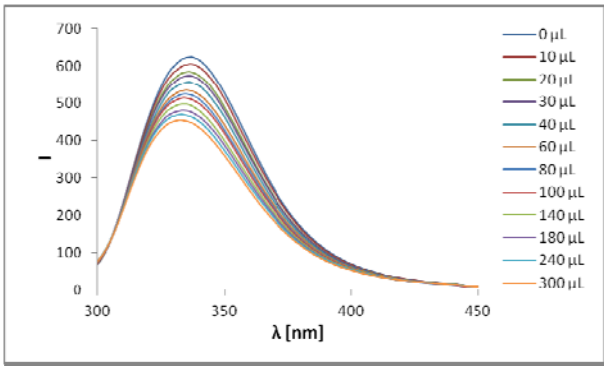

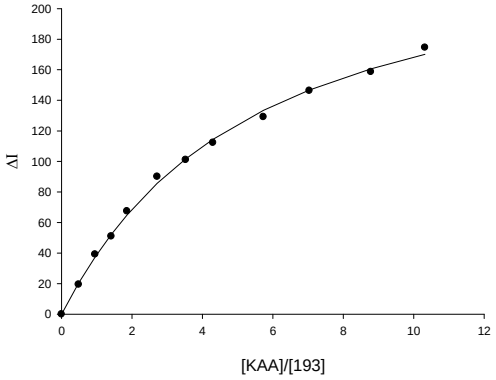

K_a [M^{-1}] = 10000 ± 7 %

K_d [µM] = 100 ± 7 %

Fluorescence titration of the tweezer 193 with KLVFF in phosphate buffer (10mM. pH 7.6)

λ_{exc} = 285 nm λ_{em} = 336 nm	Receptor **193**	Guest KLVFF
Amount [mg]:	0.143	0.328
Volume [mL]:	9.523	0.669
Concentration [mol/L]:	$2.18 \cdot 10^{-05}$	$7.51 \cdot 10^{-04}$

Guest V (µL)	Receptor V (µL)	[Receptor] [mol/L]	[Guest] [mol/L]	[Guest]/ [Receptor]	F.I. ($I_{334\ nm}$)	ΔI_{obs}	ΔI_{calc}
0	700	2.18E-05	0.00E+00	0.00	601.226	0.000	0.000
10	710	2.18E-05	1.06E-05	0.49	577.714	23.512	26.907
20	720	2.18E-05	2.09E-05	0.96	550.459	50.767	47.965
30	730	2.18E-05	3.09E-05	1.42	541.506	59.720	64.568
40	740	2.18E-05	4.06E-05	1.86	523.536	77.690	77.811
60	760	2.18E-05	5.93E-05	2.72	500.276	100.950	97.294
80	780	2.18E-05	7.70E-05	3.53	489.437	111.789	110.716
100	800	2.18E-05	9.39E-05	4.31	482.214	119.012	120.413
140	840	2.18E-05	1.25E-04	5.74	463.563	137.663	133.358
180	880	2.18E-05	1.54E-04	7.05	463.559	137.667	141.538
240	940	2.18E-05	1.92E-04	8.80	454.119	147.107	149.336
300	1000	2.18E-05	2.25E-04	10.33	445.093	156.133	154.318

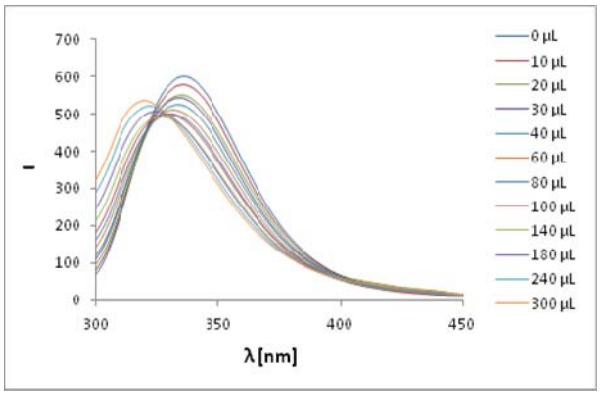

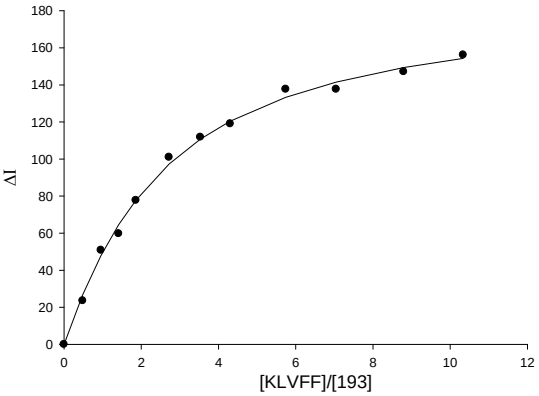

K_a [M^{-1}] = 22500 ± 8 %

K_d [µM] = 44 ± 8 %

Fluorescence titration of the tweezer 193 with $IAPP_{1-7}$ in phosphate buffer (10mM. pH 7.6)

λ_{exc} = 285 nm λ_{em} = 336 nm	Receptor **193**	Guest $IAPP_{1-7}$
Amount [mg]:	0.099	0.310
Volume [mL]:	6.593	0.560
Concentration [mol/L]:	$2.18 \cdot 10^{-05}$	$7.51 \cdot 10^{-04}$

Guest V (µL)	Receptor V (µL)	[Receptor] [mol/L]	[Guest] [mol/L]	[Guest]/ [Receptor]	F.I. ($I_{334\ nm}$)	ΔI_{obs}	ΔI_{calc}
0	700	2.18E-05	0.00E+00	0.00	633.538	0.000	0.000
10	710	2.18E-05	1.06E-05	0.49	592.929	40.609	33.451
20	720	2.18E-05	2.09E-05	0.96	569.126	64.412	59.450
30	730	2.18E-05	3.09E-05	1.42	552.716	80.822	79.789
40	740	2.18E-05	4.06E-05	1.86	535.244	98.294	95.887
60	760	2.18E-05	5.93E-05	2.72	517.558	115.980	119.329
80	780	2.18E-05	7.70E-05	3.53	496.209	137.329	135.292
100	800	2.18E-05	9.38E-05	4.30	492.579	140.959	146.722
140	840	2.18E-05	1.25E-04	5.74	476.164	157.374	161.842
180	880	2.18E-05	1.54E-04	7.04	469.739	163.799	171.312
240	940	2.18E-05	1.92E-04	8.79	453.468	180.070	180.279
300	1000	2.18E-05	2.25E-04	10.33	435.893	197.645	185.978

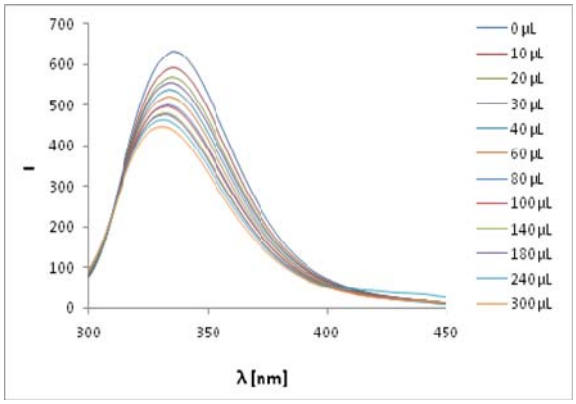

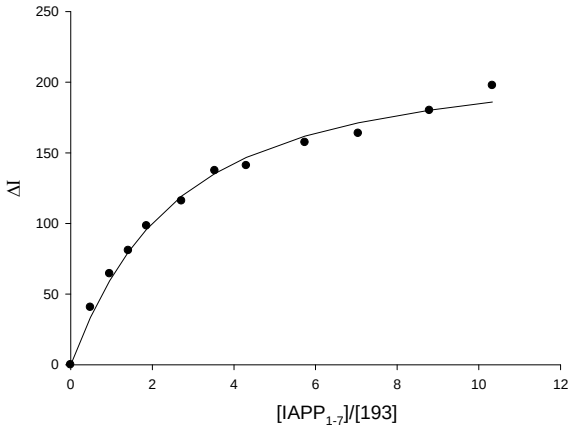

K_a [M^{-1}] = 24100 ± 12 %

K_d [µM] = 41 ± 12 %

Fluorescence titration of the tweezer 193 with $IAPP_{2-14}$ in phosphate buffer (10mM. pH 7.6)

λ_{exc} = 285 nm λ_{em} = 336 nm	Receptor **193**	Guest $IAPP_{2-14}$
Amount [mg]:	0.199	0.758
Volume [mL]:	13.252	0.741
Concentration [mol/L]:	$2.18 \cdot 10^{-05}$	$7.50 \cdot 10^{-04}$

Guest V (µL)	Receptor V (µL)	[Receptor] [mol/L]	[Guest] [mol/L]	[Guest]/ [Receptor]	F.I. ($I_{334\ nm}$)	ΔI_{obs}	ΔI_{calc}
0	700	2.18E-05	0.00E+00	0.00	452.757	0.000	0.000
10	710	2.18E-05	1.06E-05	0.48	437.479	15.278	16.095
20	720	2.18E-05	2.08E-05	0.96	425.005	27.752	29.491
30	730	2.18E-05	3.08E-05	1.41	406.789	45.968	40.742
40	740	2.18E-05	4.05E-05	1.86	394.084	58.673	50.280
60	760	2.18E-05	5.92E-05	2.72	384.079	68.678	65.480
80	780	2.18E-05	7.69E-05	3.53	380.939	71.818	76.970
100	800	2.18E-05	9.38E-05	4.30	370.615	82.142	85.912
140	840	2.18E-05	1.25E-04	5.73	357.585	95.172	98.849
180	880	2.18E-05	1.53E-04	7.04	352.933	99.824	107.709
240	940	2.18E-05	1.92E-04	8.79	333.641	119.116	116.724
300	1000	2.18E-05	2.25E-04	10.32	322.837	129.920	122.802

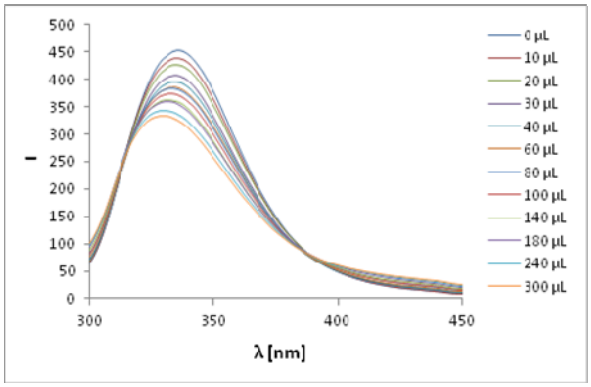

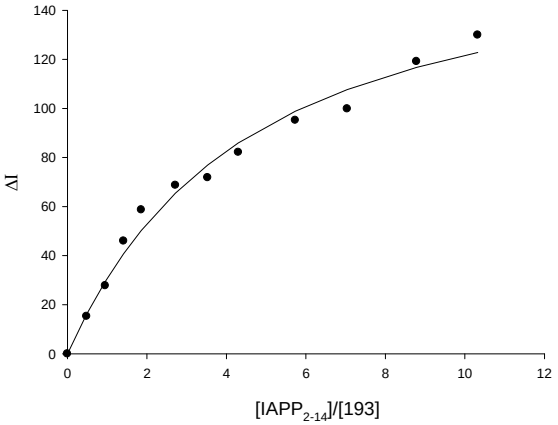

K_a [M^{-1}] = 12200 ± 17 %

K_d [µM] = 82 ± 17 %

5.4.3.2 Fluorescence titrations of the ethoxycarboxymethyl phosphate tweezer 196

Fluorescence titration of the tweezer 196 with AcLysOMe · HCl in phosphate buffer (10mM, pH 7.6)

λ_{exc} = 285 nm	Receptor **196**	Guest AcLysOMe · HCl
Amount [mg]:	0.170	0.190
Volume [mL]:	8.996	1.742
Concentration [mol/L]:	$2.579 \cdot 10^{-05}$	$4.57 \cdot 10^{-04}$

Guest V (µL)	**Receptor V (µL)**	**[Receptor] [mol/L]**	**[Guest] [mol/L]**	**[Guest]/ [Receptor]**	**F.I. (I_{343})**	**ΔI_{obs}**	**ΔI_{calc}**
0	700	2.579E-05	0.000E+00	0.00	591.106	0.000	0.000
10	710	2.579E-05	6.437E-06	0.25	570.014	21.092	24.011
20	720	2.579E-05	1.269E-05	0.49	546.695	44.411	44.747
30	730	2.579E-05	1.878E-05	0.73	529.350	61.756	62.678
40	740	2.579E-05	2.470E-05	0.96	515.369	75.737	78.225
50	750	2.579E-05	3.047E-05	1.18	496.607	94.499	91.753
60	760	2.579E-05	3.608E-05	1.40	484.978	106.128	103.574
70	770	2.579E-05	4.155E-05	1.61	477.336	113.770	113.953
80	780	2.579E-05	4.687E-05	1.82	466.028	125.078	123.109
100	800	2.579E-05	5.713E-05	2.22	454.219	136.887	138.455
140	840	2.579E-05	7.617E-05	2.95	430.803	160.303	160.746
180	880	2.579E-05	9.348E-05	3.62	417.400	173.706	175.973
240	940	2.579E-05	1.167E-04	4.52	399.394	191.712	191.344
300	1000	2.579E-05	1.371E-04	5.32	388.433	202.673	201.601

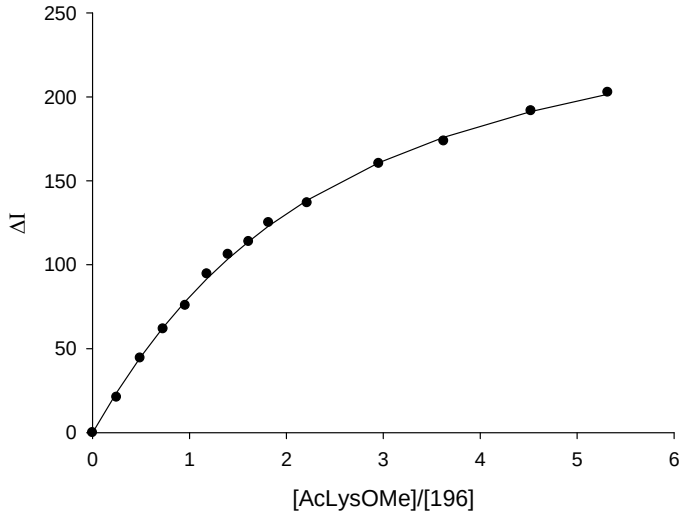

K_a [M^{-1}] = 22600 ± 4 %

K_d [µM] = 44 ± 4 %

ΔI_{max} = 277

Fluorescence titration of the tweezer 196 with AcArgOMe · HCl in phosphate buffer (10mM, pH 7.6)

λ_{exc} = 284 nm	Receptor **196**	Guest AcArgOMe · HCl
Amount [mg]:	0.170	0.145
Volume [mL]:	8.996	1.189
Concentration [mol/L]:	$2.579 \cdot 10^{-05}$	$4.57 \cdot 10^{-04}$

Guest V (µL)	**Receptor V (µL)**	**[Receptor] [mol/L]**	**[Guest] [mol/L]**	**[Guest]/ [Receptor]**	**F.I. (I_{343})**	**ΔI_{obs}**	**ΔI_{calc}**
0	700	2.579E-05	0.000E+00	0.00	561.433	0.000	0.000
10	710	2.579E-05	6.440E-06	0.25	549.806	11.627	11.898
20	720	2.579E-05	1.270E-05	0.49	536.256	25.177	22.538
30	730	2.579E-05	1.879E-05	0.73	529.390	32.043	32.087
40	740	2.579E-05	2.472E-05	0.96	518.275	43.158	40.689
50	750	2.579E-05	3.048E-05	1.18	512.216	49.217	48.466
60	760	2.579E-05	3.610E-05	1.40	506.225	55.208	55.521
80	780	2.579E-05	4.690E-05	1.82	495.273	66.160	67.806
100	800	2.579E-05	5.716E-05	2.22	484.497	76.936	78.114
140	840	2.579E-05	7.621E-05	2.96	469.835	91.598	94.370
180	880	2.579E-05	9.353E-05	3.63	453.226	108.207	106.548
240	940	2.579E-05	1.167E-04	4.53	440.114	121.319	119.927
300	1000	2.579E-05	1.372E-04	5.32	432.272	129.161	129.569

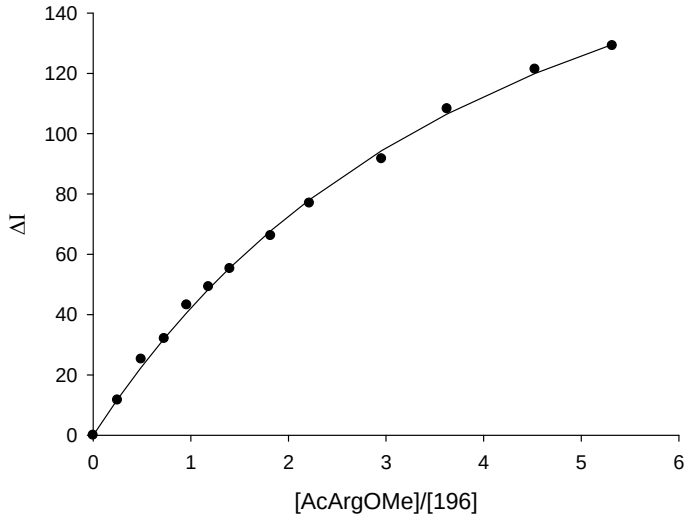

K_a [M^{-1}] = 10900 ± 7 %

K_d [µM] = 92 ± 7 %

ΔI_{max} = 227

Fluorescence titration of the tweezer 196 with KLVFF in phosphate buffer (10mM. pH 7.6)

λ_{exc} = 285 nm λ_{em} = 343 nm	Receptor **196**	Guest KLVFF
Amount [mg]:	0.153	0.330
Volume [mL]:	9.578	0.674
Concentration [mol/L]:	$2.18 \cdot 10^{-05}$	$7.50 \cdot 10^{-04}$

Guest V (µL)	Receptor V (µL)	[Receptor] [mol/L]	[Guest] [mol/L]	[Guest]/ [Receptor]	F.I. ($I_{334\ nm}$)	ΔI_{obs}	ΔI_{calc}
0	700	2.18E-05	0.00E+00	0.00	635.542	0.000	0.000
10	710	2.18E-05	1.06E-05	0.48	615.693	19.849	13.354
20	720	2.18E-05	2.08E-05	0.96	608.846	26.696	24.810
30	730	2.18E-05	3.08E-05	1.41	604.937	30.605	34.713
40	740	2.18E-05	4.05E-05	1.86	589.550	45.992	43.339
60	760	2.18E-05	5.92E-05	2.72	575.477	60.065	57.583
80	780	2.18E-05	7.69E-05	3.53	565.820	69.722	68.815
100	800	2.18E-05	9.37E-05	4.30	564.477	71.065	77.868
140	840	2.18E-05	1.25E-04	5.73	543.174	92.368	91.507
180	880	2.18E-05	1.53E-04	7.04	533.346	102.196	101.257
240	940	2.18E-05	1.91E-04	8.78	527.565	107.977	111.549
300	1000	2.18E-05	2.25E-04	10.32	513.093	122.449	118.717

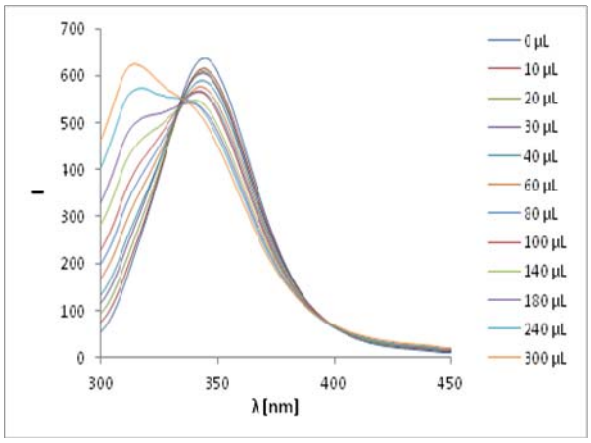

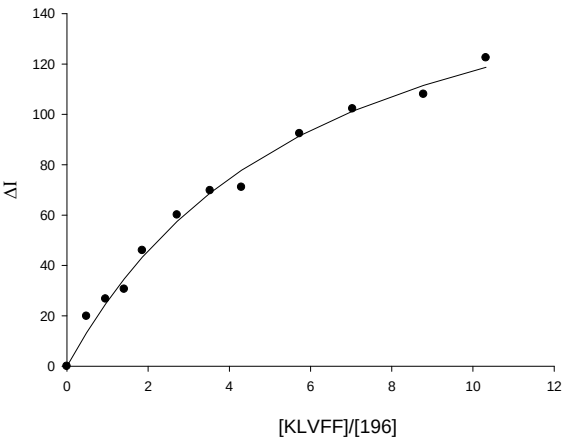

K_a [M^{-1}] = 8790 ± 14 %

K_d [µM] = 114 ± 14 %

Fluorescence titration of the tweezer 196 with $IAPP_{1-7}$ in phosphate buffer (10mM. pH 7.6)

λ_{exc} = 285 nm λ_{em} = 343 nm	Receptor **196**	Guest $IAPP_{1-7}$
Amount [mg]:	0.153	0.393
Volume [mL]:	9.578	0.710
Concentration [mol/L]:	$2.18 \cdot 10^{-05}$	$7.51 \cdot 10^{-04}$

Guest V (µL)	Receptor V (µL)	[Receptor] [mol/L]	[Guest] [mol/L]	[Guest]/ [Receptor]	F.I. ($I_{334\ nm}$)	ΔI_{obs}	ΔI_{calc}
0	700	2.18E-05	0.00E+00	0.00	636.672	0.000	0.000
10	710	2.18E-05	1.06E-05	0.49	608.513	28.159	24.008
20	720	2.18E-05	2.09E-05	0.96	596.917	39.755	44.672
30	730	2.18E-05	3.09E-05	1.42	573.907	62.765	62.593
40	740	2.18E-05	4.06E-05	1.86	561.312	75.360	78.247
60	760	2.18E-05	5.93E-05	2.72	526.643	110.029	104.200
80	780	2.18E-05	7.70E-05	3.53	512.296	124.376	124.760
100	800	2.18E-05	9.38E-05	4.30	494.406	142.266	141.397
140	840	2.18E-05	1.25E-04	5.74	472.700	163.972	166.580
180	880	2.18E-05	1.54E-04	7.04	451.611	185.061	184.670
240	940	2.18E-05	1.92E-04	8.79	434.884	201.788	203.851
300	1000	2.18E-05	2.25E-04	10.33	417.406	219.266	217.262

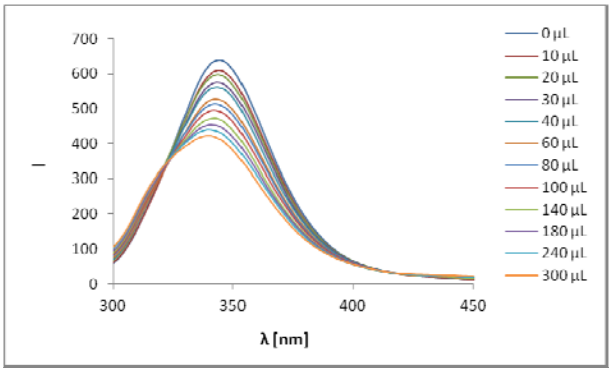

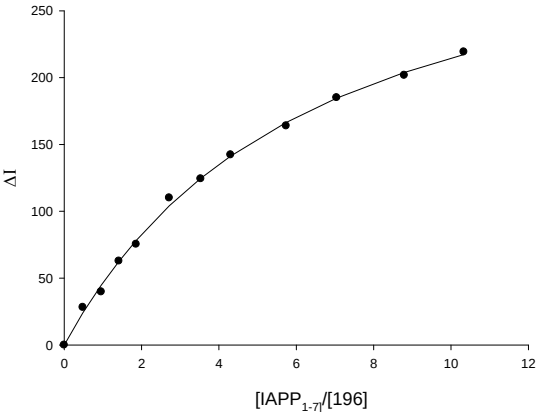

K_a [M^{-1}] = 8440 ± 6 %

K_d [µM] = 118 ± 6 %

Fluorescence titration of the tweezer 196 with $IAPP_{2-14}$ in phosphate buffer (10mM. pH 7.6)

λ_{exc} = 285 nm λ_{em} = 343 nm	Receptor **196**	Guest $IAPP_{2-14}$
Amount [mg]:	0.134	0.713
Volume [mL]:	3.388	0.697
Concentration [mol/L]:	$2.18 \cdot 10^{-05}$	$7.50 \cdot 10^{-04}$

Guest V (µL)	Receptor V (µL)	[Receptor] [mol/L]	[Guest] [mol/L]	[Guest]/ [Receptor]	F.I. ($I_{334\ nm}$)	ΔI_{obs}	ΔI_{calc}
0	700	2,18E-05	0,00E+00	0,00	574,307	0,000	0,000
10	710	2,18E-05	1,06E-05	0,48	531,805	42,502	19,721
20	720	2,18E-05	2,08E-05	0,96	513,578	60,729	36,388
30	730	2,18E-05	3,08E-05	1,41	514,928	59,379	50,594
40	740	2,18E-05	4,06E-05	1,86	504,512	69,795	62,805
60	760	2,18E-05	5,92E-05	2,72	499,696	74,611	82,622
80	780	2,18E-05	7,69E-05	3,53	488,894	85,413	97,929
100	800	2,18E-05	9,38E-05	4,30	473,532	100,775	110,054
140	840	2,18E-05	1,25E-04	5,73	459,571	114,736	127,959
180	880	2,18E-05	1,53E-04	7,04	433,034	141,273	140,486
240	940	2,18E-05	1,92E-04	8,79	422,963	151,344	153,465
300	1000	2,18E-05	2,25E-04	10,32	395,952	178,355	162,356

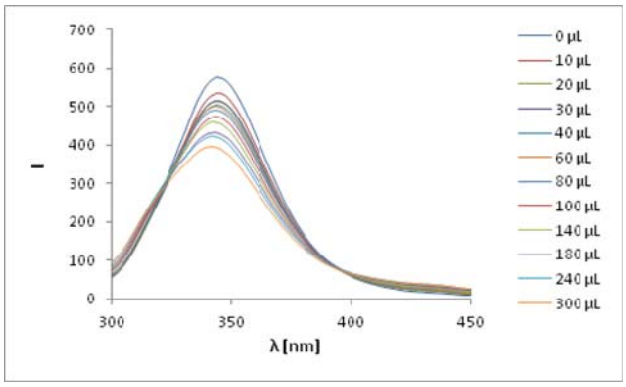

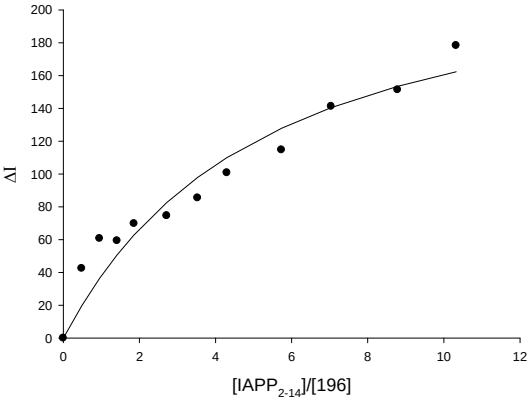

K_a [M^{-1}] = 10400 ± 36 %

K_d [µM] = 96 ± 36 %

5.4.3.3 Fluorescence titration of the glycerol phosphate tweezer 198

Fluorescence titration of the tweezer 198 with Ac-Lys-OMe · HCl in phosphate buffer (10mM, pH 7.6)

λ_{exc} = 285 nm	Receptor **198**	Guest Ac-Lys-OMe · HCl
Amount [mg]:	0.092	0.80
Volume [mL]:	4.628	0.733
Concentration [mol/L]:	$2.579 \cdot 10^{-05}$	$4.572 \cdot 10^{-04}$

Guest V (µL)	**Receptor V (µL)**	**[Receptor] [mol/L]**	**[Guest] [mol/L]**	**[Guest]/ [Receptor]**	**F.I. (I_{341})**	**ΔI_{obs}**	**ΔI_{calc}**
0	700	2.579E-05	0.000E+00	0.00	629.793	0.000	0.000
10	710	2.579E-05	6.440E-06	0.25	626.381	3.412	6.137
20	720	2.579E-05	1.270E-05	0.49	615.687	14.106	11.926
30	730	2.579E-05	1.879E-05	0.73	610.584	19.209	17.396
40	740	2.579E-05	2.472E-05	0.96	603.899	25.894	22.571
50	750	2.579E-05	3.048E-05	1.18	603.652	26.141	27.475
60	760	2.579E-05	3.610E-05	1.40	595.550	34.243	32.128
80	780	2.579E-05	4.690E-05	1.82	588.319	41.474	40.753
100	800	2.579E-05	5.715E-05	2.22	585.336	44.457	48.574
140	840	2.579E-05	7.620E-05	2.95	569.057	60.736	62.215
180	880	2.579E-05	9.352E-05	3.63	554.742	75.051	73.705
240	940	2.579E-05	1.167E-04	4.53	543.420	86.373	87.897
300	1000	2.579E-05	1.372E-04	5.32	528.916	100.877	99.365

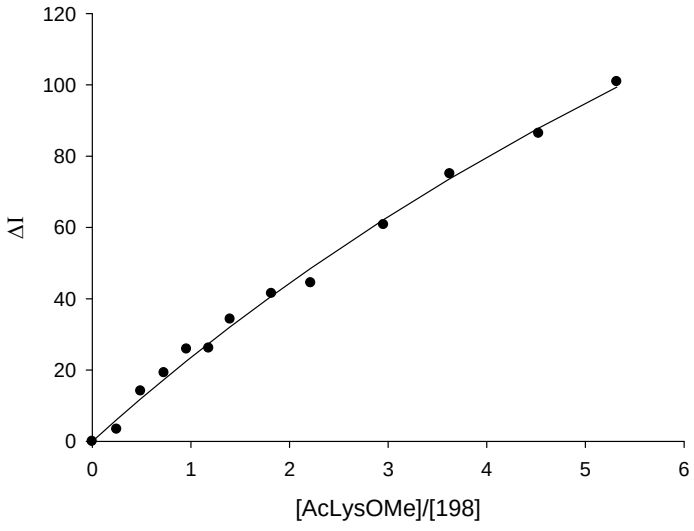

K_a [M^{-1}] = 2760 ± 23 %

K_d [µM] = 362 ± 23 %

ΔI_{max} = 375

Fluorescence titration of the tweezer 198 with Ac-Arg-OMe · HCl in phosphate buffer (10mM, pH 7.6)

λ_{exc} = 285 nm	Receptor **198**	Guest Ac-Arg-OMe · HCl
Amount [mg]:	0.092	0.70
Volume [mL]:	4.628	0.574
Concentration [mol/L]:	$2.579 \cdot 10^{-05}$	$4.573 \cdot 10^{-04}$

Guest V (µL)	**Receptor V (µL)**	**[Receptor] [mol/L]**	**[Guest] [mol/L]**	**[Guest]/ [Receptor]**	**F.I. (I_{341})**	**ΔI_{obs}**	**ΔI_{calc}**
0	700	2.579E-05	0.000E+00	0.00	571.170	0.000	0.000
10	710	2.579E-05	6.440E-06	0.25	567.731	3.439	4.317
20	720	2.579E-05	1.270E-05	0.49	560.881	10.289	8.436
30	730	2.579E-05	1.879E-05	0.73	554.084	17.086	12.370
40	740	2.579E-05	2.472E-05	0.96	555.087	16.083	16.132
50	750	2.579E-05	3.048E-05	1.18	550.623	20.547	19.732
60	760	2.579E-05	3.610E-05	1.40	545.689	25.481	23.181
80	780	2.579E-05	4.690E-05	1.82	545.687	25.483	29.661
100	800	2.579E-05	5.716E-05	2.22	537.385	33.785	35.638
140	840	2.579E-05	7.621E-05	2.95	525.274	45.896	46.299
180	880	2.579E-05	9.353E-05	3.63	514.754	56.416	55.525
240	940	2.579E-05	1.167E-04	4.53	504.183	66.987	67.248
300	1000	2.579E-05	1.372E-04	5.32	493.678	77.492	76.999

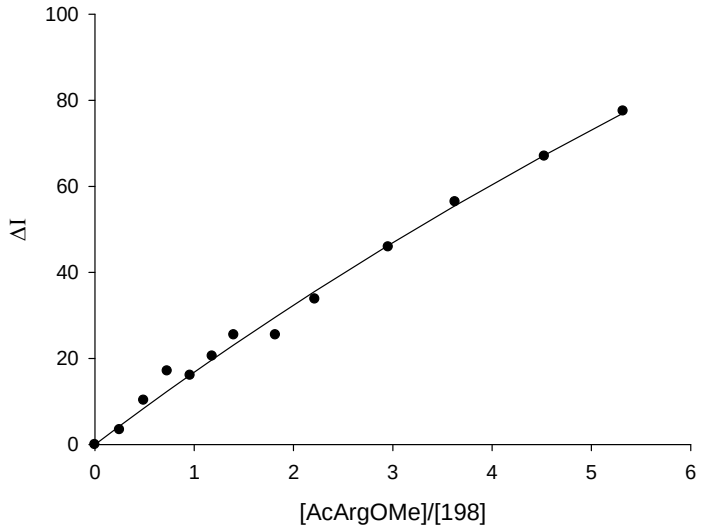

K_a [M^-] = 1620 ± 42 %

K_d [µM] = 617 ± 42 %

ΔI_{max} = 437

5.5 Isothermal titration calorimetry (ITC) studies of the tweezers 133 and 161 complexes

5.5.1 ITC experiments of the phosphate tweezer 133 complexes

ITC titration of the tweezer **133** (0.1 mM) with AcLysOMe (1.0 mM) in phosphate buffer (10 mM, pH 7.6)

Nr.	K_a [M^{-1}]	n	ΔH[kcal/mol]	-TΔS[kcal/mol]	ΔG[kcal/mol]
1	69300 ± 3700	0.679 ± 0.009	-5.552 ± 0.101	-1.05	-6.60
2	67900 ± 3200	0.648 ± 0.008	-5.609 ± 0.095	-0.99	-6.60

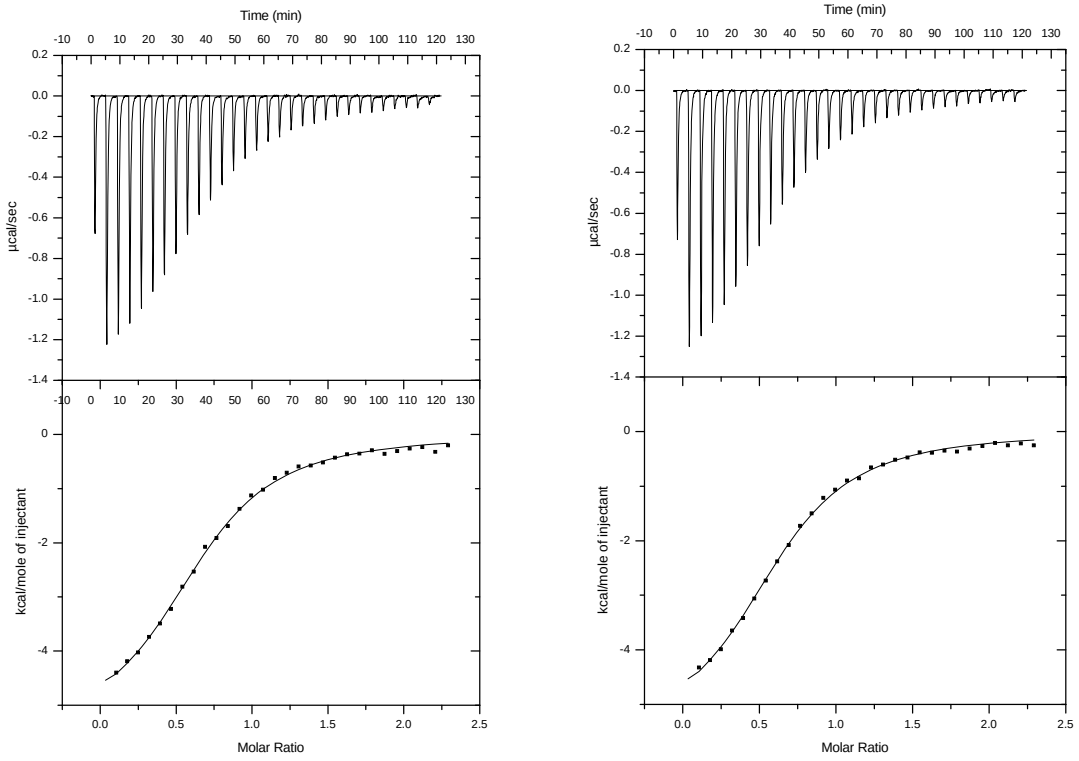

ITC titration of the tweezer **133** (0.1 mM) with AcArgOMe (1.0 mM) in phosphate buffer (10 mM, pH 7.6)

Nr.	K_a [M^{-1}]	n	ΔH[kcal/mol]	-TΔS[kcal/mol]	ΔG[kcal/mol]
1	31700 ± 1100	0.625 ± 0.010	-6.805 ± 0.145	0.67	-6.14
2	27500 ± 1700	0.613 ± 0.020	-7.249 ± 0.305	1.19	-6.06

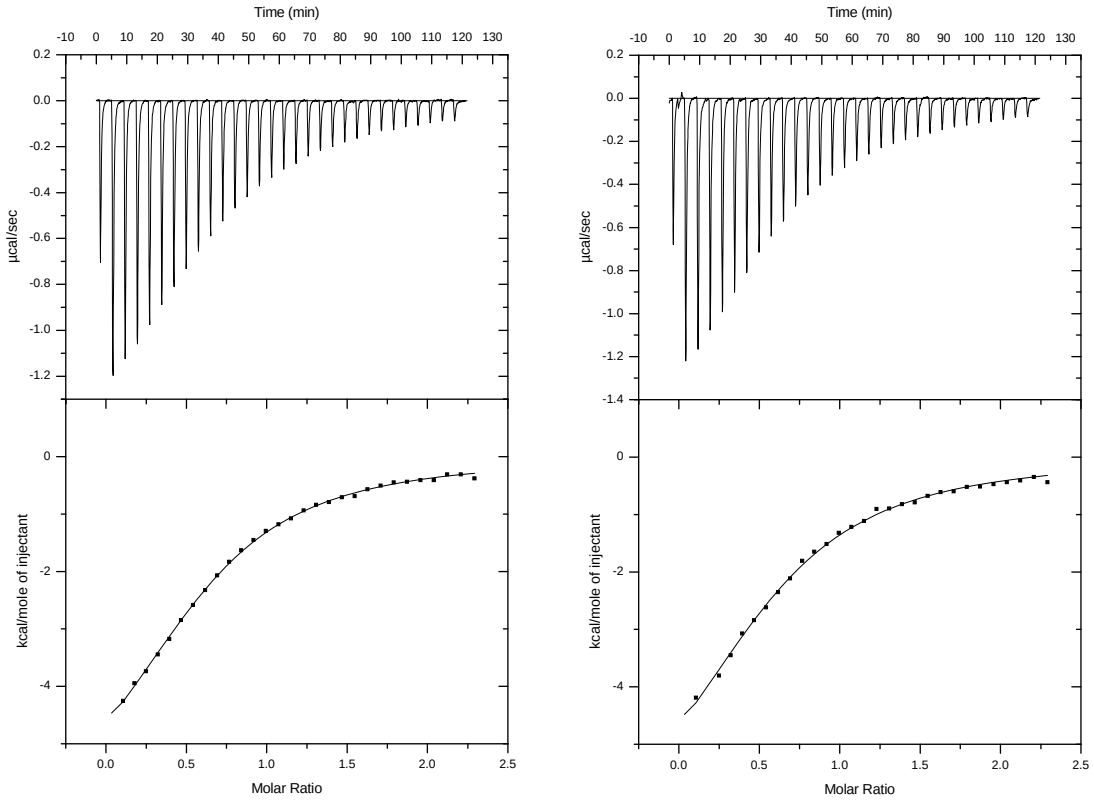

ITC titration of the tweezer **133** (0.1 mM) with KLVFF (0.65 mM) in phosphate buffer (10 mM, pH 7.6)

Nr.	K_a [M^{-1}]	n	ΔH[kcal/mol]	-TΔS[kcal/mol]	ΔG[kcal/mol]
1	65800 ± 2600	1.02 ± 0.005	-6.293 ± 0.055	-0.28	-6.57
2	65300 ± 3300	0.983 ± 0.007	-6.466 ± 0.084	-0.10	-6.57

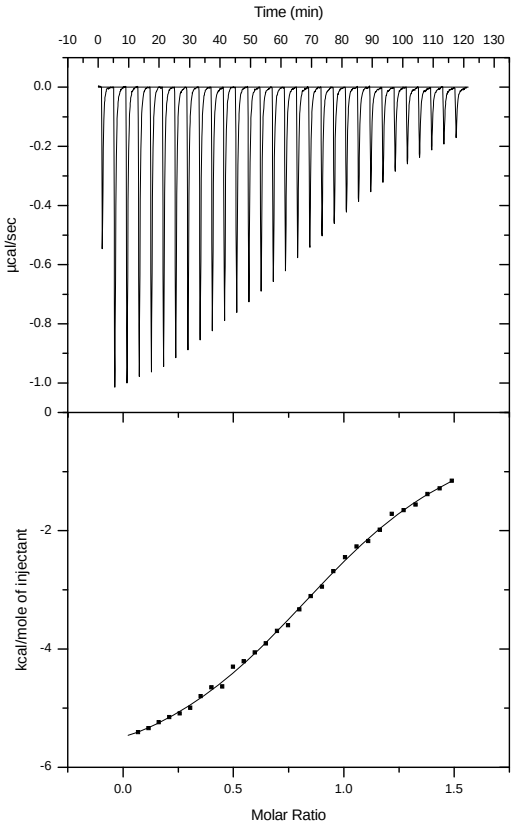

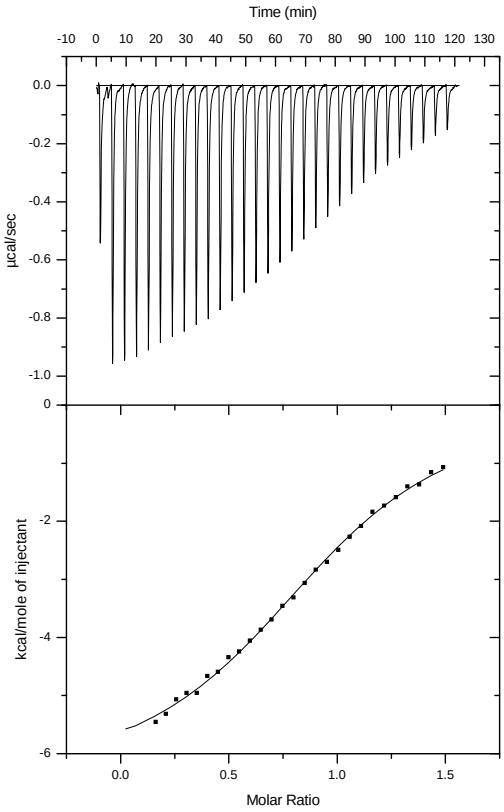

ITC titration of the tweezer **133** (0.1 mM) with $IAPP_{1-7}$ (0.65 mM) in phosphate buffer (10 mM, pH 7.6)

Nr.	K_a [M^{-1}]	n	ΔH[kcal/mol]	-TΔS[kcal/mol]	ΔG[kcal/mol]
1	168000 ± 5300	1.21 ± 0.003	-6.442 ± 0.024	-0.69	-7.13
2	151000 ± 5300	1.16 ± 0.004	-6.366 ± 0.03	-0.70	-7.07

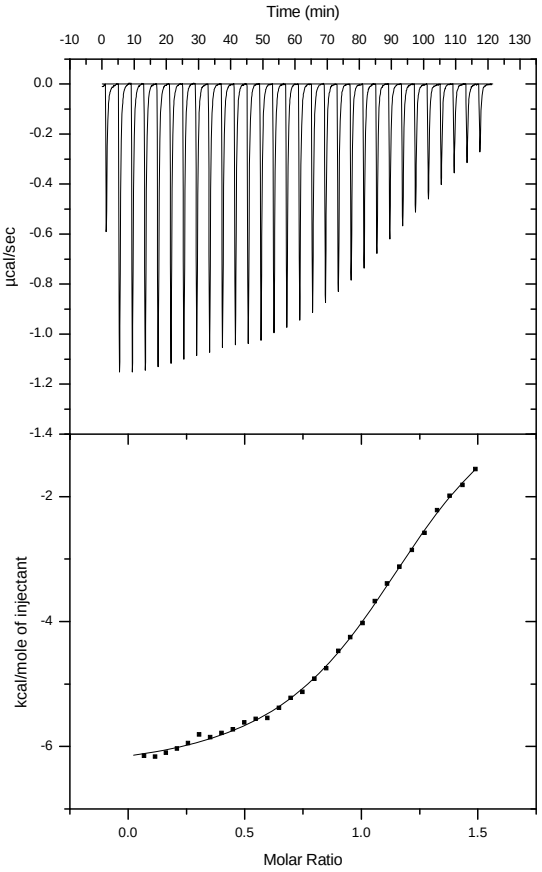

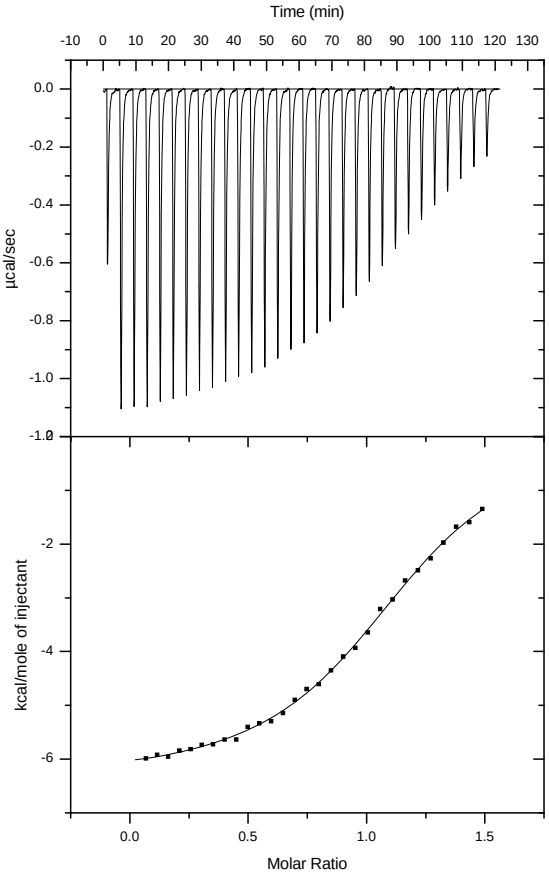

ITC titration of the tweezer **133** (0.1 mM) with $IAPP_{2-14}$ (0.65 mM) in phosphate buffer (10 mM, pH 7.6)

Nr.	K_a [M^{-1}]	n	ΔH[kcal/mol]	-TΔS[kcal/mol]	ΔG[kcal/mol]
1	6360 ± 1630	1.00 ± 0.18	-5.378 ± 1.63	0.19	-5.19
2	6980 ± 2600	1.42 ± 0.11	-4.756 ± 1.08	-0.49	-5.25

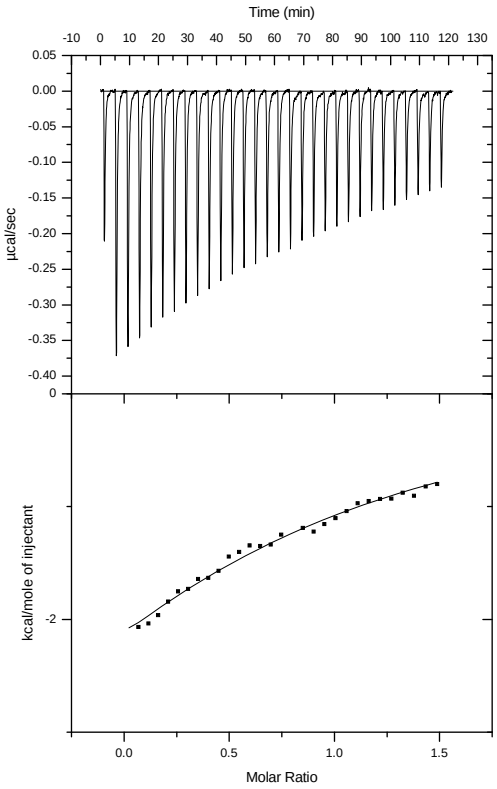

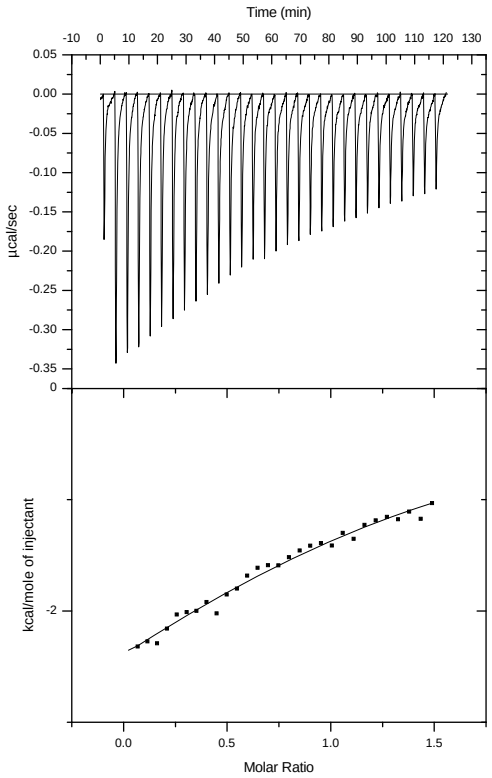

ITC titration of the tweezer **133** (0.1 mM) with AcLysOMe (1.0 mM) in methanol

Nr.	K_a [M^{-1}]	n	ΔH[kcal/mol]	-TΔS[kcal/mol]	ΔG[kcal/mol]
1	7510 ± 900	1.49 ± 0.064	7.985 ± 0.643	-13.28	-5.30
2	5820 ± 1000	1.25 ± 0.13	10.150 ± 1.64	-15.31	-5.16

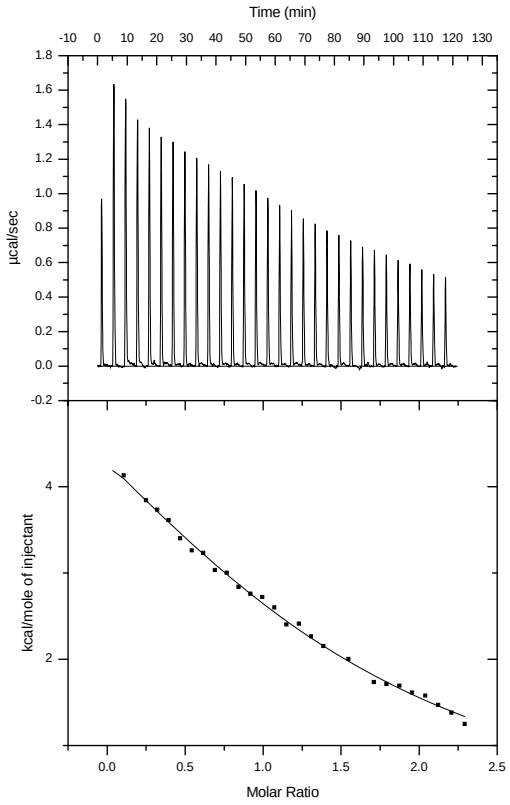

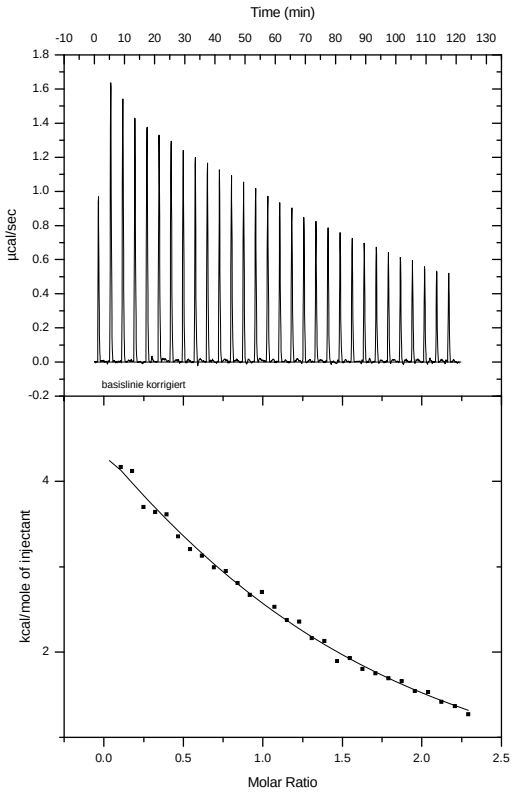

5.5.2 ITC experiments of the sulfate tweezer 161 complexes

ITC titration of the tweezer **161** (0.1 mM) with AcLysOMe (1.0 mM) in phosphate buffer (10 mM, pH 7.6)

Nr.	K_a [M^{-1}]	n	ΔH[kcal/mol]	-TΔS[kcal/mol]	ΔG[kcal/mol]
1	36200 ± 1600	0.823 ± 0.011	-8.171 ± 0.159	1.96	-6.21
2	33000 ± 1800	0.782 ± 0.015	-8.403 ± 0.226	2.24	-6.16

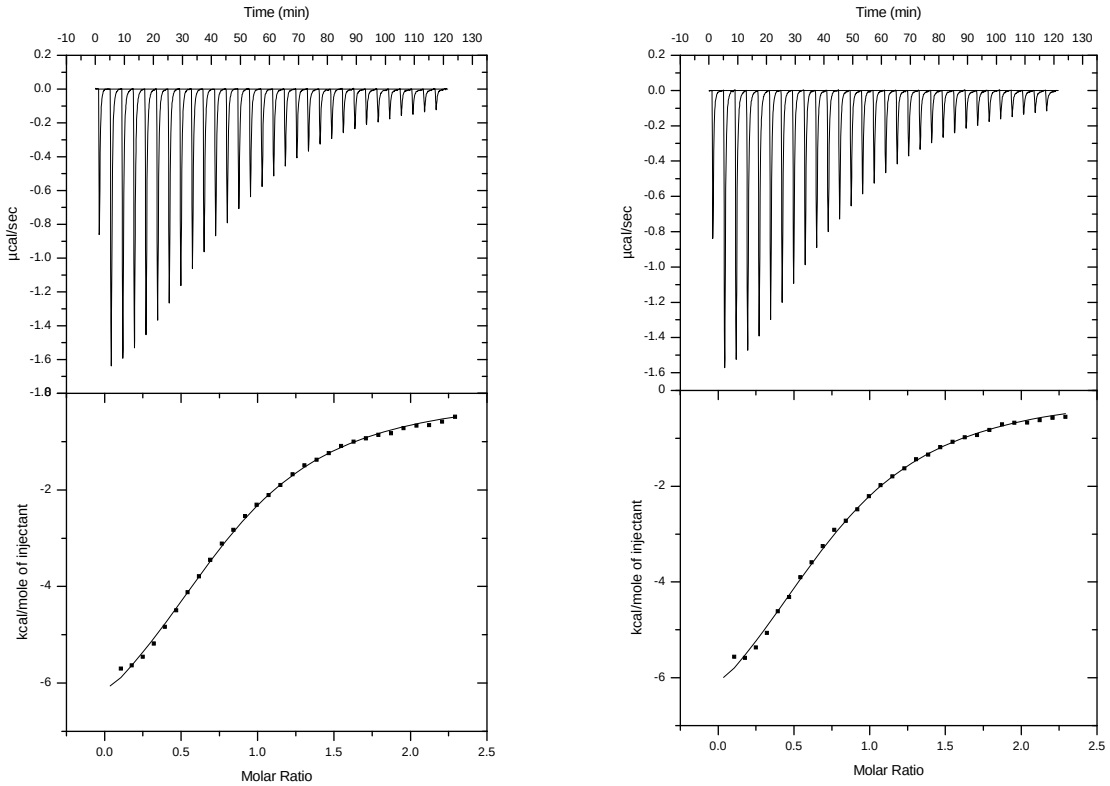

The ITC titration of the tweezer **161** (0.1 mM) with AcArgOMe (1.0 mM) in phosphate buffer (10 mM, pH 7.6)

Nr.	K_a [M^{-1}]	n	ΔH[kcal/mol]	-TΔS[kcal/mol]	ΔG[kcal/mol]
1.	11300 ± 1000	0.904 ± 0.048	-5.92 ± 0.045	0.387	-5.53
2.	9490 ± 1100	0.816 ± 0.071	-6.75 ± 0.796	1.317	-5.43

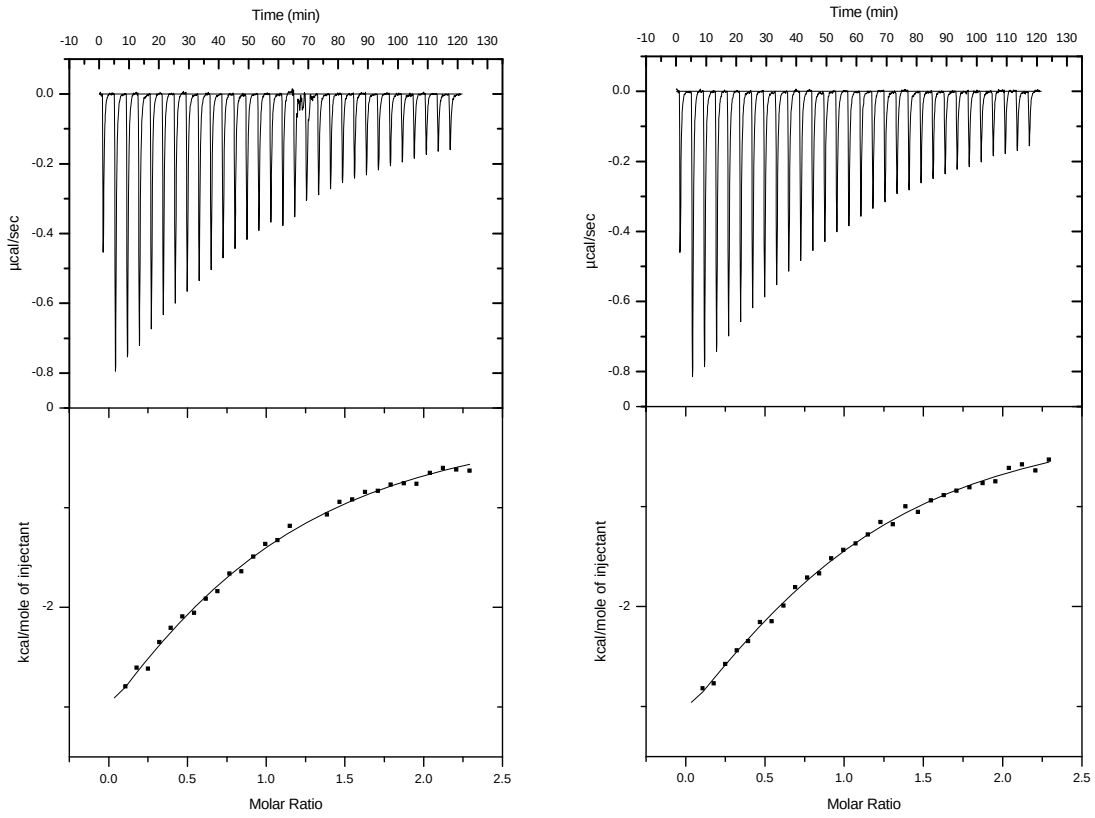

5.6 Crystal structure

5.6.1 Crystal structure of dimethoxy phosphate octyl tweezer 182

The crystals of the tweezer **182** were obtained by dissolving 10 mg of the tweezer **182** in 3 ml methanol/n-pentane mixture (5:1) and allowing the solution to stand at room temperature for 3-5 days. The crystal structure was solved on an X-ray diffractometer by Dr. Christöph Wolper at University of Duisburg-Essen.

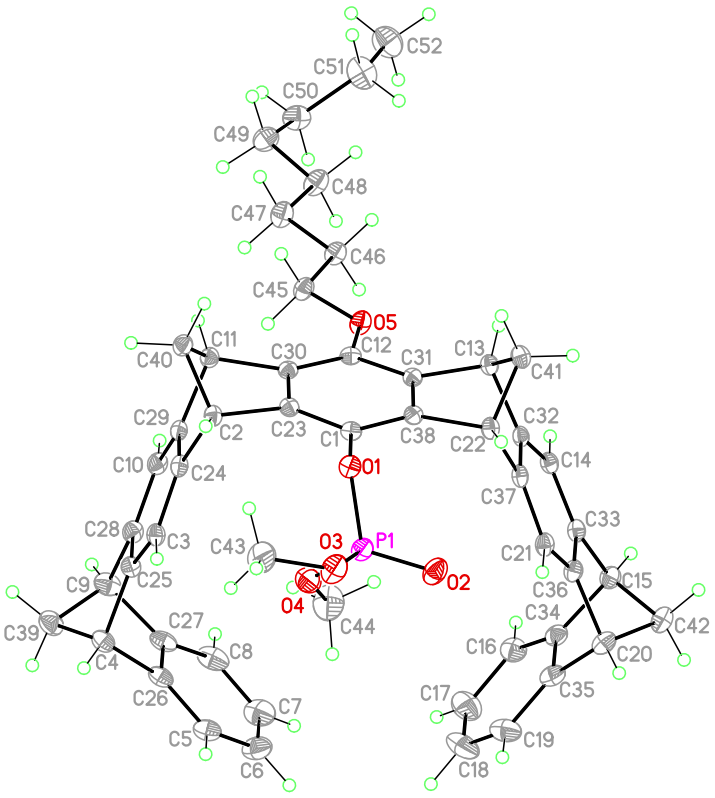

5.6.1.1 Crystal data and structure refinement for the tweezer 182

Identification code	sd_182p1
Empirical formula	$C_{52}\ H_{51}\ O_5\ P * C\ H_4\ O$
Formula weight	818.94 Da
Density (calculated)	1.261 g cm^{-3}
F(000)	1744
Temperature	100(1) K

Crystal size	0.32 x 0.12 x 0.07 mm	
Crystal color	colourless	
Crystal description	needle	
Wavelength	0.71073 Å	
Crystal system	monoclinic	
Space group	$P2_1/c$	
Unit cell dimensions	a = 14.804(3) Å	α = 90°
	b = 18.391(3) Å	β = 103.622(8)°
	c = 16.298(3) Å	γ = 90°
Volume	4312.7(12) Å^3	
Z	4	
Cell measurement reflections used	9887	
Cell measurement theta min/max	2.39° to 27.08°	
Diffractometer control software	Bruker AXS APEX 2 Vers.3.0/2009	
Diffractometer measurement device	Bruker D8 KAPPA series II with APEX II area detector system	
Diffractometer measurement method	Data collection strategy APEX 2/COSMO	
Theta range for data collection	1.80° to 27.11°	
Completeness to theta = 27.11°	99.3 %	
Index ranges	-18<=h<=18, -23<=k<=23, -19<=l<=20	
Computing data reduction	Bruker AXS APEX 2 Vers.3/2009	
Absorption coefficient	0.116 mm^{-1}	
Absorption correction	Semi-empirical from equivalents	
Empirical absorption correction	Bruker AXS APEX 2 Vers.3/2009	
Max. / min. transmission	0.75 / 0.66	
R(merg) before/after correction	0.0777 / 0.0394	
Computing structure solution	Bruker AXS SHELXTL Vers. 2008/4/(c) 2008	
Computing structure refinement	Bruker AXS SHELXTL Vers. 2008/4/(c) 2008	
Refinement method	Full-matrix least-squares on F^2	
Reflections collected	78132	
Independent reflections	9461 [R(int) = 0.0375]	
Data / restraints / parameters	7636 / 0 / 549	
Goodness-of-fit on F^2	1.033	

Weighting details	$w = 1/[\square^2 (Fo^2)+ (0.0597*P)^2+2.6078*P]$ where $P = (Fo^2+2Fc^2)/3$
Final *R* indices [*I*>2sigma(*I*)]	*R*1 = 0.0414, *wR*2 = 0.1067
R indices (all data)	*R*1 = 0.0573, *wR*2 = 0.1187
Largest diff. peak and hole	0.358 and -0.418 eÅ^{-3}
Treatment of hydrogen atoms	Riding model on idealized geometries with the 1.2 fold isotropic displacement parameters of the equivalent Uij of the corresponding carbon atom. The methyl groups are idealized with tetrahedral angles in a combined rotating and rigid group refinement with the 1.5 fold isotropic displacement parameters of the equivalent Uij of the corresponding carbon atom. Hydrogen atom position H(60) taken from a Fourier-map and also refined as riding group with the 1.5 fold isotropic displacement parameters of the equivalent Uij of the corresponding oxygen atom.
Disorder	Octoxy carbon atoms C(50, 51) disordered over two sites with SOF 0.9 and 0.1 together with the riding hydrogen atoms Methyl hydrogen atoms H(52A to H52C) disordered over two sites with SOF 0.9 and 0.1

Table 5.1 Atomic coordinates (x 10^4) and equivalent isotropic displacement parameters (Å^2 x 10^3) for sd_182p1. U(eq) is defined as one third of the trace of the orthogonalized Uij tensor.

	x	y	z	U(eq)
P(1)	1802(1)	6862(1)	4694(1)	18(1)
O(1)	706(1)	6958(1)	4567(1)	15(1)

O(2)	2165(1)	6154(1)	5026(1)	25(1)
O(3)	1932(1)	7008(1)	3791(1)	27(1)
O(4)	2239(1)	7531(1)	5241(1)	25(1)
O(5)	-809(1)	7302(1)	7396(1)	18(1)
C(1)	334(1)	7061(1)	5281(1)	13(1)
C(2)	26(1)	8464(1)	4988(1)	14(1)
C(3)	1609(1)	9185(1)	5565(1)	15(1)
C(4)	3070(1)	9914(1)	6481(1)	18(1)
C(5)	4363(1)	8951(1)	7181(1)	22(1)
C(6)	4711(1)	8555(1)	7923(1)	28(1)
C(7)	4338(1)	8639(1)	8622(1)	30(1)
C(8)	3608(1)	9122(1)	8612(1)	26(1)
C(9)	2474(1)	10057(1)	7640(1)	21(1)
C(10)	862(1)	9403(1)	7016(1)	16(1)
C(11)	-593(1)	8684(1)	6116(1)	15(1)
C(12)	-474(1)	7290(1)	6679(1)	13(1)
C(13)	-258(1)	5862(1)	6885(1)	13(1)
C(14)	1191(1)	5454(1)	8104(1)	14(1)
C(15)	2821(1)	4988(1)	9036(1)	17(1)
C(16)	3792(1)	6141(1)	9736(1)	22(1)
C(17)	4482(1)	6630(1)	9644(1)	32(1)
C(18)	4916(1)	6562(1)	8980(1)	35(1)
C(19)	4668(1)	6007(1)	8382(1)	29(1)
C(20)	3534(1)	4880(1)	7944(1)	20(1)
C(21)	2080(1)	5282(1)	6730(1)	16(1)
C(22)	432(1)	5677(1)	5788(1)	14(1)
C(23)	10(1)	7737(1)	5443(1)	13(1)
C(24)	732(1)	8932(1)	5597(1)	14(1)
C(25)	2095(1)	9572(1)	6264(1)	16(1)
C(26)	3644(1)	9431(1)	7171(1)	18(1)
C(27)	3273(1)	9517(1)	7884(1)	20(1)
C(28)	1730(1)	9667(1)	6980(1)	17(1)
C(29)	360(1)	9051(1)	6300(1)	14(1)
C(30)	-388(1)	7862(1)	6139(1)	13(1)
C(31)	-187(1)	6606(1)	6476(1)	13(1)
C(32)	733(1)	5609(1)	7275(1)	13(1)
C(33)	2099(1)	5200(1)	8231(1)	15(1)
C(34)	3556(1)	5588(1)	9156(1)	18(1)

C(35)	3994(1)	5519(1)	8480(1)	21(1)
C(36)	2537(1)	5126(1)	7560(1)	16(1)
C(37)	1164(1)	5510(1)	6600(1)	14(1)
C(38)	221(1)	6488(1)	5799(1)	13(1)
C(39)	2876(1)	10556(1)	7042(1)	23(1)
C(40)	-884(1)	8798(1)	5143(1)	16(1)
C(41)	-446(1)	5392(1)	6066(1)	16(1)
C(42)	3350(1)	4387(1)	8666(1)	21(1)
C(43)	1692(1)	7698(1)	3359(1)	33(1)
C(44)	2650(2)	7474(1)	6141(1)	38(1)
C(45)	-1250(1)	7936(1)	7628(1)	17(1)
C(46)	-1600(1)	7726(1)	8397(1)	17(1)
C(47)	-2091(1)	8342(1)	8745(1)	21(1)
C(48)	-2390(1)	8113(1)	9540(1)	22(1)
C(49)	-2936(1)	8695(1)	9890(1)	22(1)
C(50)	-3093(1)	8514(1)	10756(1)	24(1)
C(51)	-3640(2)	7821(1)	10769(1)	31(1)
C(50A)	-3654(11)	8327(9)	10444(10)	18(3)
C(51A)	-3105(13)	7951(10)	11216(12)	27(4)
C(52)	-3924(1)	7688(1)	11608(1)	33(1)
O(60)	4072(1)	8872(1)	949(1)	64(1)
C(61)	4488(2)	9548(1)	920(1)	43(1)

Table 5.2 Bond lengths [Å] and angles [°] for sd_182p1.

P(1)-O(2)	1.4626(12)	C(13)-C(41)	1.5605(19)
P(1)-O(3)	1.5528(12)	C(14)-C(32)	1.391(2)
P(1)-O(4)	1.5662(12)	C(14)-C(33)	1.391(2)
P(1)-O(1)	1.5961(11)	C(15)-C(34)	1.530(2)
O(1)-C(1)	1.4118(17)	C(15)-C(33)	1.535(2)
O(3)-C(43)	1.453(2)	C(15)-C(42)	1.557(2)
O(4)-C(44)	1.453(2)	C(16)-C(34)	1.376(2)
O(5)-C(12)	1.3737(17)	C(16)-C(17)	1.397(2)
O(5)-C(45)	1.4291(17)	C(17)-C(18)	1.386(3)
C(1)-C(23)	1.380(2)	C(18)-C(19)	1.401(3)
C(1)-C(38)	1.385(2)	C(19)-C(35)	1.380(2)
C(2)-C(24)	1.527(2)	C(20)-C(35)	1.525(2)
C(2)-C(23)	1.5322(19)	C(20)-C(36)	1.529(2)
C(2)-C(40)	1.555(2)	C(20)-C(42)	1.560(2)
C(3)-C(25)	1.392(2)	C(21)-C(37)	1.388(2)
C(3)-C(24)	1.392(2)	C(21)-C(36)	1.391(2)
C(4)-C(26)	1.526(2)	C(22)-C(38)	1.5239(19)
C(4)-C(25)	1.537(2)	C(22)-C(37)	1.531(2)
C(4)-C(39)	1.560(2)	C(22)-C(41)	1.563(2)
C(5)-C(26)	1.380(2)	C(23)-C(30)	1.414(2)
C(5)-C(6)	1.402(2)	C(24)-C(29)	1.401(2)
C(6)-C(7)	1.387(3)	C(25)-C(28)	1.406(2)
C(7)-C(8)	1.396(3)	C(26)-C(27)	1.407(2)
C(8)-C(27)	1.381(2)	C(31)-C(38)	1.395(2)
C(9)-C(27)	1.523(2)	C(32)-C(37)	1.407(2)
C(9)-C(28)	1.525(2)	C(33)-C(36)	1.403(2)
C(9)-C(39)	1.554(2)	C(34)-C(35)	1.410(2)
C(10)-C(29)	1.387(2)	C(45)-C(46)	1.514(2)
C(10)-C(28)	1.389(2)	C(46)-C(47)	1.526(2)
C(11)-C(29)	1.529(2)	C(47)-C(48)	1.524(2)
C(11)-C(30)	1.5413(19)	C(48)-C(49)	1.531(2)
C(11)-C(40)	1.556(2)	C(49)-C(50)	1.520(2)
C(12)-C(31)	1.393(2)	C(49)-C(50A)	1.690(16)
C(12)-C(30)	1.396(2)	C(50)-C(51)	1.513(3)
C(13)-C(32)	1.5279(19)	C(51)-C(52)	1.543(3)
C(13)-C(31)	1.5351(19)	C(50A)-C(51A)	1.50(2)

C(51A)-C(52)	1.573(18)	C(31)-C(12)-C(30)	116.90(13)
O(60)-C(61)	1.393(3)	C(32)-C(13)-C(31)	107.15(11)
		C(32)-C(13)-C(41)	98.40(11)
O(2)-P(1)-O(3)	112.79(7)	C(31)-C(13)-C(41)	97.98(11)
O(2)-P(1)-O(4)	114.98(7)	C(32)-C(14)-C(33)	116.52(13)
O(3)-P(1)-O(4)	106.03(7)	C(34)-C(15)-C(33)	104.93(12)
O(2)-P(1)-O(1)	114.82(6)	C(34)-C(15)-C(42)	98.84(12)
O(3)-P(1)-O(1)	101.95(6)	C(33)-C(15)-C(42)	99.33(12)
O(4)-P(1)-O(1)	105.01(6)	C(34)-C(16)-C(17)	118.41(16)
C(1)-O(1)-P(1)	119.31(9)	C(18)-C(17)-C(16)	120.74(16)
C(43)-O(3)-P(1)	122.64(11)	C(17)-C(18)-C(19)	121.02(16)
C(44)-O(4)-P(1)	122.38(11)	C(35)-C(19)-C(18)	118.13(16)
C(12)-O(5)-C(45)	121.20(11)	C(35)-C(20)-C(36)	105.39(12)
C(23)-C(1)-C(38)	118.13(13)	C(35)-C(20)-C(42)	98.61(12)
C(23)-C(1)-O(1)	119.95(12)	C(36)-C(20)-C(42)	99.12(12)
C(38)-C(1)-O(1)	121.77(12)	C(37)-C(21)-C(36)	116.40(13)
C(24)-C(2)-C(23)	105.27(11)	C(38)-C(22)-C(37)	106.99(11)
C(24)-C(2)-C(40)	99.03(11)	C(38)-C(22)-C(41)	97.98(11)
C(23)-C(2)-C(40)	98.81(11)	C(37)-C(22)-C(41)	98.60(11)
C(25)-C(3)-C(24)	116.60(13)	C(1)-C(23)-C(30)	121.96(13)
C(26)-C(4)-C(25)	105.11(12)	C(1)-C(23)-C(2)	130.34(13)
C(26)-C(4)-C(39)	98.97(12)	C(30)-C(23)-C(2)	107.66(12)
C(25)-C(4)-C(39)	98.69(12)	C(3)-C(24)-C(29)	121.89(13)
C(26)-C(5)-C(6)	117.96(15)	C(3)-C(24)-C(2)	131.76(13)
C(7)-C(6)-C(5)	120.89(16)	C(29)-C(24)-C(2)	106.24(12)
C(6)-C(7)-C(8)	121.27(16)	C(3)-C(25)-C(28)	121.13(13)
C(27)-C(8)-C(7)	117.71(16)	C(3)-C(25)-C(4)	132.35(14)
C(27)-C(9)-C(28)	105.32(12)	C(28)-C(25)-C(4)	106.37(12)
C(27)-C(9)-C(39)	99.24(12)	C(5)-C(26)-C(27)	120.87(15)
C(28)-C(9)-C(39)	98.87(12)	C(5)-C(26)-C(4)	132.50(14)
C(29)-C(10)-C(28)	116.47(14)	C(27)-C(26)-C(4)	106.55(13)
C(29)-C(11)-C(30)	105.11(11)	C(8)-C(27)-C(26)	121.29(15)
C(29)-C(11)-C(40)	99.28(11)	C(8)-C(27)-C(9)	131.88(15)
C(30)-C(11)-C(40)	99.35(11)	C(26)-C(27)-C(9)	106.75(13)
O(5)-C(12)-C(31)	114.11(12)	C(10)-C(28)-C(25)	122.12(13)
O(5)-C(12)-C(30)	128.99(13)	C(10)-C(28)-C(9)	131.03(14)

C(25)-C(28)-C(9)	106.79(13)	C(45)-C(46)-C(47)	113.76(12)
C(10)-C(29)-C(24)	121.66(13)	C(48)-C(47)-C(46)	111.63(13)
C(10)-C(29)-C(11)	131.15(13)	C(47)-C(48)-C(49)	114.10(13)
C(24)-C(29)-C(11)	107.04(12)	C(50)-C(49)-C(48)	113.76(14)
C(12)-C(30)-C(23)	120.02(13)	C(48)-C(49)-C(50A)	111.9(5)
C(12)-C(30)-C(11)	134.99(13)	C(51)-C(50)-C(49)	113.34(15)
C(23)-C(30)-C(11)	104.93(12)	C(50)-C(51)-C(52)	113.78(16)
C(12)-C(31)-C(38)	122.79(13)	C(51A)-C(50A)-C(49)	110.4(12)
C(12)-C(31)-C(13)	130.21(13)	C(50A)-C(51A)-C(52)	99.6(12)
C(38)-C(31)-C(13)	106.99(12)		
C(14)-C(32)-C(37)	121.71(13)		
C(14)-C(32)-C(13)	131.84(13)		
C(37)-C(32)-C(13)	106.39(12)		
C(14)-C(33)-C(36)	121.57(13)		
C(14)-C(33)-C(15)	131.77(13)		
C(36)-C(33)-C(15)	106.60(12)		
C(16)-C(34)-C(35)	120.98(15)		
C(16)-C(34)-C(15)	132.75(15)		
C(35)-C(34)-C(15)	106.19(13)		
C(19)-C(35)-C(34)	120.70(15)		
C(19)-C(35)-C(20)	132.25(15)		
C(34)-C(35)-C(20)	106.96(13)		
C(21)-C(36)-C(33)	121.96(13)		
C(21)-C(36)-C(20)	131.30(14)		
C(33)-C(36)-C(20)	106.71(12)		
C(21)-C(37)-C(32)	121.74(13)		
C(21)-C(37)-C(22)	131.31(13)		
C(32)-C(37)-C(22)	106.92(12)		
C(1)-C(38)-C(31)	120.07(13)		
C(1)-C(38)-C(22)	133.11(13)		
C(31)-C(38)-C(22)	106.79(12)		
C(9)-C(39)-C(4)	94.15(12)		
C(2)-C(40)-C(11)	94.06(11)		
C(13)-C(41)-C(22)	93.95(11)		
C(15)-C(42)-C(20)	94.10(11)		
O(5)-C(45)-C(46)	106.11(12)		

Table 5.3 Anisotropic displacement parameters ($Å^2 x\ 10^3$) for sd_182p1. The anisotropic displacement factor exponent takes the form: $-2\pi^2 [h^2 a^{*2} U11 + ... + 2 h k a^* b^* U12]$

	U11	U22	U33	U23	U13	U12
P(1)	20(1)	20(1)	16(1)	4(1)	8(1)	4(1)
O(1)	19(1)	18(1)	10(1)	0(1)	5(1)	1(1)
O(2)	28(1)	25(1)	25(1)	6(1)	13(1)	9(1)
O(3)	34(1)	30(1)	22(1)	8(1)	18(1)	10(1)
O(4)	23(1)	26(1)	25(1)	3(1)	4(1)	-3(1)
O(5)	23(1)	17(1)	15(1)	0(1)	10(1)	4(1)
C(1)	13(1)	16(1)	9(1)	-1(1)	3(1)	-1(1)
C(2)	16(1)	12(1)	13(1)	1(1)	2(1)	0(1)
C(3)	19(1)	13(1)	13(1)	2(1)	4(1)	0(1)
C(4)	18(1)	19(1)	17(1)	-2(1)	4(1)	-5(1)
C(5)	17(1)	29(1)	19(1)	-2(1)	3(1)	-4(1)
C(6)	19(1)	36(1)	28(1)	3(1)	2(1)	3(1)
C(7)	25(1)	42(1)	20(1)	9(1)	-1(1)	-3(1)
C(8)	22(1)	38(1)	16(1)	-2(1)	4(1)	-9(1)
C(9)	20(1)	24(1)	20(1)	-9(1)	5(1)	-5(1)
C(10)	19(1)	14(1)	17(1)	-3(1)	6(1)	2(1)
C(11)	16(1)	13(1)	16(1)	0(1)	4(1)	1(1)
C(12)	12(1)	16(1)	11(1)	-1(1)	2(1)	0(1)
C(13)	16(1)	12(1)	12(1)	0(1)	4(1)	0(1)
C(14)	17(1)	12(1)	14(1)	-1(1)	5(1)	-2(1)
C(15)	18(1)	17(1)	15(1)	1(1)	3(1)	2(1)
C(16)	21(1)	26(1)	18(1)	0(1)	1(1)	-1(1)
C(17)	31(1)	33(1)	28(1)	-5(1)	0(1)	-10(1)
C(18)	27(1)	41(1)	36(1)	1(1)	5(1)	-15(1)
C(19)	20(1)	40(1)	26(1)	3(1)	7(1)	-3(1)
C(20)	19(1)	22(1)	18(1)	0(1)	5(1)	6(1)
C(21)	21(1)	12(1)	15(1)	-2(1)	7(1)	1(1)
C(22)	18(1)	12(1)	12(1)	-1(1)	4(1)	0(1)
C(23)	13(1)	14(1)	12(1)	0(1)	1(1)	-1(1)
C(24)	18(1)	11(1)	14(1)	0(1)	2(1)	1(1)
C(25)	16(1)	15(1)	17(1)	1(1)	3(1)	-1(1)
C(26)	16(1)	22(1)	16(1)	-3(1)	3(1)	-7(1)

C(27)	16(1)	26(1)	16(1)	-5(1)	3(1)	-8(1)
C(28)	18(1)	15(1)	17(1)	-4(1)	3(1)	0(1)
C(29)	16(1)	11(1)	17(1)	1(1)	4(1)	2(1)
C(30)	11(1)	14(1)	13(1)	-2(1)	1(1)	0(1)
C(31)	12(1)	15(1)	11(1)	1(1)	1(1)	-1(1)
C(32)	16(1)	9(1)	15(1)	-1(1)	5(1)	0(1)
C(33)	19(1)	12(1)	13(1)	0(1)	2(1)	-1(1)
C(34)	16(1)	20(1)	17(1)	3(1)	0(1)	3(1)
C(35)	16(1)	26(1)	20(1)	2(1)	2(1)	4(1)
C(36)	18(1)	13(1)	17(1)	-2(1)	5(1)	2(1)
C(37)	20(1)	9(1)	13(1)	-1(1)	4(1)	-1(1)
C(38)	13(1)	13(1)	12(1)	-2(1)	2(1)	0(1)
C(39)	23(1)	20(1)	26(1)	-5(1)	4(1)	-6(1)
C(40)	16(1)	15(1)	17(1)	2(1)	2(1)	2(1)
C(41)	19(1)	14(1)	14(1)	-1(1)	3(1)	-2(1)
C(42)	24(1)	18(1)	20(1)	1(1)	3(1)	5(1)
C(43)	37(1)	37(1)	26(1)	16(1)	12(1)	6(1)
C(44)	45(1)	36(1)	27(1)	-2(1)	-8(1)	-1(1)
C(45)	20(1)	16(1)	18(1)	0(1)	7(1)	5(1)
C(46)	20(1)	18(1)	14(1)	1(1)	6(1)	3(1)
C(47)	26(1)	20(1)	18(1)	2(1)	10(1)	5(1)
C(48)	26(1)	24(1)	17(1)	1(1)	8(1)	7(1)
C(49)	22(1)	24(1)	22(1)	-2(1)	7(1)	4(1)
C(50)	23(1)	28(1)	21(1)	-7(1)	7(1)	0(1)
C(51)	40(1)	32(1)	20(1)	-4(1)	8(1)	-6(1)
C(52)	38(1)	35(1)	29(1)	1(1)	12(1)	-5(1)
O(60)	40(1)	52(1)	91(1)	21(1)	-8(1)	-10(1)
C(61)	38(1)	51(1)	39(1)	-1(1)	6(1)	-10(1)

Table 5.4 Hydrogen coordinates (x 10^4) and i displacement parameters (Å^2 x 10^3) for sd_182p1.

___	x	y	z	U(eq)
H(2)	85	8442	4389	17
H(3)	1863	9099	5090	18
H(4)	3349	10041	5997	22
H(5)	4613	8890	6699	26
H(6)	5210	8224	7946	34
H(7)	4584	8363	9117	36
H(8)	3351	9178	9091	31
H(9)	2266	10301	8112	25
H(10)	624	9461	7505	19
H(11)	-1040	8857	6449	17
H(13)	-717	5820	7245	16
H(14)	900	5519	8559	17
H(15)	2579	4854	9539	20
H(16)	3492	6189	10188	27
H(17)	4656	7014	10039	38
H(18)	5389	6898	8932	42
H(19)	4956	5967	7921	34
H(20)	3883	4658	7551	23
H(21)	2380	5236	6278	19
H(22)	546	5475	5252	16
H(39A)	3448	10813	7336	28
H(39B)	2414	10906	6728	28
H(40A)	-1446	8519	4870	20
H(40B)	-962	9317	4981	20
H(41A)	-1035	5519	5661	19
H(41B)	-421	4863	6183	19
H(42A)	2956	3961	8453	25
H(42B)	3929	4229	9066	25
H(43A)	1047	7822	3355	49
H(43B)	1759	7657	2777	49
H(43C)	2107	8079	3653	49
H(44A)	2430	7028	6360	58
H(44B)	2467	7896	6431	58
H(44C)	3328	7459	6238	58
H(45A)	-1774	8088	7161	21

H(45B)	-802	8342	7764	21
H(46A)	-1067	7559	8846	20
H(46B)	-2035	7312	8248	20
H(47A)	-1668	8765	8875	25
H(47B)	-2645	8494	8309	25
H(48A)	-1829	7985	9980	26
H(48B)	-2779	7670	9413	26
H(49A)	-2595	9161	9927	27
H(49B)	-3547	8763	9490	27
H(50A)	-3420	8909	10941	28
H(50B)	-2501	8468	11150	28
H(51A)	-3273	7417	10662	37
H(51B)	-4191	7839	10319	37
H(50C)	-4060	7980	10101	22
H(50D)	-4030	8700	10608	22
H(51C)	-2683	8290	11596	33
H(51D)	-2743	7538	11072	33
H(52A)	-4267	7242	11576	50
H(52B)	-3376	7658	12060	50
H(52C)	-4304	8084	11713	50
H(52D)	-3672	7432	12125	50
H(52E)	-4273	8100	11723	50
H(52F)	-4324	7370	11218	50
H(60)	3431	8857	562	97
H(61A)	4090	9929	1065	65
H(61B)	4573	9634	349	65
H(61C)	5094	9556	1324	65

6 References

[1] P. L. Toogood*, J. Med. Chem.* **2002**, *45*, 1543–1558.

[2] M. A. DePristo, *HFSP Journal* **2007**, *1*, 94–98.

[3] F. U. Hartl, & M. Hayer-Hartl, *Science **2002,*** **295**, 1852–1858.

[4] R. J. Ellis, *Curr. Opin. Struct. Biol.* **2001***, 11*, 114–119.

[5] C. M. Dobson, *Nature* **2002**, *426*, 884-890.

[6] D. J. Selkoe, *Physiol Rev.* **2001**, *81*, 741-66.

[7] J. L. Cummings, *N Engl J Med.* **2004**, *351*, 56-67.

[8] Worldwide Cost Estimate For Alzheimer's And Dementia Is US$315.4 Billion. *Alzheimer's disease International* **2009** [updated 2009; cited March 24, 2009]; Available from: http://www.alz.co.uk/media/nr090324.html.

[9] 2009 Alzheimer's disease facts and figures, *Alzheimers Dement.* **2009,** *5*, 234-70.

[10] Alzheimer's disease facts and figures, *Alzheimer's & Dementia* **2008**, *4*, 110-33.
Every 72 seconds someone in America develops Alzheimer's **2007**: Available from: http://www.alz.org/news_and_events_rates_rise.asp.

[11] Worldwide Cost Estimate For Alzheimer's And Dementia Is US$315.4 Billion. *Alzheimer's disease International* **2009** [updated 2009; cited March 24, 2009]; Available from: http://www.alz.co.uk/media/nr090324.html.

[12] A. Shanmugam, B. H. Monien, G. Bitan, *Nova Science Publishers, Inc.* **2008**, 193-250.

[13] B. H. Monien, L.G. Apostolova, G. Bitan, *Expert Rev Neurother.* **2006**, *6*, 1293-306.

[14] P. R. Turner, K. O'Connor, W. P. Tate, **W. C**. Abraham, *Progress in Neurobiology* **2003**, *70*, 1-32.

[15] J. A. Hardy, *Science* **1992**, *256*, 184-185.

[16] M. D. Kirkitadze, G. Bitan, D. B. Teplow, *J Neurosci Res.* **2002,** *69*, 567-77.

[17] D. M. Walsh, D. J. Selkoe, *Protein Peptide Lett.* **2004**, *11*, 213-28.

[18] W. L. Klein, Jr. W. B. Stine, D. B. Teplow, *Neurobiol Aging.* **2004***, 25*, 569-80.

[19] A. F. Rahimi, A. Shanmugam, G. Bitan, *Curr Alzheimer Res.* **2008**, *5,* 319-41.

[20] R. S. Harrison, P. C. Sharpe, Y. Singh, D. P. Fairlie, *Rev Physiol Biochem Pharmacol.* **2008**, *159*, 1-77.

[21] R. Tycko, *Q Rev Biophys.* **2006**, *39*, 1-55.

[22] R. Nelson, D. Eisenberg, *Adv Protein Chem.* **2006**, *73*, 235-82.

[23] D. B. Teplow, N. D. Lazo, G. Bitan, S. Bernstein, T. Wyttenbach, M.T. Bowers, *Acc Chem Res.* **2006**, *39*, 635-45.

[24] T. Lührs, C. Ritter, M. Adrian, D. R. -Loher, B. Bohrmann, H. Döbeli, D. Schubert, R.

Riek, *Proc Natl Acad Sci USA* **2005**, *102*, 17342-47.

[25] A. T. Petkova, Y. Ishii, J. J. Balbach, O. N. Antzutkin, R. D. Leapman, F. Delaglio, *Proc Natl Acad Sci USA* **2002**, *99*, 16742-7.

[26] A. T. Petkova, R. D. Leapman, Z. Guo, W. M. Yau, M. P. Mattson, R. Tycko, *Science* **2005**, *307*, 262-5.

[27] A. T. Petkova, W. M. Yau, R. Tycko, *Biochemistry* **2006**, *45*, 498-512.

[28] N. D. Lazo, M. A. Grant, M. C. Condron, A. C. Rigby, D. B. Teplow, *Protein Sci.* **2005**, *14*, 1581-96.

[29] J. M. Borreguero, B. Urbanc, N. D. Lazo, S. V. Buldyrev, D. B. Teplow, and H. E. Stanley, *Proc Natl Acad Sci USA* **2005**, *102*, 6015-6020.

[30] M. G. Krone, A. Baumketner, S. L. Bernstein, T. Wyttenbach, N. D. Lazo, D. B. Teplow, *J Mol Biol.* **2008**, *381*, 221-8.

[31] L. Cruz, B. Urbanc, J. M. Borreguero, N. D. Lazo, D. B. Teplow, H. E. Stanley, *Proc Natl Acad Sci USA* **2005**, *102*, 18258-63.

[32] A. Baumketner, S. L. Bernstein, T. Wyttenbach, N. D. Lazo, D. B. Teplow, M. T. Bowers, *Protein Sci.* **2006**, *15*, 1239-47.

[33] T. Schrader, S. Koch, *Mol. BioSyst.* **2007**, *3*, 241-48.

[34] H. Yin, A. D. Hamilton, *Angew. Chem. Int. Ed.* **2005***, 44*, 4130.

[35] M. W. Peczuh, A. D. Hamilton, *Chem. Rev.* **2000,** *100*, 2479.

[36] S. Fletcher and A. D. Hamilton, *J. R. Soc. Interface* **2006***, 3*, 215.

[37] V. Martos, P. Castreño, J. Valero and J. De Mendoza, *Current Opinion in Chemical Biology* **2008***, 12*, 698.

[38] S. Dutt, C. Wilch, T. Schrader, *chem. Commun.* **2011**, *47*, 5376-83.

[39] R. Zadmard, T. Schrader, *J. Am. Chem. Soc.* **2005**, *127*, 904-915.

[40] A. W. Coleman, S. G. Bott, S. D. Morley, C. M. Means, K. D. Robinson, H. Zhang, J. L. Atwood, *Angew. Chem. Int. Ed.* **1988**, *27*, 1361–1362.

[41] M. Selkti , A. W. Coleman , I. Nicolis , N. D. -Guével , F. Villain , A. Tomas, C. de Rango, *Chem. Commun.*, **2000**, *2*, 161–162.

[42] G. Arena, A. Casnati , A. Contino, A. Magrì, F. Sansone, D. Sciotto, R. Ungaro, *Org. Biomol. Chem.* **2006**, *4*, 243–249.

[43] C. S. Beshara, C. E. Jones, K. D. Daze, B. J. Lilgert, F. A. Hof, *ChemBioChem* **2010**, *11*, 63–66.

[44] F. Perret, A. W. Coleman, *Chem. Commun.* **2011**, *47*, 7303–7319.

[45] S. N. Gradl, J. P. Felix, E. Y. Isacoff, M. L. Garcia, D. Trauner, *J. Am. Chem. Soc.*

2003*, 125*, 12668.

[46] F. M. Ashcroft, *Ion Channels and Disease: Channelopathies;* Academic Press, San Diego, **2000**.

[47] C. Ader, R. Schneider, S. Hornig, P. Velisetty, E. M. Wilson, A. Lange, K. Giller, I. Ohmert, M.-F. Martin-Eauclaire, D. Trauner, S. Becker, O. Pongs, M. Baldus**,** *Nat. Struct. Mol. Bio.* **2008***, 15*, 605.

[48] V. Martos, S. C. Bell, E. Santos, E. Y. Isacoff, D. Trauner, J. de Mendoza, *Proc. Natl. Acad. Sci. USA* **2009**, *106*, 10482.

[49] A. J. Levine, *Cell* **1997***, 88*, 323.

[50] S. Gordo, V. Martos, E. Santos, M. Menéndez, C. Bo, E. Giralt, J. de Mendoza, *Proc. Natl. Acad. Sci. USA* **2008**, *105*, 16426.

[51] R. E. McGovern, H. Fernandes, A. R. Khan, N. P. Power, P. B. Crowley, *Nature Chemistry* **2012***, 4*, 527–533.

[52] B. C. Cunningham, J. A. Wells, *Science* **1989***, 244*, 1081-1085.

[53] S. S. Peacock, D. M. Walba, F. C. A. Gaeta, R. C. Helgeson, D. J. Cram, *J. Am. Chem. Soc.* **1980**, *102*, 2043-2052.

[54] J. L. Sessler, A. Andrievsky, *Chem. Eur. J.* **1998**, *4*, 159-167

[55] V. Král, S.L. Springs, J. L. Sessler, *J. Am. Chem. Soc.* **1995**, *117*, 8881-8882.

[56] J. L. Sessler, A. Andrievsky, P. A. Gale, V. Lynch, *Angew. Chem. Int. Ed.* **1996**, *35*, 2782-2785.

[57] J. Chin, S. S. Lee, K. J. Lee, S. Park, D. H. Kim, *Nature* **1999**, *401*, 254-257.

[58] A. Galán, D. Andreu, A. M. Echavarren, P. Prados, J. de Mendoza, *J. Am. Chem. Soc.* **1992**, *114*, 1511-1512.

[59] P. Breccia, M. V. Gool, R. P.-Fernández, S. M.-Santamaría, F. Gago, P. Prados, J. de Mendoza, *J. Am. Chem. Soc.* **2003**, *125*, 8270-8284.

[60] R. P. Bonar-Law, L. G. Mackay, C. J. Walter, V. Marvaud, J. K. M. Sanders, *Pure Appl. Chem.* **1994**, *66*, 803.

[61] H.-J. Schneider, *Angew. Chem. Int. Ed.* **2009**, *48*, 3924–3977.

[62] C. P. Mandl, B. König, *J. Org. Chem.* **2005**, *70*, 670–674.

[63] J. N. H. Reek, J. A. A. W. Elemans, R. J. M. Nolte, *J. Org. Chem.* **1997**, *62*, 2234–2243.

[64] B. Escuder, A. E. Rowan, M. C. Feiters, R. J. M. Nolte, *Tetrahedron* **2004**, *60*, 291-300.

[65] Bell, T. W., Khasanov, A. B., Drew, M. G. B., Filikov, A., James, T. L., *Angew. Chem.*

Int. Ed. **1999**, *38*, 2543–2547.

[66] S. M. Ngola, P. C. Kearney, S. Mecozzi, K. Russell, and D. A. Dougherty, *J. Am. Chem. Soc.*, **1999**, *121*, 1192-1201.

[67] M. Kruppa, C. Mandl, S. Miltschitzky, B. König, *J. Am. Chem. Soc.* 2005, *127*, 3362 – 3365.

[68] Folmer-Andersen JF, Lynch VM, Anslyn EV, *Chem. Eur. J.* **2005**, *11*, 5319-26.

[69] O. Rusin, N. N. St. Luce, R. A. Agbaria, J. O. Escobedo, S. Jiang, I. M. Warner, F. B. Dawan, K. Lian, R. M. Strongin, *J. Am. Chem. Soc.* **2004**, *126*, 438–439.

[70] C. Schmuck, V. Bickert *Org. Lett.* **2003**, *5*, 4579 - 4581.

[71] C. Schmuck, *Coord. Chem. Rev.* **2006**, *250*, 3053-3067.

[72] L. A. Logsdon, C. L. Schardon, V. Ramalingam, S. K. Kwee, A. R. Urbach, *J. Am. Chem. Soc.* **2011**, *133*, 17087–17092.

[73] A. M. Burger, A. K. Seth, *Eur. J. Cancer* **2004**, *40*, 2217-2229.

[74] R. N. Dutnall, S. T. Tafrov, R. Sternglanz, V. Ramakrishnan, *Cell* **1998**, *94*, 427-438.

[75] J. Taunton, C. A. Hassig, S. L. Schreiber, *Science* **1996**, *272*, 408-411.

[76] A. D. Ellington, *Curr. Biol.* **1993**, *3*, 375-377.

[77] G. Varani, *Acc. Chem. Res.* **1997**, *30*, 189-195.

[78] D. H. Williams, B. Bardsley, *Angew. Chem., Int. Ed.* **1999**, *38*, 1173-1193.

[79] L. O. Tjernberg, C. Lilliehook, D. J. E Callaway, J. Naslund, S. Hahne, J. Thyberg, , L. Terenius, C. Nordstedt, *J. Biol. Chem.* **1997**, *272*, 12601-12605.

[80] R. O. Hynes. *Cell* **1992**, *69*, 11-25.

[81] H. Li, S. Ilin, W. Wang, E. M. Duncan, J. Wysocka, C. D. Allis, D. J. Patel, *Nature* **2006**, *442*, 91-95.

[82] F. -G. Klärner1, T. Schrader, J. Polkowska, F. Bastkowski, P. Talbiersky, M. C. Kuchenbrandt, T. Schaller, H. de Groot, M. Kirsch, *Pure Appl. Chem.* **2010**, *4*, 991–999.

[83] P. Talbiersky, F. Bastkowski, F. -G. Klärner, T. Schrader, *J. Am. Chem. Soc.* **2008**, *130*, 9824–9828.

[84] F. -G. Klärner and B. Kahlert, *Acc. Chem. Res.* **2003,** *36*, 919-932.

[85] F.-G. Klärner, T. Schrader, *Acc. Chem. Res.* **2012**, DOI: 10.1021/ar300061c.

[86] M. Kirsch, P. Talbiersky, J. Polkowska, F. Bastkowski, T. Schaller, H. de Groot, F. Klärner, T. Schrader, *Angew. Chem. Int. Ed.* **2009**, *48*, 2886-2890.

[87] M. Fokkens, T. Schrader, F. -G. Klärner, *J. Am. Chem. Soc.* **2005**, *127*, 14415–14421.

[88] S. Sinha, D. H. J. Lopes, Z. Du, E. S. Pang, A. Shanmugam, A. Lomakin, P.

Talbiersky, A. Tennstaedt, K. McDaniel, R. Bakshi, P.-Y. Kuo, M. Ehrmann, G. B. Benedek, J. A. Loo, F.-G. Klärner, T. Schrader, C.Wang and G. Bitan, *J. Am. Chem. Soc.* **2011**, 133, 16958–16969.

[89] F. Bastkowski, Universität Duisburg-Essen, Essen, *Dissertation* **2008.**

[90] P. M. Talbiersky, Universität Duisburg-Essen, Essen, *Dissertation* **2009.**

[91] P. W. Sorensen, J. M. Fine, V. Dvornikovs, C. S. Jeffrey, F. Shao, J. Z. Wang, L. A. Vrieze, K. R. Anderson, T. R. Hoye, *Nat. Chem. Biol.* **2005**, *1*, 324-328.

[92] J. M. Fine, P. W. Sorensen, *J. Chem. Ecol.* **2005**, *31*, 2205-2210.

[93] M. Foot, M. Mulholland, *J. Pharm. Biomed. Anal.* **2005**, *38*, 397-407.

[94] S. Iida, H. Tsuiji, Y. Nemoto, Y. Sano, M. A. Reddish, T. Irimura, *Oncol. Res.* **1998**, *10*, 407-414.

[95] H. Tsuiji, J. C. Hong, Y. S. Kim, Y. Ikehara, H. Narimatsu, T. Irimura, *Biochem. Biophys. Res. Commun.* **1998**, *253*, 374-381.

[96] J. R. Bundgaard, J. Vuust, J. F. Rehfeld, *J. Biol. Chem.* **1997**, *272*, 21700-21705.

[97] J. E. Rose, P. D. Leeson, D. Gani, *J. Chem. Soc. Perkin Trans. 1* **1994**, 3089-3094.

[98] H. Luecke and F. A. Quiocho, *Nature* **1990**, *347*, 402-406.

[99] J. W. Pflugrath and F. A. Quiocho, *J. Mol. Bid.* **1988**, *200*, 163-180.

[100] J. N. Vos, P. Westerduin and Constant A.A. van Boeckel, *Bioorganic &Medicinal Chemistry* Letters. **1991,** *3*, 143-146.

[101] M. C. Cartagena, Dissertation, Universität Duisburg-Essen, Essen, *Dissertation* **2007.**

[102] T. C. Öberg, A. -L. Noresson, H. Leffler and U. J. Nilsson, *Chem. Eur. J.* **2011**, *17*, 8139 – 8144.

[103] M. Kamieth, Dissertation, Universität Essen, *Dissertation* **1998.**

[104] I. M. Pastor, M. Yus, *Curr. Org. Chem.* **2005**, *9*, 1-29.

[105] C. Schneider, *Synthesis* **2006**, *23*, 3919-44.

[106] A. Heydari, M. Mehrdad, A. Maleki, N. Ahmadia, *Synthesis* **2004**, *10***,** 1563-65.

[107] J. Chen, W. Shun, *Tetrahedron Letters* **1995**, *36*, 2370-80.

[108] K. Kitaori, Y. Furukawa, H. Yoshimoto, J. Otera, *Tetrahedron* **1999**, *55*, 14381-14390.

[109] R. S. Lankalapalli, A. Ouro, L. Arana, A. Gomez-Munoz, R. Bittman, *J. Org. Chem.* **2009**, *74*, 8844–8847.

[110] H. Griesser, M. Tolev, A. Singh, T. Sabirov, C. Gerlach, C. Richert, *J. Org. Chem.* **2012**, *77*, 2703−2717.

[111] J. J. Steffens, E. J. Sampson, I. J. Siewers, S. J. Benkovic, *J. Am. Chem. Soc.*, **1973,** *95*, 936–938.

[112] M. Fokkens, Universität Duisburg-Essen, Essen, *Dissertation* **2005.**

[113] C. Wilch, Dissertation, Universität Duisburg-Essen, Essen, *Dissertation* **2012.**

[114] K. A. Connors: *Binding Constants*, John-Wiley & Sons, New York **1987.**

[115] K. Hirose, *J. Incl. Phenom. Macro. Chem.* **2001**, *39*, 193-209.

[116] P. Thordarson, *Chem. Soc. Rev.,* **2011**, *40*, 1305–1323.

[117] J. Polkowska, F. Bastkowski, T. Schrader, F.-G. Klärner, J. Zienau, F. Koziol, C. Ochsenfeld, *J. Phys. Org. Chem.* **2009**, *22*, 779-790.

[118] *TableCurve 2D* 5.01, SYSTAT Software, Inc., Richmond, CA.

[119] *SigmaPlot*, version 10.0, Systat Software, Inc., San Jose CA.

[120] E. Freire, O. L. Mayorga, M. Straume, *Anal. Chem.* **1990**, *62,* 950A-959A.

[121] VP-ITC, *MicroCal*, LLC, Northampton, MA.

[122] W. Blokzijl, J. Engberts, *Angew. Chem. Int. Ed.* **1993**, *32*, 1545-79.

[123] E. A. Meyer, R. K. Castellano, F. Diederich, *Angew. Chem. Int. Ed.* **2003,** *42*, 1210-1250.

[124] S. B. Ferguson, E. M. Sandford, E. M. Seward, F. Diederich, *J. Am. Chem. Soc.*, **1991,** *113*, 5410–19.

[125] D. B. Smithurd, T. B. Wyman, F. Diederich, *J. Am. Chem. Soc.*, **1991,** *113*, 5420–26.

[126] F. Diederich, D. B. Smithurd, E. M. Sandford, S. B. Ferguson, D. R. Carcanague, I Chao, K. N. Houl, *Acta Chem. Scand.* **1992**, *46*, 205-215.

[127] A.P. de Silva, H. Q. N. Gunaratne, T. Gunnlaugsson, A. J. M. Huxley, C. P. McCoy, J. T. Rademacher, T. E. Rice, *Chem. Rev.* **1997**, *97*, 1515.

[128] R. A. Agbaria, D. Gill*, J. Phys. Chem.* **1988**, *92*, 1052-55.

[129] N. D. -Guével, F. Perret, A. W. Coleman, J. -P. Morel and N. M.-Desrosiers, *J. Chem. Soc*., *Perkin Trans.* **2002**, *2*, 524–532.

[130] J. Dziemidowicz, D. Witt, J. Rachoń, J Incl Phenom Macrocycl Chem **2008**, *61*, 381–391.

[131] K. D. Collins, G. W. Neilson, J. E. Enderby, *Biophysical Chemistry* **2007**, *128*, 95–104.

[132] Y. Marcus, *J. Chem. Soc., Faraday Trans.* **1991**, *87*, 2995-2999.

[133] R. A. Rossi, J. F. Bunnett, *J. Org. Chem.* **1973**, *37*, 3570.

[134] M. Mizuno, M. Yamano, *Org. Lett.* **2005**, *7*, 3629.

[135] S. L. Tunis, M. E. Minshall, *Am. J. Manag. Care* **2008**, *14*, 131-140.

[136] A. D. A., *Diabetes Care* **2006**, *29*, S43-48.

[137] M. C. Argossi, A. Nicolucci, A*cta Biomed* **2009**, *80*, 93-101.

[138] P. Hogan, T. Dall, P. Nikolov, *Diabetes Care* **2003**, *26*, 917-932.

[139] P. Westermark, C. Wernstedt, , T. D. O'Brien, D. W. Hayden, K. H. Johnson, *Am. J. Pathol.* **1987**, *127*, 414-417.

[140] E. L. Saafi, B. Lysonarkowska, S. Zhang, J. Kistler, G. J. Cooper, *Cell Biol. Int.* **2000**, *25*, 339-350.

[141] K. A. Schug, W. Lindner, *Chem. Rev.* **2005,** *105*, 67-113.

[142] D. D. Perrin, W. L. F. Armatego, *Purification of Laboratory Chemicals,* 3rd. ed., Pergamon Press, New York, **1988**.

[143] W. C. Still, M. Kahn, A. Mitra, *J. Org. Chem.* **1978**, *43*, 2923-2925.

[144] H. E. Gottlieb, V. Kotyar, A. Nudelman, *J. Org. Chem.* **1997**, *62*, 7512-7515.

[145] C. S. Wilcox, *Frontiers in Supramolecular Chemistry and Photochemistry*; H. J. Schneider, H. Durr, Eds.; VCH: Weinheim, **1990.**

[146] K. A. Connors, *Binding Constants*; John Wiley and Sons: New York, **1987**.

[147] T. Wiseman, S. Williston, J. F. Brandts, L. -N Lin, *Anal. Biochem.* **1989**, *179*, 131-137.

‘‘The biography is not included in the online version for reasons of data protection’’

‘‘The biography is not included in the online version for reasons of data protection’’